THEORETICAL STUDIES ON ORGANIC SEMICONDUCTORS

A thesis submitted to the

UNIVERSITY OF SALFORD

by

HAROLD MORRIS

for the degree of

DOCTOR OF PHILOSOPHY

ABSTRACT

The thesis is concerned with the calculation of carrier mobilities in organic molecular crystals.

Five models which have been proposed to account for the transport of charge carriers in such crystals are discussed and evaluated in the light of the most recent improvements in the estimates of transfer integrals; and from these five, two have been chosen for further consideration.

Numerical calculations have therefore been made for several aromatic hydrocarbons and heterocycles under conditions in which the electron - lattice interactions are both strong and weak, and for which the crystal wave function may be represented respectively by localized molecular wave functions, and by Bloch sums of molecular wave functions within the crystal.

The use of molecular orbitals based on single Slater - type atomic orbitals in the calculations of energy band structures has been assessed; and a procedure, based on a simple configuration - interaction treatment, has been developed for the consideration of the effects of band - band interactions in those crystals wherein the molecular energy levels, which give rise to the energy bands in the solid, are degenerate.

A study has also been made of the effects on the calculated mobilities in anthracene of the temperature dependence of the transfer integrals.

ACKNOWLEDGEMENTS

TABLE OF CONTENTS

CHAPTER (1)

INTRODUCTION

The behaviour of materials when subjected to an applied field of varying intensity led initially to their classification into (1) conductors (i.e. those such as copper and graphite that readily conduct electricity) and (2) insulators (i.e. those such as diamond that did not).

The conduction properties of metals were accountable by Drude and Sommerfield in terms of free-electron theory (15); whilst the distinction between conductors and insulators was resolvable in terms of the band theory of solids. The origin and mathematical description of energy bands in high resistivity solids is discussed at some length in Chapter 2; so for the moment it is sufficient to give a purely descriptive account of the processes involved.

When atoms (or molecules) condense to form a solid, the discrete atomic energy levels are broadened due to nuclear-electronic and electronic-electronic interactions. Thus the discrete energy levels of the atom degenerate into broad energy bands in the solid. The two extremes cited above are illustrated in figure (1.1).
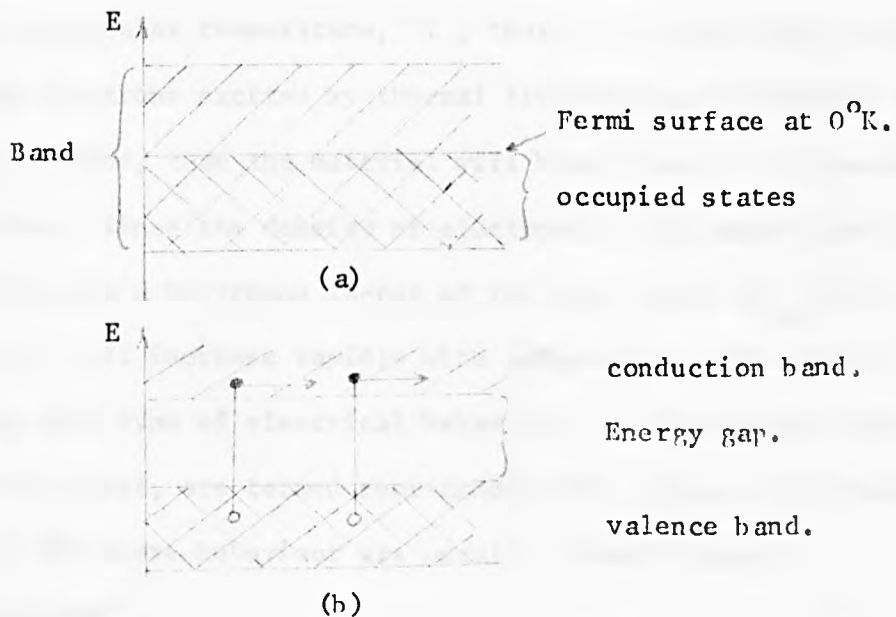
Figure (1.1)

Figure (1.1) (a) shows the band picture of a typical monovalent metal. In the ground state electrons with paired spins will fill the lower half of the energy band and hence this will be incapable of supporting conduction. However, there are current carrying states in the band an infinitesimal distance in energy above the top of the filled band, thermal fluctuations will, therefore, be sufficient to excite electrons into these levels and the solid will be a good conductor. Because of the very low energy of activation of excess carriers the conductivity will show little temperature dependence, except in so far as this governs the mechanism by which the carriers are scattered.

The second situation shown in figure (1.1) (b), illustrates the case for a solid having a full valence band above which is an energy gap, E gap, followed by a conduction band. In the ground state such a system will be incapable of supporting conduction since a finite excitation energy is required to carry electrons over the energy gap into the band of higher energy. If the necessary energy cannot be supplied by the thermal or electric fields, then the solid will act as an insulator. However, if the energy gap is relatively small such that at a particular temperature, T , there is a small but finite density of electrons excited by thermal fluctuations or by other means in the upper band, then the material will have a small but observable conductivity. Since the density of electrons in the upper band is characterized by a Boltzmann factor of the type $\exp(- E_{gap}/k_0 T)$, the conductivity will increase rapidly with temperature. Materials exhibiting this type of electrical behaviour, of which many organic solids form a part, are termed semi-conductors. Organic materials exhibiting the above behaviour are usually termed "Organic semi-conductors".

The first paper on the subject is considered to be that of Stoletov (1), who, in 1888, observed the existence of the photo voltaic effect in dye films irradiated with ultraviolet light. Later Pochettino (2) in 1906 reported the photo conductivity of anthracene which was studied further by Byk and Borak (3) and Volmer (4), however, it was not until the 1940's that the study of the electrical properties of organic solids began to gain momentum.

The study of semi-conduction processes in organic solids, especially compounds of biological interest, received a stimulus after Szent-Gyorgyi's (5-7) publications on their biological implications appeared in 1941. In the years that followed many papers were published on both theoretical and experimental aspects of the role of electronic conduction in biological processes (8). Brillouin (26) has suggested that the periodic structure of deoxyribonucleic acid (DNA) should give rise to an energy band structure and several calculations (27), based on simplified model structures and using the SCF-LCAO - crystal orbital method (24), have been reported.

A further stimulation was provided with the widespread success of inorganic semi-conductors in the field of electronics. However, the range of inorganic materials is only a fraction compared to the immense number of organic materials that are available which led to the idea of synthesising a particular molecule for a definite purpose. A rather intriguing example of this is the proposal by Little (25) of a possible structure for a superconducting polymer which, according to Little, should remain superconducting at and well above room temperature.

In a large proportion of the earlier work on the dark conductivity of organic solids, the experiments took the form of

determining the temperature variation of the resistivity (or conductance). It was found that the conductivity, σ, invariably obeyed the equation

$$\sigma = \sigma_0 \exp(- E/2k_0T) \qquad (1.1)$$

where k_0 is the Boltzmann constant and σ_0 is a constant, largely temperature independent and termed the specific conductivity. From the gradient of the $\log_e(\sigma)$ vs $1/T$ curve the value of E was determined. The value of E usually in the region $0.5 \rightarrow 3.0$ eV. was then ascribed to the energy band gap for intrinsic carrier generation. However, more recent photo conductive experiments indicate that this is very much an over simplification of the mechanism of charge carrier generation and that the true energy gap for intrinsic generation of charge carriers is, for anthracene at least, much higher (9). Pope, Kallmann and Giachmo (9) estimate that the band gap for intrinsic carrier generation is greater than the energy of the singlet state in the isolated molecule.

The mechanism of carrier generation in organic molecular crystals, particularly anthracene, has been extensively studied and various mechanisms have been proposed, however, the subject is far too diverse to discuss here. The review article of Le Blanc (10) and the references quoted therein contain more detailed information.

On the basis of solid state theory the conductivity, σ, is related to the velocity with which a carrier moves under a unit electric field, μ, through the equation :

$$\sigma = nze\mu \qquad (1.2)$$

when only one type of carrier is present, and

$$\sigma = \sum_i z_i e n_i \mu_i \qquad (1.3)$$

where 'i' types of charge carrier are present and z_i, n_i, and v_i are the charge, number and drift mobility, respectively of specimen i. e is the charge of the electron. The drift mobility, often shortened to simplify the mobility, μ , of charge carriers is a more fundamental property of the crystal than the conductivity, σ , and can be considered as providing a measure of the ease of which an electron, or hole, can move from molecule to molecule in the solid. The study of mobilities of excess carriers in organic single crystals has been enhanced by the introduction and wide spread use of Kepler's (11) pulsed photo conductivity technique and the discovery by Kallmann and Pope (12) of techniques for forming ohmic injecting contacts. Room temperature measurements of the drift mobility indicate that, for aromatic hydrocarbons, they are of the order 1 cm^2/volt-sec and, for the relatively few cases in which the mobility along different crystal axes has been determined, anisotropic. Temperature dependence studies indicate that the mobility almost always varies as some inverse power of the absolute temperature. Kepler (11) found a T^{-1} dependence for the hole mobility along the a axis in anthracene. Bogus (14) observed a variation T^{-2} between 230° and 270°k, Delacote (15), $T^{-1.7}$ between 280° and 400°k for hole conduction in the c' (a × b) direction while Raman et al (16) observed dependences of $T^{-1.4} - T^{-2.3}$ for different crystals between 295° and 333°k. Belper (17) found a $T^{-1.5}$ variation for both holes and electrons in the ab plane of pyrene, $T^{-1.3}$ and $T^{-2.0}$, for holes and electrons respectively, along the c' axis. A notable exception to this kind of temperature dependence is the electron mobility along the c' axis in anthracene which has a temperature variation of $T^{+0.3}$.

In contrast the mobilities in ferrocene and triphenylamine are very much smaller than 1 cm^2/volt sec. and are temperature activated (18) suggesting a different mechanism to that in higher mobility crystals.

The T^{-n} temperature dependence of the drift mobility observed for aromatic hydrocarbons is qualitatively the same as that found in inorganic semi-conductors, known to be ameniable by energy band treatment, while the much lower, thermally activated mobilities in ferrocene and triphenylamine are similar to those in nickel oxide crystals with small amounts of lithium as impurity (19). Yamashuta and Kurowasa (20, 21) have explained the experimental features of N_1O in terms of the Heitler-London scheme in which the electron or hole is bound to a particular site for a sufficient length of time to polarize the surroundings resulting in the carrier becoming self trapped. On the basis of this model, Yamashuta and Kurowasa established an upper limit for the mobility of 0.6 cm^2/volt-sec.

The qualitative agreement of the temperature dependence of the drift mobility in aromatic hydrocarbons and inorganic semi-conductors has led several authors to attempt theoretical treatments of the transport in organic crystals by the standard Bloch band theory method (38). By considering the crystal to be absolutely and perfectly rigid and treating phonon interactions as small perturbations which scatter carriers between eigenstates within an energy band, reasonable agreement with the observed drift mobilities were obtained. In addition the Hall effect in anthracene was predicted to be anomolous in both sign and magnitude (100), a point which has since been verified experimentally (22).

Several alternative models of charge carrier transport have been proposed in which conduction occurs via resonance transfer between

localized states. These together with the energy band model are discussed in greater detail in Chapter (2).

This thesis is concerned with the calculation of the mobility of excess carriers in organic homomolecular (23) crystals, these form the simplest type of organic solid. Because of the lack of data relating to the mechanism of conduction it was necessary to calculate the mobility by two models corresponding to the cases where the mean free path of the carriers is either greater than or less than the lattice spacing. At the instigation of this work calculations had been restricted to naphthalene, anthracene and a few simple polyphenyls and subsequently these have been extended to include a series of condensed polyacenes and a number of nitrogen containing heterocyclic molecules.

CHAPTER (2)

THEORIES OF THE TRANSPORT MECHANISM IN ORGANIC MOLECULAR CRYSTALS

2.1 Introduction

The proposed models of charge carrier conduction in organic solids can be roughly divided into two groups (1) those in which the carrier moves via a series of localized states (44,47-63) and (2) those in which conduction occurs in a wave-like motion, the carriers being periodically scattered by lattice phonons, crystal defects etc. The models in the localized state group can be further subdivided into those in which the carrier is envisaged as tunnelling through a series of potential barriers (47-50, 52-54), 59-63), which are termed tunnelling models, and those in which the transfer probability distribution is randomized after each transfer (44,55,56,65), i.e. the carrier is arbitrarily assumed to be scattered after each transfer, such models are termed resonance transfer (65) or hopping (44) models. The model of Gosar and Choi (51) cannot be strictly assigned to either of these two subgroups, but in many ways it has strong connections with the latter.

It is the object of this chapter to discuss some of the more sophisticated of the above models in the light of more recently reported values for the energy transfer integrals and also with a view to the extension of the models to molecules other than naphthalene and anthracene. Since, in general, the extent of electron-phonon coupling is unclear it is necessary in several cases to calculate the mobility of excess carriers in both the localized and delocalized representations. For convenience the models are discussed in two sections corresponding to the two groups outlined above.

In section (3.4) the conditions to be satisfied for the energy band model to be applicable are outlined

2.2 Tunnelling and Hopping models

Of the tunnelling models of carrier transport the most refined are those of Keller and Rast (60) and Keller (63) which are essentially extensions of the models of Eley et al in which the temperature

dependence of the mobility is incorporated into the model by allowing
the energy barrier to vary sinusoidally as a result of lattice
vibrations. Such variations are predicted to give the mobility a linear
dependence with temperature, the slope of the curve being either positive
or negative depending upon the parameters chosen. Application of the
method to anthracene revealed that the parameters which gave good
agreement with the experimentally measured mobilities (69,75) gave rise
to a temperature dependence opposite to that obtained experimentally (69)
while those chosen to give a negative temperature dependence led to rather
high values for the mobility. The temperature dependence of the model
has been criticised by Tredgegold (64) who pointed out that within the
framework of the model the mobility should always increase with
increasing temperature. An additional anomaly in the model, as mentioned
by Keller and Rast (60), is that the mobility of excess electrons, which
are associated with the first excited state of the free molecule, will
always be greater than that of excess holes, which are associated with
the highest bonding molecular orbital.

The resonance transfer model of conduction in organic molecular
crystals was first proposed by Kearns (65). Based on time-dependent
perturbation theory, the time in which an electron, localized on
molecule i, takes to move to a neighbouring molecule j is given
by (66)

$$t_{ij} = \tfrac{1}{2}h / |<\psi_j|H'|\psi_i> - <\psi_j|\psi_i><\psi_i|H'|\psi_i>| \qquad (2.1)$$

where H' describes the perturbation of the donor molecule i,
produced by the neighbour j, ψ_i, ψ_j are the molecular wave functions
of molecules i and j. The mobility of charge carriers can be
related to t_{ij} through (67,68) :

$$\mu = a^2 e/(k_0 T t_{ij}) \qquad (2.2)$$

where a is the transfer distance and k_0 the Boltzmann constant.
Mobilities calculated on this model are predicted to vary approximately
inversely with temperature, T . Application to crystalline
anthracene (65) showed the predicted anisotropy of the hole mobility
along the crystallographic axes a, b and c' (a × b) to be :

$$\mu_{bb} \sim 2\mu_{aa} \sim 5\mu_{c'c'} \qquad (2.3)$$

where μ_{ii} are the diagonal elements of the mobility tensor, $\underline{\mu}$,
corresponding to the mobility along axis i . This is in good agreement
with experiment (69,75) but the predicted anisotropy of the electron in
the ab plane was

$$\mu_{aa} \sim 2\mu_{bb} , \qquad (2.4)$$

opposite to that observed experimentally. The absolute values of the
mobilities calculated by Kearns (65), were $\sim$ 5 times too low, which,
in view of the approximations used to estimate the integrals in
equation (2.1) can be considered to be reasonable results.

In the above model the effects of electron-phonon interactions
are not considered explicitly. This problem has however been treated
in some detail by Goser and Choi (51) who studied the effects of the
fluctuations of the polarization energy and the transfer integrals on
the electron and hole motion in crystalline anthracene. The acoustic
and intermolecular vibrations of the lattice displace or change the
orientation of the molecules within the crystal resulting in
fluctuations in the polarization energy, thus coupling the electrons
with the phonons, and the energy transfer integrals. The latter types
of interaction has also been studied by Friedman (70). In a very
elegant piece of mathematical analysis in which the wave functions of
the charge carriers are represented by Wannier functions (76,77) and

the mobility calculated using the linear response theory of Kubo and

Tomita (72,73), Gosar and Choi derive the following expression for the

mobility tensor, $\underline{\mu}$:

$$\underline{\mu} = \frac{\pi e}{k_0 T} \sum_j (\underline{r}_j - \underline{r}_i)(\underline{r}_j - \underline{r}_i) \{J_{ij}^2 + \sum_\lambda |u(i,j,\lambda)|^2$$

$$[2n(\lambda) + 1]\}/\alpha(i,j) \qquad (2.5)$$

where J_{ij} is the transfer integral between molecules i and j whose

geometrical centres, at equilibrium, are defined by the vectors $\underline{r}_i$ and

$\underline{r}_j$ respectively. The parameters $u(i,j,\lambda)$ and $\alpha(i,j)$ contain the

effects of electron-phonon interactions and $n(\lambda)$ is the thermodynamic

equilibrium number of phonons in mode λ . The second term in curly

brackets represent the contribution to the mobility $\underline{\mu}$ from phonon

assisted tunnelling and can be related to the transfer integrals, J_{ij} ,

through

$$\sum_\lambda |u(i,j,\lambda)|^2 [2n(\lambda) + 1] = \frac{1}{\pi^2} \frac{k_0 T}{\rho s^2} r_{ij} \left(\frac{\partial J_{ij}}{\partial r_{ij}}\right)^2$$

$$\int_0^{q_{max} \times r_{ij}} (1 - \frac{\sin(x)}{x}) \, dx \qquad (2.6)$$

where q_{max} is the wave number corresponding to the Debye frequency;

$q_{max} = 12\pi^2/V_c$, V_c being the volume of the unit cell, ρ is the

density of the crystal, and s the velocity of sound in the solid.

Gosar and Choi assumed the differential in equation (2.6) to be of the

form,

$$\frac{\partial J_{ij}}{\partial r_{ij}} = A J_{ij} \qquad (2.7)$$

where A is constant, and using a value $A = 0.4$ nm. estimated that the

effect of phonon assisted tunnelling is to effectively increase the

energy transfer integral by between 35 and 69% depending upon the value

selected for the velocity of sound. Using the energy transfer integrals

of Katz et al (40), Gosar and Choi obtained values of the elements of

the mobility tensor in very good agreement with those obtained

experimentally for all but electronic conduction along the $\underline{c}'$ axis.

The lack of agreement along this axis they claimed was a result of

inaccuracies in the transfer integrals.

The calculation of transfer integrals has been investigated by

Glaeser and Berry (44) who showed that they could be expressed as :

$$J_{ij} = \left[J(resonance) + \Delta J(resonance) + J(electrostatic) \right] \cdot S_{ij} \qquad (2.8)$$

where J(resonance) is a sum of terms involving the neutral molecule

potentials (for excess electrons) or positive ion-molecule potential

(for holes) and terms arising from the intermolecular exchange.

ΔJ(resonance) gives the correction to these terms which results from

the use of polarized orbitals. J(electrostatic) represents the

off-diagonal elements of the long range interaction between the

access charge and the induced dipoles on neighbouring molecules. S_{ij}

is the product of overlaps of neutral molecules polarized by a charge

at i with a neutral molecule polarized by a charge at j . Glaeser

and Berry considered two cases, one in which the outmost orbital was

polarized, the second in which all seven orbitals were polarized.

Explicit calculation (44) of ΔJ(resonance) and J(electrostatic)

for the first case showed the two integrals to be of opposite sign and

very much less than J(resonance) thus neglect of those interactions

introduces errors well within the computation errors of J(resonance).

Thus for this case the principle effect of including polarization has

in the overlap factor, S_{ij} , which serves to reduce J(resonance) by

a factor of about a half. For the second case the term ΔJ(resonance)

was found to be extremely small, the overlap factor S_{ij} very close to unity while the term J(electrostatic) was an order of magnitude smaller than J(resonance). Therefore for this second case the effects of polarization can be neglected. The two functions described above represent the two extremes of the polarization and the true effect will be a compromise of the two.

The carrier mobilities, calculated using the integrals of Glaeser and Berry (44) for the two extremes of polarization and the method of Gosar and Choi (51), are shown in table (2.1). From these it can be seen that transfer integrals, incorporating the effects of molecular exchange of the excess electron or hole, serve to vastly increase the calculated values of the mobilities which, with the exception of the electron in the $\underline{c}'$ direction, are of the order of 4 - 10 times too large. The high values of the mobility probably arise as a result of inaccuracies in the calculated values of the polarization fluctuation constant, α, the accuracy of which Gosar and Choi claim is only an order of magnitude value. This is substantiated by the essentially correct prediction of the mobility anisotropy and the ratio μ_+/μ_-, but again the electron mobility along the $\underline{c}'$ axis is an exception to the rule. A possible method of overcoming the problem is to treat the constant, α, as an adjustable parameter. However, this would put the model on par with the energy band model, which is treated in a later section, since, strictly speaking, both models would only be capable of predicting mobility ratios. It is worth noting that if the expression for the mobility on the Gosar - Choi model is written in the form

$$\mu_{ij} = \frac{\pi e}{k_0 T} \frac{1}{\alpha} \sum_j (\underline{r}_j - r_i)(r_j - r_i) J_{ij}'^2 \qquad (2.9)$$

where J_{ij}' is the transfer integral, including the effects of phonon assisted tunnelling, between molecules i and j, it is very similar

Gosar and Choi				Glaeser and Berry			Expt.
I	II	III	IV	I	II	V	VI
11.8	12.4	1.6	7.1	5.8	1.2	0.95	1.7±0.2
9.5	10.0	5.4	4.5	1.7	1.1	0.98	1.1±0.1
0.04	0.04	0.07	0.01	0.3	0.2	0.15	0.4

(a)

I	II	III	IV	I	II	V	VI
6.6	6.6	3.3	3.7	0.9	0.6	0.56	1.2±0.2
16.2	16.2	7.3	8.3	1.8	1.2	1.02	1.8±0.2
5.4	5.4	1.4	1.6	1.8	1.2	1.02	0.8

(b)

Table(2.1)

Values of the mobilities* of excess electrons(a) and holes(b)

computed using the Gosar-Choi and Glaeser-Berry models.

I   calculated using the integrals from Ref(44)(no polarization)

and $s = 1.77 \times 10^3$ m/sec.

II calculated using the integrals from Ref(44)(no polarization)

and $s = 3.44 \times 10^3$ m/sec.

IIIcalculated using the integrals from Ref(44)(outer most orbital

polarized) and $s = 1.77 \times 10^3$ m/sec.

IV calculated using the integrals from Ref(44)(outer most orbital

polarized) and $s = 3.44 \times 10^3$ m/sec.

V   values taken from Ref(44).

VI Ref(11).

*units: 1×10^{-4} m^2/volt-sec.

to the band-model expression for the mobility in the mean free time
approximation (38) :

$$\mu_{ij} = \frac{e\tau_0}{k_0 T} <<v_i \, v_j>> \qquad (2.10)$$

with τ_0 proportional to $\frac{1}{\alpha}$ and the velocities v_j to $(\underline{r}_j - r_i)J_{ij}{}'$.
These similarities are reflected in the predicted anisotropy of the
mobility tensor, which is rather fortuitous since extension of the
Gosar - Choi method to other organic molecular-crystals is limited to the
few crystals in which the velocity of sound is known.

An alternative method for the mobilities of excess carrier in organic
solids has been proposed by Glaeser and Berry (44). In some ways the
model has close similarities with the resonance transfer model of
Kearns (65). As this model has been used extensively in this thesis the
model will be treated in rather more detail than has been given to the
previous models.

The crystal wave function is constructed as an antisymmetrized
product of molecular wave functions in which one molecule is either a
positive or a negative ion and the remaining molecules are perturbed by
the ionic molecule. If, at time $t = 0$ the charge is localized on
molecule 1 then the exact (non stationary state) wave function is
given by :

$$\Phi(0) = A \, \Psi_i(2a \pm 1) \prod_{j \neq i} \Psi_j{}^{(i)}(2a) \qquad (2.11)$$

where a is the number of filled orbitals in the neutral molecule,
$\Psi_i(2a \pm 1)$ denotes the wave function of appropriate molecular ion,
$\Psi_j{}^{(i)}(2a)$ is the wave function of a molecule in the field of this ion
as A is the normalized antisymmetrising operator, permuting electrons
between the molecules.

In the Glaeser-Berry model (44) the excess charge originally localized on molecule 1 (say) moves slowly onto other molecules so that, at a particular time, t , the crystal wave function $\Phi(t)$ becomes a supposition of Ψ_1 and other Ψ_i's , where Ψ_i is the molecular wave function of the i-th molecule. After a short time, Δt , it is supposed that the charge is relocalized on a molecule, j , in the near neighbourhood of molecule 1. Thus the wave function $\Phi(\Delta t)$ is given by :

$$\Phi(\Delta t) = \Psi_j$$

Physically this means that in time Δt the excess carrier has jumped from molecule 1 to molecule j. An additional assumption is made that the only transitions of importance are one step jumps whose jump probabilities and frequencies are independent of each other. This assumption is justified by the small values and rapid depreciation of the perturbation matrix elements (the transfer integrals). This being the case the system can be treated as a two state system and the wave function $\Phi(t)$ can be expanded in the wave functions Ψ_i of the unperturbed time dependent wave equation where the expansion coefficients are time dependent.

Within the assumptions of the model outlined above the charge localized on molecule 1 at $t = 0$ moves to molecule i in time

$$t_i = h/4|J_i| \tag{2.12}$$

where $|J_i|$ is the transfer integral between molecule 1 and i . This expression is similar to that used by Kearns (65), however, on their model the oscillation frequency is calculated on the assumption that molecules 1 and i are effectively isolated such that resonance transfer occurs only between these two molecules in which case

$$t_i = h/2|J_i|$$

However, the Glaeser - Berry model requires that there are several available states so that the wave function localized about molecule 1 at short times is

$$\Phi(t) \approx \Psi_1 + \sum_{i \neq j} \sin(2|J_i|t/h)\Psi_i \qquad (2.13)$$

The probability that the electron jumps to a particular site j will be

$$\tau(\underline{r}_j) = t_j^{-1}/\sum_i t_i^{-1} \qquad (2.14)$$

where $\underline{r}_j$ is the vector connecting the geometrical centres of molecules 1 and j and the summation i goes over all molecules in the neighbourhood of molecule 1. On the assumption that the probability distributions, $\tau(\underline{r})$, are randomized after each jump the system can be treated as a stationary Markoff process. This enables the basic probability distribution $\tau(\underline{r}_i)$ to be related to the probability distribution, $w(x|y,t)$, of the particle at position y, originally at x, after time t, after a large number of jumps (78). In effect the second moments of the probability distribution $w(x|y,t)$ are simply given by the second moments of the distribution $\tau(\underline{r}_i)$ multiplied by the number of jumps. All that remains is to relate the probability distribution to the diffusion.

Letting the probability of finding a particle, originally at x at time $t = 0$, after time Δt at position y be $w(x|y,t + \Delta t)$ then by the Smoluckowski equation

$$w(x|y,t + \Delta t) = \int dz\, w(x|z,t)w(z|y,\Delta t) \qquad (2.15)$$

Consider the integral

$$\int dy\, R(y) \frac{\partial}{\partial t} w(x|y,t) \qquad (2.16)$$

where R(y) is any function obeying the relation

$$R(y) \to 0 \quad y \to \pm \infty$$

Rewriting equation (2.16) in the form

$$\int dy \, R(y) \, \frac{\partial w}{\partial t}(x|y,t) = \underset{\Delta t \to 0}{Lt} \int dy \, R(y) \, [w(x|y,t+\Delta t) - w(x|y,t)] \qquad (2.17)$$

and substituting for $w(x|y,t+\Delta t)$ from equation (2.15) gives

$$\underset{\Delta t \to 0}{Lt} \{ \int dy \, R(y) \int dz \, w(x|z,t)w(z|y,\Delta t) - \int dy \, R(y)w(x|y,t) \} \qquad (2.18)$$

Rearranging the order of the first double integration term in equation (2.18) in the form

$$\int dz \, w(x|z,t) \int dy \, R(y) \, w(z|y,\Delta t) \qquad (2.19)$$

expanding the arbitrary function R(y) as a power series about z :

$$R(y) = R(z) + (y-z)R'(z) + \frac{1}{2}(y-z)^2 \, R''(z) + 0(3)$$

and ignoring terms $0(3)$, equation (2.19) becomes

$$\int dz \, w(x|z,t)\{R(z) \int dy \, w(z|y,\Delta t) + R'(z) \int dy(y-z) \, w(z|y,\Delta t)$$
$$+ \frac{1}{2} R''(z) \int dy(y-z)^2 \, w(z|y,\Delta t) \} \qquad (2.20)$$

Since the probability of finding the particle somewhere within the system is 1,

$$\int dy \, w(z|y,\Delta t) = 1 \qquad (2.21)$$

and assuming that there is an even probability of the particle moving backwards or forwards, i.e. $w(z|y,\Delta t)$ is an even function, then

$$\int dy(y-z) \, w(z|y,\Delta t) = 0 \qquad (2.22)$$

thus equation (2.20) reduces to

$$\int dz \, (w(x|z,t) \, [R(z) + \frac{1}{2} R''(z) \quad dy(y-z)^2 \, w(z|y,\Delta t)] \qquad (2.23)$$

Substitution of equation (2.23) into equation (2.18) leads to

$$\int dy\ R(y)\ \frac{\partial}{\partial t}\ w(x|y,t)\ =\ \underset{\Delta t \to 0}{Lt}\ \int dz\ w(x|z,t)\ R(z)$$

$$+ \frac{1}{2} \int dz\ w(x|z,t)\ R''(z)\ \int dy(y-z)^2 w(z|y,\Delta t)$$

$$- \int dy\ R(y)\ w(x|y,t) \tag{2.24}$$

The first and last terms of equation (2.24) are identical apart from the dummy variable of integration and therefore cancel leaving

$$dy\ R(y)\ \frac{\partial}{\partial t}\ w(x|y,t)\ = \frac{1}{2} \int dz\ R''(z)\ w(x|y,t)$$

$$\underset{\Delta t \to 0}{Lt}\ \int (y-z)^2\ w(z|y,\Delta t)dy \tag{2.25}$$

The second integration, over variable y, in equation (2.25) is just the second moment of the distribution function w and since the basic probability distribution, τ, is independent of the initial position of the particle this will be reflected in the distribution function w. Then the quadratic moment, B, of the distribution will be independent of z and equation (2.25) reduces to

$$\int dy\ R(y)\ \frac{\partial}{\partial t} w(x|y,t)\ = \frac{B}{2} \int dz\ R''(z)\ w(x|z,t) \tag{2.26}$$

Partial integration of the second integral, together with a change of the dummy variable from z to y gives :

$$\int dy\ R(y) \left[\frac{\partial}{\partial t}\ w(x|y,t)\ -\ \frac{B}{2}\ \frac{\partial^2}{\partial y^2}\ w(x|y,t) \right]\ =\ 0 \tag{2.27}$$

which must hold for all functions R(y) therefore

$$\frac{\partial}{\partial t}\ w(x|y,t)\ =\ \frac{B}{2}\ \frac{\partial^2}{\partial y^2}\ w(x|y,t) \tag{2.28}$$

This is a special form of the more general Fokker-Plank equation.
Comparison of equation (2.28) with the normal diffusion equation (39)
shows that the diffusion D is simply $\frac{B}{2}$ therefore

$$D = \frac{1}{2} \text{ Second moment of the distribution function}$$

Thus

$$D_{\alpha\beta} = \frac{N}{2} \sum_i \tau(\underline{r}_i) \, x_\alpha^{(i)} x_\beta^{(i)} \tag{2.29}$$

where $x_\alpha^{(i)}$ is the component of the vector $\underline{r}_i$ in the direction α,
and N is the number of jumps. $D_{\alpha\beta}$ can be related to the mobility tensor
through the Einstein equation

$$\mu_{\alpha\beta} = \frac{e \, D_{\alpha\beta}}{k_0 T} \tag{2.30}$$

The number of jumps per second is given by

$$N = \sum_i \tau(\underline{r}_i)/t_i \tag{2.31}$$

Mobilities calculated on this model (44) give fair agreement with the
experimentally observed values both in the anisotropy and magnitude of the
mobilities, however, the model has been criticized (51) in that in no way
are the effects of phonon interactions taken into account. This problem
was noted by Glaeser and Berry (44) who stated that to consider such a
probability distribution would require a detailed analysis of the
acoustical phonon spectrum as well as an estimate of how the various
transfer integral were affected, an accurate treatment of which at the
moment is out of the question. The second term, that of variation of
transfer integrals with displacement from equilibrium, could be incorporated
into the Glaeser-Berry scheme in a semi-quantitative sort of way by
including in the expression for the transfer integral, J_{ij} (equation (2.6)),
a term of the type (51)

$$\frac{1}{\pi s} \quad \frac{k_0 T}{p r_{ij}} \quad \sum \frac{(-1)^n (q_{max} \times r_{ji})^{2n+1}}{(2n+1)(2n+1)!} \qquad (2.32)$$

The symbols used in equation (2.32) have been defined previously (see equation (2.5)). The effect of inclusion of such a term would be to increase the transfer integrals by between 35 and 69% (51) depending upon the value used for the velocity of sound, s . The mobility of excess electrons and holes in anthracene have been calculated on the Glaeser-Berry model using the transfer integral of Glaeser and Berry (44) and incorporates the term representing the fluctuation of the transfer integrals, the results are given in table (2.1) together with the mobility as calculated by Glaeser and Berry. As can be seen from the table the calculated values of the mobility are in good agreement with those experimentally determined, however, the predicted anisotropy of the mobility, with the exception of the electron mobility along the c'-axis, is not as good as that of the Gosar-Choi model. In addition neglect of phonon interactions still predict values of the mobility within a factor of 2. As has been previously stated the velocity of sound in organic solids is, generally speaking, unknown, therefore the results quoted in this thesis are for the case where phonon assisted transfer is neglected.

2.3   The energy band model of conduction in organic molecular cystals
2.3(i)   Origins of energy bands in solids

On the basis of the energy band model the quantum states of an organic molecular crystal can be traced back to their origin in the isolated molecules of which the solid is composed. If one imagines that the N molecules of the crystal, N being a large number, are arranged in their lattice positions but at many times their normal separations such that the interactions between the molecules are negligible, then the quantum state distribution for such a system would be essentially that of an N-fold degenerate molecular state. As the molecules are brought to their

equilibrium positions each energy level associated with a particular

quantum state will be modified since the molecular wave functions

overlap and the quantum states will no longer be restricted to single

molecules but instead will extend over the whole crystal. Thus each

molecular energy level leads to a band of energy levels in the crystal.

In the process of splitting the number of quantum states in the atom or

molecule remains invariant: i.e. the number of quantum states in the

energy band will be the same as the number of quantum states from which

it is produced. Furthermore the width of the energy band arising from a

particular molecular energy level will be independent of the number of

molecules in the crystal but will be dependent upon the magnitude of the

interactions between molecules in the near vicinity of one another.

2.3(ii) Construction of the crystal wave function - The Bloch Theorem

The periodicity of a crystal can be described by specifying a set of

vectors $\underline{R}_i$ such that if $f(\underline{r})$ is any function which is periodic with

the lattice then the function $f(\underline{r})$ is unchanged upon displacement by

any vector $\underline{R}_i$

$$f(\underline{r} + \underline{R}_i) = f(\underline{r}) \tag{2.33}$$

The vectors $\underline{R}_i$ can be expressed in terms of three primitive

translation vectors $\underline{a}_1$, $\underline{a}_2$ and $\underline{a}_3$

i.e. $\underline{R}_i = n_{i1}\underline{a}_1 + n_{i2}\underline{a}_2 + n_{i3}\underline{a}_3$ \hfill (2.34)

where n_{ij} are integers.

Such periodic behaviour can be described in terms of a set of

translation operators $\{\underline{\varepsilon}|\underline{R}_i\}$ where $\{\underline{\varepsilon}|\underline{R}_i\}$ has the property that if

$f(\underline{r})$ is any function of position

$$\{\underline{\varepsilon}|\underline{R}_i\}f(\underline{r}) = f(\underline{r} + \underline{R}_i) \tag{2.35}$$

The translation operators $\{\underline{\varepsilon}_i|\underline{R}_i\}$ form an Abelian group of unit

element, $\underline{\varepsilon}$.

If the potential energy of an electron at position $\underline{r}$ is denoted $V(\underline{r})$ then since the potential energy must be periodic with the lattice

$$V(\underline{r}) = V(\underline{r} + \underline{R}_i) \tag{2.36}$$

As a result the translation operators commute with the Hamiltonian for an electron in a periodic potential and thus if the Hamiltonian of the system is denoted H

$$[\{\epsilon|\underline{R}_i\}, H] = 0 \tag{2.37}$$

Consequently the wave function of an electron in a periodic potential may be chosen to be simultaneously an eigenfunction of the energy and all the translations. If $\Phi(\underline{r})$ is such an eigenfunction then

$$\{\epsilon|\underline{R}_i\} \Phi(\underline{r}) = \Phi(\underline{r} + \underline{R}_i) = \lambda_i \Phi(\underline{r}) \tag{2.38}$$

and

$$|\Phi(\underline{r} + \underline{R}_i)|^2 = |\lambda_i|^2 |\Phi(\underline{r})|^2 \tag{2.39}$$

But the wave function of the electron must have the periodicity of the lattice

$$|\Phi(\underline{r} + \underline{R}_i)|^2 = |\Phi(\underline{r})|^2 \tag{2.40}$$

and λ_i must be a complex number of modulus unity i.e. $\lambda_i = \exp(i\,\theta_i)$.

If the two translation operators $\{\epsilon|\underline{R}_i\}$, $\{\epsilon|\underline{R}_j\}$ act in succession then the subsequent translation is equivalent to that produced by the single translation operator $\{\epsilon|\underline{R}_i + \underline{R}_j\}$

$$\{\epsilon|\underline{R}_i\} \{\epsilon|\underline{R}_j\}\Phi(\underline{r}) = \Phi(\underline{r} + \underline{R}_i + \underline{R}_j) = \lambda_i \lambda_j \Phi(\underline{r})$$

and $\{\epsilon|\underline{R}_i + \underline{R}_j\}\Phi(\underline{r}) = \lambda_{i+j}\Phi(\underline{r})$

Therefore the product of the eigenvalues corresponding to the different translations must be equal to the eigenvalue of the combined translation. This condition is satisfied if

$$\theta_i = \underline{k} \cdot \underline{R}_i$$

where $\underline{k}$ is an arbitrary vector that is the same for each operation

$$\phi(\underline{r} + \underline{R}_i) = e^{i\,\underline{k}\cdot\underline{R}_i}\,\phi(\underline{r}) \tag{2.41}$$

This result is known as the Bloch theorem (80) and the vector $\underline{k}$ is referred to as the wave vector.

2.3(iii) Derivation of the energy expression

The energy of a crystal, $E(\underline{k})$, with Hamiltonian, H, and wave function $\Omega(\underline{k})$ can be expressed:

$$E(\underline{k}) = \frac{\langle \Omega(\underline{k})|H|\Omega(\underline{k})\rangle}{\langle \Omega(\underline{k})|\Omega(\underline{k})\rangle} \tag{2.42}$$

Expanding the crystal wave function $\Omega(\underline{k})$ as a Bloch function of the molecular wave functions, Ψ_ℓ, gives:

$$E(\underline{k}) = \sum_m \sum_\ell \frac{\exp(i(\underline{r}_m - \underline{r}_\ell))\,\langle\phi_\ell|H|\phi_m\rangle}{\sum_m \sum_\ell \langle\phi_\ell|\phi_m\rangle \exp(i(\underline{r}_m - \underline{r}_\ell))} \tag{2.43}$$

which can be expressed as

$$E(\underline{k}) = \frac{\sum_\ell \{\langle\phi_\ell|H|\phi_\ell\rangle + \sum_{m\neq\ell}\exp(i\,\underline{k}\cdot(\underline{r}_m-\underline{r}_\ell))\langle\phi_\ell|H|\phi_m\rangle\}}{\sum_\ell \{\langle\phi_\ell|\phi_\ell\rangle + \sum_{m\neq\ell}\exp(i\,\underline{k}\cdot(\underline{r}_m-\underline{r}_\ell))\langle\phi_\ell|\phi_m\rangle\}} \tag{2.44}$$

Setting $\ell = 0$ and suppressing the summation over ℓ the above equation reduces to

$$E(\underline{k}) = \frac{\langle\phi_0|H|\phi_0\rangle + \sum_{m\neq 0}\exp(i\,\underline{k}\cdot\underline{r}_m)\langle\phi_0|H|\phi_m\rangle}{1 + \sum_{m\neq 0}\exp(i\,\underline{k}\cdot\underline{r}_m)\langle\Psi_0|\Psi_m\rangle} \tag{2.45}$$

It is generally assumed (38-43) that the overlap integral $\langle \Psi_0 | \Psi_m \rangle$ is zero. Furthermore, it is assumed that the Hamiltonian, H, can be partitioned into terms representing all the potential energy terms involving the excess electron, H_1, and the remaining terms representing the Hamiltonian in the absence of the excess electron, H_0. Thus

$$H = H_0 + H_1 \qquad (2.46)$$

The wave function, Ψ_ℓ, for a crystal containing an excess electron sited on molecule ℓ is of the form:

$$\Psi_\ell = A \, \phi_\ell^n(1) \, \psi_\ell(2a) \prod_{j \neq \ell} \psi^{(\ell)}(2a) \qquad (2.47)$$

where ϕ_ℓ^n is the n-th molecular orbital occupied by the excess electron on molecule ℓ. $\psi_\ell(2a)$ is the molecular wave function of molecule ℓ, $\psi_j^{(\ell)}$ is the wave function of the molecule at j in the presence of the excess charge on molecule ℓ, and A is the normalized antisymmetrizer permuting electrons between the molecules. If the perturbations due to the excess electron are small (i.e. if the effects of polarization are negligible) the above expression reduces to (2.48). Note that this assumption is consistent with the zero overlap approximation

$$\Psi_\ell = A \, \phi_\ell^n(1) \, \psi_\ell(2a) \prod_{j \neq \ell} \psi_j(2a) \qquad (2.48)$$

Making use of the approximation that the functions Ψ_ℓ are eigenfunctions of H_0, and invoking the zero overlap approximation, the $\underline{k}$ dependent part of $E(\underline{k})$ can be expressed as (41):

$$E'(\underline{k}) = \sum_{m \neq 0} \exp(i\underline{k} \cdot \underline{r}_m) \, \langle \phi_0 | H_1 | \phi_m^n \rangle \qquad (2.49)$$

where $H_1 = V_{cryst}(r) - V_0(r)$

and V_{cryst} and V_0 are the crystal potential and the neutral

molecule potential respectively. It is generally assumed (38 - 43)

that the crystal potential can be approximated by a linear

combination of neutral molecule potentials :

$$V_{cryst}(\underline{r}) = \sum_n V_n(\underline{r} - r_n) \tag{2.50}$$

with $V_n(\underline{r} - r_n)$ of the form (41)

$$V_n(\underline{r} - r_n) = V_{core} + \sum_{i=0}^{a} (2J_n^{\ i} - K_n^{\ i}) \tag{2.51}$$

The summation over i runs over the occupied molecular

orbitals $\phi_n^{\ i}(\mu)$ of molecule n where μ stands for the space

coordinates x^μ, y^μ, z^μ of the occupying i electron. $J_n^{\ i}$ and

$K_n^{\ i}$ are the coulomb and exchange operators of the i-th molecular

orbital of the n-th molecule defined by :

$$J_n^{\ i} \phi_{n'}^{\ j}, (1) = <\phi_n^{\ i}(2) \ |\frac{e^2}{r_{12}}| \ \phi_n^{\ i}(2)> \ \phi_{n'}^{\ j},(1)$$

$$\tag{2.52}$$

$$K_n^{\ i} \phi_{n'}^{\ j}, (1) = <\phi_n^{\ i}(2) \ |\frac{e^2}{r_{12}}| \ \phi_{n'}^{\ j}(2)> \ \phi_n^{\ j} (1)$$

and V_{core} is the potential energy operator of the core electrons

and the atomic nucleii. In the approximation that the core states

can be considered localized at the nucleus on which they are centred,

i.e. exchange interactions of the type defined in equation (2.52) are

neglected, then V_{core} can be expressed as

$$V_{core} = - \sum_{A=1}^{M} Z_A/R_A - \sum_i <\theta_A^{(i)}(2)|r_{12}^{-1}|\theta_A^{(i)}(2)> \tag{2.53}$$

$$\text{core states}$$

R_A is the distance of the electron from the A-th nucleus of nuclear charge Z_A, $\theta_A^{(i)}$ is the atomic wave function of the i-th core state and r_{12} is the distance between electrons 1 and 2. In practise the atomic core states are constructed from the wave functions of the 1s, 2s, $2p_\sigma$ and $2p_\pi$ atomic states for first row elements.

Substituting equation (2.53) and equation (2.52) into equation (2.51) and the resulting expression for $V_n(\underline{r} - \underline{r}_n)$ into equation (2.49) it can be shown that the energy wave vector relationship is

$$E'(\underline{k}) = \sum_{m \neq 0} \exp(i\underline{k} \cdot \underline{r}_m) \{ \langle \phi_0^n(1) | - \sum_{A=1}^{M} \{ Z_A/R_A$$

$$- \sum_{\substack{i \text{ core} \\ \text{store}}} \langle \theta_A^{(i)}(2) | r_{12}^{-1} | \theta_A^{(i)}(2) \rangle \} | \phi_m^n(1) \rangle$$

$$+ 2 \langle \phi_0^n(1) | \sum_{i=1}^{a} \langle \phi_m^i(2) | r_{12}^{-1} | \phi_m^i(2) \rangle | \phi_0^n(2)$$

$$+ \langle \phi_0^n(1) | \sum_{i=0}^{a} \langle \phi_m^i(2) | r_{12}^{-1} | \phi_m^n(2) \rangle | \phi_0^i(2) \rangle \} \qquad (2.54)$$

Expanding the molecular orbitals, ϕ, in terms of a basis set of atomic orbitals, u, $E'(\underline{k})$ becomes :

$$E'(\underline{k}) = \sum_{m \neq 0} \exp(i\underline{k} \cdot \underline{r}_m) \sum_{\alpha, \beta}^{m} c_\alpha^n c_\beta^n [\langle u_\alpha | - \sum_{A=1}^{m} Z_A/R_A$$

$$- \sum_{\substack{i \text{ core} \\ \text{store}}} \langle \theta_A^{(i)} | r_{12}^{-1} | \theta_A^{(i)} \rangle | u_\beta \rangle$$

$$+ \sum_{i=1}^{a} \sum_{\delta, \gamma}^{m} c_\delta^i c_\gamma^i \{ 2 \langle u_\alpha | \langle u_\delta | r_{12}^{-1} | u_\gamma \rangle | u_\beta \rangle$$

$$- \langle u_\alpha | \langle u_\delta | r_{12}^{-1} | u_\beta \rangle | u_\gamma \rangle \}] \qquad (2.55)$$

Katz et al (40) have carried out band structure calculations in which three centre terms were included and the potential was represented by

$$V_\ell(\underline{r} - r_\ell) = - e^2 \sum_A Z_A/R_A + 2 \sum_{i=0}^{a} J_\ell^i \qquad (2.56)$$

The notation here is the same as that of equation (2.51). Their results showed that the exclusion of just four-centre terms resulted in values for the transfer integrals which were about 30% larger than those obtained by the exclusion of three- and four- centre terms. However in their potential equation (2.56) they omitted the electron exchange terms, K_ℓ^i , which tend to increase the two-centre contribution to the transfer integrals by a factor of three but at the same time add little to the three-centre contribution. This then reduces the relative contribution of the three-centre terms in a potential of the form of equation (2.51) to approximately 10%.

Since the three centre terms are extremely tedious to calculate and require large amounts of computer time, the two centre approximation (38, 39, 41, 42, 43, 45) is used throughout this thesis and multicentre terms are negative. Thus equation (2.55) reduces to

$$E'(\underline{k}) = \sum_{m \neq 0} \exp(i\underline{k}\cdot r_m) \{ \sum_{\alpha,\beta}^{N} c_\alpha^n c_\beta^n \langle u_\alpha |- Z_\alpha/R_\beta | u_\beta \rangle$$

$$+ \langle u_\alpha / \sum_{\substack{i \text{ occ} \\ \text{core states}}} \langle \theta_\alpha^{(i)}(2) | r_{12}^{-1} | \theta_\alpha^{(i)}(2) \rangle | u_\beta \rangle$$

$$+ 2 \sum_{i=1}^{a} c_\alpha^i c_\alpha^i \langle u_\alpha | \langle u_\alpha | r_{12}^{-1} | u_\alpha \rangle | u_\beta \rangle$$

$$- \sum_{i=1}^{a} c_\alpha^i c_\alpha^i \langle u_\alpha | \langle u_\alpha | r_{12}^{-1} | u_\alpha \rangle | u_\beta \rangle \} \qquad (2.57)$$

Now $2 \sum_{i=1}^{a} (c_\alpha^i) = \rho_\alpha$, the π-electron density at centre α, therefore equation (2.57) becomes :

$$
\begin{aligned}
E'(\underline{k}) = {} & \sum_{m \neq 0} \exp(i\underline{k} \cdot r_m) \{ \sum_{\alpha,\beta}^{N} c_\alpha^n c_\alpha^n \langle u_\alpha | - Z_\alpha / R_\alpha | u_\beta \rangle \\
& + \sum_{\substack{i \text{ core} \\ \text{states}}} \langle u_\alpha | \langle \theta_\alpha^{(i)}(2) | r_{12}^{-1} | \theta_\alpha^{(i)}(2) \rangle | u_\beta \rangle \\
& + \frac{\rho_\alpha}{2} \langle u_\alpha | \langle u_\alpha | r_{12}^{-1} | u_\alpha \rangle | u_\beta^{-1} \rangle \}
\end{aligned}
\tag{2.58}
$$

A similar derivation can be used to determine the energy band structure of a crystal containing excess holes. It should be noted that in the above derivation it is inherently assumed that the concentration of excess electrons or holes is small so that carrier-carrier interactions are negligible. This has been found to be the case so far where the average carrier concentration at room temperature is in the region $1_{10}12$ cm^{-3}.

In the derivation of the energy band structure up to this point no mention has been made as to the effects of interactions of the excess electron or hole with molecular vibrations. Such interactions can be classified into two categories; (a) the interaction of the excess charge carrier with low frequency intermolecular modes and (b) the interaction of the excess carriers with high frequency (h ω_0 ~ 0.2 eV) internal vibrations of the constituent molecules. Interactions of type (a) serve to scatter the carrier within the energy band and are discussed in a later section, whereas the interactions of type (b) give rise to a series of vibronic sub-bands, separated from the ground state vibronic sub-band by h ω_0 and modified by a vibrational overlap factor. Electronic motion in these vibronic sub-bands corresponds to the simultaneous presence of an

electron in the conduction band together with one or more vibrational quanta. The existence of these vibrational bands has been detected experimentally (46). Because of the small interaction of the delocalized carrier as a large, non-polar, aromatic molecule and also of the largeness of the optical quantum the coupling of the excess carriers with the intermolecular vibrations is weak. Thus the molecular wave function Ψ_ℓ can be represented as :

$$\Psi_\ell = A \, \phi_\ell^n(1) \, \psi_\ell(2a) \, \chi_\ell \prod_{j \neq \ell} (\psi_j(2a) \, \chi_j) \qquad (2.59)$$

This representation corresponds to the weak coupling limit of vibronic interaction (41). χ_ℓ is the ground state vibrational wave function of the j-th molecule, and it is assumed that all vibrational wave functions are the same except for that of the molecule with an excess electron or hole. The effect of using a wave function of this type is to premultiply the transfer integral of equation (2.58) by a constant factor $|\langle \chi_1 | \chi_0 \rangle|^2$, where χ_1 is the vibrational wave function of the positive or negative ion and χ_0 that of the free molecule.

In summary, the approximations used in the tight binding approximation are :

(1) The perturbation of near neighbours due to the presence of the excess electron or hole are small in which case the wave functions of the molecule, ℓ, obeys the relation

$$H_0 \, \Psi_\ell = E \, \Psi_\ell ,$$

H_0 being the Hamiltonian of the free molecule.

(2) The overlap of molecular wave functions is small and can be neglected i.e.

$$\int \Psi_0^* \, \Psi_\ell \, d\tau = \delta_{\ell 0}$$

- 33 -

(3)   The crystal potential can be constructed as a linear combination of neutral molecule potentials

(4)   Multicentre terms are relatively small and can be neglected.

For crystals obeying the above assumptions the energy band structure can be written

$$E'(\underline{k}) = \sum_{m \neq 0} |\langle \chi_1 | \chi_0 \rangle|^2 \exp(i\underline{k} \cdot r_m) \{ \sum_{\alpha, \beta}^{N} c_\alpha^n c_\beta^n$$

$$\langle u_\alpha | - Z_\alpha / R_\alpha | u_\beta \rangle + \sum_{\substack{i \text{ core} \\ \text{states}}} \langle u_\alpha | \langle \theta_\alpha^{(i)}(2) | r_{12}^{-1} | \theta_\alpha^{(i)}(2) \rangle | u_\beta \rangle$$

$$+ \frac{\rho_\alpha}{2} \langle u_\alpha | \langle u_\alpha | r_{12}^{-1} | u_\alpha \rangle | u_\beta \rangle \} \tag{2.60}$$

It should be noted that the transfer integrals will be the same for both the localized and energy band approximations, the various terms in the band expression being the off-diagonal elements of the Hamiltonian in the localized representation (44). The mathematical methods used to evaluate the various integrals in equation (2.60) are discussed in appendix (1).

2.3(iv)   Conditions imposed by the energy band model.

The approximations used in energy band theory have been described by Slater (81) as

(i)   the use of a one electron potential

(ii)   the neglect of multiplet structure on individual atoms

(iii)   the treatment of electron-lattice interaction as a small perturbation.

For high mobility semiconductors only approximation (i) is not strictly applicable, but even here the band description is formally valid although the values of parameters used are not

calculable from a one electron potential. However, as pointed out
by Ioffe (82, 83), many semiconductors with mobilities less than
100 cm^2 v.sec^{-1} have a nominal free path which is less than the
wave length of thermal electrons, in contradiction of assumption
(iii), since in this case one has strong electron lattice
coupling. Difficulties arising in the use of energy band theory
in describing low mobility semiconductors have been discussed by
Ioffe (82) and more recently by Frohlich and Sewell (84). The
latter authors derived the inequality

$$B\tau > h/4\pi \qquad (2.61)$$

as the limitation on the validity of the band model where B is
half the band width and τ is the relaxation time of the carrier.
Requirements for the validity of the band model can also be expressed
in terms of the mobility as follows.

The current density j_i in the direction i is given by

$$j_i = \frac{-e^2 \, F}{h^2} \int \frac{\partial E(\underline{k})}{\partial k_i} \frac{\partial E(\underline{k})}{\partial k_i} \frac{\partial f(\underline{k})}{\partial E(\underline{k})} \, d\underline{k} \qquad (2.62)$$

where $f(\underline{k})$ is the Maxwell distribution function and F is the
applied field. An alternative method of writing the above is

$$j_i = \frac{e^2 \, F}{k_0 T} \, n << (v_i(\underline{k}) \, v_i(\underline{k}) \, \tau(\underline{k})) >> \qquad (2.63)$$

where n is the concentration of electrons, the double angular
brackets indicating the appropriate averaging over the band. The
mobility μ will, therefore, be given by

$$\mu = \frac{e}{k_0 T} << v_i(\underline{k}) \, v_i(\underline{k}) \, \tau(\underline{k}) >> \qquad (2.64)$$

We now make the assumption that the relaxation time $\tau(\underline{k})$ can be treated as being independent of k, i.e. $\tau(\underline{k}) \equiv \tau_0$, and that the resulting statistical average $<<v_i(\underline{k}) \, v_i(\underline{k})>>$ can be replaced by v_{max}^2 which is of the same order if $2J < kT$.

$$\mu = \frac{e \, \tau_0}{k_0 T} \, v_{max}^2 \qquad (2.65)$$

The order of v_{max} has been given, for lattice constant a, as

$$v_{max} \simeq 2Ba/h \qquad (2.66)$$

$$\mu \simeq \frac{4e \, \tau_0}{h^2 \, kT} \, B^2 \, a^2 \qquad (2.67)$$

Now $2B\tau_0 > h$

$$\mu > \frac{2e}{kT} \, B \, a^2 \qquad (2.68)$$

which, for $a \sim 5 \, \overset{o}{A}$, reduces to

$$\mu > \frac{6B}{kT} \quad cm^2 \, | \, volt-sec. \qquad (2.69)$$

$$\mu > 232B \quad \text{at room temperature.}$$

Application of scattering theory leads to the relation between mobility and temperature dependence of the form

$$\mu \propto T^{-3/2} \qquad (2.70)$$

Equation (2.70) does not hold when the maximum velocity, v_{max}, of an electron on a band is less than s, the velocity of sound, since use of band theory demands that both energy and wave vector are conserved and if $v_{max} < s$ then the emission or absorption of acoustic phonons cannot take place with conservation of both energy and wave vector. The above criterion places a limitation

on the band width as follows.

The velocity of a charge carrier in a state of given k is

$$v(\underline{k}) = \frac{1}{h} \frac{\partial E(\underline{k})}{\partial \underline{k}}$$ (2.72)

Using the approximation introduced by Glarum (57) the component of the velocity along the x-axis is given by

$$v_x = \frac{a}{h} (B^2 - E^2)^{\frac{1}{2}}$$ (2.72)

where a is again the lattice spacing and

$$- B < E < B$$ (2.73)

As before the order of v_{max} is given by

$$v_{max} = \frac{2 B a}{h}$$ (2.74)

which, in terms of the velocity of sound is given by

$$v_{max} = \frac{2 B s}{k \theta}$$ (2.75)

where θ is the Debye temperature for the lattice. Since v_{max} cannot be less than s it follows that, for band theory to be valid

$$2 B > k \theta$$ (2.76)

Glarum (31) gives a similar condition for the validity of the band model

$$B > h \omega_o$$ (2.77)

where all the lattice vibrations are assumed to have the same frequency, ω_o.

Finally it should be noted that conduction occurring via a wavelike motion is strongly dependent upon the translational symmetry of the crystal, therefore any reduction in this symmetry, as in the case of the solid melting, will considerably reduce the mobility of the carriers whereas carrier transport due to a hopping motion does not rely on translational symmetry and should thus be about equally effective for liquids and solids.

CHAPTER (3)

On the use of single Slater wave functions in band structure

calculations with special reference to naphthalene.

3.1   Introduction.

3.2   Construction of symmetry adapted wave functions.

3.3   Method of calculation.

3.4   Numerical calculations.

3.5   Numerical results and band structure.

3.6   The mobility tensor.

    (i)   Variation of the calculated mobility ratios

        with screening parameter and vibrational overlap factor.

    (ii)   Optimum value of the screening parameter, ζ .

    (iii)   Effects of small rotations of the molecules on the

        calculated mobilities.

    (iv)   The validity of the energy band model.

3.7   Discussion and conclusion.

3.1 Introduction

The tight binding approximation, as first used by LeBlanc (38) in the calculation of the energy band structure of crystalline anthracene, forms one of the most significant theoretical advances towards the understanding of electronic processes in organic molecular crystals. Using a single Slater function, with screening parameter $\zeta = 30.7$ nm^{-1}, to represent the carbon $2p_z$ atomic wave function Le Blanc showed that the essential features of the anisotropy of the mobility tensor could be understood in terms of an energy band model. In his work Le Blanc assumed that a molecular crystal with two molecules per unit cell could be related to a hypothetical crystal with one molecule per unit cell. However, this has since been shown to be incorrect (40) as symmetry considerations demand there be two energy bands for both the electrons and holes each corresponding to the two molecules per unit cell.

Naphthalene has been considered under the same approximations as above by Thaxton, Jarnagin and Silver (39), while further developments have been made by Katz et al (40) who replaced the single Slater functions by SCF atomic orbitals of Clementi and Rootaan (89) and obtained energy band widths increased by a factor of 5. Inclusion of an exchange potential (44,41), of the type defined by equation (2.52), page (28), in the neutral molecule potential further increases the calculated band widths to 0.1, 0.2 eV for electrons and holes respectively. Using the calculated elements of the mobility tensor and the experimental data of Silver et al (39) it can be shown that the uncertainty in the energy of the scattered carriers is of the order of the band width and the mean free paths of excess carriers

is less than the lattice spacing, thus casting some doubt on the validity of the energy band model (84) as a method of describing the transport of excess carriers in naphthalene - antracene type crystals.

In the calculations sited above the molecules are assumed to be non-vibrating and fixed at their lattice positions. Silbey et al (41) have shown that inclusion of the effects of molecular vibrations serves to reduce the electronic matrix elements by a factor $|<\chi_1|\chi_0>|^2$, where χ_0 and χ_1 are the vibrational wave functions of the neutral molecule and positive or negative ion respectively. For the symmetric ground, first and second excited state vibrational modes the vibrational overlap factors have the values (74) 0.605, 0.305 and 0.08 respectively. In addition, as discussed in chapter (2), page (14), polarization effects serve to reduce the transfer integrals by up to a factor of 2. Therefore inclusion of the above effects reduce the band widths by between $\frac{1}{4}$ and $\frac{1}{20}$ depending upon the vibrational state of the molecular ion. Silbey et al (41(a)), in their original paper, estimated the mean free path of excess carriers in crystalline anthracene to be of the order 1 nm for vibrational overlap factor 0.5, thus removing the apparent violation of the uncertainty principle. However, the above calculations were found to be in error and in the erratum (41(b)) the effects of molecular vibrations were not included.

The question of proper representation of wave functions at large distances is not a new one in fact as long ago as 1931 Slater and Kirkwood (85) showed, in the calculation of the polarizability of the helium atom, that considerable improvement in the quantities dependent upon the tail of the wave function could be achieved by using Slater functions with reduced screening parameters. More recently McClelland (86) has shown that the electronic excitation levels in benzene can be calculated using single Slater functions

with $\zeta = 22.7 \text{ nm}^{-1}$ to represent the carbon $2p_z$ atomic wave functions.

This leads us to believe that, with suitable adjustment of the

screening parameter, results comparable to those calculated with SCF

wave functions can be obtained using a single Slater function with a

considerable saving in labour.

It is the purpose of this chapter to investigate the effects of

molecular vibrations on the calculated values of the mobility ratios

while, at the same time, attempting to assess the use of single Slater

functions in energy band structure calculations.

3.2 Construction of symmetry adapted wave functions

Naphthalene crystallizes in the monoclinic system with space

group C_{2h}^5 and has two molecules per unit cell. The factor group

of the space group contains the following operations :

(i)   inversion at any site

(ii)   reflection in the ac plane followed by an a/2 glide in the

       ac plane

(iii) a two fold rotation about the b axis followed by a b/2

       glide along this axis.

The factor group, including the identity operation, is, therefore,

isomorphous with the point group C_{2h} . Group theory demands that

the cell wave functions belonging to the k = 0 representation

must transform like the irreducible representations of the factor

group and, since all the irreducible representations of C_{2h} are

one dimensional, symmetry adapted wave functions for k = 0 can

be constructed by utilizing the projection operator

$$P^i = \frac{1}{n} \sum_R \chi^i(R) R \qquad (3.1)$$

where R is a symmetry operation in C_{2h}, $\chi^i(R)$ the character

of R for the i-th irreducible representation, and n is the order
of the group C_{2h} .

The transformations of the one site wave functions under the
group operations are :

$$\sigma_{ac} \psi_1(0) = \psi_2(0)$$

$$i \ \psi_1(0) = -\psi_1(0)$$

$$i \ \psi_2(0) = -\psi_2(0)$$

$$C_2^b \ \psi_1(0) = -\psi_2(0)$$

The symmetry adapted functions can be obtained by means of the
projection operator equation (3.1) in the form

$$\phi_i(0) = P^i \psi_2(0)$$

where i represents any of the irreducible representations of the
C_{2h} point group. The representations Ag and Bg give only
vanishing results owing to the odd parity of the molecular wave
functions, and for the representations Au and Bu

$$\phi_-(k) = \frac{1}{\sqrt{2}} (\psi_1(0) - \psi_2(0))$$

and

$$\phi_+(k) = \frac{1}{\sqrt{2}} (\psi_1(0) + \psi_2(0)) .$$

When $\underline{k} \neq 0$ the unit cell wave functions are given by

$$\phi_\pm(k) = \frac{1}{\sqrt{2}} (\psi_1(k) \pm \psi_2(k))$$

but the symmetries of $\phi_+(k)$ or $\phi_-(k)$ depend on the group of the
wave vector $\underline{k}$. If the vector connecting the centres of molecules 1
and 2 is $\underline{r}$ it can be shown that as a consequence of the translational

symmetry of the crystal

$$\Psi_1(k) = \Psi_1(0)$$

and
$$\Psi_2(k) = e^{i\underline{k}\cdot\underline{r}}\Psi_2(0) \;.$$

The general symmetry adapted wave functions are therefore

$$\Phi_\pm(k) = \frac{1}{\sqrt{2}}(\Psi_1(0) \pm e^{i\underline{k}\cdot\underline{r}}\,\Psi_2(0)) \tag{3.2}$$

Thus, when the molecules come together to form the solid, each

molecular energy level will split into two components due to the

symmetric and antisymmetric combinations of the one site wave

functions in the cell giving rise to two energy states for the

excess electron and two for the hole.

The crystal wave function is constructed, in the Bloch

representation, as a linear combination of unit cell wave functions.

If the vector locating the origin of the i-th unit cell is $\underline{r}_i$ then

$$\Omega_\pm(k) = \sum_i \exp(i\underline{k}\cdot\underline{r}_i)\,\Phi_{i\pm}(k) \tag{3.3}$$

where the summation i runs over all cells in the crystal.

Substitution for $\Phi_\pm(k)$ and replacing the summation over all unit

cells by a summation over all molecules in the crystal equation (3.3)

becomes

$$\Omega_\pm(k) = \sum_j (-)^L \exp(i\cdot\underline{k}\cdot\underline{r}_j)\Psi_j \tag{3.4}$$

where $L = 0$ if $\underline{r}_j$ contains $n\,\underline{b}$ and $L = 1$ if $\underline{r}_j$ contains

$(n + \tfrac{1}{2})\underline{b}$.

The single site functions Ψ_j are taken to be an antisymmetrized

product of molecular wave functions in which one molecule is represented as either a positive or negative ion. The effect of molecular vibrations are included by taking the molecular wave functions as being the product of an electronic part and a vibrational part. This representation corresponds to the weak-coupling limit of vibronic interaction. Symbolically, the wave function corresponding to the electron or hole on molecule 'ℓ' is

$$\Psi_\ell = A \phi_\ell \psi_\ell(2a) \prod_{j \neq \ell} \psi_j(2a) \chi_j \qquad (3.5)$$

where ϕ_ℓ is the lowest unoccupied molecular orbital in the case of an excess electron, highest occupied for an excess hole, χ_j is the ground state vibrational wave function of the j-th molecule, A is the antisymmetrizing operator permuting electrons between the molecule and is of the form (74)

$$A = \{(2a)^{2N}/(4Na)!\}^{\frac{1}{2}} \sum_P (-1)^P P \qquad (3.6)$$

where N is the number of unit cells in the crystal.

3.3 Method of calculation

As has been shown in chapter (2) (equation (2.54), page (29)) the energy dependence upon the wave vector when the effects of intermolecular overlap have been neglected may be written as

$$E'_\pm(k) = \sum_\ell (\pm 1)^L \cos(\underline{k} \cdot \underline{r}_\ell) E_\ell \qquad (3.7)$$

where E_ℓ is given by

$$E_\ell = |\langle \chi_1 | \chi_0 \rangle|^2 \{ \sum_{\alpha, \beta}^N c_\alpha^n c_\beta^n \langle u_\alpha | -Z_\alpha/R_\alpha | u_\beta \rangle$$

$$+ \sum_{\substack{i \text{ core} \\ \text{states}}} \langle u_\alpha | \langle \theta_\alpha^{(i)}(2) | r_{12}^{-1} | \theta_\alpha^{(i)}(2) \rangle | u_\beta \rangle$$

$$+ \frac{\rho_\alpha}{2} \langle u_\alpha | \langle u_\alpha | r_{12}^{-1} | u_\alpha \rangle | u_\beta \rangle \} \qquad (3.8)$$

the symbols have been defined in chapter (2), page (29), and $L = 1$ if $\underline{r}_\ell$ contains $(n + \frac{1}{2})\underline{b}$ or $L = 0$ if $\underline{r}_\ell$ contains $n\,\underline{b}$.

The amount of labour involved in the numerical calculation of the electronic part of the transfer integrals, E_ℓ, can be considerably reduced if the core electrons are considered as point charges at the nucleus on which they are centred. If the number of electrons contributed to the pi-system by the centre α is n_α then equation (3.8) becomes :

$$E_\ell = |\langle\chi_1|\chi_0\rangle|^2 \sum_{\alpha,\beta} \langle u_\alpha|-n_\alpha/R_\alpha|u_\beta\rangle$$

$$+ \frac{P_\alpha}{2} \langle u_\alpha|\langle u_\alpha|r_{12}^{-1}|u_\alpha\rangle|u_\beta\rangle \qquad (3.9)$$

In forthcoming sections this approximation is referred to as the pi-electron approximation.

The matrix elements involving the operator r_{12}^{-1} in equation (38) and equation (3.9) give rise to the so-called hybrid integral. Evaluation of such integrals (discussed in appendix (1), page (232)) is very involved and considerable simplification can be obtained if it is assumed that the charge distribution of the second electron, $|u_\alpha|^2$, can be considered as concentrated at the nucleus α. The problem then reduces to the calculation of two-centre, one electron integrals which, by comparison, are easily evaluated. In this approximation equation (3.9) reduces to

$$E_\ell = |\langle\chi^1|\chi^0\rangle|^2 e^2 \sum_{\alpha,\beta} c_\alpha c_\beta \langle u_\alpha(\underline{r} - \underline{r}_\ell)|\frac{P_\alpha}{2} - n_\alpha|u_\beta(r)\rangle \qquad (3.10)$$

The integrals between the molecule at the origin and the molecules at the corners and side centres of the unit cell have been calculated using equations (3.8), (3.9) and (3.10). This is equivalent to the calculation of the integrals between the molecule at position

numbered (1), figure (3.1), and the molecules in position (2) through (10). Neglecting interactions with other molecules the energy dependence on $\underline{k}$ is

$$
\begin{aligned}
E_{\pm}^{1}(\underline{k}) = \quad & 2E_2 \cos(\underline{k} \cdot \underline{c}) + 2E_3 \cos(\underline{k} \cdot \underline{b}) + \\
& 2E_4(\cos(\underline{k} \cdot (\underline{b} + \underline{c})) + \cos(\underline{k} \cdot (\underline{b} - \underline{c}))) \\
& + 2E_5 \cos(\underline{k} \cdot \underline{a}) + 2E_6 \cos(\underline{k} \cdot (\underline{c} + \underline{a})) \\
& + 2E_7(\cos(\underline{k} \cdot (\underline{a} + \underline{b})) + \cos(\underline{k} \cdot (\underline{a} - \underline{b}))) \\
& + 2E_8(\cos(\underline{k} \cdot (\underline{a} + \underline{b} + c)) + \cos(\underline{k} \cdot (\underline{a} - \underline{b} + c))) \\
& \pm 2E_9(\cos(\underline{k} \cdot \tfrac{1}{2}(\underline{a} + \underline{b})) + \cos(\underline{k} \cdot \tfrac{1}{2}(\underline{a} - b))) \\
& \pm 2E_{10}(\cos(\underline{k} \cdot (\tfrac{1}{2}(\underline{a} + \underline{b}) + \underline{c})) + \cos(\underline{k} \cdot (\tfrac{1}{2}(\underline{a} - \underline{b}) + \underline{c}))) \; .
\end{aligned} \tag{3.11}
$$

The energy bands can be more readily visualized if the special cases when the wave vector, $\underline{k}$, is parallel to a reciprocal lattice vector $\underline{a}^{-1}$, $\underline{b}^{-2}$ or $\underline{c}^{-3}$ are considered. The relationships between energy and wave vector is then

$$
\begin{aligned}
E_{\pm}(\underline{k} \,||\, \underline{a}^{-1}) = \; & 2(E_2 + E_3 + 2E_4) + 2(E_5 + E_6 + 2E_7 + 2E_8) \\
& \cos(\underline{k} \cdot \underline{a}) \pm 4(E_9 + E_{10}) \cos(\underline{k} \cdot \underline{a}/2)
\end{aligned}
$$

$$
\begin{aligned}
E_{\pm}(\underline{k} \,||\, \underline{b}^{-1}) = \; & 2(E_2 + E_5 + E_6) + 2(E_3 + 2E_4 + 2E_7 + 2E_8) \\
& \cos(\underline{k} \cdot \underline{b}) \pm 4(E_9 + E_{10}) \cos(\underline{k} \cdot \underline{b}/2)
\end{aligned}
$$

$$
\begin{aligned}
E_{\pm}(\underline{k} \,||\, \underline{c}^{-1}) = \; & 2(E_3 + E_5 + E_7 \pm 2E_9) \\
& + 2(E_2 + 2E_4 + E_6 + 2E_8 \pm 2E_{10}) \cos(\underline{k} \cdot \underline{c}) \; .
\end{aligned} \tag{3.12}
$$

3.4 Numerical Calculations

The first step in numerical calculation of the transfer integrals is choice of a suitable wave function for the positive or negative ion. Following the example of Le Blanc and Katz the excess electron or hole is assigned to the lowest unoccupied, highest

occupied, molecular orbital of the neutral molecule. The molecular
orbitals of the neutral molecule are approximated by a linear
combination of neutral carbon $2p_z$ wave functions u_i. The
analytical form of the electron and hole wave functions are therefore

$$\phi(\underline{r} - \underline{r}_n) = \sum_i c_i^j u_i \qquad (3.13)$$

where c_i^j are the Hueckel coefficients, calculated without the inclusion
of overlap, for the lowest unoccupied and highest occupied molecular
orbital respectively. The neutral carbon $2p_z$ wave functions, u_i,
are taken to be single Slater $2p_z$ functions characterized by the
screening parameter ζ.

$$u_i = \underline{n}_i \cdot \underline{r} \left(\frac{\zeta_i^5}{\pi} \right)^{\frac{1}{2}} \exp(-\zeta_i r) \qquad (3.14)$$

where $\underline{n}_i$ is the unit vector defining the direction of the $2p$
orbital. The two centre integrals can be simplified by expanding in
the form

$$\langle u_i | F_{op} | u_j \rangle = \frac{-(\underline{n}_i \cdot \underline{R}_{ij})(\underline{n}_j \cdot \underline{R}_{ij})}{\pi R_{ij}^2} \langle P_\sigma | F_{op} | P_\sigma \rangle$$

$$+ \frac{2}{\pi} \left(\underline{n}_i \cdot \underline{n}_j - \frac{(\underline{n}_i \cdot \underline{R}_{ij})(\underline{n}_j \cdot \underline{R}_{ij})}{R_{ij}^2} \right) \langle P_\pi | F_{op} | P_\pi \rangle \qquad (3.15)$$

where $\underline{n}_i$, n_j are unit vectors defining the direction of the orbitals
u_i and u_j, $\underline{R}_{ij}$ is the vector connecting atoms i and j. F_{op}
represents either the nuclear attraction or electron repulsion
operator, p_π and p_σ are Slater $2p_\pi$ and $2p_\sigma$ atomic orbitals
respectively.

The one-electron integrals were evaluated in closed form by
expanding the integrals in prolate spheroidal coordinates. The
resulting integrals can be expressed as a sum of products of functions,

$A_n(\alpha)$, $B_n(\beta)$, (34) which are easily calculated. The two electron

integrals are calculated using the Zeta function expansion method of

Coulson and Barnett, which has been discussed in appendix (I),

page (252). For a given basis set of internuclear distance

R = 4.5 (0.125)16.0 au. the values of the integral for a particular

internuclear distance. R_{ij} are obtained by interpolation using

Aitken's method. It is found that by using a large basis set in R

very high accuracies are obtained for the interpolated integrals and

that the order of polynomial used in the interpolation has little

effect on the accuracy of the result. Since the one electron integrals

are relatively simple to evaluate these are determined for each

individual R_{ij} . It should be noted that, for the two-electron

integrals, once a set of integrals have been calculated for basis

set R and screening parameter ζ further sets of integrals of

basis R' and screening parameter ζ' can be obtained using the relation

$$\frac{I(\alpha_j)}{\zeta} = \frac{I'(\alpha_j)}{\zeta'}$$

$$\alpha_j = \zeta R_j = \zeta' R_j'$$

(3.16)

where the elements of the new basis set R' is given by

$$R_j' = \frac{R_j \zeta}{\zeta'}$$

(3.17)

where R_j' and R_j are the j-th elements of the basis sets R'

and R respectively.
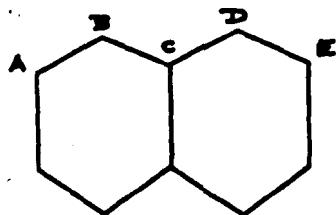
fig (3.2).

Naphthalene showing the numbering of the atoms
in the molecule.

	x	y	z
A	0.716	0.092	2.816
B	0.934	0.960	1.892
C	0.390	0.611	0.297
D	0.614	1.483	-0.685
E	0.083	1.121	-2.195

a	b	c	beta
8.235	6.003	8.658	122 55

Table(3.1)

Atomic co-ordinates* and unit cell constants* of naphthalene.

* units: 1_b-1 nm.

3.5 Numerical results and band structure

The crystal data for naphthalene was taken from Abrahams et al (90) and is listed in table (3.1). The transfer and overlap integrals, calculated between the molecules at position 1, the corner of the unit cell, and the remaining molecules within the unit cell, for various values of the screening parameter, ζ , are given in tables (3.2) and (3.3) respectively. As was expected a decrease in screening parameter, ζ , results in an increase in magnitude of the transfer integral due to the slower rate at which the Slater functions fall off with intermolecular distance. In table (3.2) the vibration overlap integral is taken as unity. The plots of the excess electron and hole band structure, for screening parameter 24.57 nm^{-1}, along the reciprocal crystal axes are given in figures (3.3) and (3.4). The shapes of the energy bands for any other cases are not shown as variation of the screening parameter, in general, alters only the band widths, the shape of the band remaining unaltered. If needed these can be calculated using the results of table (3.2) and equation (3.12). The electron repulsion, nuclear attraction and transfer integrals calculated in the pi-electron and localised core approximations (equation (3.9) and equation (3.10) respectively) are given in table (3.4). It can be seen that these approximations are quite good when the centres of the interacting molecules are separated by large distances, unfortunately, these interactions contribute little to the band structure. There is an overall error of about 25% for the pi-electron approximation and over 30% for the localised core approximation which although large are to be expected since in the pi-electron approximation a large proportion of the neutral potential is neglected while the localised core approximation amounts to a complete neglect of the coulomb part, J_n^i , of the molecular potential.

Screening parameter

Position	20.8	22.7	24.6	26.5	28.3	30.7
0,0,1	13.71	1.68	-3.74	-5.19	-3.06	-4.49
0,1,0	64.32	58.63	45.07	32.80	23.52	14.41
0,1,1	0.58	0.26	0.09	0.33	0.02	0.00
1,0,0	-0.16	-0.01	0.02	0.11	0.00	0.00
1,0,1	8.70	5.99	3.23	1.42	0.81	0.32
1,1,0	-0.41	-0.18	-0.07	-0.24	-0.01	0.00
1,1,1	-0.12	0.00	-0.03	-0.13	-0.01	0.00
$\frac{1}{2},\frac{1}{2},0$	-276.94	-218.35	-168.35	-120.34	-65.41	-45.48
$\frac{1}{2},\frac{1}{2},1$	44.42	26.08	15.62	7.69	3.56	5.21

(a)

Screening parameter

Position	20.8	22.7	24.6	26.5	28.3	30.7
0,0,1	7.94	1.39	-0.66	-0.23	0.06	1.28
0,1,0	-408.59	-302.26	-210.64	-142.35	-91.61	-51.84
0,1,1	3.53	1.42	0.53	0.19	0.07	0.00
1,0,0	2.30	1.02	0.45	0.19	0.08	0.02
1,0,1	71.66	28.21	14.24	6.87	3.22	1.20
1,1,0	2.26	0.99	0.33	0.12	0.04	0.00
1,1,1	0.21	0.00	0.05	-0.02	0.01	0.00
$\frac{1}{2},\frac{1}{2},0$	257.89	155.69	76.07	47.03	35.04	6.33
$\frac{1}{2},\frac{1}{2},1$	-217.55	-142.28	-90.47	-58.85	-34.55	-20.81

(b)

Table(3.2)

Variation of transfer integrals* with screening parameter for
excess electrons(a) and holes(b) in crystalline naphthalene.
*units: 10^{-4} eV.

/

Screening parameter

Position	20.8	22.7	24.6	26.5	28.3	30.7
0,0,1	-6.08	-2.2	-0.30	0.45	0.63	0.54
0,1,0	-6.42	-7.01	-6.34	-5.17	-3.92	-2.58
0,1,1	-0.20	-0.09	-0.04	-0.01	0.00	0.00
1,0,0	0.10	0.02	0.00	0.00	0.00	0.00
1,0,1	-2.59	-1.56	-0.85	-0.46	-0.23	-0.09
1,1,0	-0.14	0.06	0.02	0.01	0.00	0.00
1,1,1	0.03	0.00	0.01	0.00	0.00	0.00
$\frac{1}{2},\frac{1}{2},0$	32.64	28.95	23.55	17.99	13.08	8.33
$\frac{1}{2},\frac{1}{2},1$	-9.59	-6.00	-3.56	-2.02	-1.09	-0.48

(a)

Screening parameter

Position	20.8	22.7	24.6	26.5	28.3	30.7
0,0,1	-3.13	-1.14	-0.33	-0.04	0.04	0.05
0,1,0	59.18	49.67	37.52	26.49	17.83	10.34
0,1,1	-1.29	-1.42	-0.20	-0.08	0.00	0.00
1,0,0	-0.72	-1.53	-0.15	-0.06	-0.03	0.00
1,0,1	-14.25	-7.89	-4.12	-2.04	-0.98	-0.37
1,1,0	-0.84	-0.34	-0.33	-0.05	-0.02	0.00
1,1,1	-0.05	0.00	-0.02	0.00	0.00	0.00
$\frac{1}{2},\frac{1}{2},0$	-55.96	-35.63	-21.32	-12.06	-6.44	-2.68
$\frac{1}{2},\frac{1}{2},1$	41.04	27.92	18.26	11.59	7.18	3.86

(b)

Table(3.3)

Variation of Overlap integrals* with screening parameter for excess electrons(a) and holes(b) in crystalline naphthalene.

*units: $1\text{\tiny$\mathbf{M}$}-4$.
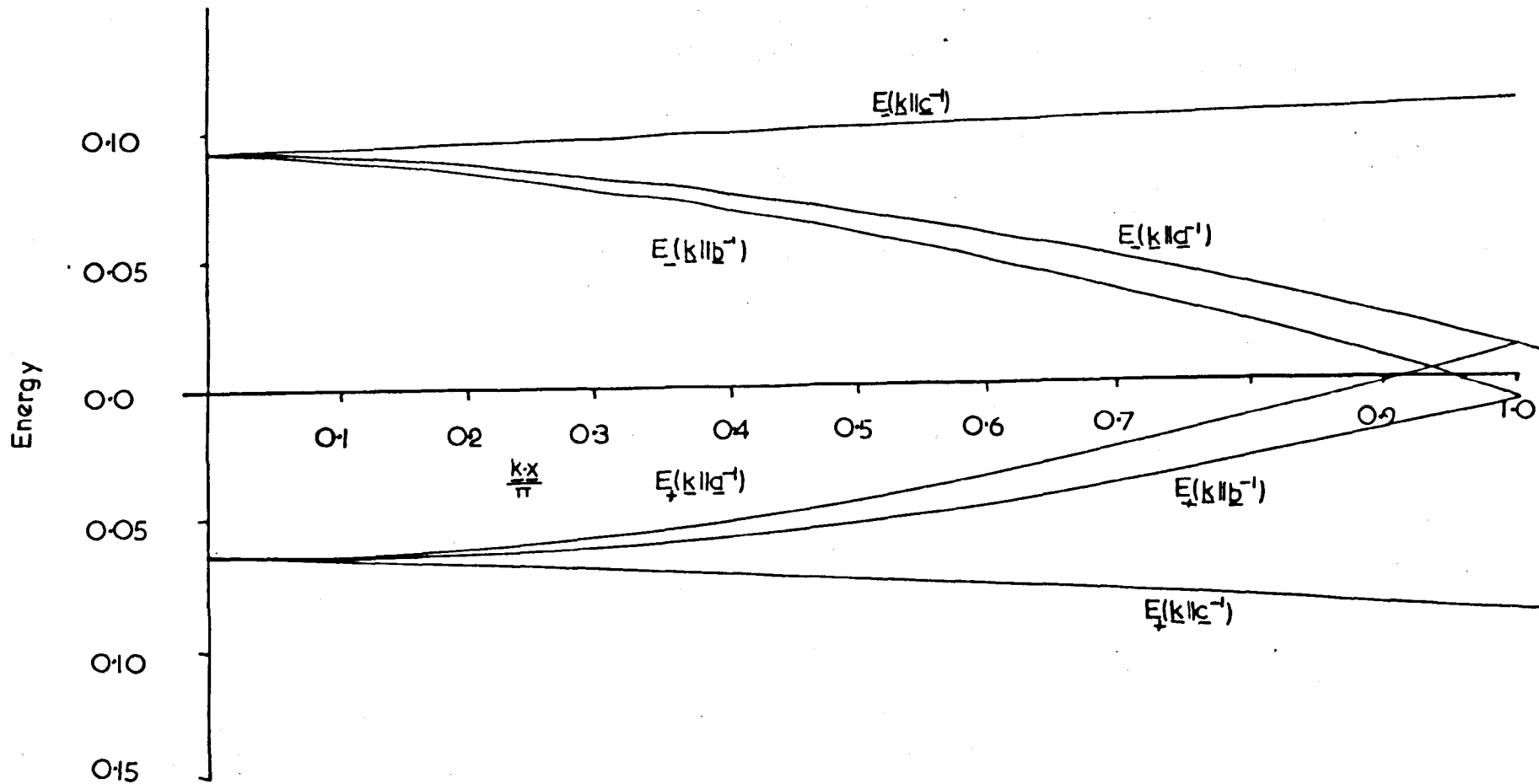
Figure (3.3)

Energy band structure of excess electrons in naphthalene.
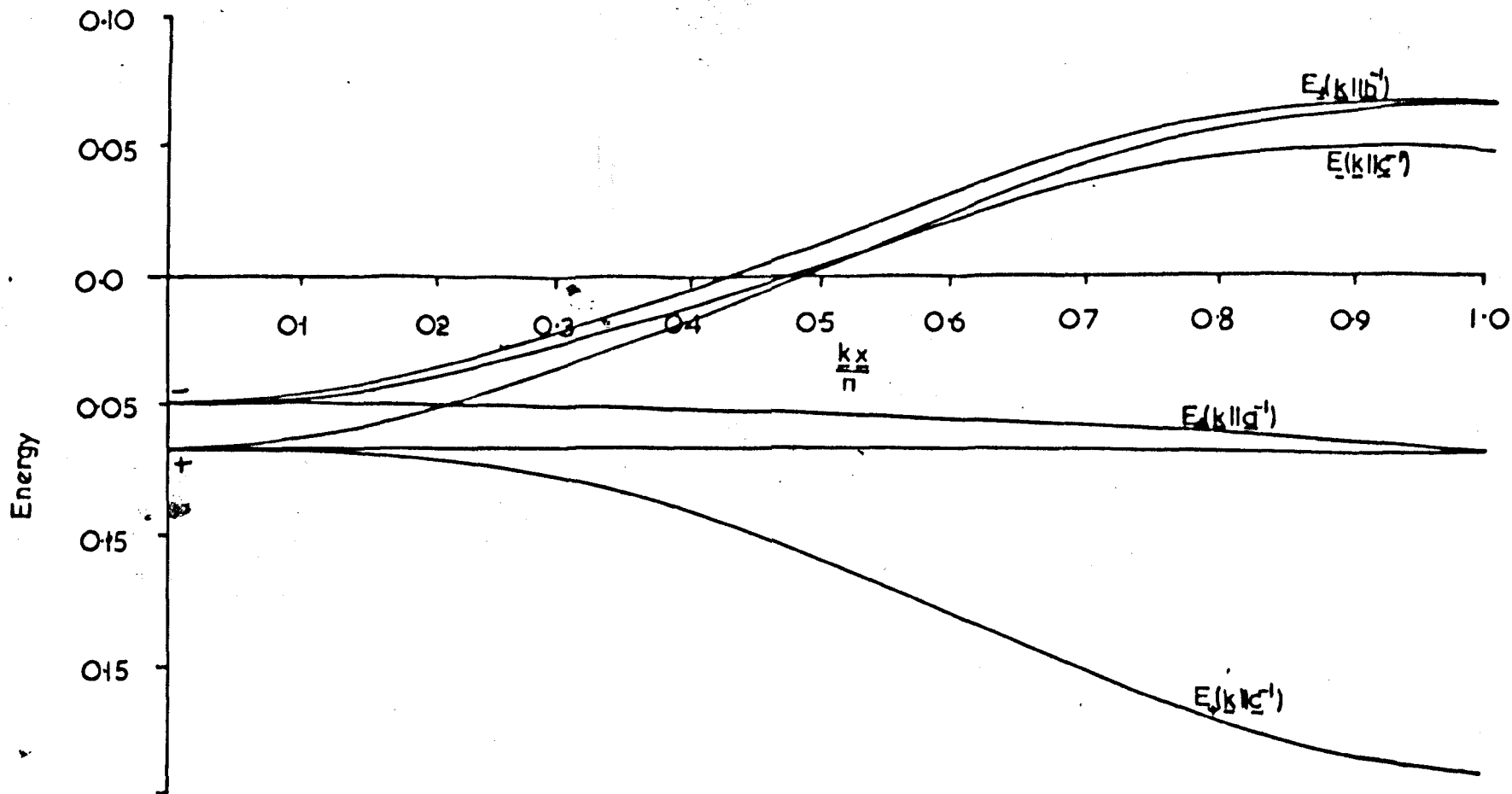
Figure (3.4)

Energy band structure of excess holes in crystalline naphthalene.

Position	Nuclear Attraction	Electron Repulsion	Transfer integral			Error	
			I	II	III	I	II
0,0,1	-0.62	-0.69	-0.07	-0.31	-0.66	-	-
0,1,0	63.76	26.92	36.84	31.88	45.07	18.26	29.27
0,1,1	0.18	0.09	0.10	0.09	0.09	-	-
1,0,0	0.02	0.01	0.01	0.01	0.02	-	-
1,0,1	5.47	2.54	2.93	2.73	3.23	-	-
1,1,0	-0.13	-0.06	-0.07	-0.06	-0.07	-	-
1,1,1	-0.06	-0.03	-0.03	-0.03	-0.03	-	-
$\frac{1}{2},\frac{1}{2},0$	-220.66	-98.23	-122.38	-110.33	-168.35	27.31	34.46
$\frac{1}{2},\frac{1}{2},1$	23.79	11.53	12.26	11.90	15.62	21.51	33.84

(a)

Table(3.4)

Comparison of methods for the calculation of transfer integrals*.

Figures refer to excess electrons in crystalline naphthalene.

I   Calculated using eqn(3.14)

II Calculated using eqn(3.15)

III Calculated using eqn(3.13)

*units: $1_{\text{}} -4$ eV.

Position	Nuclear Attraction	Electron Repulsion	Transfer integral			Error	
			I	II	III	I	II
0,0,1	-0.62	-0.69	-0.07	-0.31	-0.66	-	-
0,1,0	-318.46	-138.33	-180.13	-159.23	-210.64	14.48	24.40
0,1,1	0.97	0.46	0.51	0.49	0.53	-	-
1,0,0	0.80	0.38	0.42	0.40	0.45	-	-
1,0,1	24.45	11.40	13.05	12.23	14.24	8.39	14.15
1,1,0	0.61	0.28	0.32	0.30	0.33	-	-
1,1,1	0.10	0.04	0.05	0.05	0.05	-	-
$\frac{1}{2},\frac{1}{2},0$	140.72	66.06	74.66	70.36	76.07	1.85	7.51
$\frac{1}{2},\frac{1}{2},1$	-138.87	-63.13	-75.74	-69.43	-90.47	16.28	23.26

(b)

Table(3.4)

Comparison of methods for the calculation of transfer integrals*.

Figures refer to excess holes in crystalline naphthalene.

I   Calculated using eqn(3.14)

II   Calculated using eqn(3.15)

III Calculated using eqn(3.13)

*units: $1_{10}-4$ eV.

The electron and hole band structures are similar to those given by Katz et al showing the major splitting in the $\underline{c}^{-1}$ direction with much smaller splittings in the $\underline{a}^{-1}$ and $\underline{b}^{-1}$ directions. The degeneracy of the two components of the electron and hole bands at $\underline{k} = \pi \underline{a}^{-1}$ and $\underline{k} = \pi \underline{b}^{-1}$ arises as a consequence of the existence of a two fold screw axis in the $\underline{b}$ direction and a glide plane in the $\underline{a}$ direction in the Naphthalene crystal. The group of the wave vector $\underline{k}$ at these points has only a two dimensional representation resulting in E_+ and E_- being degenerate. The degeneracy and subsequent invertion of the two energy bands along the $\underline{c}^{-1}$ axis observed by Katz et al has no origins in the symmetry of the crystal and arises simply as a consequence of the magnitudes and signs of the transfer integrals. Such behaviour is only observed by us for the case where the screening parameter is 1.4. The energy band widths along the $\underline{a}^{-1}$, $\underline{b}^{-1}$ and $\underline{c}^{-1}$ directions and splitting in the $\underline{c}^{-1}$ directions, for an excess electron and hole, for various values of screening parameter, ζ, and vibrational overlap factor unity, together with the energy band widths calculated using the transfer integrals obtained using an SCF wave function and including exchange are given in table (3.5).

3.6 The mobility tensor

3.6(i) Variation of the calculated mobility ratios with screening parameter and vibrational overlap factor

In order to calculate the elements of the mobility tensor it is usually assumed that the scattering of carriers can be described in terms of a relaxation time function $\tau(\underline{k})$ (91). The mobility of the carriers along an axis i is then related to the velocity of the carriers along the axis through:

$$\mu_{ii} = \frac{e}{k_0 T} \langle\langle v_i(\underline{k})\, v_i(\underline{k})\, \tau(\underline{k}) \rangle\rangle \qquad (3.18)$$

Screening parameter

	20.8	22.7	24.6	26.5	28.3	30.7	SCF
$E(\underline{k}\parallel\underline{a}^{-J})$ +	4.50	7.47	5.99	4.47	2.44	1.60	7.15
−	4.80	7.92	6.23	4.54	2.50	1.62	8.12
$E(\underline{k}\parallel\underline{b}^{-J})$ +	3.36	5.34	4.31	3.20	1.53	1.03	4.49
−	5.94	10.04	7.91	5.82	3.41	2.19	10.78
$E(\underline{k}\parallel\underline{c}^{-J})$ +	2.24	2.41	1.23	0.48	0.20	0.25	1.13
−	1.31	1.76	1.27	0.75	0.37	0.58	0.94
$\underline{c}$ splitting	12.85	19.55	14.72	10.24	5.52	4.06	13.20

(a)

Screening parameter

	20.8	22.7	24.6	26.5	28.3	30.7	SCF
$E(\underline{k}\parallel\underline{a}^{-J})$ +	4.77	1.78	0.04	0.18	0.16	0.53	2.62
−	1.54	0.71	1.19	0.76	0.12	0.63	1.62
$E(\underline{k}\parallel\underline{b}^{-J})$ +	14.25	11.36	8.93	6.14	3.63	2.65	16.96
−	17.48	12.43	7.78	5.20	3.67	1.49	17.96
$E(\underline{k}\parallel\underline{c}^{-J})$ +	13.92	10.08	6.65	4.43	2.63	1.57	11.32
−	20.98	12.68	7.83	4.99	2.90	1.76	13.64
$\underline{c}$ splitting	38.03	23.84	13.22	8.47	5.57	2.17	25.96

(b)

Table(3.5)

Variation of the calculated energy bandwidths*

and band-splitting in crystalline naphthalene

with screening parameter, ζ.

* units: 1×-2 eV.

where $v_i(\underline{k})$ is the i-th component of the velocity vector $\underline{v}(\underline{k})$, k_0 the Boltzmann constant, e the charge on the electron and the double angular brackets indicate an average over the Boltzmann distribution of electrons within the energy band. The functional forms of $\tau(\underline{k})$ are generally considered (40) each involving an isotropic scattering parameter :

(1) $\tau(\underline{k})$ $= \tau_0$,   constant free time

(2) $\tau(\underline{k})|\underline{v}(\underline{k})|$ $= \lambda$,   constant free path

where $\underline{v}(\underline{k})$ is the velocity associated with the wave function $\Psi(\underline{k})$ and is given by :

$$\underline{v}(\underline{k}) = \frac{1}{h} \nabla_{\underline{k}} E(\underline{k}) \tag{3.19}$$

The components of the mobility tensor in the mean free time and mean free path approximations are given by :

$$\mu_{ij} = \frac{e\tau_0}{k_0 T} <<v_i(\underline{k})v_j(\underline{k})>>$$

$$\tag{3.20}$$

and $$\mu_{ij} = \frac{e\lambda}{k_0 T} <<v_i(\underline{k})v_j(\underline{k})/|\underline{v}(\underline{k})|>> .$$

For molecules crystallizing in the structure $P2_1/a$ containing two molecules per unit cell the functions in angular brackets are given by :

$$<<v_i(\underline{k})v_j(\underline{k})>> = \frac{\int \{ \frac{\partial^2 E_+(\underline{k})}{\partial k_i \partial k_j} f_+^B(\underline{k}) + \frac{\partial^2 E_-(\underline{k})}{\partial k_i \partial k_j} f_-^B \} d\underline{k}}{h^2 \int \{f_+^B(\underline{k}) + f_-^B(k)\} d\underline{k}}$$

and $$\tag{3.21}$$

$$<<v_i(\underline{k})v_j(\underline{k})/\underline{v}(\underline{k})>> = \frac{\int \{ \frac{\partial^2 E_+(\underline{k})}{\partial k_i \partial k_j} f_+^B(\underline{k}) + \frac{\partial^2 E_-(\underline{k})}{\partial k_i \partial k_j} f_-^B \} d\underline{k}}{h \int \{|\frac{\partial E_+(\underline{k})}{\partial k}| f_+^B(\underline{k}) + |\frac{\partial E_-(\underline{k})}{\partial k}| f_-^B\} d\underline{k}}$$

where $f_{\pm}^{B}(\underline{k})$ are the Boltzmann distribution functions of the positive and negative branches of the energy band. It should be noted that, since the creation of an excess hole requires the movement of an electron from its position in the valence band to the conduction band, the energy of excess holes is measured downwards from the top of the valence band.

The mobility tensor calculated using equation (3.18) through equation (3.21) and the energy equation (3.11) gives the elements of the mobility tensor in a coordinate system whose axes are parallel to the unit cell vectors $\underline{a}$, $\underline{b}$ and $\underline{c}$. To facilitate comparison with experiment the elements of the mobility tensor are transformed to the orthogonal coordinate system of $\underline{a}$ and $\underline{b}$ unit cell vectors and the vector $\underline{c}'$ ($\underline{a} \times \underline{b}$). If the coordinates of a point X in the crystallographic coordinate system, denoted by the vector $\underline{x}$, are transformed to the coordinate Y in the orthogonal system, where $\underline{x}$ and $\underline{y}$ are related through

$$\underline{Y} = \underline{\alpha} \cdot \underline{x} \tag{3.22}$$

$\underline{\alpha}$ being a 3×3 matrix,
then the elements of the mobility tensor in the orthogonal coordinate system, $\underline{\mu}'$, are related to those in the crystallographic system, $\underline{\mu}'$, by

$$\mu_{ij}' = \sum_{i'j'} \alpha_{i'i} \, \alpha_{j'j} \, \mu_{i'j'} \tag{3.23}$$

To calculate the mobility tensors from equation (3.18) an assumption must be made as to the value of the mean free path and mean free time parameters. Accurate calculation of these by present methods is out of the question but one can obtain an order of magnitude value from the uncertainty principle. As discussed in Chapter (2), section (3), page (34) for energy band theory to be physically meaningful the mean-

free time, τ_0 , must be greater than h/band width since the
uncertainty in the energy, h/τ_0 , must be less than the band width.
Similarly the mean free path, λ , must be greater than the lattice
spacing. Thus the equations for the mobility become

$$\mu_{ii} > h \, e <v_i(\underline{k})v_i(\underline{k})>/B_i k_0 T \qquad (3.24)$$

and

$$\mu_{ii} > e \, X_i <v_i(\underline{k})v_i(\underline{k})/|\underline{v}(\underline{k})|>/k_0 T \qquad (3.25)$$

where B_i and X_i are the band widths and lattice distances in
direction i . Alternatively the values of τ_0 and λ can be
calculated to give the observed mobility along a particular axis and
using this value the mobility along the remaining two axes estimated.

The elements of the mobility tensor, without the constant
premultiplicative factors $\dfrac{e \, \tau_0}{k_0 T}$ and $\dfrac{e \, \lambda}{k_0 T}$, along the $\underline{b}$ axis together
with the ratios of the components of the mobility tensor along the
orthogonal axes $\underline{a}$, $\underline{b}$ and $\underline{c}'$ for several values of the screening
parameter, ζ , are given in table (3.6). A 1% change in screening
parameter produces a 40% change in the elements of the mobility
tensor, however, with the exception of $\mu_{c'c'}/\mu_{bb}$ for electrons, the
mobility ratios remain approximately constant, decreasing approximately
1 % per percentage increase in screening parameter, ζ .

The variation of the mobility ratios with vibrational overlap
factor, $|<\chi_1|\chi_0>|^2$, for screening parameter, $\zeta = 22.68^{nm^{-1}}$ is
shown in table (3.7) and are compared with values calculated using the
SCF integrals of Glaeser and Berry (44). It can be seen that the
agreement for the mobility ratios, calculated using the two wave
functions, is very good, although the ratio μ_{aa}/μ_{bb} for excess holes
shows a larger variation with vibrational overlap for the SCF case as a
result of the larger band width in the $\underline{a}$ direction (see table (3.5),
section (5), page (58)). The remaining mobility ratios show only

Screening parameter /100

	0.208	0.227	0.246	0.265	0.283	0.307
$\langle vbvb\rangle$*	6.565	4.239	4.347	1.334	0.462	0.169
$\langle vbvb/\underline{v}(\underline{k})\rangle$**	1.153	0.957	0.759	0.558	0.330	0.185
$\dfrac{\mu_{aa}}{\mu_{bb}}$	1.790 (1.526)	1.721 (1.504)	1.704 (1.508)	1.679 (1.514)	1.459 (1.393)	1.794 (1.632)
$\dfrac{\mu_{cc}}{\mu_{bb}}$	0.181 (0.175)	0.086 (0.093)	0.050 (0.055)	0.027 (0.029)	0.020 (0.023)	0.088 (0.087)
$\dfrac{\mu_{cc}}{\mu_{aa}}$	0.101 (0.114)	0.050 (0.062)	0.029 (0.036)	0.016 (0.019)	0.014 (0.017)	0.049 (0.053)

(a)

Screening parameter /100

	0.208	0.227	0.246	0.265	0.283	0.307
$\langle vbvb\rangle$*	33.366	18.176	8.616	3.934	1.645	0.503
$\langle vbvb/\underline{v}(\underline{k})\rangle$**	2.336	1.909	1.406	0.972	0.614	0.372
$\dfrac{\mu_{aa}}{\mu_{bb}}$	0.274 (0.318)	0.192 (0.224)	0.102 (0.121)	0.087 (0.105)	0.117 (0.139)	0.013 (0.017)
$\dfrac{\mu_{cc}}{\mu_{bb}}$	0.619 (0.592)	0.508 (0.482)	0.452 (0.418)	0.428 (0.396)	0.359 (0.347)	0.379 (0.326)
$\dfrac{\mu_{cc}}{\mu_{aa}}$	2.259 (1.862)	2.646 (2.152)	4.430 (3.443)	4.894 (3.757)	3.085 (2.496)	29.150 (19.176)

(b)

Table(3.6)

Variation of the mobility ratios, μ_{ii}/μ_{jj}, of excess electrons(a) and holes(b) in crystalline naphthalene, calculated in the mean free time and mean free path (in parentheses) approximations, with screening parameter. Vibrational overlap factor 0.1.

* units: 1×6 m^2/sec^2.

**units: 1×3 m/sec.

Vibrational

Overlap		0.1	0.2	0.5	1.0	Expt.
$\dfrac{\mu_{aa}}{\mu_{bb}}$	I	1.583	1.600	1.657	1.632	1.00
		(1.413)	(1.491)	(1.773)	(2.331)	
	II	1.481	1.496	1.541	1.499	
		(1.386)	(1.463)	(1.724)	(2.176)	
$\dfrac{\mu_{cc}}{\mu_{bb}}$	I	0.090	0.089	0.087	0.078	0.57
		(0.054)	(0.059)	(0.080)	(0.128)	
	II	0.089	0.088	0.087	0.078	
		(0.070)	(0.079)	(0.110)	(0.176)	

(a)

Vibrational

Overlap		0.1	0.2	0.5	1.0	Expt.
$\dfrac{\mu_{aa}}{\mu_{bb}}$	I	0.102	0.097	0.085	0.073	0.64
		(0.124)	(0.112)	(0.090)	(0.079)	
	II	0.121	0.114	0.097	0.083	
		(0.144)	(0.128)	(0.100)	(0.086)	
$\dfrac{\mu_{cc}}{\mu_{bb}}$	I	0.452	0.429	0.373	0.315	0.29
		(0.339)	(0.306)	(0.240)	(0.194)	
	II	0.418	0.393	0.336	0.284	
		(0.324)	(0.288)	(0.234)	(0.188)	

(b)

Table(3.7)

Variation of the mobility ratios,calculated in the mean free time and mean free path(in parentheses) approximations, with vibrational overlap factor.

I - calculated using single Slater function with $\zeta = 22.7$ nm^{-1}.

II- calculated using the transfer integrals of Glaeser and Berry(44).

slight variation with vibrational overlap, the ratios for excess electrons showing a slight increase, the ratios for excess holes showing a slight decrease. Similar results are obtained using different values of the screening parameter, ζ. Thus it can be concluded that the anisotropy of the mobility tensor can be determined without accurate specific knowledge of either the screening parameter or the vibration overlap factor. However, accurate determination of the energy band widths necessitates a detailed knowledge of both the aforementioned factors.

3.6(ii)   Optimum value of the screening parameter, ζ.

It is widely accepted (40) that the use of SCF wave functions as a basis for constructing molecular orbitals leads to a more accurate description of the wave function at large distances from the origin. The problem is, therefore, to determine the best value of ζ to reproduce the SCF wave function at large r. To this end it is required to derive a suitable function involving the difference between an SCF and a single Slater function which when minimized, by variation of ζ, over the required range of r will yield the appropriate value of ζ.

If the SCF and Slater functions are denoted $\psi(SCF, R)$ and $\psi(\zeta, r)$ respectively, then minimization of the function :

$$f_1(\zeta) \; = \; \int_0^\infty (\psi(SCF, r) - \psi(\zeta, r))^2 \, dr \qquad (3.26)$$

should yield the normal (30.7 nm^{-1}) value of the screening parameter, ζ, as the largest contributions to $f_1(\zeta)$ will come from those regions of r which contribute most to the energy in the normal variation method: i.e. the function $\psi(\zeta, r)$ will be most accurate for small r.

Minimization of $f_1(\zeta)$ using a Simplex technique (188) verified the above arguments. At the other extreme calculation of the function

$$f_2(\zeta) = \int_0^x (\psi(SCF, r) - \psi(\zeta, r))/\psi(SCF, r))^2 \, dr$$

showed the contributions to $f_2(\zeta)$ to be approximately constant for all values of r. Hence by incorporating the weighting function $g(r) = 1/\psi(SCF, r)$ equal weights can be added to all parts of the curve, i.e. the tail of the wave function will contribute just as much to $f_2(\zeta)$ in the minimization procedure as will parts of the wave function for smaller r. Unfortunately one is now left with the problem of where to terminate the integration over r.

The above functions $f_1(\zeta)$ and $f_2(\zeta)$ are really the two extremes of the problem one placing equal weights on all parts of the curve the other strongly weighting the curve for small values of r. In the calculation of transfer integrals a weighting function, similar to $g(r)$, is required which has maximum weight at those values of r which contribute most to the transfer integral. Such a weighting can be applied by minimizing the function

$$f_3(\zeta) = \int_0^\infty g'(r)(\psi(SCF, r) - \psi(\zeta, r)^2 \, dr \qquad (3.27)$$

where $\quad g'(r) = \phi_A(1) <\phi_A(2) |r_{12}^{-1}| \phi_A(2)> \phi_B(1)$

is essentially the radial profile of the hybrid integral, numerical values of which can be obtained by inserting the appropriate "write" statements in the program given in appendix (1). As the wave functions ϕ_A and ϕ_B are centred on different nuclei the function $g'(r)$ will be a function of the intermolecular distance, R, and also the screening parameters of the wave functions, ϕ_i. Strictly speaking the function $g'(r)$ should be evaluated for every value of ζ required

in the minimization of $f_3(\zeta)$, however, this is prohibitive in terms of computer time, therefore, $f_3(\zeta)$ was minimized, for several values of the internuclear distance R between 0.3 nm. and 0.6 nm., with $g'(r)$ calculated assuming all the ϕ's to be $2p_z$ atomic orbitals characterized by a screening parameter $\zeta = 30.7$ nm^{-1}. The values of ζ obtained in this way were in the region 22.7 to 24.6 nm^{-1}; of a similar order of magnitude to those obtained by McClelland (86). Thus use of a screening parameter in this range rather than the normal value of $\zeta = 30.7$ nm^{-1} should lead to more accurate values of the energy band widths. Comparison of the elements of the mobility tensor (table (3.6), page (62)) and calculated band widths (table (3.5), page (58)) with their SCF counterparts reflect the above conclusion.

3.6(iii) Effects of small rotation of the molecules on the calculated mobilities.

Accurate X-ray crystallographic studies on organic molecular crystals have shown (98) that the molecules in a crystal are able, under normal conditions, to rotate about their equilibrium positions through angles up to approximately 4°. The effects of such rotations on the calculated principle transfer integrals and mobility ratios are shown in table (3.8) and table (3.9) respectively. The molecules have been rotated through $\pm 1^\circ, \pm 2^\circ$ and $\pm 4^\circ$ about the a, b and c axes. The magnitude of the changes induced are quite large, the interaction most affected being that between the molecule at the origin and the molecule at position ($\frac{1}{2}$, $\frac{1}{2}$, 0) where a rotation of $\pm 2^\circ$ about a produces a 50% change in the transfer integral. For all rotations the clockwise and anticlockwise motions compensate each other and the net result is the equilibrium value. However, the calculations infer that in the region of dislocations, where angles much larger than used here are to be expected, the mobility pattern could be drastically

Position	Rc(-1°)	Rb(-1°)	Ra(-1°)	Equilib.	Ra(+1°)	Rb(+1°)	Rc(+1°)
(0,1,0)	-206.94 (44.77)	-213.09 (45.73)	-194.92 (31.91)	-210.64 (45.07)	-227.17 (58.70)	-207.80 (44.34)	-213.82 (45.24)
($\frac{1}{2}$,$\frac{1}{2}$,0)	-87.70 (166.64)	-71.78 (153.73)	-103.95 (170.19)	-76.13 (168.35)	-47.78 (165.62)	-78.61 (182.19)	-66.55 (167.95)
($\frac{1}{2}$,$\frac{1}{2}$,1)	88.71 (-15.30)	91.81 (-13.11)	86.03 (-15.59)	90.47 (-15.61)	94.67 (-14.86)	88.74 (-18.04)	92.11 (-15.90)

Position	Rc(-2°)	Rb(-2°)	Ra(-2°)	Equilib.	Ra(+2°)	Rb(+2°)	Rc(+2°)
(0,1,0)	-202.76 (44.32)	-215.12 (46.28)	-180.31 (19.74)	-210.64 (45.07)	-245.42 (73.22)	-204.61 (43.52)	-216.50 (45.26)
($\frac{1}{2}$,$\frac{1}{2}$,0)	-100.96 (162.24)	-68.83 (134.41)	-130.14 (171.10)	-76.13 (168.35)	-20.46 (161.43)	-78.62 (197.98)	-58.36 (166.02)
($\frac{1}{2}$,$\frac{1}{2}$,1)	93.68 (-14.93)	86.54 (-10.62)	81.51 (-12.76)	90.47 (-15.61)	98.56 (-15.55)	92.78 (-20.38)	86.54 (-16.21)

Position	Rc(-4°)	Rb(-4°)	Ra(-4°)	Equilib.	Ra(+4°)	Rb(+4°)	Rc(+4°)
(0,1,0)	-220.67 (44.38)	-197.73 (41.74)	-280.45 (99.75)	-210.64 (45.07)	-153.23 (8.38)	-218.81 (47.28)	-193.24 (43.13)
($\frac{1}{2}$,$\frac{1}{2}$,0)	-44.44 (160.59)	-86.94 (229.83)	29.45 (229.83)	-76.13 (168.35)	-180.94 (171.97)	-69.54 (97.82)	-128.23 (151.55)
($\frac{1}{2}$,$\frac{1}{2}$,1)	96.55 (-16.76)	81.22 (-26.37)	107.33 (-7.02)	90.47 (-15.61)	73.06 (-15.59)	92.68 (-4.17)	82.73 (-14.08)

Table(3.8)

Fluctuations in the major resonance integrals* of excess electrons and holes (in parentheses) in crystalline naphthalene on rotation of the molecules through a small angle ±a about one of the crystallographic axes.

*units: 1$_\text{m}$-4 eV.

	$R_z(-1°)$	$R_y(-1°)$	$R_x(-1°)$	Equil.	$R_x(1°)$	$R_y(1°)$	$R_z(1°)$	Exp.
$\langle vbvb\rangle$	266.09	232.58	259.69	271.38	287.11	311.26	270.58	
	(841.23)	(867.68)	(782.91)	(853.79)	(951.36)	(834.65)	(867.37)	
$\dfrac{u_{aa}}{u_{bb}}$	1.65	1.61	1.76	1.65	1.51	1.69	1.65	1.0
	(0.29)	(0.25)	(0.36)	(0.26)	(0.19)	(0.26)	(0.23)	0.64
$\dfrac{u_{c'c'}}{u_{bb}}$	0.04	0.04	0.04	0.04	0.04	0.05	0.04	0.57
	(0.44)	(0.46)	(0.44)	(0.45)	(0.44)	(0.44)	(0.46)	0.29

	$R_z(-2°)$	$R_y(-2°)$	$R_x(-2°)$	Equil.	$R_x(2°)$	$R_y(2°)$	$R_z(2°)$	Exp.
$\langle vbvb\rangle$	253.24	186.70	251.19	271.38	307.76	360.73	265.35	
	(841.68)	(870.91)	(736.45)	(853.79)	(1086.00)	(818.90)	(869.70)	
$\dfrac{u_{aa}}{u_{bb}}$	1.64	1.53	1.84	1.65	1.34	1.72	1.64	1.0
	(0.35)	(0.22)	(0.50)	(0.26)	(0.15)	(0.28)	(0.20)	0.64
$\dfrac{u_{c'c'}}{u_{bb}}$	0.04	0.03	0.03	0.04	0.04	0.05	0.05	0.57
	(0.49)	(0.40)	(0.42)	(0.45)	(0.42)	(0.49)	(0.40)	0.29

	$R_z(-4°)$	$R_y(-4°)$	$R_x(-4°)$	Equil.	$R_x(4°)$	$R_y(4°)$	$R_z(4°)$	Exp.
$\langle vbvb\rangle$	249.38	473.81	353.27	271.38	249.00	116.86	223.21	
	(903.39)	(767.60)	(1410.53)	(853.79)	(706.78)	(907.46)	(814.33)	
$\dfrac{u_{aa}}{u_{bb}}$	1.64	1.77	1.00	1.65	1.88	1.29	1.63	1.0
	(0.19)	(0.29)	(0.14)	(0.26)	(0.84)	(0.23)	(0.44)	0.64
$\dfrac{u_{c'c'}}{u_{bb}}$	0.05	0.07	0.01	0.04	0.05	0.01	0.04	0.57
	(0.48)	(0.40)	(0.38)	(0.45)	(0.35)	(0.44)	(0.39)	0.29

Table(3.9)

Effects of small rotations on the mean square velocities and mobility ratios of excess electrons and holes(in parenthesis) in naphthalene.

*units: 10^6 m^2/sec^2.

changed. In addition the presence in the lattice of impurity molecules is expected to cause slight reallignment of molecules in the near vicinity so modifying the interactions between host molecules. Finally, the magnitude of the change induced shows very clearly that the formulation of crystal structures, for compounds of which the exact crystal structure is unknown, from the crystal structures of similar compounds can lead to erroneous results when used in band structure calculations.

3.6(iv)   The validity of the Energy band model.

In Chapter (2), section (3), page (33), several criteria were outlined which must be obeyed for the energy band model to be applicable to the conduction process in a particular molecular crystal. These can be summarised briefly as :

(1)   Band width > k θ (equation (2.76)), where θ is the Debye temperature.

(2)   Band width > h/τ_0 (equation (2.61)) - the uncertainty principle.

(3) λ >   lattice spacing.

Assuming the Debye temperature for naphthalene to be similar to that of anthracene (92) then criterion (1) states that the band width must be greater than 0.007 eV . The remaining two criterion can be rearranged as in equation (2.29) and equation (2.30) such that the minimum values of the calculated mobilities serve as the criterion. Numerical values for these quantities are shown in table (3.10).

For the remaining screening parameters, with the exception of ζ = 20.7 nm^{-1}, the calculated mobilities are less than those quoted in table (3.10). For values calculated in the mean free time approximation the uncertainty principle is obeyed for all values of the vibrational overlap factor. However, for values calculated in the mean free path approximation only those values corresponding to a

Vibrational Overlap	Electron			Hole		
	a	b	c	a	b	c
0.1	0.14	0.09	0.01	0.03	0.30	0.14
0.2	0.29	0.18	0.02	0.05	0.50	0.21
0.5	0.56	0.34	0.03	0.09	1.05	0.39
1.0	0.73	0.45	0.04	0.10	1.41	0.44
Expt.	0.7	0.7	0.4	0.9	1.4	0.4

(a)

Vibrational Overlap	Electron			Hole		
	a	b	c	a	b	c
0.1	0.40	0.28	0.02	0.05	0.37	0.13
0.2	0.79	0.53	0.03	0.12	1.08	0.33
0.5	1.93	1.09	0.09	0.22	2.40	0.58
1.0	3.78	1.62	0.21	0.24	3.00	0.58
Expt.	0.7	0.7	0.4	0.9	1.4	0.4

(b)

Table(3.10)

Minimum values of the mobility* for various values of the vibrational overlap factor calculated such that the Energy band model is internally consistant. Screening parameter $\mathfrak{Z}$ = 22.7 nm^{-1}.

(a) Mean free time approximation.

(b) Mean free path approximation.

* units: 1×10^{-4} m /volt-sec.

vibrational overlap factor < 0.2 obey criterion (3). As stated earlier the vibrational overlap factor is ~0.5 and in addition polarization effects (44) serve to reduce the transfer integrals by a factor of up to 2. Thus the combination of these two effects could culminate in criterion (3) being satisfied, while at the same time any changes in the calculated band widths would be insufficient to cause a contradiction of criterion (1). However, it is only fair to point out that the applicability of the energy band model has so far not been conclusively proved. For the remaining screening parameter ζ = 20.7 nm^{-1} and 24.6 nm^{-1} the results obtained are similar to those of ζ = 0.227 nm^{-1}, while for ζ = 26.5 nm^{-1} and upwards criteria (2) and (3) are obeyed for practically any value of the vibrational overlap factor. It should however be noted that for the larger screening parameters criterion (1) is in danger of being contradicted for values of the vibrational overlap factor which are substantially less than unity.

3.7   Discussion and conclusion

The anisotropy of the mobility tensor of excess electrons and holes in crystalline naphthalene have been calculated on the energy band model using single Slater functions with modified orbital exponents to represent the carbon $2p_z$ atomic wave function. Results in good agreement with those obtained using SCF atomic orbitals can be obtained using a screening parameter in the range 22.7 to 24.6 nm^{-1}, however, both sets of wave functions give only fair agreement with experiment.

The general lack of agreement between theory and experiment could arise as a result of :

(a)   the assumptions used in the calculation of the mobility ratio are incorrect in that the relaxation time function $\tau(\underline{k})$ is not isotropic.

(b)   energy bands other than the first conduction band are involved in the migration of charge carriers.

(c)   the energy band model is not applicable to the mechanism of transport in crystalline naphthalene.

With regard to point (a) we can only re-iterate what has already been stated, i.e. that the accurate calculation of the relaxation time function is beyond the scope of present methods, however, an approximate estimation of $\tau(\underline{k})$ for anthracene (70) indicated that $\tau(\underline{k})$ was indeed isotropic. Similarly with point (c) it has been shown in section (6) that inclusion of molecular vibrations and polarization effects can lead to mobility values consistent with the uncertainty principle. Thus there is no theoretical reason why the energy band model should not be applicable. This leaves point (b). Jager (124) using the LCAO-HCO method of Ladik (125) has estimated the energy band width of the second conduction band in anthracene to be of the same order of magnitude as the first conduction band, and experimentally injection of excess electrons into higher conduction bands has been observed in crystalline anthracene (9,87). Point (b) is therefore a feasible proposition. The symmetry of the molecular orbitals which would be employed as a basis in the construction of the crystal wave function for the second conduction band are such that qualitatively one would expect the second conduction band to be similar to the hole band. Thus the overall ratios μ_{aa}/μ_{bb} would decrease whilst $\mu_{c'c'}/\mu_{bb}$ would increase bringing the theoretical results more in line with experiment. Furthermore, if electrons were injected from the first conduction band they would leave hole vacancies in the conduction band, thus, the hole mobility ratios would attain some electron character, viz. μ_{aa}/μ_{bb} would increase and $\mu_{c'c'}/\mu_{bb}$ would decrease, again bringing the ratios more in line with experiment. This point is considered in greater detail in the next chapter.

CHAPTER (4)

On the energy band structure and carrier mobilities in

crystalline anthracene.

4.1 Introduction

In the past decade anthracene has received considerable attention as a prototype molecular crystal and the literature has been inundated with experimental values of the resistivity and energy gaps (93). Single crystal and mobility measurements, however, are somewhat rare. and the complete anisotropy of the mobility has only been determined by Kepler (11). Theoretical calculations (39, 40, 41, 43) have shown that the major features of the mobility anisotropy can be understood in terms of an energy band model, the only exception being electronic conduction along the axis perpendicular to the ab plane where the calculated mobility is too low by a factor of about 100. In the above mentioned calculations electronic conduction was assumed to occur only in the lowest conduction band. The precise location of this band is not known with any degree of certainty although it has been suggested that it lies above the first singlet state (101). Hence the photo conduction band gap is above 3.1 eV., and may be greater than 3.7 eV (102). Several workers have claimed that intrinsic photo generation of carriers only occurs with photo energies in excess of 4 eV (9, 151, 103) and that the photo conduction spectrum shows two maxima 4.4 eV (9, 151, 103) and 5.5 eV (103) indicating that electrons can be excited to bands of a higher energy than the first conduction band. Sano, Pope and Kallmann (103,), in an electro luminescence experiment, have shown that electrons can be injected from the normal conduction band into higher energy bands under the effect of an applied field, thus producing holes in the conduction band. It is partially the purpose of this chapter to investigate the nature of the second conduction band on the assumption that, like the first, the band can be treated in the tight binding approximation.

The calculation of the energy band structure of the second conduction band in anthracene is complicated by the fact that the molecular energy level giving rise to the band is degenerated. Thus, corresponding to the two molecular energy levels there will exist two energy bands in the close proximity of one another and subsequently interactions between the two bands cannot be neglected. A procedure for the calculation of such bands is outlined in section (2).

The temperature dependence of the mobility of charge carriers has been studied experimentally by several authors (11, 14, 16, 38, 94, 95) and the general confensus is that electrons and holes have a different temperature dependence of the type T^{-n}, with n usually between 1 and 2. The only exception to this is that the drift mobility of excess electrons along the axis perpendicular to the ab plane is found to be virtually temperature independent (11, 109, 110, 111). Because of the absence of crystal data only very approximate methods have previously been used (40) to estimate the effects of temperatures on the calculated mobilities. However, since the publication of the earlier work Mason (98) has completed a study of the thermal expansion properties of the anthracene crystal thus facilitating a more detailed study which is reported in section (5).

4.2 The energy band structure of molecular crystals with nearly degenerate bands.

In the two centre approximation, with zero overlap, the energies of the two symmetry states $\Omega_\ell^{\pm}(\underline{k})$, in the absence of all other states, are given by :

$$\langle \Omega_\ell^{\pm}(\underline{k})|H|\Omega_\ell^{\pm}(\underline{k})\rangle = E_\ell^{(0)} + \sum_{n \neq 0} |\langle \phi_\ell|V(\underline{r} - \underline{r}_n)|\phi_\ell\rangle$$

$$+ \sum_{n \neq 0} (\pm 1)^n |\langle \chi^1|\chi^0\rangle|^2 \langle \phi_\ell|V(\underline{r} - \underline{r}_n)\phi_\ell\rangle$$

$$\cos(\underline{k} \cdot \underline{r}_n) \qquad\qquad (4.1)$$

where $E_\ell^{(0)}$ is the energy of molecular orbital ϕ_ℓ in the free molecule, $\Omega_\ell^{\pm}(\underline{k})$ are the symmetry adapted crystal wave functions formed as a Bloch sum of molecular orbitals ϕ_ℓ. The difference in energy between the highest occupied and lowest unoccupied molecular orbitals in anthracene is about 4 eV. It is therefore justifiable to neglect the possibility of band mixing between crystal states formed with the above two molecular orbitals as a basis set, and the band energies can be obtained by direct substitution of the appropriate integrals into equation (4.1). The second and third lowest unoccupied levels of anthracene, of symmetry b_{2g} and a_u respectively, are degenerate in the Hueckel approximation. Hence the centres of the energy bands formed from these molecular orbitals will lie close together and one must subsequently expect an appreciable amount of band mixing. The energies of the resulting states will be the solutions of the determinant

$$\begin{vmatrix} H_{b_{2g},b_{2g}}^{\pm} - E & H_{b_{2g},a_u}^{\pm} \\ H_{a_u,b_{2g}}^{\pm} & H_{a_u,a_u}^{\pm} - E \end{vmatrix} = 0$$

where $H_{\ell,m}^{\pm} = \langle \Omega_\ell^{\pm} | H | \Omega_m^{\pm} \rangle$ 　　　　　　　　　　(4.2)

$$= E_\ell^{(0)} \delta_{\ell m} + \sum_{n \neq 0} C_n^{\ell,m} + \sum_{n \neq 0} (\pm 1)^n E_n^{\ell,m} \cos(\underline{k} \cdot \underline{r}_n) \quad (4.3)$$

where $\delta_{\ell m}$ is the Kronecker δ function,

$$C_n^{\ell,m} = \langle \phi_\ell(\underline{r}) | V(\underline{r} - \underline{r}_n) | \phi_m(\underline{r}) \rangle \quad (4.4)$$

and $\quad E_n^{\ell,m} = \langle \phi_\ell(\underline{r} - \underline{r}_n) | V(\underline{r} - \underline{r}_n) | \phi_m(\underline{r}) \rangle \quad (4.5)$

The two solutions of the determinant for each symmetry are given by :

$$W_{\pm}^{\mp}(\underline{k}) = \tfrac{1}{2} \{ H_{a_u,a_u}^{\pm} + H_{b_{2g},b_{2g}}^{\pm}$$

$$\pm (H_{a_u,a_u}^{\pm} - H_{b_{2g},b_{2g}}^{\pm})^2 + 4 H_{a_u,b_{2g}}^{\pm 2} \}^{\tfrac{1}{2}} \} \qquad (4.6)$$

thus the energy dependence on the wave vector $\underline{k}$ depends not only on the last term in equation (3.1) but on the other terms also.

Expanding the molecular orbitals, ϕ , in terms of their constituent atomic orbitals, u , and substituting the potential in the manner given in chapter (2) (equations (2.9) through (2.13)) then :

$$E_n^{\ell,m} = |\langle \chi^1|\chi^0\rangle|^2 \{ -e^2 \sum_{\alpha,\beta} c_\alpha^\ell \, c_\beta^m$$

$$\langle u_\alpha | Z_\alpha/R_\alpha - \sum_{j \text{ occ}} \theta_\alpha^{(j)} |r_{12}^{-1}| \theta_\alpha^{(j)} | u_\beta \rangle$$

$$- \frac{\rho_\alpha}{2} \langle u_\alpha | \langle u_\alpha | r_{12}^{-1} | u_\alpha \rangle | u_\beta \rangle \} \qquad (4.7)$$

where c_j^i is the coefficient of centre j of the molecular orbital ϕ_i the remaining symbols have been defined in chapter (2).
Similarly

$$C_n^{\ell,m} = \{ -e^2 \sum_{\alpha,\beta} c_\beta^\ell \, c_\beta^m \, \langle u_\beta | Z_\alpha/R_\alpha | u_\beta \rangle$$

$$- \langle u_\beta | \sum_{j \text{ occ}} \theta_\alpha^{(j)} | r_{12}^{-1} | \theta_\alpha^{(j)} | u_\beta \rangle$$

$$- \frac{\rho_\alpha}{2} (\langle u_\beta | \langle u_\alpha | r_{12}^{-1} | u_\alpha \rangle | u_\beta \rangle$$

$$- \langle u_\beta | \langle u_\alpha | r_{12}^{-1} | u_\beta \rangle | u_\alpha \rangle) \} \qquad (4.8)$$

Of the last two terms in equation (4.8) the latter represents the exchange interaction between the atomic orbitals u_α and u_β the former being the coulomb interaction between the charge distribution $|u_\beta|^2$ and $|u_\alpha|^2$. The fourth term is ~ 1000 times smaller than the third (at $\zeta \times R \approx 7.0$) and is neglected. $C_n^{\ell,m}$ therefore reduces to

$$C_n^{\ell m} = \{-e^2 \sum_{\alpha,\beta} c_\beta^\ell c_\beta^m \langle u_\beta | Z_\alpha / R_\alpha | u_\beta \rangle$$

$$- \langle u_\beta | \sum_{j=occ} \phi_\alpha^{(j)} | r_{12}^{-1} | \phi_\alpha^{(j)} | u_\beta \rangle$$

$$- \rho_\alpha \langle u_\beta | \langle u_\alpha | r_{12}^{-1} | u_\alpha | \rangle u_\beta \rangle \} \qquad (4.9)$$

For aromatic hydrocarbons the electron density, ρ_α, at centre α is unity and for large internuclear distances the electron charge distributions

$$\sum_{j=occ} \phi_\alpha^{(j)} \phi_\alpha^{(j)} \quad \text{and} \quad u_\alpha u_\alpha$$

can be considered as localized on the centre α. Thus the last two terms of equation (4.9) reduce to

$$\langle u_\beta(r) | Z_\alpha / R_\beta | u_\beta(r) \rangle$$

and hence

$$C_n^{\ell,m} = 0.0 .$$

To test the validity of the above approximation we have calculated the nuclear attraction and electronic repulsion parts within the square brackets of equations (7) and (9) using the molecular integral tables of Kotani et al (34). The results are given in table (4.1).

	$E_n^{\ell,m}$			$C_n^{\ell,m}$		
ζR	Electron Repulsion ζ	Nuclear Attraction ζ	Difference	Electron Repulsion ζ	Nuclear Attraction ζ	Difference
5.0	0.1743525	0.1931544	0.018809	0.74638501	0.75218740	0.00580239
6.0	0.0867993	0.0941924	0.207391	0.63743608	0.63891160	0.00147552
7.0	0.0415234	0.0443784	0.002855	0.55358831	0.55393868	0.00035037
8.0	0.0192620	0.023512	0.001892	0.48820259	0.48828160	0.00007901

Table (4.1)

Nuclear attraction and electron repulsion parts of the hybrid, E, and coulomb, C, integrals.

For screening parameter $\zeta = 30.7$ nm^{-1} the internuclear distances corresponding to the values in table (4.1) are 0.163, 0.195, 0.228 and 0.261 nm . These are considerably smaller than the average internuclear distance in anthracene, the smallest internuclear distance being 0.367 nm, however it does show that $C_n^{\ell,m}$ is decreasing at a faster rate than $E_n^{\ell,m}$ and that in the region R = 0.370 nm to 1.058 nm will be several orders of magnitude less. It should be noted at this point that the above arguments only apply to molecules having an even distribution of electrons. For cases where there is polarization of the π-electron system, leading to greater densities at certain atoms, the above conclusions to not apply.

4.3 Molecular orbitals

Following the procedure outlined in Chapter (3), page (47), the wave function for the positive ion was obtained by assigning the excess hole to the highest occupied molecular orbital in the neutral molecule. For the excess electron the molecular orbital of the ion was obtained by assigning the electron to the first, second or third lowest unoccupied molecular orbital giving rise to the first, second or third

conduction bands. The molecular orbital coefficients are taken as the Hueckel coefficient (108) of the appropriate energy level.

The use of Hueckel molecular orbitals in band structure calculations has recently been criticised by Mathur and Singh (105). Their criticisms are based on the following two inconsistencies :

"(1)   One is not justified in combining resonance integrals between molecules situated far apart at different molecules with Hueckel coefficients because in calculating Hueckel molecular orbitals one neglects all resonance integrals except those between nearest neighbours.

(2)   The atomic orbitals centred on a given molecule, when calculating intermolecular resonance integrals, are non-orthogonal, whereas Hueckel coefficients are based on the assumption of orthogonality."

With these criticisms in mind Mathur and Singh have developed a modified procedure for determining molecular orbital coefficients. These coefficients, together with those calculated using the Hueckel approximation are given in table (4.2).

4.4   Numerical results and energy band structure

The crystal data used is taken from Mason (98). The unit cell constants and atomic coordinates were determined both at $95^{\circ}K$ and $290^{\circ}K$. X-ray photographs were also taken by Mason at temperatures intermediate to these two temperatures and no discontinuous changes in unit cell constants were observed. Precision measurements on the single film showed the thermal expansion coefficients to be markedly anisotropic the maximum value being approximately in the direction of N, the axis perpendicular to the molecular plane. Calculated torsional oscillations, at $290^{\circ}K$ about the molecular axes L, M and N are 3.6°, 2.7° and 3.1° respectively in reasonable agreement with the earlier

Symm.	m	1.	2.	3.	4.	1.	2.	3.	4.
AxSy	7	0.220	0.311	-0.091	-0.440	0.24269	0.30648	-0.10231	-0.45530
SxSy	8	0.220	-0.311	-0.091	0.440	-0.27584	0.37937	0.05053	-0.47861
AxAy	9	-0.204	0.408	-0.204	0.000	0.24353	-0.51270	0.30056	0.00000
SxAy	10	-0.354	0.000	0.354	0.000	0.47415	-0.04131	0.43256	0.00000

Table(4.2)

Molecular orbital coefficients, c , in the Hueckel and Mathur-Singh approximations.
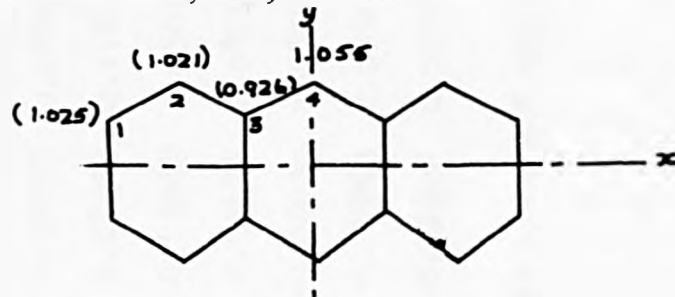
fig(4.1)

Numbering of the atoms in anthracene. The figures in parentheses refer to the electron densities calculated in the Mathur-Singh approximation.

Crystal data for anthracene(98).

	a nm.	b nm	c nm.	beta.
290 K	0.8562	0.6038	1.1184	124 42
95 K	0.8443	0.6002	1.1124	125 36

Fractional atomic coordinates.

atom	95° K x/a	y/b	z/c	290° K x/a	y/b	z/c
1	0.08600	0.02361	0.36797	0.08893	0.02818	0.36586
2	0.11750	0.15677	0.28348	0.11849	0.15836	0.28041
3	0.05888	0.07961	0.13963	0.05878	0.08054	0.13804
4	0.08835	0.20949	0.05174	0.08712	0.20829	0.04766
5	0.02972	0.13458	-0.09030	0.03077	0.13087	-0.08990
6	0.06056	0.26109	-0.18263	0.05911	0.26461	-0.18260
7	0.00399	0.18707	-0.31804	0.00260	0.18099	-0.31673

Inclination of the molecular axes L,M and N to the orthogonal axes a,b and c .

	95° K a	b	c	290° K a	b	c
L	120.74	97.52	31.88	L 119.61	97.32	30.68
M	107.67	153.76	108.75	M 108.51	153.44	108.36
N	36.51	114.97	65.22	N 35.97	115.38	66.23

Table(4.3)

values of Cruickshank (112). The translational vibrations are a good deal more isotropic having $\sqrt{u^2}$ values of 0.022, 0.017 and 0.016 nm respectively. At 95°K the molecules are much more rigidly fixed in the lattice, the rotational amplitudes being 0.9°, 0.9° and 1.6° respectively with translational amplitudes of 0.013, 0.007 and 0.009 nm. The unit cell data at 95°K and 290°K together with the atomic coordinates and the orientations of the crystal to the molecular axes are given in table (4.3). It should be noted that the atomic coordinates in table (2) of Mason's paper are wrongly quoted, the corrected coordinates are given in table (4.3).

Intermolecular transfer integrals have been calculated for the excess hole and the three conduction bands using the normal Slater screening parameter, $\zeta = 30.7$ nm^{-1}, the modified screening parameter, $\zeta = 24.7$ nm^{-1} and Hueckel coefficients for both temperatures. The results are listed in tables (4.4), and table 4.5). The principle transfer integrals for the electron and hole bands at the two temperatures show only a small variation, E_3, (see figure (3.1), page (46)), decreasing by about 10% whilst E_9 and E_{10} show a rather larger increase. The temperature dependence of the transfer integrals in the higher conduction bands is more complicated.

Transfer integrals have also been calculated using the molecular orbitals coefficients of Mathur and Singh. The results, using the normal Slater screening parameter are given in table (4.6). With the exception of E_{10} for the electron the integrals for the electron and hole bands are comparable to but rather smaller than their Hueckel equivalents. E_{10} for the electron band is larger by a factor of about 10 than the same calculated using Hueckel molecular orbitals. For the higher conduction bands the differences in the transfer integrals is much larger reflecting the large differences between the two sets of coefficients.

	95°K		290°K		95°K			290°K		
Position	$\langle 8\bar{1}8 \rangle$	$\langle 7\bar{1}7 \rangle$	$\langle 8\bar{1}8 \rangle$	$\langle 7\bar{1}7 \rangle$	$\langle 9\bar{1}9 \rangle$	$\langle 10\bar{1}10 \rangle$	$\langle 10\bar{1}9 \rangle$	$\langle 9\bar{1}9 \rangle$	$\langle 10\bar{1}10 \rangle$	$\langle 10\bar{1}9 \rangle$
(0,0,1)	1.07	1.06	0.51	0.10	-0.90	2.64	-1.52	-0.42	-0.34	0.31
(0,1,0)	39.32	-51.98	45.31	-58.07	81.30	-6.81	28.69	84.49	-6.58	27.90
(0,1,1)	-	-0.01	-	-0.01	-	0.01	-	-	0.01	-
(1,0,0)	0.05	0.03	0.01	0.24	-0.04	-0.05	0.02	-0.06	0.01	-0.02
(1,0,1)	-0.19	-1.01	-0.16	-0.77	0.25	0.55	0.53	0.22	0.43	-3.86
(1,1,0)	0.01	-0.01	0.08	-0.01	-0.02	-	0.01	0.01	-	-
(1,1,1)	-	-	-	-	-0.01	-	-	-	-	-
($\frac{1}{2}$,$\frac{1}{2}$,0)	-137.97	-67.06	-115.21	-47.247	-1.02	18.59	-31.10	15.44	14.35	-18.19
($\frac{1}{2}$,$\frac{1}{2}$,1)	0.26	23.65	-0.34	19.05	7.00	-31.94	-3.33	6.12	-27.58	-5.58

Table(4.4)

Transfer integrals* for the excess hole and first three conduction bands in crystalline anthracene computed at 95°K and 290°K using Hueckel molecular orbitals as basis in the Bloch sum and a single Slater function with ζ = 30.7 nm^{-1}. to represent the carbon atomic wavefunction. The numbers within the angular brackets refer to the number of the molecular orbital used to calculate the transfer integral.

* units: 1_{D}-4 eV.

| | 95° K | | 290° K | | 95° K | | | 290° K | | |
Position	<8I8>	<7I7>	<8I8>	<7I7>	<9I9>	<10I10>	<10I9>	<9I9>	<10I10>	<10I9>
(0,0,1)	-4.93	-2.07	-3.84	-2.62	4.21	2.48	2.46	3.41	4.33	-0.43
(0,1,0)	166.71	-210.45	161.67	-218.18	321.45	-53.20	159.96	332.51	-46.50	151.23
(0,1,1)	-0.03	-0.22	-0.03	-0.22	0.06	0.17	-0.05	0.06	0.17	-0.03
(1,0,0)	0.73	0.01	0.44	0.05	-2.41	0.24	-0.75	-1.75	0.18	-0.58
(1,0,1)	-1.02	-10.96	-1.08	-9.00	-1.76	7.11	-8.91	1.89	5.90	-4.90
(1,1,0)	0.03	-0.09	0.02	-0.09	-0.05	0.07	0.01	-0.42	0.05	-0.15
(1,1,1)	0.03	-0.08	0.02	-0.09	-0.14	0.02	-0.04	-0.11	0.18	-0.05
($\frac{1}{2}$,$\frac{1}{2}$,0)	-410.66	-207.94	-376.62	-148.97	8.26	99.22	330.64	31.87	71.84	73.58
($\frac{1}{2}$,$\frac{1}{2}$,1)	-8.71	106.12	-1.96	91.77	43.13	-129.46	40.68	28.98	107.41	14.64

Table (4.5)

Transfer integrals* for the excess hole and first three conduction bands in crystalline anthracene computed at 95° K and 290° K using Hueckel molecular orbitals as basis in the Bloch sum and a single Slater function with ς = 24.6 nm . to represent the carbon atomic wavefunction. The numbers within the angular brackets refer to the number of the molecular orbital used to calculate the transfer integral.

* units: 1_D-4 eV.

	95°K		290°K		95°K			290°K		
Position	$\langle 8\overline{1}8\rangle$	$\langle 7\overline{1}7\rangle$	$\langle 8\overline{1}8\rangle$	$\langle 7\overline{1}7\rangle$	$\langle 9\overline{1}9\rangle$	$\langle 10\overline{1}10\rangle$	$\langle 10\overline{1}9\rangle$	$\langle 9\overline{1}9\rangle$	$\langle 10\overline{1}10\rangle$	$\langle 10\overline{1}9\rangle$
(0,0,1)	1.25	-1.48	0.31	0.11	5.09	-1.13	-2.36	-0.67	-0.41	2.72
(0,1,0)	20.39	-36.96	31.01	-43.94	-5.62	127.88	17.05	-6.44	132.50	19.64
(0,1,1)	-	-0.01	-	-0.01	0.01	-	-	0.01	-	-
(1,0,0)	0.12	0.03	0.06	-	0.05	-0.11	0.02	-	-0.12	-0.07
(1,0,1)	-0.41	-0.68	-0.32	-0.51	-0.32	0.20	-0.99	-0.18	0.20	0.71
(1,1,0)	0.01	-0.01	0.01	-0.01	-	-	-	-	-0.01	-
(1,1,1)	-	-	-	-	-	-	-	-	-	-
($\frac{1}{2},\frac{1}{2}$,0)	-120.51	-24.02	-97.48	-16.28	-80.78	24.83	-185.28	-54.98	55.14	-137.38
($\frac{1}{2},\frac{1}{2}$,1)	4.03	31.99	2.41	26.01	-40.52	8.99	-25.83	-35.97	8.21	-19.25

Table (4.6)

Transfer integrals* for the excess hole and first three conduction bands in crystalline anthracene computed at 95°K and 290°K using Mathur and Singh molecular orbitals as basis in the Bloch sum and a single Slater function with $\varsigma = 30.7$ nm^{-1}. to represent the carbon atomic wavefunction. The numbers within the angular brackets refer to the number of the molecular orbital used to calulate the transfer integral.

* units: 1_D-4 eV.

The energy band structures of excess electrons and holes along the three crystallographic axes, computed using the transfer integrals calculated, at $95^{\circ}K$ and $290^{\circ}K$, with Hueckel coefficients, are illustrated in figure (4.2) and figure (4.3). The general shapes of the valence and first conduction bands calculated using Mathur - Singh coefficients are similar to those shown in figure (4.3) and figure (4.4) and subsequently are not reproduced here. Figure (4.4) shows the energy bands, at $95^{\circ}K$, calculated using equation (4.3) i.e. without taking into account the effects of band interactions. It is easily seen from the diagram that there will be a considerable amount of band mixing. The conduction bands resulting from band mixing are displayed in figure (4.5) and the resultant effect is that the two conduction bands are forced apart, each band imparting some of its character onto the other. The energy zero for these bands is arbitrarily chosen as the energy of the Hueckel molecular orbitals in the free molecule. The separation of the centroids of the two conduction bands at $\underline{k} = 0$ and with vibrational overlap factor = 1.0 is of the order 0.03 eV in both cases therefore thermal energy will be sufficient to excite electrons from one band to the other and so increasing the range of allowed $E(\underline{k})$ values for the wave vector $\underline{k}$. The energy band structure of the second and third conduction bands calculated at $95^{\circ}K$ using Mathur and Singh coefficients is shown in figure (4.6). The band at $290^{\circ}K$ is very similar to the $95^{\circ}K$ band. A comparison of figure (4.5) and figure (4.6) illustrates the large differences between the second conduction bands. The general shapes of the second and third conduction bands will be discussed in more detail later in connection with the Hall effect.

The energy band widths for the valence and first conduction bands at $95^{\circ}K$ and $290^{\circ}K$ for Hueckel molecular orbitals and Mathur-Singh molecular orbitals are given in tables (4.7). The values are calculated
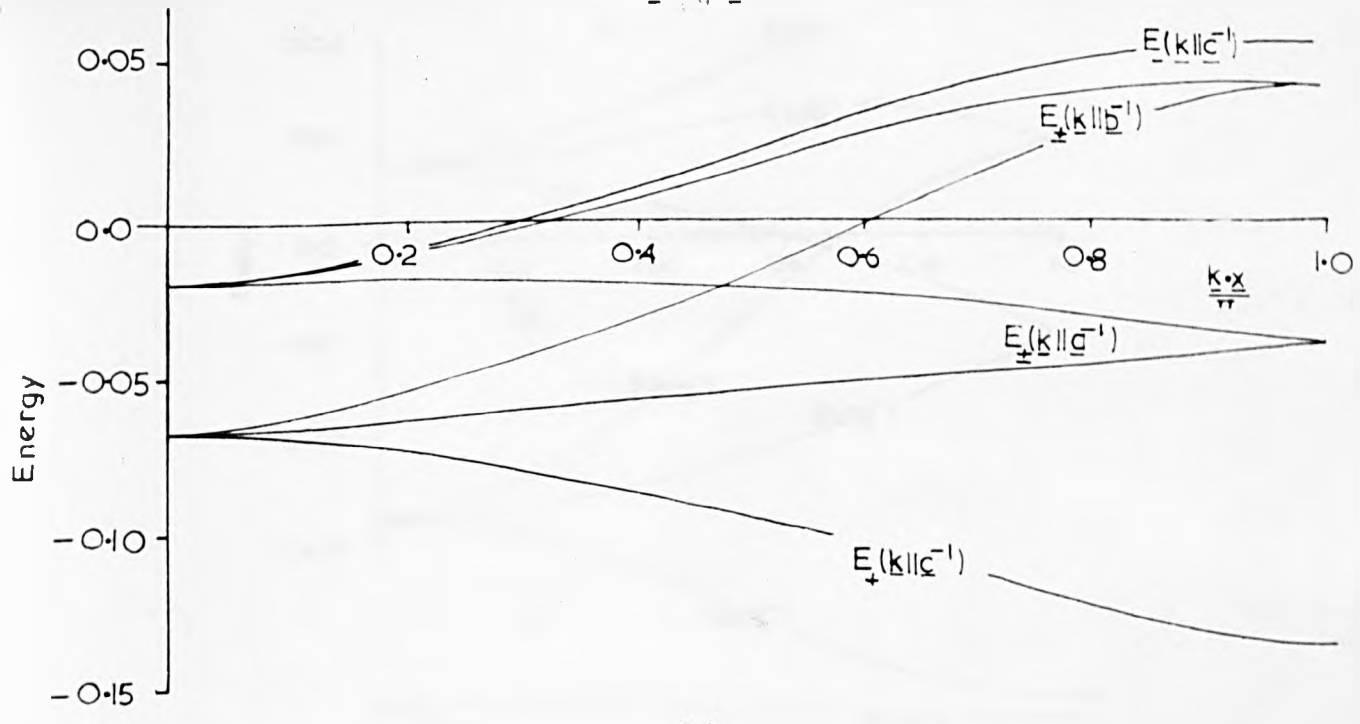
(a)
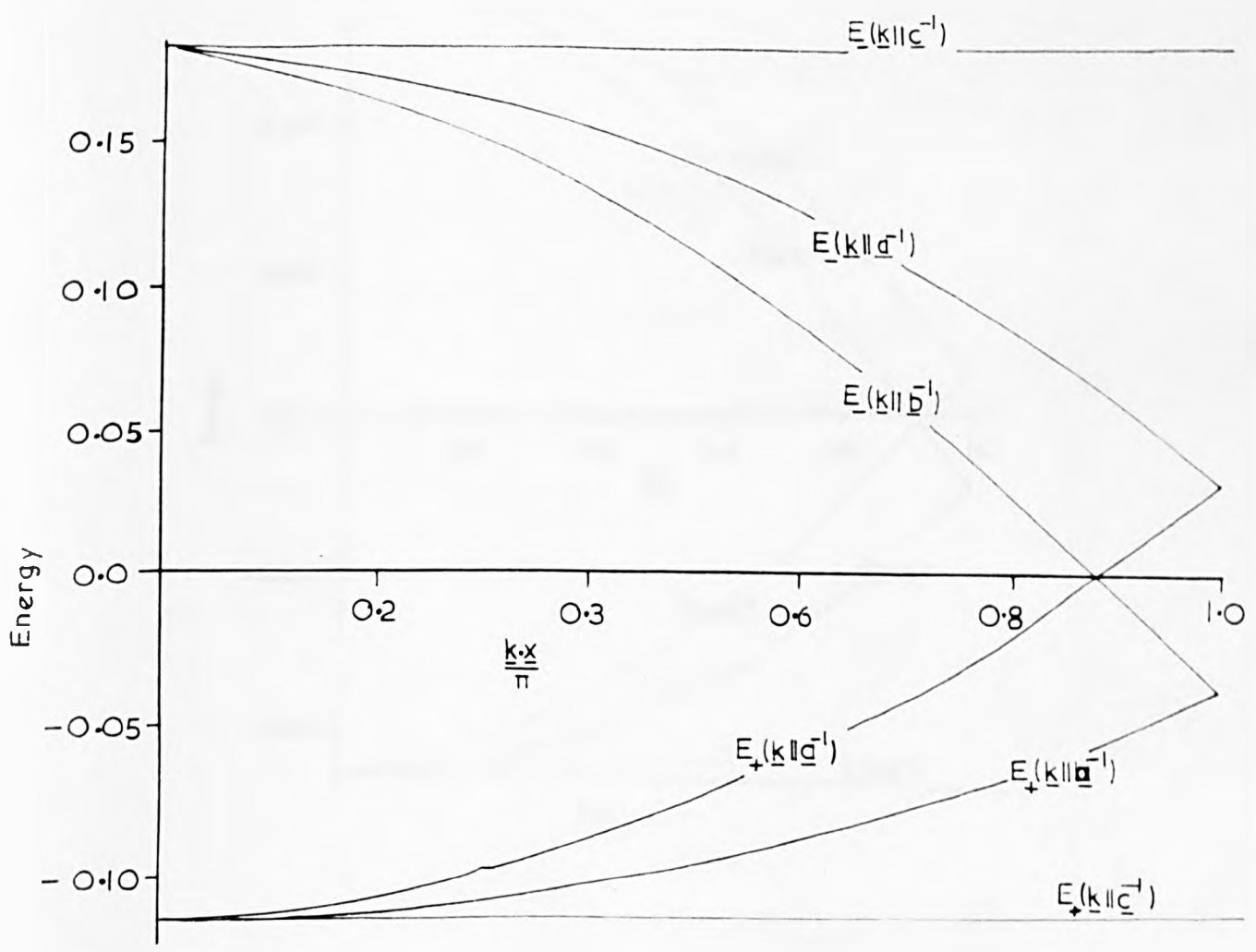
(b)

Figure (4.2)

Energy band structure of excess holes (a) and electrons (b) in crystalline anthracene at 300°K computed using Huckel molecular orbitals as basis in the Bloch sum.

(a)

(b)
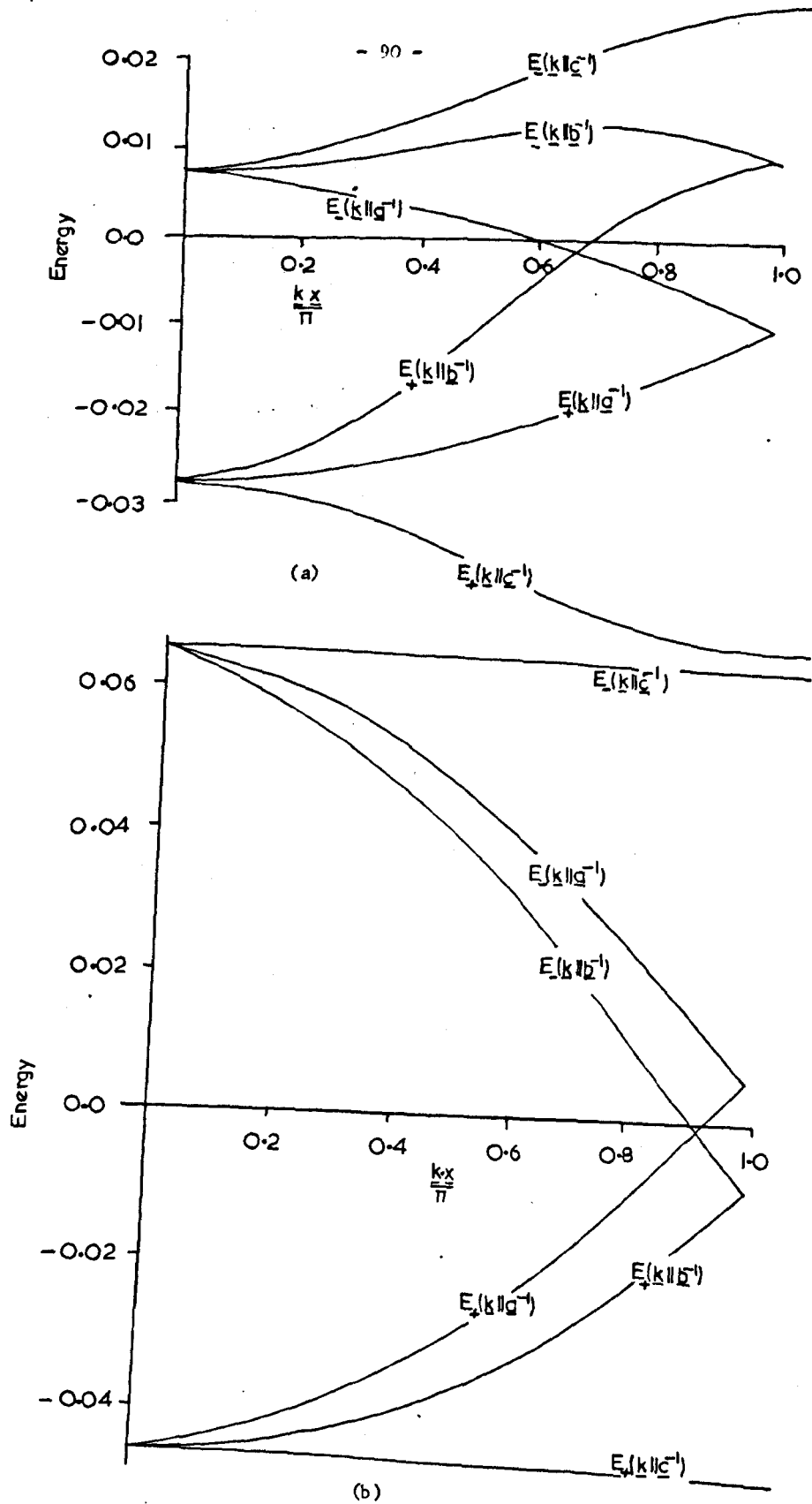
Figure (4.3)

Energy band structure of excess holes (a) and electrons (b)
in crystalline anthracene at 95°K. Computed using Hueckel
molecular orbitals as basis in the Bloch sum.
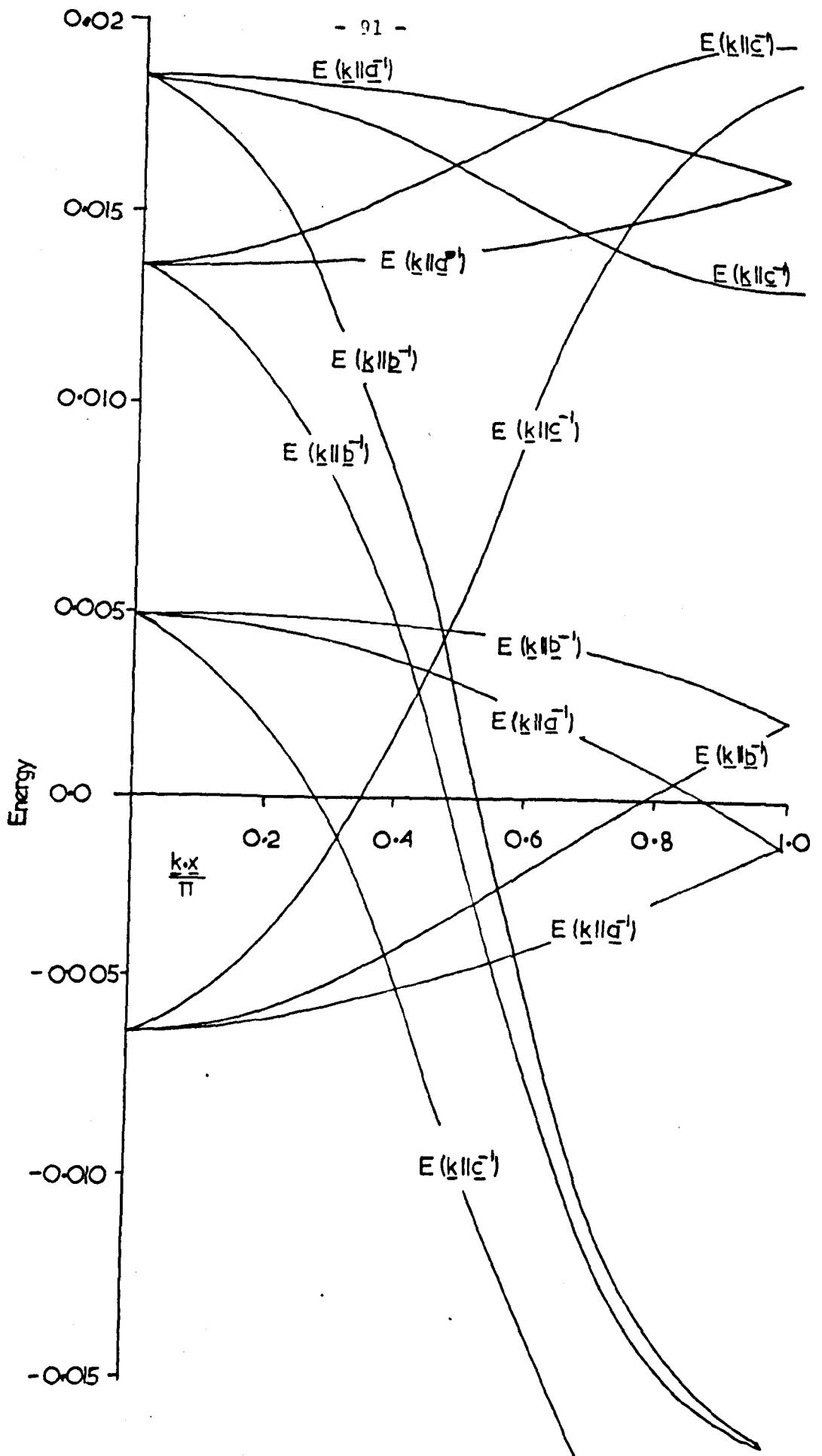
Figure (4.4)

The energy band structures of the second and third
conduction bands at 95°K, calculated using equation (4.3)
showing the overlapping of the two energy bands.
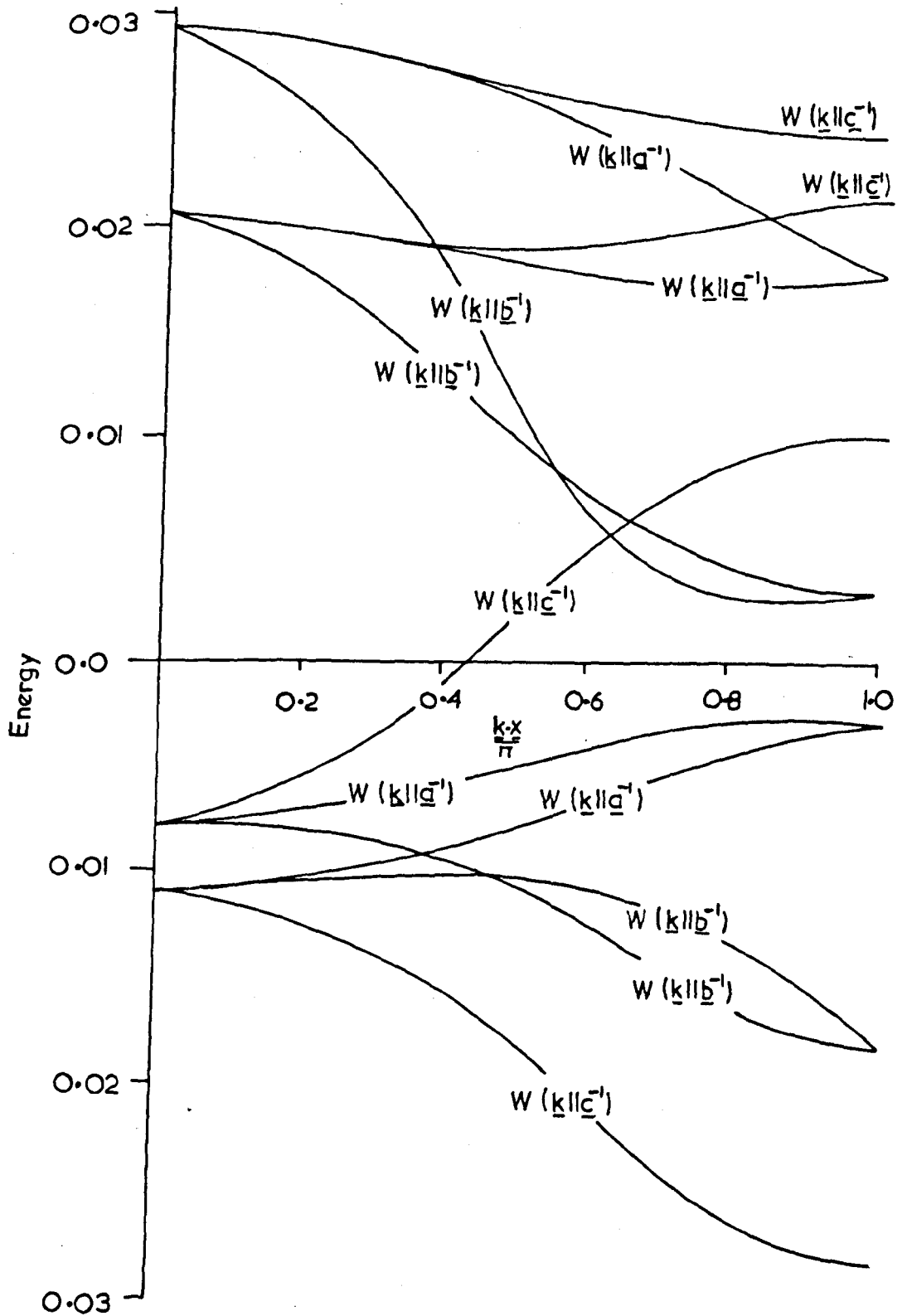
Figure (4.5)

The energy band structures of the second and third conduction bands
in crystalline anthracene after taking into account energy band mixing.
The basis set used in the Bloch sum are the Hueckel molecular orbitals
for the second and third lowest unoccupied states in the free molecule.
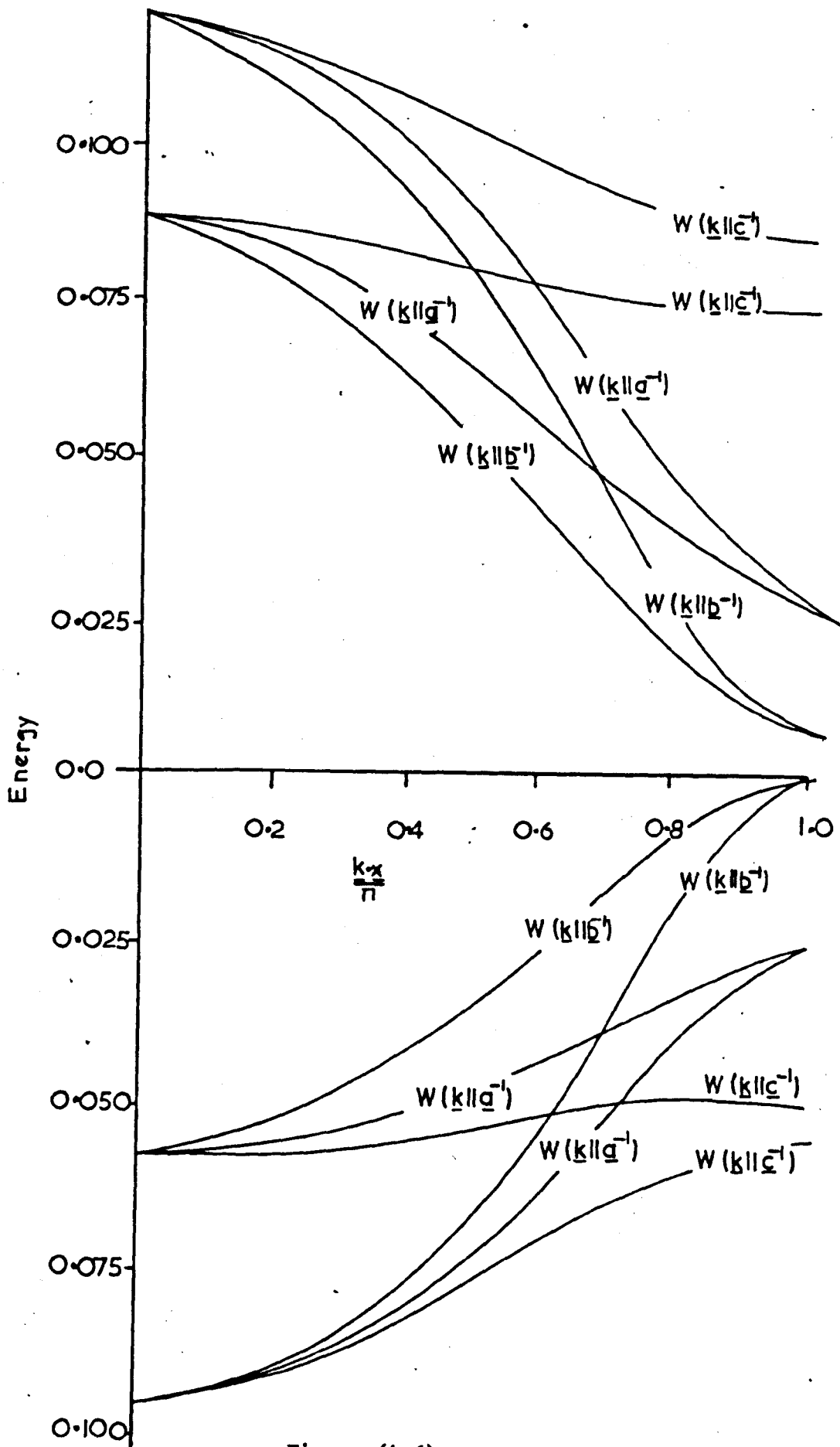
Figure (4.6)

The energy band structure of the second and third conduction bands
in crystalline anthracene after taking into account band mixing.
The basis set used in the bloch sum are Mathur - Singh molecular
orbitals for the second and third lowest unoccupied state in the
free molecule.

		Hole			1st Cond.			2nd Cond.		3rd Cond.	
		I	II	III	I	II	III	I	II	I	II
$E(k \parallel a')$	+	1.80	0.29	4.52	5.50	4.67	16.78	0.28	6.21	0.54	9.72
	−	1.70	0.35	3.62	5.50	4.65	16.77	1.17	9.35	0.84	5.85
$E(k \parallel b')$	+	3.80	1.16	12.52	3.90	3.84	10.10	1.72	8.51	0.96	7.12
	−	0.30	1.80	4.33	7.80	5.48	23.44	2.62	11.65	0.66	3.26
$E(k \parallel c')$	+	1.80	2.47	7.94	0.10	0.36	0.94	0.13	1.61	1.76	3.98
	−	1.90	2.65	9.04	0.01	0.29	0.46	0.43	3.46	1.66	0.78
c splitting		7.30	4.48	25.12	11.06	9.96	32.16	0.33	12.90	3.73	0.66

(a)

Table (4.7)

Energy bandwidths* and splitting at $\underline{k} = \underline{c}/\pi$ in crystalline anthracene, for vibrational overlap unity, at 95° K(a) and 290° K(b).

I   Calculated using Hueckel coefficients and $\mathcal{S} = 30.7$ nm⁻¹.

II   Calculated using Mathur and Singh coefficients and $\mathcal{S} = 30.7$ nm⁻¹.

III Calculated using Hueckel coefficients and $\mathcal{S} = 24.6$ nm⁻¹.

		Hole			1st Cond.			2nd Cond.		3rd Cond.	
		I	II	III	I	II	III	I	II	I	II
$E(k \parallel a^{-1})$	+	1.20	0.39	2.66	4.60	3.81	15.17	0.73	5.32	0.37	6.43
	−	1.10	0.41	1.92	4.60	3.79	15.12	0.18	6.03	0.49	4.93
$E(k \parallel b^{-1})$	+	3.50	1.37	11.05	2.80	2.56	8.68	2.28	7.88	1.17	3.94
	−	1.20	2.15	6.47	6.40	5.04	21.61	1.73	8.59	1.05	2.44
$E(k \parallel c^{-1})$	+	1.50	2.06	6.85	−	0.19	0.35	0.52	1.04	2.24	3.30
	−	1.60	2.10	7.83	−	0.19	0.04	0.38	2.98	1.34	0.80
c splitting		5.30	3.88	19.26	0.92	7.79	29.97	0.40	1.23	3.70	1.00

(b)

Table(4.7)

Energy bandwidths* and splitting at $\underline{k} = \underline{c}/\pi$ in crystalline anthracene, for vibrational overlap unity, at 95°K(a) and 290°K(b).

I   Calculated using Hueckel coefficients and $\varsigma = 30.7 \text{ nm}^{-1}$.

II   Calculated using Mathur and Singh coefficients and $\varsigma = 30.7 \text{ nm}^{-1}$.

III Calculated using Hueckel coefficients and $\varsigma = 24.6 \text{ nm}^{-1}$.

on the assumption that the vibrational overlap factor is unity.
Jortner et al (74) have estimated that the vibrational overlap factor
reduces the band widths by $\frac{1}{4}$ to $\frac{1}{5}$ and in addition Glaeser and Berry (44)
have shown that polarization of the crystal by the excess carriers
further reduces the band width by $\frac{1}{2}$. The actual band widths will
therefore be approximately 1/10 those listed in the tables, i.e.
0.005 eV ($\zeta = 30.7$ nm^{-1}), 0.01 eV ($\zeta = 20.5$ nm^{-1}) in reasonable
agreement with the value 0.006 as determined by Delacote and Schott (22).
The energy band widths of the second and third conduction bands are
given in table (3.7).

It is interesting to note that the band width, in the $\underline{c}'$
direction , of the second conduction band is several orders of
magnitude larger than for the first (cf. figures (4.5) and
figure (4.3)) indicating that electrons in this band can have an
appreciable mobility in this direction.

4.5 Mobility tensor

4.5(i) General

The components of the mobility tensor for the hole and first
conduction bands have been calculated using the methods of Chapter (3).
The component of the mobility tensor along the $\underline{b}$ axis, without the
premultiplicative factors $\frac{e \tau_0}{k_0 T}$ and $\frac{e \lambda}{k_0 T}$, computed at 95°K and
290°K using Hueckel coefficients and the normal ($\zeta = 30.7$ nm^{-1}). Slater
screening parameters, together with the ratios of the non-zero elements
of the tensor to this are given in table (4.8). Due to the larger values
of the band widths and smaller value of $k_0 T$, the mobility ratios at
95°K show a stronger dependence on vibrational overlap factor. With
the exception of the electron mobility in the $\underline{c}'$ direction, the
calculated room temperature mobility ratios, computed using vibrational

	Electron			Hole		
Vibrational Overlap	0.1	0.5	1.0	0.1	0.5	1.0
$\langle vbvb\rangle$*	1.571	19.209	43.635	0.791	12.135	27.214
$\langle vbvb/\underline{v}(\underline{k})\rangle$**	0.635	2.064	3.045	0.361	1.391	1.773
$\dfrac{\mu_{aa}}{\mu_{bb}}$	1.879	2.738	3.268	0.935	1.193	1.673
	(1.670)	(2.200)	(2.359)	(0.934)	(1.148)	(1.542)
$\dfrac{\mu_{cc}}{\mu_{bb}}$	-	0.001	0.002	0.550	0.847	1.526
	(0.001)	(0.003)	(0.007)	(0.531)	(0.786)	(1.295)
$\dfrac{\mu_{ac}}{\mu_{bb}}$	-0.001	-0.001	-0.001	-0.176	-0.269	-0.483
	-	(-0.002)	(-0.005)	(-0.240)	(-0.347)	(-0.452)

(a)

	Electron			Hole		
Vibrational Overlap	0.1	1.0	Exp.	0.1	1.0	Expt.
$\langle vbvb\rangle$*	1.409	81.44		0.794	64.795	
$\langle vbvb/\underline{v}(\underline{k})\rangle$**	0.601	4.218		0.399	3.582	
$\dfrac{\mu_{aa}}{\mu_{bb}}$	1.562	2.169	1.7	0.495	0.495	0.5
	(1.493)	(1.991)		(0.526)	(0.508)	
$\dfrac{\mu_{cc}}{\mu_{bb}}$	-	-	0.4	0.373	0.391	0.4
	-	-		(0.372)	(0.384)	
$\dfrac{\mu_{ac}}{\mu_{bb}}$	-	-		-0.108	-0.112	
	-	-		(-0.150)	(-0.152)	

(b)

Table(4.8)

Calculated mobility ratios of excess electrons and holes in crystalline anthracene computed in the mean free time and free path(in parentheses) approximations at $95°$K (a) and $290°$K (b) using Hueckel coefficients and screening parameter $\mathcal{T} = 30.7 nm^{-1}$.

* units: $1\text{\tiny D}6 \ m^2/sec^2$.

**units: $1\text{\tiny D}3 \ m/sec$.

overlap factor, 0.1, are in good agreement with the experimental values of Kepler (11). However, the electron mobility ratio $\frac{\mu_{c'c'}}{\mu_{bb}}$ is too low by a factor of the order 1000. Electronic conduction along this axis will be discussed later in connection with conduction in higher energy bands.

4.5(ii)   Electron mobility along the c' axis

The band width of the first conduction band along the c' axis is very small and gives rise to very low values for the electron mobility in this direction. The mobility of electrons under consideration is promoted by resonance interactions between molecules whose centres are connected by the lattice vectors $\frac{1}{2}\underline{a} + \frac{1}{2}\underline{b} + \underline{c}$ and $\frac{1}{2}\underline{a} - \frac{1}{2}\underline{b} + \underline{c}$. The symmetry of the molecular wave functions is such that these interactions nearly vanish when the molecules are at their equilibrium position and it has been suggested that slight displacements from equilibrium, as in lattice vibrations, would result in large increases in these interactions. As stated in section (4), page (81), the angular oscillations of the molecule at $290^{\circ}K$ are approximately 3°, therefore, the resonance interactions have been calculated after rotating the molecule at $(\frac{1}{2}\underline{a}, \frac{1}{2}\underline{b}, \underline{c})$ through $\pm 2^{\circ}$. The results indicate that, although there is an increase in the interaction, the magnitude is such that the calculated mobility ratios are still far too low.

An alternative possibility is that carrier migration occurs via injection of carriers into higher conduction bands of sufficient width to support conduction on an appreciable scale. As can be seen from table (4.7) the band width of the second conduction band along the c' axis is several orders of magnitude larger than that of the first conduction band and this should result in a relatively high value for the mobility in this direction. The calculated mobility ratios of excess electrons in the second and third conduction bands are

given in table (4.9) from which it can be seen that the mobility of excess electrons along the $\underline{c}'$ axis is indeed much higher. To calculate the overall mobility ratios the relative number of carriers within each band is needed but this is unknown. However, 20% of the free electrons in the second conduction band would be sufficient to give the observed mobility ratio. Such a figure would give a value to the ratio $\dfrac{\mu_{aa}}{\mu_{bb}}$ of the order 1.4 which is still in reasonable agreement with experiment.

The effect of injecting electrons into higher conduction bands on the hole mobility ratios is rather complicated since it depends upon whether the electrons are injected from the first conduction band, in which case excess holes are created in the first conduction band, or injected directly from the valence band into the second conduction band. Generation of holes within the first conduction band by injection of electrons into higher conduction bands under the influence of an applied voltage has been suggested by Pope et al (9, 103). This effect should be particularly important in conduction along the c' axis since, due to the extreme narrowness of the energy band, acceleration of excess electrons under the influence of an applied field is practically impossible unless electrons are injected into a higher conduction band, the nearest of which is separated by about 2 eV. Direct injection of electrons into high energy conduction bands is known to occur via exiton-exiton and photon-photon annihilation processes (9, 106, 107). Under the conditions of Kepler's experiment the majority of carriers were generated by exiton-surface processes, however, exiton-exiton and photon-photon effects may have been present to a lesser extent. The effect of including these mechanisms of carrier production on the hole mobility ratios would be to increase $\dfrac{\mu_{aa}}{\mu_{bb}} \sim 0.6$ and $\dfrac{\mu_{c'c'}}{\mu_{bb}} \sim 0.3$, for screening parameter $\zeta = 30.7$ nm^{-1},

	2nd Cond.			3rd Cond.		
Vibrational Overlap	0.1	0.5	1.0	0.1	0.5	1.0
$\langle vbvb \rangle$*	0.550	13.942	54.928	1.179	30.626	127.83
$\langle vbvb/\underline{v}(\underline{k}) \rangle$**	0.326	1.690	3.390	0.526	2.739	5.707
$\dfrac{\mu_{aa}}{\mu_{bb}}$	1.141 (0.741)	1.005 (0.645)	0.937 (0.600)	0.318 (0.356)	0.287 (0.314)	0.255 (0.280)
$\dfrac{\mu_{cc}}{\mu_{bb}}$	2.491 (1.116)	2.171 (0.978)	2.030 (0.923)	0.449 (0.384)	0.484 (0.400)	0.508 (0.410)
$\dfrac{\mu_{ac}}{\mu_{bb}}$	-0.696 (-0.394)	-0.619 (-0.357)	-0.594 (-0.348)	-0.130 (-0.139)	-0.139 (-0.141)	-0.145 (-0.139)

(a)

	2nd Cond.			3rd Cond.		
Vibrational Overlap	0.1	0.5	1.0	0.1	0.5	1.0
$\langle vbvb \rangle$*	0.576	14.234	58.919	0.857	21.275	93.975
$\langle vbvb/\underline{v}(\underline{k}) \rangle$**	0.341	1.725	3.834	0.468	2.324	4.830
$\dfrac{\mu_{aa}}{\mu_{bb}}$	0.724 (0.561)	0.682 (0.519)	0.602 (0.434)	0.197 (0.203)	0.202 (0.207)	0.176 (0.195)
$\dfrac{\mu_{cc}}{\mu_{bb}}$	2.256 (1.109)	2.092 (1.023)	1.818 (0.836)	0.539 (0.424)	0.574 (0.443)	0.496 (0.424)
$\dfrac{\mu_{ac}}{\mu_{bb}}$	-0.588 (-0.356)	-0.546 (-0.338)	-0.470 (-0.275)	-0.130 (-0.120)	-0.137 (-0.124)	-0.122 (-0.122)

(b)

Table (4.9)

Calculated mobility ratios of excess electrons in the second and third conduction bands in crystalline anthracene computed in the mean free time and free path (in parentheses) approximations at $95°$ K (a) and $290°$ K (b) using Hueckel coefficients and screening parameter $\varsigma = 30.7$ $n\bar{m}'$.

* units: 1×6 m^2/sec^2

**units: 1×3 m/sec.

which are in good agreement with experiment.

4.5(iii)   Comparison of the results obtained using the modified (ζ = 24.6 nm^{-1}.) and normal (ζ = 30.7 nm^{-1}.) Slater functions to represent the $2p_z$ atomic wave functions.

The elements of the mobility tensor, calculated in the mean free time and free path approximations, without the premultiplicative factors $\dfrac{e \tau_0}{k_0 T}$ and $\dfrac{e \lambda}{k_0 T}$, along the $\underline{b}$ - axis and ratios of the non-zero elements of the tensor to this are given in table (4.10). Because of the relatively large band widths ($\sim$ 5 $k_0 T$ for vibrational overlap unity) obtained using the modified screening parameter, the mobility ratios show a much stronger dependence on the vibrational overlap factor than the same calculated using the normal Slater function. For a vibrational overlap factor 0.1 the mobility ratios of the excess hole and first conduction band show fair agreement with experiment. However, as with the normal Slater function the calculated mobility along the $\underline{c}'$ axis is too low by a factor of about 1000. For higher values of the vibrational overlap factor all the mobility ratios progressively increase so lessening the agreement with experiment.

As was discussed in the previous section, to explain the relatively large mobility along the $\underline{c}'$ axis, electronic conduction in higher energy bands must be assumed. The percentage of the total number of electrons which would need to be in the second conduction band to give the required mobility ratio is considerably higher than needed using the normal screening parameter ($\sim$ 50% as compared to 20%). However, the resulting values of the mobility ratios $\dfrac{\mu_{aa}}{\mu_{bb}}$ and $\dfrac{\mu_{c'c'}}{\mu_{bb}}$ of 1.87 and 0.45 are in good agreement with the experimental values of 1.7 and 0.4 (11). The effects on the hole mobility ratios would again be to bring them more in line with experiment.

	Hole			1st Cond.		
Vibrational Overlap	0.1	0.5	1.0	0.1	0.5	1.0
$\langle vbvb \rangle$*	10.222	186.960	501.360	13.818	150.710	299.130
$\langle vbvb/\underline{v}(\underline{k}) \rangle$**	1.394	5.868	9.237	1.809	5.292	7.024
$\dfrac{\mu_{aa}}{\mu_{bb}}$	0.385 (0.410)	0.387 (0.398)	0.424 (0.437)	1.616 (1.576)	2.609 (2.353)	3.656 (2.925)
$\dfrac{\mu_{cc}}{\mu_{bb}}$	0.647 (0.581)	0.709 (0.611)	0.816 (0.718)	0.001 (0.002)	0.003 (0.009)	0.007 (0.022)
$\dfrac{\mu_{ac}}{\mu_{bb}}$	-0.184 (-0.190)	-0.193 (-0.197)	-0.205 (-0.216)	-0.001 (-0.001)	-0.001 (-0.001)	-0.001 (-0.001)

	2nd Cond.			3rd Cond.		
Vibrational Overlap	0.1	0.5	1.0	0.1	0.5	1.0
$\langle vbvb \rangle$*	19.905	448.790	891.340	44.018	666.690	1890.600
$\langle vbvb/\underline{v}(\underline{k}) \rangle$**	1.908	8.669	9.908	2.916	10.856	15.766
$\dfrac{\mu_{aa}}{\mu_{bb}}$	2.124 (1.555)	1.342 (1.131)	1.521 (1.311)	0.967 (0.853)	1.029 (0.884)	1.841 (1.648)
$\dfrac{\mu_{cc}}{\mu_{bb}}$	0.929 (0.559)	1.189 (0.845)	2.185 (1.577)	0.207 (0.226)	0.341 (0.341)	0.460 (0.440)
$\dfrac{\mu_{ac}}{\mu_{bb}}$	-0.239 (-0.219)	-0.319 (-0.312)	-0.539 (-0.503)	-0.046 (-0.079)	-0.075 (-0.113)	-0.089 (-0.135)

Table(4.10)

Calculated mobility ratios of excess electrons and holes in crystalline anthracene computed in the mean free time and free path(in parentheses) approximations at 290°K using Hueckel coefficients and screening parameter $\mathfrak{z}$ = 24.6 nm^{-1}.

* units 10^6 m^2/sec^2 .

**units 10^3 m/sec.

4.5(iv)   Comparison of the results obtained using Hueckel and Mathur - Singh molecular orbitals.

It has been shown in section (5,i) that, using Hueckel molecular orbitals and a single Slater function with screening parameter $\zeta = 30.7$ nm^{-1}., mobility ratios in good agreement with those obtained experimentally are obtained. In order to test the molecular orbitals of Mathur and Singh, the calculations have been repeated using the transfer integrals computed using Mathur - Singh coefficients. The results for the valence and first conduction bands are given in table (4.11) and the same for the second and third conduction bands, including the effects of band mixing, are given in table (4.12).

If electronic conduction is considered to occur in the lowest conduction band only, then contrary to expectation, the use of the revised molecular orbital coefficients leads to a lower degree of agreement between theory and experiment. Inclusion of the second and third conduction bands in the transport scheme again results in considerable improvement in the overall values of the mobility ratios, however, to give an overall value for $\dfrac{\mu_{c'c'}}{\mu_{bb}}$ for excess electrons of 0.4, conduction would have to occur predominantly in the third conduction band which seems rather improbable.

4.5(v)   Temperature dependence

The temperature dependence of the mobility arises as a consequence of :

(a)   the temperature dependence of the relaxation time

(b)   changes in the transfer integrals arising from changes within the unit cell

(c)   changes in the distribution of carriers within the energy bands.

For vibrational overlap factor 0.1 the energy band widths of both electrons and holes at both temperatures are less than k_0T leading to

Vibrational Overlap	Hole			Electron		
	0.1	0.5	1.0	0.1	0.5	1.0
$\langle vbvb\rangle$*	0.344	6.822	19.906	1.159	18.309	47.101
$\langle vbvb/\underline{v}(\underline{k})\rangle$**	0.211	0.924	1.532	0.538	1.969	2.931
$\dfrac{\mu_{aa}}{\mu_{bb}}$	0.433 (0.439)	0.483 (0.487)	0.588 (0.592)	1.995 (1.653)	2.437 (1.955)	2.656 (2.086)
$\dfrac{\mu_{cc}}{\mu_{bb}}$	2.315 (1.651)	2.509 (1.726)	2.907 (1.919)	0.013 (0.016)	0.027 (0.039)	0.052 (0.081)
$\dfrac{\mu_{ac}}{\mu_{bb}}$	-0.621 (-0.522)	-0.681 (-0.554)	-0.803 (-0.630)	-0.012 (-0.014)	-0.019 (-0.026)	-0.030 (-0.045)

(a)

Vibrational Overlap	Hole			Electron		
	0.1	0.5	1.0	0.1	0.5	1.0
$\langle vbvb\rangle$*	0.412	9.910	37.492	0.933	19.670	62.083
$\langle vbvb/\underline{v}(\underline{k})\rangle$**	0.262	1.293	2.531	0.483	2.159	3.707
$\dfrac{\mu_{aa}}{\mu_{bb}}$	0.186 (0.195)	0.181 (0.189)	0.177 (0.183)	1.703 (1.539)	1.897 (1.692)	2.180 (1.898)
$\dfrac{\mu_{cc}}{\mu_{bb}}$	1.342 (1.026)	1.309 (0.990)	1.271 (0.950)	0.005 (0.007)	0.0ᴖ6 (0.009)	0.0ᴖ8 (0.013)
$\dfrac{\mu_{ac}}{\mu_{bb}}$	-0.326 (-0.281)	-0.317 (-0.271)	-0.308 (-0.260)	-0.006 (-0.008)	-0.007 (-0.009)	-0.0ᴖ8 (-0.011)

(b)

Table(4.11)

Calculated mobility ratios of excess electrons and holes in crystalline anthracene computed in the mean free time and free path(in parentheses) approximations at $95°$K (a) and $290°$K (b) using Mathur-Singh coefficients and screening parameter, $\varsigma = 30.7$ nm^{-1}.

* units: 1×6 m^2/sec^2.

**units: 1×3 m/sec.

	2nd Cond.			3rd Cond.		
Vibrational Overlap	0.1	0.5	1.0	0.1	0.5	1.0
$\langle vbvb \rangle$*	9.546	229.300	172.380	2.826	77.506	61.400
$\langle vbvb/\underline{v}(\underline{k}) \rangle$**	1.380	6.938	9.378	0.509	3.067	2.551
$\dfrac{\mu_{aa}}{\mu_{bb}}$	1.150	1.067	0.014	3.901	3.249	1.350
	(1.007)	(0.912)	(0.013)	(2.992)	(2.555)	(1.289)
$\dfrac{\mu_{cc}}{\mu_{bb}}$	0.249	0.210	0.010	1.038	0.995	2.201
	(0.202)	(0.166)	(0.010)	(0.656)	(0.649)	(1.704)
$\dfrac{\mu_{ac}}{\mu_{bb}}$	-0.028	-0.018	-0.002	-0.148	-0.161	-0.462
	(-0.055)	(-0.040)	(-0.003)	(-0.301)	(-0.210)	(-0.529)

(a)

	2nd Cond.			3rd Cond.		
Vibrational Overlap	0.1	0.5	1.0	0.1	0.5	1.0
$\langle vbvb \rangle$*	14.211	247.180	281.860	6.896	205.110	41.172
$\langle vbvb/\underline{v}(\underline{k}) \rangle$**	1.679	7.280	11.078	0.930	4.798	2.193
$\dfrac{\mu_{aa}}{\mu_{bb}}$	1.295	1.160	0.104	2.803	1.881	1.344
	(1.092)	(0.898)	(0.109)	(2.315)	(1.707)	(1.211)
$\dfrac{\mu_{cc}}{\mu_{bb}}$	0.196	0.127	0.012	0.675	0.938	2.734
	(0.154)	(0.098)	(0.148)	(0.473)	(0.776)	(1.858)
$\dfrac{\mu_{ac}}{\mu_{bb}}$	-0.017	-0.007	-0.001	-0.098	-0.213	-0.536
	(-0.042)	(-0.027)	(-0.003)	(-0.154)	(-0.324)	(-0.552)

(b)

Table(4.12)

Calculated mobility ratios of excess electrons in the second and third conduction bands in crystalline anthracene computed in the mean free time and free path(in parentheses) approximations at $95°K$ (a) and $290°K$ (b) using Mathur-Singh coefficients and screening parameter $\gamma = 30.7$ nm^{-1}.

* units: $1_{10}6$ m^2/sec^2.

**units: $1_{10}3$ m/sec.

an even distribution of carriers through the bands hence by using this value effect (c) can be eliminated. As previously stated in section (4.4) the unit cell constants show no discontinuous changes with temperature and it therefore seems reasonable to suppose that effect (b) leads to a temperature dependence of the type T^{-n}. Assuming for the moment that τ is constant over the temperature range $95^{\circ}K$ to $290^{\circ}K$ then for an excess electron in the first conduction band the contribution to the total temperature dependence of effect (b) is of the order $T^{-1.1}$ for excess electrons in the _ab_ plane.

Simplified calculations by Friedman (70), assuming acoustic phonon scattering, led to a temperature dependence for τ_0 of the type $T^{-1.0}$. Thus the predicted total temperature dependence should be approximately $T^{-2.1}$. A similar analysis using the elements of the mobility tensor for vibrational overlap factor unity lead to a temperature dependence in the _ab_ plane of the type $T^{-1.8}$. The latter value is in fair agreement with the observed value of Kepler (11) of $T^{-1.5}$.

Using similar arguments it can be shown that for excess holes effect (b) is highly anisotropic leading to total temperature dependence along the _a_ _b_ and _c'_ axes of $T^{-2.5}$, $T^{-2.0}$ and $T^{-2.3}$, respectively, for vibrational overlap factor 0.1, and $T^{-2.3}$, $T^{-1.2}$ and $T^{-1.4}$ for vibrational overlap factor unity. The predicted temperature dependence for hole conduction along the _c'_ axis is within the extremes of the reported values of $T^{-1.4}$ to $T^{-2.3}$ (14, 15, 16), however, Kepler (11) noted no observable anisotropy in the _ab_ plane. It is interesting to note that the anisotropy of the temperature dependence reflects the anisotropy of the thermal comparison coefficients, $\underline{\alpha}$, viz. $\alpha_a > \alpha_{c'} > \alpha_b$.

Similar trends are observed for the temperature variation computed using screening parameter $\zeta = 24.6$ nm^{-1} where the respective dependences along the a b and c' axes are :

$T^{-2.4}$, $T^{-1.8}$ and $T^{-2.1}$, for vibrational overlap factor 0.1, and $T^{-2.1}$, $T^{-0.6}$ and $T^{-2.1}$ for vibrational overlap factor unity.

For values calculated using the Mathur-Singh coefficients the predicted temperature dependences of both electrons and holes in the ab plane are similar to the values quoted above. However, for hole conduction along the c' axis the value $\sim T^{-4}$ is much higher than observed experimentally.

In the foregoing discussion the electronic conduction along the c' axis and the role of higher conduction bands in determining the temperature dependence has been omitted. The predicted temperature dependence of the mobility along the c' axis for the first conduction band is of the order T^{-3} whereas for the second and third conduction bands it is of the type T^{-2} , however, due to the relatively large band widths along the c' axis coupled with the close proximity of the two energy bands one would expect effect (a) to be of greater importance in the higher energy bands. Since, in general, effect (c) leads to a lowering of the overall temperature dependence this may be sufficient to reverse the sign of the temperature dependence for carriers in these bands.

4.5(vi)   Hall effect

The ratio of the Hall to drift mobility has been calculated in the manner outlined by Le Blanc (100).

Consider a one carrier zero transverse current Hall experiment in which the current Hall field and magnetic field vectors are parallel to the orthogonal axes a, b and c' respectively. Let the energy of the carrier of wave vector k be E(k) , its group

velocity $\underline{v}(\underline{k})$ and inverse effective mass $\underline{M}^{-1}(\underline{k})$ and assume that scattering can be accounted for with a relaxation time function $\tau(\underline{k})$. It can be shown that, for Boltzmann statistics, the ratio of Hall to drift mobilities along $\underline{a}$ is a function only of the direction of application of the applied magnetic field, B.

$$\mu^H/\mu_D \Big|_{B \parallel \underline{c}'} = \frac{k_0 T}{2} \frac{<<\tau^2 (v_a^2 M_{bb}^{-1} - 2v_a v_b M_{ab}^{-1} + v_b^2 M_{aa}^{-1})>>}{<<\tau v_a^2>> <<\tau v_b^2>>} \qquad (4.10)$$

The angular brackets indicate a statistical average over the Boltzmann distribution in $\underline{k}$ space.

For simplicity an abbreviated form of the anthracene band structure is considered which retains only those terms corresponding to intermolecular interactions between neighbours in the ab plane. Thus

$$E_{\pm}(\underline{k}) = 2E_3 \pm 4E_9 \cos(\tfrac{1}{2} \underline{k} \cdot \underline{a}) \cos(\tfrac{1}{2} \underline{k} \cdot \underline{b}) ,$$

where the symbols have their usual meanings.

Assuming the mean free time approximation to be valid then for $k_0 T >$ band width the above ratio reduces to

$$\mu_H/\mu_D \Big|_{B \parallel \underline{c}'} = -\frac{3}{2} k_0 T \ E_3/(2E_3^2 + E_9^2) \qquad (4.11)$$

from which it can be seen that the sign of the Hall effect is determined by the sign of the resonance integral between the molecule at the origin and that at position $(0, \underline{b}, 0)$. A more general calculation has been done by Hermann (104). His theoretical argument assumes the energy $E(\underline{k})$ to be a cosine function of $\underline{k}$ and for the extreme case of $\omega \ll k_0 T$ the ratio μ_H/μ_D becomes $-2.15 \ k_0 T$/band width which again predicts an anomalous Hall effect for narrow bands.

The ratios of the Hall to drift mobilities calculated using equation (4.10) are listed in table (4.13). The agreement between theory and experiment for both sets of molecular orbitals with $\zeta = 30.7$ nm^{-1} is good, however, the values calculated with the modified screening parameter are rather low. Le Blanc (100) has shown that the ratio μ^H/μ_D for $\underline{B}||\underline{a} \times \underline{b}$ is relatively insensitive to the band assymetry (i.e. the ratio E_3/E_9 but is very sensitive to the band widths. It therefore appears that the band widths calculated using the modified Slater function and S.C.F. atomic functions are too high, indicating that these wave functions over estimate the true wave function at large distances.

Because of the effects of band mixing it is not possible to determine the values of the Hall to drift mobilities by equation (4.11) in the higher bands. However, the energy bands along the $\underline{a}$ axis, figure (4.5), show either an increase in the second conduction band or a slight decrease in the third conduction band with increasing $\underline{k}$. The bands along the $\underline{b}$ axis show a very sharp decrease with increasing $\underline{k}$ indicating that E_9 is positive and E_3 more strongly negative, thus giving rise to an anomalous Hall effect in these bands. Injection of electrons into the second and third conduction bands will not alter the sign of the Hall effect, but if the electrons are injected from the first conduction band in the manner described by Sano (103), leaving behind an excess hole, the magnitude and possible sign of the Hall effect for excess holes will vary since holes in this band will have the opposite sign to those in the valence band. Such a change of sign has been observed for one of the carriers in crystalline anthracene, however, the sign of the carrier could not be determined (99).

The situation in the case of electron bands calculated using the Mathur-Singh molecular orbitals, figure (4.6), is not quite so straight-forward. Using arguments similar to those above one comes to the

Temp.	Vibrational Overlap	Hueckel = 30.7 nm		Hueckel = 24.6 nm		M-S = 30.7 nm		I	II	
		Electron	Hole	Electron	Hole	Electron	Hole	Hole	Electron	Hole
95 K	0.1	2.18	-6.45	0.91	-1.96	1.63	-13.94	-	-	-
	1.0	0.22	-0.65	0.09	-0.20	0.16	-1.39	-	-	-
290 K	0.1	9.77	-24.25	3.12	-6.97	10.17	-39.91	-25±10	13.6	-35.7
	1.0	0.98	-2.43	0.31	-0.70	1.02	-3.99			

Table(4.13)

Ratio of the Hall to Drift mobilities in crystalline anthracene.

I Figure taken from Ref(22).

II Figures calculated from data in Ref(99) assuming the mobility of excess electrons and holes in the ab plane to be 1.4_D-4 m /volt-sec(11) and the sign of the Hall effect to be anomalous(22).

conclusion that the magnitude of the Hall effect in the two bands is similar but of opposite sign. The separation of the energy bands, with vibrational overlap factor 0.1, is of the order k_0T at room temperature therefore both bands will be populated giving rise to a low value of the Hall constant.

4.6   Conclusion

The energy band structure and carrier mobilities in crystalline anthracene have been calculated in the tight binding approximation in which the wave function for a crystal containing an excess electron or hole is constructed using both Hueckel and Mathur - Singh molecular orbitals as a basis in constructing the Bloch sum. The wave functions constructed using Hueckel molecular orbitals give better agreement with experiment than their Mathur - Singh counterparts, although both predict a mobility along the $\underline{c}'$ axis several orders of magnitude lower than observed experimentally. Inclusion of higher energy bands in the transport mechanism can, under certain conditions, remove this apparent discrepancy.

CHAPTER (5)

Mobilities of excess electrons and holes in crystalline phenanthrene.

5.1 Introduction

The electrical properties of anthracene have been extensively studied both theoretically and experimentally and the molecule is now regarded as a test model for the investigation of semiconduction properties of aromatic hydrocarbons. Phenanthrene, a structural isomer of anthracene, on the other hand has received considerably less attention experimentally and no theoretical calculations relating to the mobility of excess carriers have been reported. It is the object of this chapter to investigate the electronic properties of phenanthrene and to determine whether any similarities exist between the two structural isomers.

In the absence of any conclusive data concerning the mechanism of charge carrier transport, calculations have been carried out in both the localized and Bloch representations.

5.2 Crystal and molecular wave functions

Phenanthrene crystallizes in a monoclinic lattice, space group $P2_1$, with two molecules per unit cell. The two molecules within the unit cell are related by a C_2 screw along the $\underline{b}$ axis, thus the elements of the space group are the identity, E, and the two fold rotation $C_2^{(b)}$. The point group containing these operations is C_2, therefore, using the methods given in Chapter (3), page (41), together with the character table of the point group C_2 it is easily shown that there are two symmetry adapted crystal wave functions, $\Omega_{\pm}(k)$, corresponding to the symmetric and antisymmetric combinations of the two molecular wave functions in the unit cell

$$\Omega_{\pm}(\underline{k}) = \sum_j (-1)^L \exp(i \, \underline{k} \cdot \underline{r}_j) \, \Psi j \qquad (5.1)$$

where L is 0 if the molecule j is related to the molecule at $(0, 0, 0)$ by a direct translation or 1 if the molecule is related by a screw axis

followed by the required translations, Ψ_j are taken to be antisymmetrized products of molecular wave functions in which one molecule is represented as either a positive or a negative ion and the summation over j runs over all molecules in the crystal. The structure of the molecular wave function Ψ_j, which includes the effects of molecular vibrations, has been discussed in Chapter (3), section (2), page (44), and will not be discussed further here.

The wave functions of the positive or negative ion were obtained in the same manner as those of naphthalene. However, in phenanthrene the second lowest molecular orbital is only separated from the lowest by 0.7 eV, hence the probability of electronic conduction occurring in energy bands other than the first will be much higher than in either anthracene or naphthalene where the energy difference of the two molecular orbitals is about 2 eV. Thus the excess electron is assumed to occupy either the lowest or second lowest antibonding molecular orbital; giving rise to two conduction bands, the centroids of which will be separated by about 0.7 eV. The close proximity of the two energy bands raises an additional problem which is not encountered in the instances of naphthalene and anthracene. The effects of coupling of the electrons with high frequency molecular vibrations is to split the energy bands into a series of vibrational sub bands corresponding to the different vibrational states of the molecular ion. These sub bands are separated by the vibrational quantum of the molecule which for aromatic hydrocarbons is of the order 0.2 eV, thus there exists the possibility of the third or fourth vibrational sub band of the lower energy band interacting with the zeroth vibrational component of the higher energy band. The vibrational overlap integrals for the phenanthrene molecular ions have not been evaluated, however, Miller and Murrell (131) have shown that use of a general Franck - Condon factor, equivalent to the square of the zeroth vibrational

overlap integral of the first electronic excited state of naphthalene as calculated by Jortner and Rice (74), gives good agreement between theoretically calculated and experimentally observed vibrational spectra of a series of aromatic hydrocarbons including phenanthrene. In addition there is very little difference between the zeroth, first and second vibrational overlap integrals for the first electronic excited state of anthracene and the corresponding integrals for naphthalene, thus it seems reasonable to assume that use of the vibrational overlap integrals of the naphthalene ion in calculations on phenanthrene will lead to only a small error. The sum of the squares of the zeroth, first and second vibrational overlap integrals for the naphthalene ion is 0.990, therefore, since the integrals must obey the vibration sum rule :

$$\sum_n |\langle \chi^0 | \chi^{\pm(n)} \rangle|^2 = 1.0 ,$$

the total sum of the remaining 33 ((3n - 6) - 3) vibrations must be 0.01 and hence the maximum value of the vibrational overlap integral for the third vibration state is 0.01.

The transfer integrals for the third vibrational sub band will thus be ~ $5_{10}-6$ eV. and the interaction of this band with the zeroth vibrational sub band of the second conduction band will be negligible.

5.3   Energy band structure

The relationship between the two molecules in the unit cell, together with some of the shorter intermolecular distances, is shown in figure (4.1).

Unlike anthracene neither of the two molecules in the unit cell
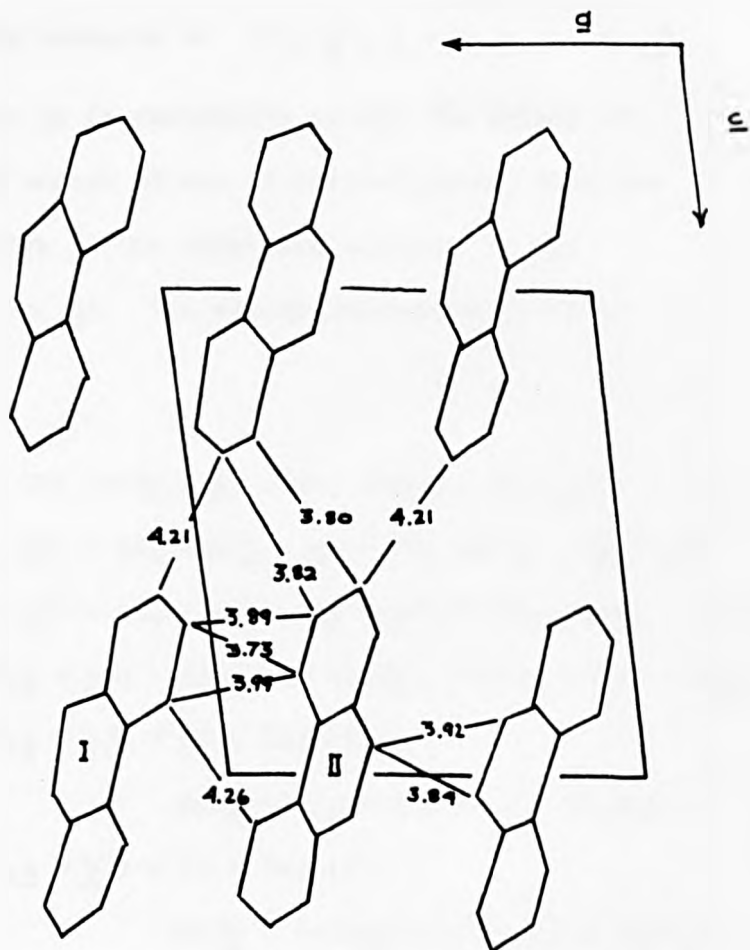
Figure (5.1)

Projection of the structure of Phenanthrene along the
b   axis showing short interactions. Molecules I and II
are related by a screw of b/2   along the b   axis.

is at the origin and if the geometrical centre of one molecule is denoted by $(x_0 \underline{a}, y_0 \underline{b}, z_0 \underline{c})$ then the vector connecting the origin to the centre of the remaining molecule is $(-x_0 \underline{a}, \frac{1}{2} + y_0 \underline{b}, - z_0 \underline{c})$.

In band structure calculations it is convenient to set the origin of the system at the geometrical centre of one of the molecules, thus the vector connecting the new centre to the remaining molecule in the unit cell is $(-2x_0 \underline{a}, \frac{1}{2}, -2z_0 \underline{c})$. The energy dependence on wave vector can then be written :

$$
\begin{aligned}
E'_{\pm}(\underline{k}) = \ & 2E_2 \, \cos(\underline{k} \cdot \underline{c}) + 2E_3 \cos(\underline{k} \cdot \underline{b}) + 2E_4 \cos(\underline{k} \cdot (\underline{b} + \underline{c})) \\
& + 2E_5 \, \cos(\underline{k} \cdot (\underline{c} - \underline{b})) + 2E_6 \cos(\underline{k} \cdot \underline{a}) + 2E_7 \cos(\underline{k} \cdot (\underline{a} + \underline{c})) \\
& + 2E_8 \, \cos(\underline{k} \cdot (\underline{a} - \underline{c})) + 2E_9 \cos(\underline{k} \cdot (\underline{a} + \underline{b})) + 2E_{10} \cos(\underline{k} \cdot (\underline{a} - \underline{b})) \\
& \pm \ E_{11}(\cos(\underline{k} \cdot (-2x_0\underline{a} + \underline{b}/2 - 2z_0\underline{c})) + \cos(\underline{k} \cdot (-2x_0\underline{a} - b/2 - 2z_0\underline{c})) \\
& \pm \ E_{12}(\cos(\underline{k} \cdot (-2x_0\underline{a} + \underline{b}/2 + (1 - 2z_0)\underline{c}) + \\
& \qquad\qquad\qquad \cos(\underline{k}(-2x_0\underline{a} - b/2 + (1 - 2z_0)\underline{c})) \\
& \pm \ E_{13}(\cos(\underline{k} \cdot (-2x_0\underline{a} + \underline{b}/2 - (1 + 2z_0)c) + \\
& \qquad\qquad\qquad \cos(\underline{k} \cdot (-2x_0\underline{a} - b/2 - (1 + 2z_0)\underline{c})) \\
& \pm \ E_{14}(\cos(\underline{k} \cdot ((1 - 2x_0)\underline{a} + \underline{b}/2 - 2z_0\underline{c}) + \\
& \qquad\qquad\qquad \cos(\underline{k} \cdot ((1 - x_0)\underline{a} - \underline{b}/2 - 2z_0\underline{c}))) \\
& \pm \ E_{15}(\cos(\underline{k} \cdot ((1 - 2x_0)\underline{a} + \underline{b}/2 - (1 + 2z_0\underline{c})) \\
& + \ \cos(\underline{k} \cdot ((1 - 2x_0)\underline{a} - b/2 - (1 + 2z_0\underline{c}))) \pm E_{16} (\cos(\underline{k}((1-2x_0)\underline{a} \\
& \qquad + b/2 + (1 - 2z_0)\underline{c})) + \cos(\underline{k} \cdot ((1 - 2z_0)\underline{a} - \underline{b}/2 + (1 - 2z_0\underline{c}))).
\end{aligned}
$$

$$(5.2)$$

The energy bands structure can be more readily visualized by considering the special cases where the wave vector, $\underline{k}$, is parallel to a reciprocal lattice vector, $\underline{a}^{-1}$, $\underline{b}^{-1}$ or $\underline{c}^{-1}$. The relationship between energy and wave vector is then

$$E'_{\pm}(\underline{k} \mid |\underline{a}^{-1}) = 2(E_3 + E_3 + E_4 + E_5) + 2(E_6 + E_7 + E_8 + E_9 + E_{10})\cos(\underline{k} \circ \underline{a})$$

$$\pm\, 2(E_{11} + E_{12} + E_{13})\cos(\underline{k} \circ 2x_0\underline{a})$$

$$\pm\, 2(E_{14} + E_{15} + E_{16})\cos(\underline{k} \circ (1 - 2x_0)\underline{a}).$$

$$E'_{\pm}(\underline{k} \mid |\underline{b}^{-1}) = 2(E_2 + E_6 + E_7 + E_8) + 2(E_3 + E_4 + E_5 + E_9 + E_{10})\cos(\underline{k} \circ \underline{b})$$

$$\pm\, 2(E_{11} + E_{12} + E_{13} + E_{14} + E_{15} + E_{16})\cos(\underline{k} \circ \underline{b}/2).$$

$$E'_{\pm}(\underline{k} \mid |\underline{c}^{-1}) = 2(E_3 + E_6 + E_9 + E_{10}) + 2(E_2 + E_4 + E_5 + E_7 + E_8)\cos(\underline{k} \circ \underline{c})$$

$$\pm\, 2(E_{11} + E_{14})\cos(\underline{k} \circ 2z_0\underline{c}) \pm 2(E_{12} + E_{16})\cos(\underline{k} \circ (1 - 2z_0)\underline{c})$$

$$\pm\, 2(E_{13} + E_{15})\cos(\underline{k} \circ (1 + 2z_0)\underline{c})$$

$$(5.3)$$

The transfer integrals, E_i, were calculated using equation (3.15) and equation (3.20) of Chapter (3) with single Slater functions, characterized by the normal, $\zeta = 30.7 \text{ nm}^{-1}$, and modified, $\zeta = 24.6 \text{ nm}^{-1}$, screening parameters to represent the carbon atomic wave functions. The molecular orbital coefficients were calculated in the Hueckel approximation without inclusion of overlap and assuming all carbon atoms equivalent. The transfer integrals, for vibrational overlap factor unity, together with the molecular overlap integrals (electronic) are given in table (5.1) and table (5.2) and the energy band structures, calculated using equation (5.3), are illustrated in figure (5.2).

The energy band structure of phenathrene is similar to that of anthracene showing considerable band splitting at $\underline{k} = 0$ and degeneracy of the two components of the energy band at $\underline{k} = \pi \underline{b}^{-1}$. However, since the phenanthrene crystal structure does not contain a $\underline{a}/2$ glide plane, the energy bands are not degenerate at $\underline{k} = \pi \underline{a}^{-1}$. The energy band widths, calculated using the modified and normal Slater screening parameters, together with the band splittings at

Position	Transfer	Overlap	Transfer	Overlap	Transfer	Overlap
0, 0, 1	-5.578	1.104	4.997	-0.883	1.192	0.603
0, 1, 0	113.972	-17.613	-32.399	7.755	-30.292	4.944
0, 1, 1	-0.148	0.005	0.017	-0.006	-0.060	0.002
0, -1, 1	0.024	-0.008	-0.018	0.006	-0.022	0.008
1, 0, 0	0.069	-0.0 1	0.074	-0.003	0.061	-0.001
1, 0, 1	0.003	-0.001	-0.003	0.001	0.087	-0.029
1, 1, 0	-	-	-	-	0.0 3	-0.001
-1, 1, 0	-	-	-	-	-	-
1, 1, 1	-	-	-	-	-	-
0, $\frac{1}{2}$, 0	-23.899	4.725	93.359	-17.0 1	75.247	-15.517
0, $\frac{1}{2}$, 1	0.005	-0.002	0.004	-0.0 2	-0.012	0.0 5
0, $\frac{1}{2}$, -1	0.632	-0.145	0.352	-0.085	-3.117	0.694
1, $\frac{1}{2}$, 0	-25.804	5.274	13.793	-1.079	43.017	-8.128
1, -$\frac{1}{2}$, -1	-	-	-	-	-	-
1, $\frac{1}{2}$, 1	-0.830	0.179	0.295	0.057	-0.054	0.070

Table(5.1)

Transfer* and Overlap** integrals for phenanthrene computed using single Slater functions with screening parameter ς = 30.7 nm^{-1}.

* units 1 $\times 10^{-4}$ eV.

** units 1 $\times 10^{-4}$.

Position	Transfer	Overlap	Transfer	Overlap	Transfer	Overlap
0, 0, 1	-23.013	4.292	14.369	-1.491	-9.890	0.084
0, 1, 0	338.307	-54.425	-127.914	15.319	-98.703	16.389
0, 1, 1	-0.280	0.093	0.386	-0.138	-0.589	0.011
0,-1, 1	0.447	-0.149	-0.256	0.077	-0.041	0.013
1, 0, 0	0.019	-0.003	0.226	-0.090	0.079	-0.037
1, 0, 1	0.100	-0.038	-0.090	0.033	1.315	-0.421
1, 1, 0	-0.039	0.019	-0.016	0.005	0.117	-0.074
-1, 1, 0	-0.010	-0.001	-0.022	-	-	-
1, 1, 1	0.014	-0.006	-0.006	0.003	0.003	-0.001
0, ½, 0	-128.967	-28.340	358.101	62.852	315.165	-51.527
0, ½, 1	0.125	0.047	0.091	0.032	-0.183	0.036
0, ½,-1	3.874	-0.833	2.436	0.538	-16.313	-3.304
1, ½, 0	-97.324	-15.454	20.649	3.606	168.834	-28.614
1, ½,-1	-0.011	-0.003	-0.011	-0.006	-0.011	0.004
1, ½, 1	-4.061	0.831	1.485	0.289	-2.353	0.637

Table(5.2)

Transfer* and Overlap** integrals for phenanthrene computed using single Slater functions with screening parameter ζ = 24.6 nm^{-1}.

* units 10^{-4} eV.

** units 10^{-4}.

(a)

(b)

(c)
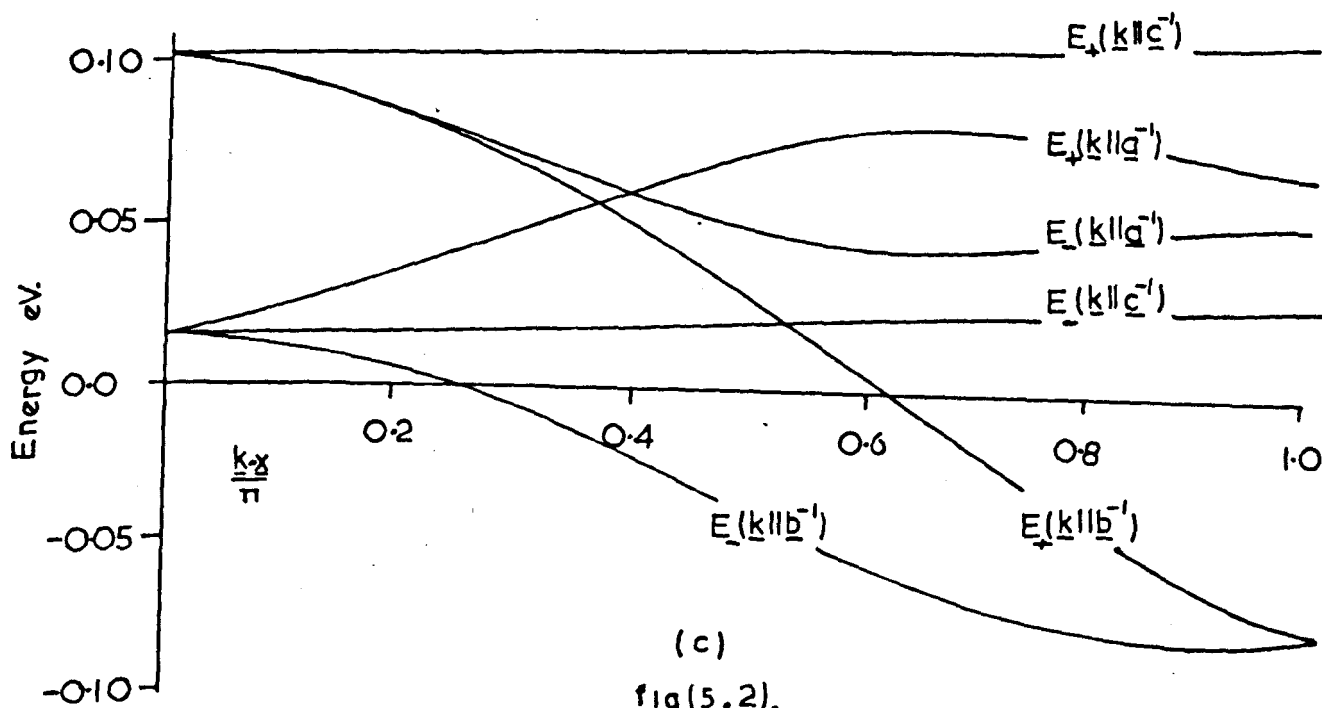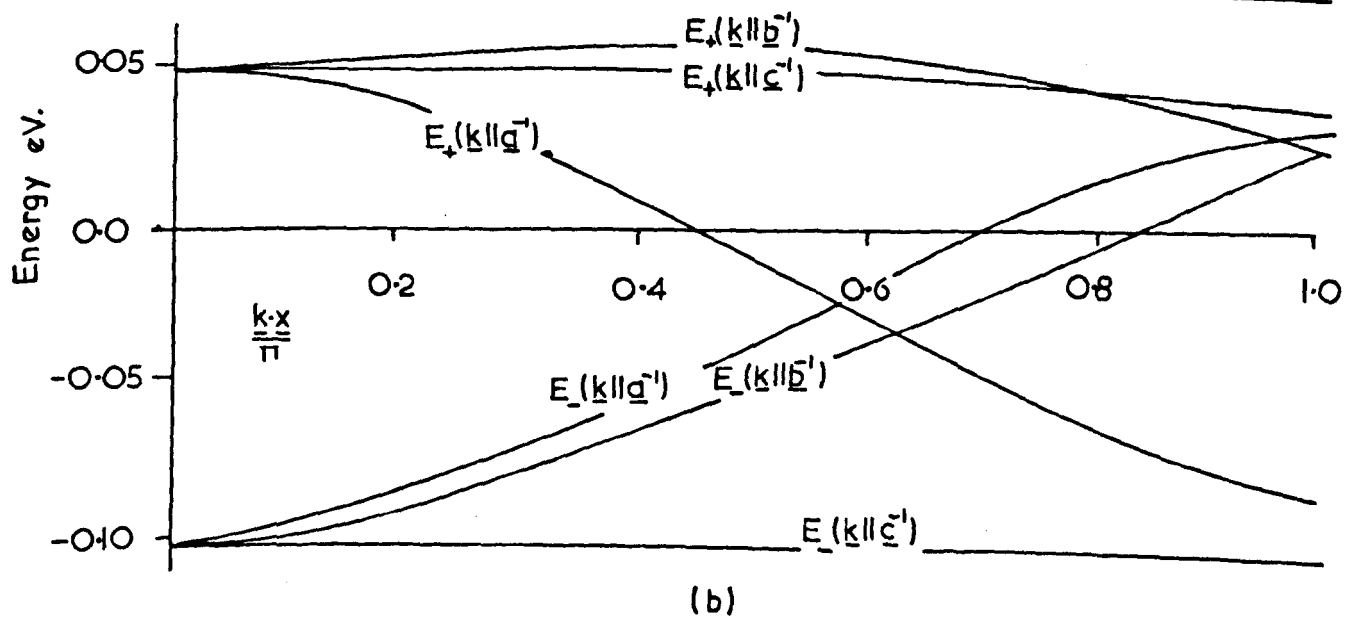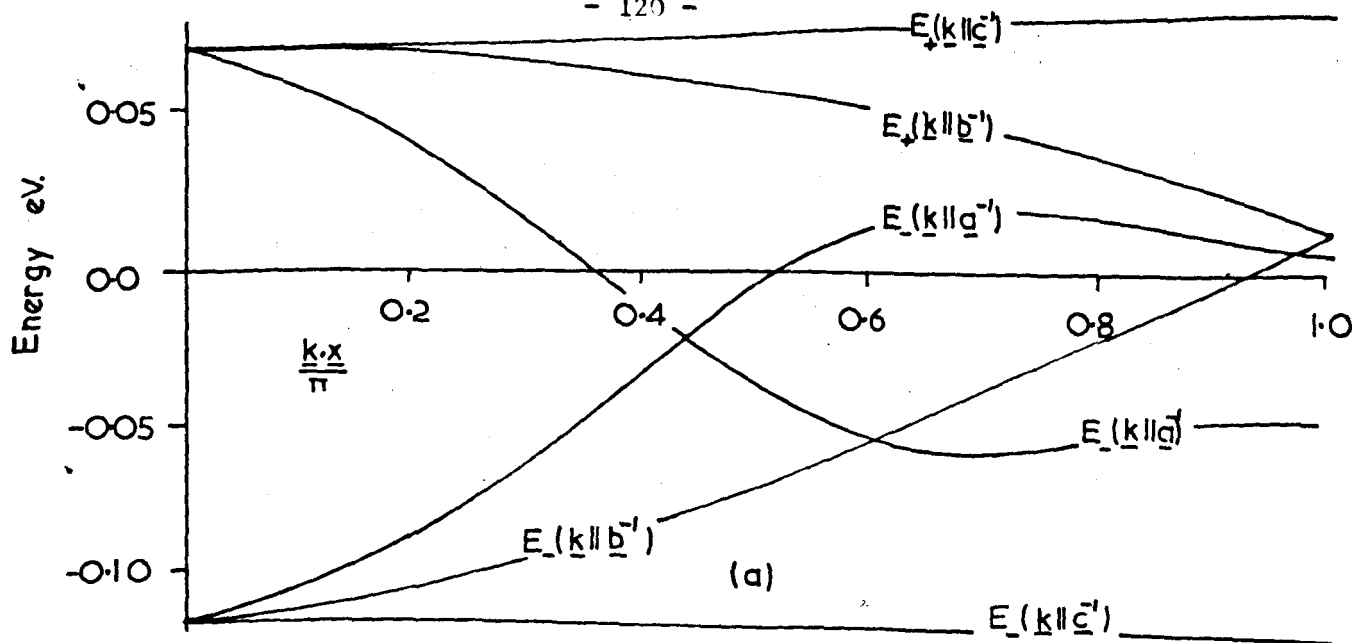
fig(5.2).

Energy band structure of excess hole (a), first (b) and
second (c) electron conduction bands in phenanthrene.

$\underline{k} = \pi \underline{a}^{-1}$ and $\underline{k} = \pi \underline{c}^{-1}$ are given in table (5.3). Note that the energy band widths quoted are for vibrational overlap unity. The polarizability of phenanthrene is extremely similar to that of anthracene (129), $2.5_{10}-2$ nm^3 compared to $2.4_{10}-2$ nm^3 and the crystal structures are not too different hence one would expect the polarization of the lattice by the excess electron or hole to be similar for the two crystals. Glaeser and Berry (44) have shown that the effects of including polarization is to reduce the transfer integrals almost linearly by a factor of 2. The vibrational overlap integrals for phenanthrene are not known, however, by comparison with naphthalene and anthracene the effects of intermolecular vibrations is to reduce the band widths linearly by factors of 0.6, 0.3 and 0.1 for the zeroth, first and second sub vibrational bands, hence the true band widths will be those given in table (5.3) multiplied by factors of 0.3, 0.15 and 0.05 for the first three vibrational levels. Thus for the lowest vibrational state the average energy band widths in the $\underline{ab}$ plane for all three sets of energy bands are 0.008 eV, using screening parameter $\zeta = 30.7$ nm^{-1}, and 0.032 eV for the modified parameter, while the band widths perpendicular to this plane are approximately an order of magnitude smaller. This is more or less what one would expect on the basis of crystal structure since the short internuclear distances, and hence large interactions, are predominantly between molecules which promote carrier transport in the $\underline{ab}$ plane.

5.4   Mobility tensor

5.4(i)   Carrier mobilities in the energy band approximation

The components of the mobility tensor, μ_{ij}, can be computed from the energy band structure using either the mean free time or mean free path approximations (132), through the relations :

	Normal			Modified		
	Hole	1st Cond	2nd Cond	Hole	1st Cond	2nd Cond
$E(\underline{k} \parallel \underline{a}^{-\prime})$ +	0.94	3.61	3.36	11.77	13.83	4.95
$E(\underline{k} \parallel \underline{a}^{-\prime})$ −	0.94	3.60	3.26	11.66	13.82	5.05
$E(\underline{k} \parallel \underline{b}^{-\prime})$ +	3.54	0.86	1.09	5.36	2.54	9.00
$E(\underline{k} \parallel \underline{b}^{-\prime})$ −	5.54	3.45	3.51	13.25	12.46	18.05
$E(\underline{k} \parallel \underline{c}^{-\prime})$ +	0.24	0.23	0.07	1.08	0.75	0.92
$E(\underline{k} \parallel \underline{c}^{-\prime})$ −	0.22	0.17	0.17	0.35	0.40	0.90
splitting at $\underline{k}.\underline{a} = \pi$	0.13	2.90	4.85	4.83	12.35	0.86
splitting at $\underline{k}.\underline{c} = \pi$	1.98	4.25	0.96	12.07	14.96	9.03

Table(5.3)

Energy bandwidths* in crystalline phenanthrene computed using single Slater functions with the normal($\mathcal{T}= 30.7$ nm^{-1}.) and modified($\mathcal{T}= 24.6$ nm^{-1}.) screening parameters. Vibrational over lap factor unity.

* units 1$_{10}$-2 eV.

$$\mu_{ij} = e \, \tau_0 \, <<v_i \, v_j>>/k_0 T \qquad (5.4)$$

and

$$\mu_{ij} = e \, \lambda \, <<v_i \, v_j/\underline{v}(\underline{k})>>/k_0 T \qquad (5.5)$$

where the symbols have their normal meanings (132). The components of the mobility tensor, without the constant multiplicative factors $e \, \tau_0/k_0 T$ and $e \, \lambda/k_0 T$, along the $\underline{b}^{-1}$ axis together with the ratios of the components along the $\underline{a}^{-1}$ and $\underline{c}'^{-1}$ axes to this are given in table (5.4).

Studies on anthracene (133) have shown that the uncertainty principle as formulated by Fröhlich and Sewell (84) is not violated and, in view of the close similarities between anthracene and phenanthrene both structurally and crystallographically, one might expect a similar situation to exist in phenanthrene. However, in addition to normal carrier - phonon scattering there is an additional problem of electron - dipole interactions which could, if of significant magnitude, reduce the mean free path to below the lattice spacing. Phenanthrene crystals are known to be piezo electric (136) an effect for which a necessary, but not sufficient, condition (135) is that a system of induced or permanent dipoles exist in an arrangement lacking central symmetry. An estimate of the value of the effective dipole moment in the crystal is $\sim 1_{10}\!-3$ D (129), hence electron - dipole interaction in phenanthrene will be of a similar order of magnitude to electron - induced dipole interactions in anthracene which have been shown to be small (44). In addition the experimentally observed trap density in phenanthrene is very similar to that of anthracene, and, as the energy band model is applicable to anthracene, it appears reasonable to assume it will also be applicable to phenanthrene. This is substantiated by the observed value of $\sigma_{solid}/\sigma_{liquid}$ which indicates that the conductivity is much higher in the solid than in

Vibrational Overlap	Hole.		1st. Cond.		2nd. Cond.	
	0.1	1.0	0.1	1.0	0.1	1.0
$\langle vbvb \rangle$*	2.497	213.809	0.425	49.596	0.361	42.219
$\langle vbvb/\underline{v}(\underline{k}) \rangle$**	1.020	8.618	0.229	2.533	0.223	2.474
$\underline{\mu}_{aa}$	0.148	0.220	9.368	8.492	7.981	7.168
μ_{bb}	(0.199)	(0.335)	(5.749)	(5.359)	(4.978)	(4.605
$\underline{\mu}_{cc}$	0.011	0.014	0.044	0.037	0.028	0.027
μ_{bb}	(0.021)	(0.028)	(0.043)	(0.035)	(0.020)	(0.021)
(μ_{aa})min.***	0.05	0.65	0.47	5.60	0.39	4.15
	(0.06)	(0.92)	(0.29)	(4.34)	(0.35)	(3.64)
(μ_{bb})min.	0.33	2.96	0.05	0.66	0.05	0.58
	(0.32)	(2.76)	(0.07)	(0.81)	(0.07)	(0.79)
(μ_{cc})min.	0.004	0.040	0.002	0.020	0.010	0.020
	(0.003)	(0.040)	(0.004)	(0.030)	(0.001)	(0.020)

Table(5.4)

Mobility ratios and minimum values of the mobility, computed in the mean free time and free path(in parentheses) approximations using single Slater functions with ς = 30.7 nm^{-1}., in crystalline phenanthrene.

* $1_{10}6$ m^2/sec .

** $1_{10}3$ m/sec.

*** $1_{10}-4$ $m^2/volt$-sec.

	Hole.		1st. Cond.		2nd. Cond.	
Vibrational Overlap	0.1	1.0	0.1	1.0	0.1	1.0
$\langle vbvb \rangle$*	22.07	1029.89	6.73	621.45	0.93	592.86
$\langle vbvb/\underline{v}(\underline{k}) \rangle$**	2.65	12.52	0.93	8.38	5.32	10.21
$\underline{\mu_{aa}}$	0.45	1.23	8.85	8.09	5.42	6.17
μ_{bb}	(0.52)	(1.68)	(5.42)	(5.64)	(9.43)	(3.38)
$\underline{\mu_{cc}}$	0.01	0.03	0.03	0.03	0.03	0.02
μ_{bb}	(0.02)	(0.07)	(0.03)	(0.02)	(0.04)	(0.02)
(μ_{aa})min.***	0.36	4.58	2.12	18.11	6.22	14.80
	(0.44)	(6.75)	(1.62)	(15.17)	(16.13)	(11.07)
(μ_{bb})min.	0.80	3.73	0.24	2.24	0.04	2.41
	(0.85)	(4.02)	(0.30)	(2.69)	(1.70)	(3.28)
(μ_{cc})min.	0.01	0.13	0.01	0.06	0.00	0.05
	(0.02)	(0.29)	(0.01)	(0.06)	(0.06)	(0.06)

Table(5.5)

Mobility ratios and minimum values of the mobility, computed in the mean free time and free path(in parentheses) approximations using single Slater functions with $\overline{s}$ = 24.6 nm^{-1}., in crystalline phenanthrene.

* 1×6 m^2/sec .

** 1×3 m/sec.

*** 1×-4 $m^2/volt\text{-}sec$.

the liquid. The observed value of $\sigma_{solid}/\sigma_{liquid} = 32$, determined [135] on a close packed polycrystalline sample, is similar to that of naphthalene obtained under similar conditions. The value obtained on single crystals of naphthalene is several orders of magnitude higher than obtained using polycrystalline samples and a similar effect might be expected for phenanthrene. Since the density of phenanthrene increases slightly on melting, the decrease in conduction is not due to larger internuclear distances and appears to be a result of the breakdown in the periodic structure of the crystal lattice. Conduction occurring via a wavelike motion is dependent upon the translational symmetry, of the lattice, therefore, any reduction in this symmetry, as in the case of melting, will considerably reduce the mobility of carriers. Conversely carrier transport due to a hopping motion does not rely on the translational symmetry and should thus be about equally effective for both liquids and solids (57). If the energy band model is applicable to the conduction mechanism of crystalline phenanthrene the uncertainty principle can be rephrased to yield approximate values of the scattering constants τ_0 and λ. Thus in the mean free time approximation the average band width, B, is related to the mean free time, τ_0, through :

$$\tau_0 > h/B \qquad (5.6)$$

Substitution of equation (5.6) into equation (5.4) gives :

$$\mu_{ii} > \frac{e\,h}{k_0 TB} <<v_i \, v_i>> \qquad (5.7)$$

Similarly, in the mean free path approximation the mean free path, λ, must be greater than the lattice spacing, a, hence, assuming λ to be isotropic and equal to the average of the lattice constants,

equation (5.5) becomes

$$\mu_{ii} > \frac{e \; a}{k_0 T} \; <<v_i \; v_i / \underline{v}(\underline{k})>> \qquad (5.8)$$

The values of the minimum mobility calculated using equation (5.7) and
equation (5.8) are shown in table (5.3).

The mean square velocities $<<v_i \; v_i>>$ and the velocity components
$<<v_i \; v_i / \underline{v}(\underline{k})>>$, calculated using vibrational overlap factor 0.1, are
similar to the corresponding values for anthracene. However, these
values show a much larger increase with increase in vibrational
overlap which results in the minimum values of the mobility, for
vibrational overlap unity, being much greater than the observed
value in anthracene. As was discussed in section (3) the effects
of coupling of the excess carriers with high frequency intramolecular
vibrations, together with polarization of the crystal by the excess
charge, serve to reduce the transfer integrals by a factor ~ 0.3.
The resultant values of the average mobility of excess electrons and
holes in the ab plane are 1.0 (6.0) and 0.6 (1.4) cm^2/volt.sec.,
respectively, while perpendicular to the ab plane the corresponding
mobilities are 0.01 (0.02) and 0.01 (0.04) cm^2/volt.sec. Thus the
mobility ratio, $\mu_{||ab} / \mu_{\perp ab}$ ~ 100 for excess electrons and ~ 60 for
excess holes, is rather larger than the value ~ 30 obtained from
the resistivity measurements of Matsumoto and Tsukada (127). However,
bearing in mind that a slight anisotropy in the energy gap, E , results
in massive changes in the anisotropy of the resistivity, ρ , the
agreement between theory and experiment is not as bad as might appear
at first sight.

5.4(ii) Carrier mobilities in the localized representation

The carrier mobilities in phenanthrene were calculated on the
Gleaser - Berry model (44) using a modification of the program outlined
in appendix (3).

The probability distributions, $\tau(\underline{r}_i)$, jump frequencies, $1/t_i$, and diagonal elements of the mobility tensor, computed using the transfer integrals of table (5.1), are given in table (5.7). The average values for the mobility in the ab plane and the mobility perpendicular to this plane are given in table (5.6) where they are compared to the corresponding values for anthracene calculated on the same model.

		Phenanthrene				Anthracene		
		Hole	Electron 1	Electron 2	Hole	Electron		Exp.
μ_{ab} (a)	I	0.281	0.321	0.218	0.118	0.288	1.5	1.4
	II	0.826	1.375	0.889	0.390	0.940		
$\mu_{c'c'}$	I	0.058	0.045	0.029	0.149	0.008	0.8	0.4
	II	0.206	0.164	0.186	0.688	0.053		

Table (5.6)

Calculated values of the mobilities in phenanthrene and anthracene computed in the simple hopping model.

(a)   units : $1_{10}-4$ m^2/volt.sec.

I   transfer integrals calculated using $\zeta = 30.7$ nm^{-1}

II   transfer integrals calculated using $\zeta = 24.6$ nm^{-1}

The calculated anisotropy of the carrier mobilities is much less than that obtained using the energy band model,   the predicted values of the mobilities in the ab plane being ~ twice that of anthracene, i.e. ~ 3 cm^2/volt.sec., while perpendicular to the ab plane the average mobility is ~ $\frac{1}{2}$ that of anthracene, giving a mobility anisotropy, $\mu_{//ab}/\mu_{\perp ab}$, of ~ 6. This is much lower than that obtained experimentally.

Position	Hole (ri)	1/ti	Electron 1 (ri)	1/ti	Electron 2 (ri)	1/ti
0,0,1	0.033	0.540	0.034	0.483	0.008	0.115
0,1,0	0.667	11.025	0.223	3.134	0.198	2.930
0,1,1	0.001	0.014	-	0.002	-	0.006
0,½,0	0.140	2.312	0.643	9.031	0.492	7.279
1,½,0	0.151	2.496	0.095	1.334	0.281	4.161
0,½,-1	0.004	0.061	0.002	0.034	0.021	0.307
1,½,1	0.005	0.080	0.002	0.029	-	0.005
Average jump frequency	2.361		2.007		2.115	
No. of jumps	8.073		6.649		5.366	
μ_{aa}**	0.12		0.44		0.28	
μ_{bb}	0.44		0.20		0.16	
μ_{cc}	0.06		0.05		0.03	

(a)

Position	Hole (ri)	1/ti	Electron 1 (ri)	1/ti	Electron 2 (ri)	1/ti
0,0,1	0.039	2.226	0.027	1.390	0.016	0.957
0,1,0	0.568	32.726	0.244	12.374	0.161	9.548
0,1,1	-	0.027	-	0.013	0.001	0.057
0, ,0	0.216	12.476	0.682	34.641	0.515	30.487
1, ,0	0.163	9.415	0.039	1.997	0.276	16.332
0, ,-1	0.0 7	0.375	0.005	0.236	0.027	1.578
1, ,1	0.0 7	0.393	0.003	0.144	0.004	0.228
Average jump* frequency	8.234		7.256		8.455	
No. of jumps	22.911		26.756		25.810	
aa**	0.53		1.89		1.21	
bb	1.12		0.84		0.59	
cc	0.21		0.16		0.19	

(b)

Table(5.7)

Jump probabilities, τ (ri), jump frequencies*, 1/ti, and mobilities in crystalline phenanthrene, computed using single Slater functions with screening parameters $\varsigma = 30.7$ nm^{-1}.(a) and $\varsigma = 24.6$ nm^{-1}.(b).

*units 1x12 sec^{-1}. **units 1x-4 m^2/volt-sec.

5.5 Comparison of phenanthrene with anthracene.

The resistivity anisotropy of phenanthrene was first studied by Matsumoto and Tsukada (127). They obtained resistivity values of $4.8_{10}15$ and $1.9_{10}14$ Ω-cm along the ab plane and perpendicular to the ab plane respectively at 288°K. Since, within the limits of experimental error, the energy gap was isotropic, having a value of 1.14 eV, they argued that the anisotropy resulted from an isotropy in the mobility tensor. The theoretical calculations reported in the previous section substantiate this reasoning. Using the above values of the resistivity and energy gap Matsumoto and Tsukada estimated the pre-exponential factor, ρ_0, to be $1.8_{10}4$ in the ab plane and $6.0_{10}4$ perpendicular to the ab plane, while the corresponding values for anthracene are seven orders of magnitude lower (189). Later studies (128, 129) cast some doubt on the purity of the crystals used in the experiment. Matsumoto (128) obtained a value for the resistivity in the ab plane of $5_{10}13$ Ω-cm while Arndt and Damask obtained a value of $9.2_{10}14$ Ω-cm perpendicular to the ab plane, thus confirming the observed anisotropy of Matsumoto and Tsukada. However, Arndt and Damask showed the log (resistivity) vs 1/T curve to consist of two straight lines of slope 1.5 eV. (T < 345°K) and 1.1 (T > 345°K). This change of gradient was accompanied by an order of magnitude decrease in the resistivity and controlled experiments on impure crystals led to a decrease and finally elimination of the effect resulting in the Matsumoto - Tsukada result. Using the Arndt and Damask values for the resistivity and energy gap the estimated value of ρ_0 in the ab plane is 0.07 Ω-cm which is within an order of magnitude of the corresponding value for anthracene.

5.6 Comments on the polarization phenomena observed in high purity phenanthrene crystals.

In this section suggestions are put forward as to the origins of the polarization phenomena observed experimentally by Arndt and Damask (129).

All experimental data quoted is taken from their paper unless otherwise stated.

The observed phenomena have been described in terms of reversible and irreversible polarization states. Crystals in the reversibly polarized states were obtained by heating the crystals to temperatures above $345^{\circ}K$ and then allowing them to cool in the presence of an applied field. Above $345^{\circ}K$ the current due to dark conductivity was observed, however, at $345^{\circ}K$ a current pulse was emitted (see figure (5.3))
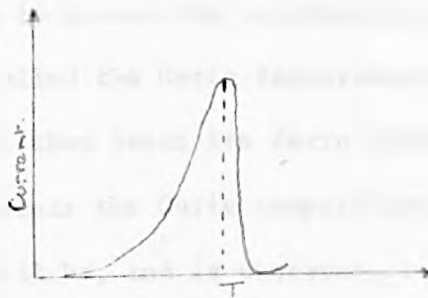
Figure (5.3)

which decreased approximately exponentially with temperature. Various other experiments were performed using different voltage bias and in all cases the current showed a pulse with a maximum at $345^{\circ}K$. From the area under the curve the charge release was calculated to be of the order $2_{10}-10$ coulombs.

Crystal without a centre of symmetry can show electrical polarization in the absence of an applied external field because of the alignment of electrical, or induced dipoles. Such polarization will not be observed under static conditions because the polarization charges are compensated by free charges. However, change of temperature will cause a change in polarization and hence some of the free carriers are liberated giving rise to a current. Such crystals are called pyro electric. If the crystals allow their spontaneous polarization to be reversed in polarity by an external field the crystals are termed Ferro electrics. The observed phenomena suggests

that phenanthrene is either pyro or ferro electric.

Phenanthrene is known to be piezo electric (136) with a piezo electric coefficient about equal to that of quartz and it is noted that substances which exhibit piezo electric phenomena often also exhibit ferro electric phenomena. A ferro electric crystal usually contains domains, that is a large number of aligned dipoles. The direction of the aligned dipoles is different in different domains and the orientation of the dipoles is opposed by thermal motion. As the temperature is increased the alignment is disturbed and at a certain temperature, called the Curie temperature, becomes completely random and the crystal then loses its ferro electric properties. Thus, if $T = 345^{o}K$ represents the Curie temperature, above this normal dark conductivity will be, and is observed.

Generally in a ferro electric material the symmetry is lower below the Curie point as the material must be polar, whereas above the Curie point it may not necessarily be polar. Hence many ferro electrics show a transition entropy which will be reflected in the heat capacity. A heat capacity anomoly has been observed in phenanthrene (129, 130) which shows a maximum of 340 cals./mole. at $345^{o}K$.

Crystals illuminated with intense white light for several minutes, and then heated with a biasing field, showed in addition to the reversible polarization, other, more permanent phenomena. A crystal in the irreversible polarized state changes to a dielectric, which suggests that polarization is largely in one direction. In addition neither chemical etching nor cleaving of the crystal impairs this ability to cling to the dielectric. This directional polarization suggests that the crystals are electrets, i.e. the electrical analogue of a magnet. Such persistent internal polarization phenomena has also been observed in benzene (137), naphthalene (138, 139) and anthracene (140 - 143).

Conclusion

The energy band structure of phenanthrene has been calculated using the tight binding model. The calculated energy band widths in the _ab_ plane, assuming vibrational overlap unity, are of a similar magnitude to anthracene being 0.055 (0.210) eV. and 0.057 (0.213) eV. for the valence and first conduction bands, respectively, while perpendicular to this plane they are an order of magnitude lower. The above figures refer to values calculated using single Slater functions with $\zeta = 30.7$ nm^{-1} and $\zeta = 24.6$ nm^{-1} (in parentheses). Coupling of the excess carriers with high frequency intramolecular vibrations and polarization effects are estimated to reduce the above band widths by a factor of about $\frac{1}{3}$. The energy band widths of the second conduction band, which is centred approximately 0.7 eV. above the first, are at a similar magnitude and show the same degree of anisotropy as the first conduction band.

The ratio of the mobility of carriers moving perpendicular to and parallel to the _ab_ plane have been calculated in both the energy band and simple hopping models. The magnitude of the mobility in the _ab_ plane is predicted to be about twice that of anthracene, i.e. ~ 3 cm^2/volt.sec., on both models, however, the anisotropy is considerably lower on the hopping model. For the energy band model

$$\mu_{\parallel \underline{ab}} \sim 100 \ \mu_{\perp \underline{ab}}$$

and in the hopping model

$$\mu_{\parallel \underline{ab}} \sim 6 \ \mu_{\perp \underline{ab}}$$

whereas the ratio calculated from resistivity studies is

$$\mu_{\parallel \underline{ab}} \sim 30 \ \mu_{\perp \underline{ab}} \qquad .$$

The available data on phenanthrene has been reviewed in the light of the calculated mobilities and the comparisons with anthracene are more pronounced than indicated by the work of Matsumoto and Tsukada (127).

CHAPTER (6)

The energy band structure and carrier mobilities in some condensed aromatic hydrocarbons.

6.1   Introduction.

6.2   Energy band structure.

6.3   Mobility tensor.

6.4   Orientation of the principle axes of the mobility tensor.

6.5   Comparison of theory with experiment.

6.6   Conclusion.

6.1 Introduction

The lower molecular weight aromatic hydrocarbons are characterised by low mobilities, high resistivities and large energy gaps. At the upper extreme in condensation of benzene rings is graphite, characterised by a relatively high mobility, which shows a high degree of anisotropy, low resistivities and low energy gaps. Intermediate between these two extremes are the condensed aromatic hydrocarbons coronene ($C_{24}H_{12}$), ovalene ($C_{32}H_{14}$) and circumanthracene ($C_{40}H_{16}$). The interplanar distance in these molecules is very similar to the graphite value of 0.335 nm. and as can be seen from figures (6.1) and figure (6.2) the normal projection of two parallel molecules shows a marked resemblence to the graphite structure as viewed along the c -axis. It seems reasonable, therefore, to expect those molecular crystals to have an appreciable value for the mobility.

No mobility measurements have been reported in the literature for any of the above compounds although values for the resistivity and energy gaps have been determined (190 - 196), and these are listed in Table (6.1) along with the methods of measurement.

Table (6.1)

Molecule	Resistivity (Ω cm)	ΔE(eV)	Method of measurement	Ref.
Coronene	$1.7_{10}17$	1.7	compressed powder	190
	$1.0_{10}18$	1.6	deposited film	190
		2.3	compressed powder	191
		2.55	evaporated film	192
	$1_{10}17 - 1_{10}18$	1.60	evap.film - sand.cell	193
	$1_{10}12 - 1_{10}13$	1.65	" " - surf.cell	193
Ovalene	$2.3_{10}15$	1.13	compressed powder	194
	$2.3_{10}15$	1.14	compressed powder	195
	-	2.0	evaporated film	192
Circumamthracene	$6.0_{10}12$	1.8	single crys.$\parallel$ b axis	196
	$2.5_{10}13$	1.9	evap.film - surf.cell	
	$1.0_{10}16 - 1.0_{10}17$	1.7	evap.film - sand.cell	

Experimental data on coronene, ovalene and circumanthracene.

c
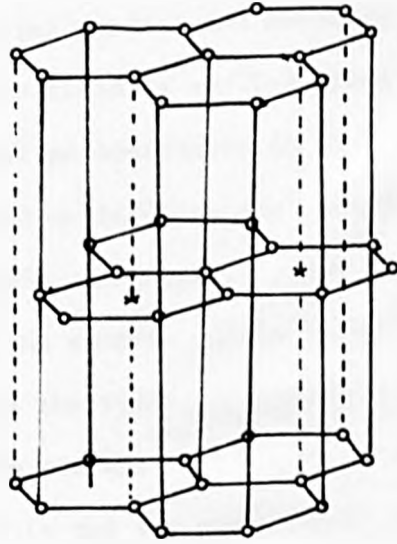
Figure (6.1)

Crystal structure of ideal graphite.
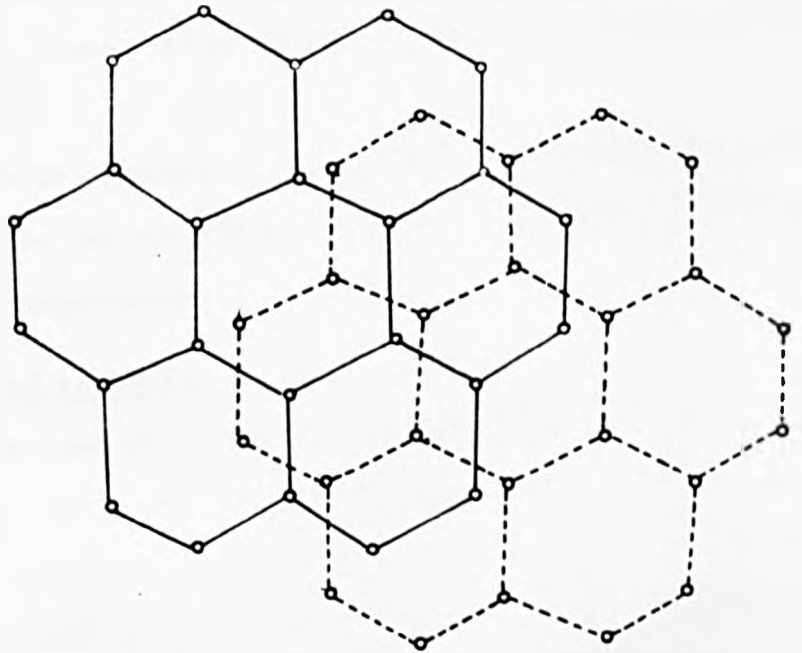
Figure (6.2)

Normal projection of two parallel molecules of ovalene.

An approximate value for the anisotropy in coronene and circumanthracene can be obtained by comparing the values of the resistivities obtained using surface and sandwich cells. In the former method the electric field is applied along the surface of the film and in the latter perpendicular to it. Electron micro diffraction and X-ray studies indicate that the films consist of a number of single crystals, arranged in close packing, with their ab planes parallel to the surface of the film. Hence, the sandwich cell effectively measures the resistance along the $\underline{c}'$ axis while the surface cell measures the average resistance in the ab plane. Since the energy gaps obtained in the two experiments are very similar it seems reasonable to suppose that the carrier density is fairly isotropic. Therefore, an order of magnitude value of the mobility ratio in the $\underline{ab}$ plane to that along the $\underline{c}'$ axis can be obtained from the ratios of the corresponding conductivities indicating that the mobility along the $\underline{c}'$ axis is several orders of magnitude less than in the ab plane. No anisotropy values have been reported for the ab plane.

It is thus the purpose of this chapter to calculate the energy band structure and the anisotropy of the mobility tensor in coronene, ovalene and circumanthracene.

6.2   Energy band structure

The energy band structure of circumanthracene has been reported by Harada et al (197). The transfer integrals were calculated using single Slater functions to represent the carbon $2p_z$ atomic wave function, the normal Goeppert - Meyer and Sklar potential (202), and atomic coordinates constructed from the atomic coordinates of coronene (199) and the unit cell data of Robertson et al (198). Unfortunately the Geoppert - Meyer and Sklar potential does not

include the effects of electron exchange and the contribution of these terms to the transfer integral are far larger than their coulombic counterparts. In the following sections an attempt is made to obtain an order of magnitude correction for the exchange contributions to the original integrals of Harada. Such a correction will be very approximate but will give an idea of the magnitudes of the interactions involved.

The crystal data for coronene (199) and ovalene (200) together with the Hueckel coefficients and symmetry of the excess electron and hole wave functions are given in table (6.2). The highest bonding and lowest anti-bonding orbitals in ovalene are separated from the nearest energy levels by about 1.3 eV and hence band mixing effects will be negligible and the calculation of the energy band structure straightforward. However, in coronene both the highest occupied and lowest unoccupied energy levels are degenerate, subsequently the energy bands constructed with these molecular orbitals as a basis will interact considerably giving rise to two sets of energy bands for both the electron and the hole. Hence when determining the energy band structure of these bands the methods developed in Chapter (4), section (2), page (76) must be used.

The necessary transfer integrals for coronene and ovalene have been computed using a single Slater function with both the modified and normal Slater screening parameters. The results of the calculation using the modified screening parameter are given in table (6.3). To facilitate the comparison of the present results with those of Harada et al (197) the transfer integral, for the normal Slater screening parameter, are quoted as a sum of the contributions from the coulomb and exchange interactions separately. From the magnitude of the two contributions to the transfer integral for ovalene it can be seen

	Coronene				Ovalene	
	Hole		Electron		Hole	Electron
Atom	I	II	I	II		
1	0.00000	-0.27490	0.00000	0.27490	0.37905	-0.37905
2	0.33570	0.01520	0.33570	0.01520	0.06372	0.06372
3	0.18000	0.28310	0.18000	0.28310	-0.24710	0.24710
4	-0.28310	0.13750	-0.28310	0.13750	-0.14671	-0.14671
5	-0.15470	-0.29830	-0.15470	-0.29830	0.19783	-0.19783
6	0.00000	-0.17860	0.00000	-0.17860	0.14309	0.14309
7	-0.15470	0.08930	-0.15470	0.08930	-0.16604	-0.16604
8	-	-	-	-	-0.11090	0.11090
9	-	-	-	-	0.065	.165
Symm.	AxSy	SxSy	SxAy	AxSy	AxSy	SxSy

Table(6.2)

Molecular orbital coefficients of the molecular energy levels
giving rise to the electron and hole energy bands in coronene and
ovalene.
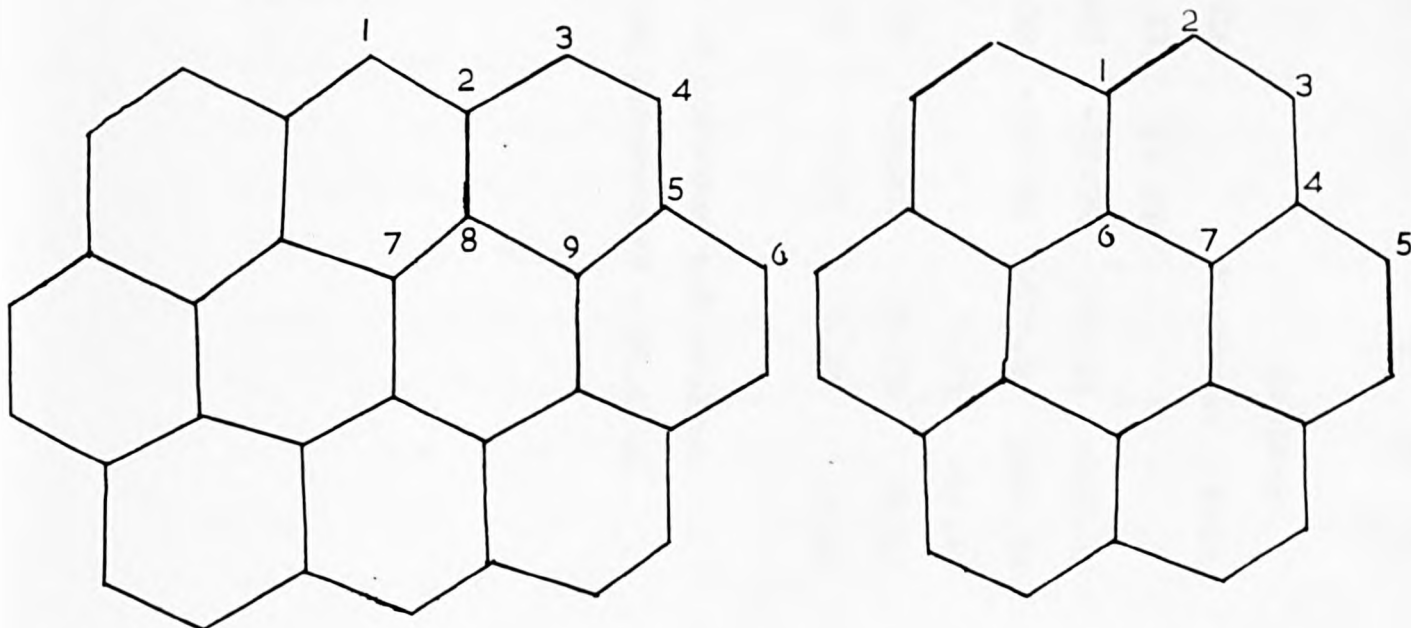
Numbering of the atoms in coronene and ovalene.

	Coronene						Ovalene	
	Electron			Hole			Electron	Hole
Position	⟨I I⟩	⟨II II⟩	⟨I II⟩	⟨I I⟩	⟨II II⟩	⟨I II⟩		
0,0,1	27.95	-46.04	8.99	-25.35	-15.25	-85.99	363.91	-473.70
0,1,0	-334.48	2383.04	12.73	65.65	-660.32	-322.83	1675.21	3121.04
0,1,1	-	-	-	-	-	-	4.25	-11.01
$\frac{1}{2}\frac{1}{2}$,0	12.56	-38.80	-28.93	90.76	-4.07	-19.18	31.56	15.90
$\frac{1}{2}\frac{1}{2}$,1	2.57	7.90	4.43	-3.11	-14.32	1.23	4.49	-7.14

Table(6.3)

Transfer integrals* for excess electrons and holes in coronene and ovalene computed using single Slater functions with screening parameter τ = 24.6 nm^{-1}.

*units $1_{10}-4$ eV.

that the effects of including exchange interactions is to increase the
interactions between the molecule at the origin and those at the
corners of the unit cell by a factor of 4 whilst the interactions
with molecules at the centre of the _ab_ faces are increased by a
factor of about 6. In order to obtain an approximate value for the
energy band widths we have multiplied the integrals of Harada by the
appropriate factor. It should be emphasised that this is a rather
drastic approximation, however, in the absence of accurate atomic
refinements and because of the remote possibility of obtaining any (201)
there appears to be no other alternative. The transfer integrals for
coronene and ovalene together with the modified integrals of Harada
are given in table (6.4). There are two points of interest in the
calculated interaction between the molecule at the origin and that at
the position (0, 1, 0). Firstly, the magnitude of the interactions for
ovalene and circumanthracene are in the reverse order to that which
would be expected from considerations of increasing ring size
coupled with little change in the intermolecular distances, i.e. the
more condensed hydrocarbon would be expected to have the larger value.
Secondly, the interactions of the electrons and the holes have the
same relative sign.

The reason for these apparent anomalies can be traced to the
symmetry properties of the two sets of molecular wave functions.
The relative phases of the Hueckel coefficients in circumanthracene
are such that all the interactions between atoms which are very
close together (~ 0.35 nm) cancel with equivalent interactions in
other parts of the molecule giving rise to a smaller overall
interaction than one might at first expect. Similar cancellations
occur in ovalene but to a lesser extent and the sign of the products

Coronene / Ovalene / Circumanthracene

Position	⟨I I⟩ Coul.	Exch.	Tran.	⟨II II⟩ Coul.	Exch.	Tran.	⟨I II⟩ Tran.	Ovalene Coul.	Exch.	Tran.	Circumanthracene Coul.	Approx Tran.
0,0,1	-0.23	-3.41	-3.64	4.08	4.89	8.97	2.47	20.11	64.08	84.19	-21.25	-84.90
0,1,0	160.80	435.45	596.24	-24.34	-68.31	-92.97	5.66	89.14	271.45	360.59	-53.69	-214.75
$\frac{1}{2},\frac{1}{2},0$	-0.36	-4.74	-5.11	0.37	1.69	2.05	-11.30	0.49	3.85	4.34	0.77	4.61
$\frac{1}{2},\frac{1}{2},1$	0.10	0.59	0.69	0.06	0.24	0.30	0.29	0.09	0.41	0.50	0.13	0.78

(a)

Position	⟨I I⟩ Coul.	Exch.	Tran.	⟨II II⟩ Coul.	Exch.	Tran.	⟨I II⟩ Tran.	Ovalene Coul.	Exch.	Tran.	Circumanthracene Coul.	Approx Tran.
0,0,1	-2.37	-5.27	-7.64	-4.50	-4.96	-9.46	15.90	-24.17	-78.71	-102.88	21.73	86.89
0,1,0	-31.64	-22.62	-54.26	-57.43	-151.64	-208.89	-107.37	199.50	534.89	734.39	-55.99	-223.99
$\frac{1}{2},\frac{1}{2},0$	4.27	13.12	17.38	-0.30	-0.90	-1.19	-3.39	0.38	2.68	3.06	-0.75	-4.50
$\frac{1}{2},\frac{1}{2},1$	-0.07	-0.30	-0.37	-0.21	-1.21	-1.42	0.10	-0.06	-0.45	-0.51	-0.18	-1.32

(b)

Table(6.4)

Coulomb and exchange contributions to the transfer integrals* of excess electrons(a) and holes(b) in coronene, ovalene and circumanthracene.

The figures in angular brackets refer to the molecular orbital of the free molecule.

*units: $1\text{\textsc{x}}{-}4$ eV.

of the Hueckel coefficients is negative for the large

non-cancelling terms for both electrons and holes giving rise to

transfer integrals which are positive for both carriers.

The energy band structure of excess electrons and holes in

crystalline coronene, calculated including the effects of energy

band interactions, are illustrated in figure (6.3) and figure (6.4).

The rather strange behaviour of the energy bands along the $\underline{b}$ axis

requires some comment.

The energy bands of excess electrons show, in addition to the

normal maximum and minimum at the centre and edge of the Brillouin

zone, a minimum, a maximum in the case of the band of lower energy,

at approximately $\underline{k} = \underline{\pi} \, \underline{a}^{-1}/2$. The origin of the effect lies in the

structure and relative positions of the two "pure" energy bands

resulting from the degenerate energy levels of the lowest

antibonding molecular orbital in the free molecules. The phrase

"pure" energy band is used to describe the energy band resulting from

one of a pair of near degenerate molecular levels calculated

assuming the second band to be absent. Such bands will not exist

physically but are extremely helpful in understanding the structure

of energy bands resulting from the mixing of two or more such bands.

Figure (6.5) shows the structure of these bands along the reciprocal

lattice axes, $\underline{a}^{-1}$, $\underline{b}^{-1}$ and $\underline{c}^{-1}$. To distinguish between the energy

bands resulting from the degenerate molecular energy levels I and II

the notation $E_{\pm}(\underline{k})$ has been modified slightly to include the

molecular energy level as a superscript: viz $E_{\pm}^{I}(\underline{k}||\underline{x}^{-1})$ denotes

the two components of the energy band in the $\underline{x}^{-1}$ direction calculated

using the molecular orbital coefficients of energy level I . As can

be seen from figure (6.5) the "pure" energy bands along the $\underline{a}^{-1}$

and $\underline{c}^{-1}$ axes are reasonably well separated whereas along the $\underline{b}^{-1}$

- 145 -
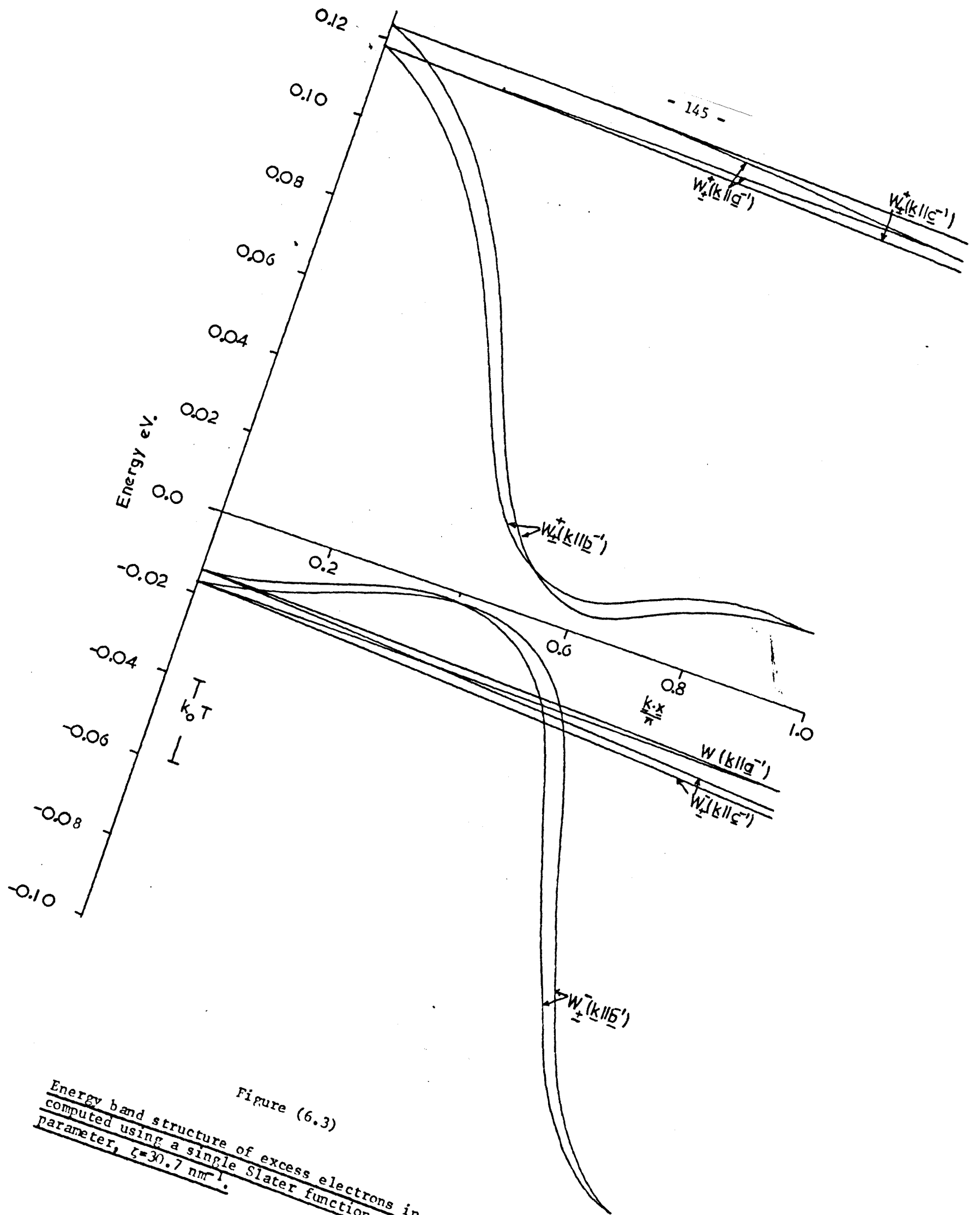
Figure (6.3)

Energy band structure of excess electrons in coronene computed using a single Slater function with screening parameter, $\zeta = 30.7$ nm^{-1}.
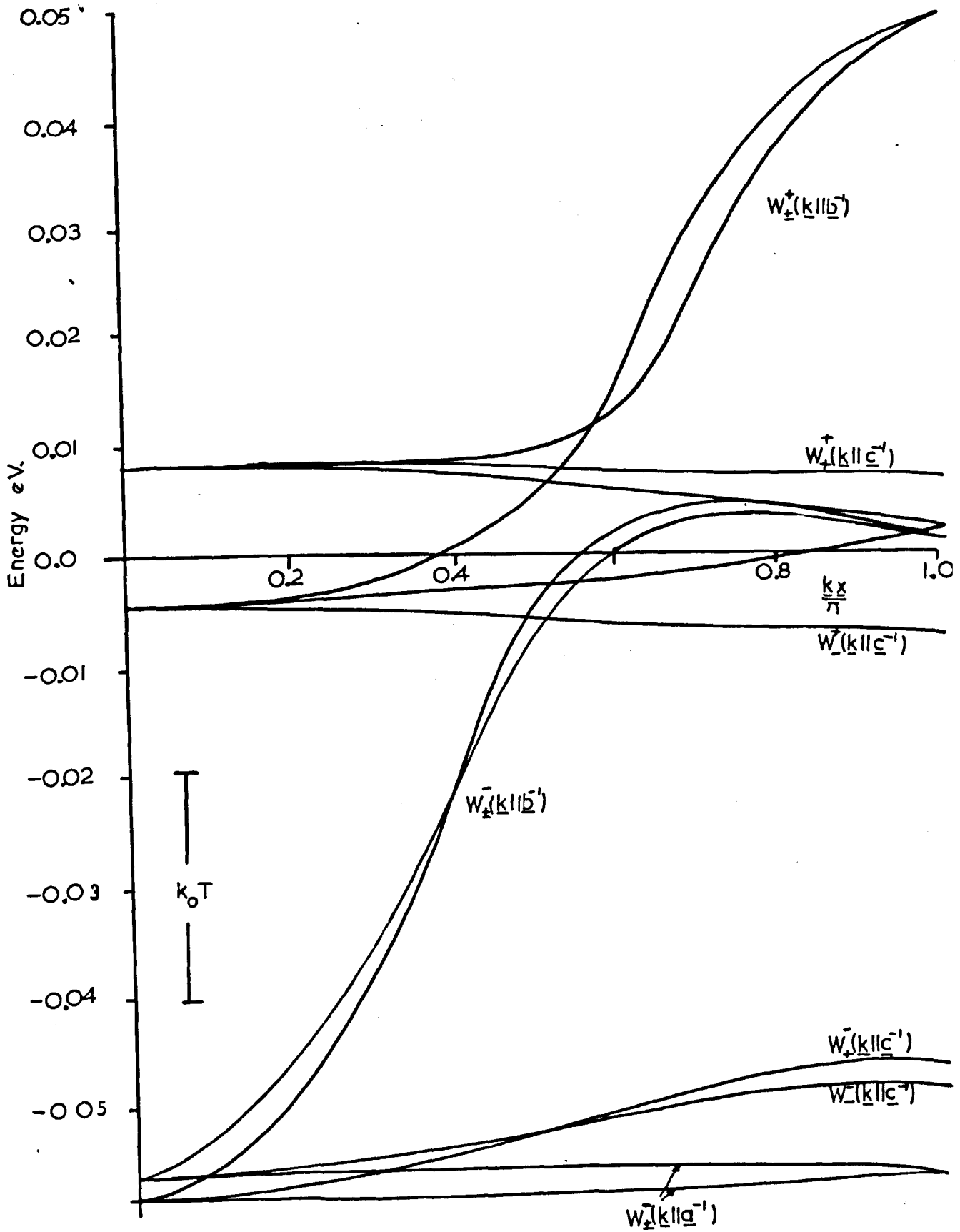
Figure (6.4)

Energy band structure of excess holes in crystalline coronene computed using a single Slater function to represent the carbon $2p_z$ wave function with screening parameter, $\zeta = 30.7$ nm^{-1}.
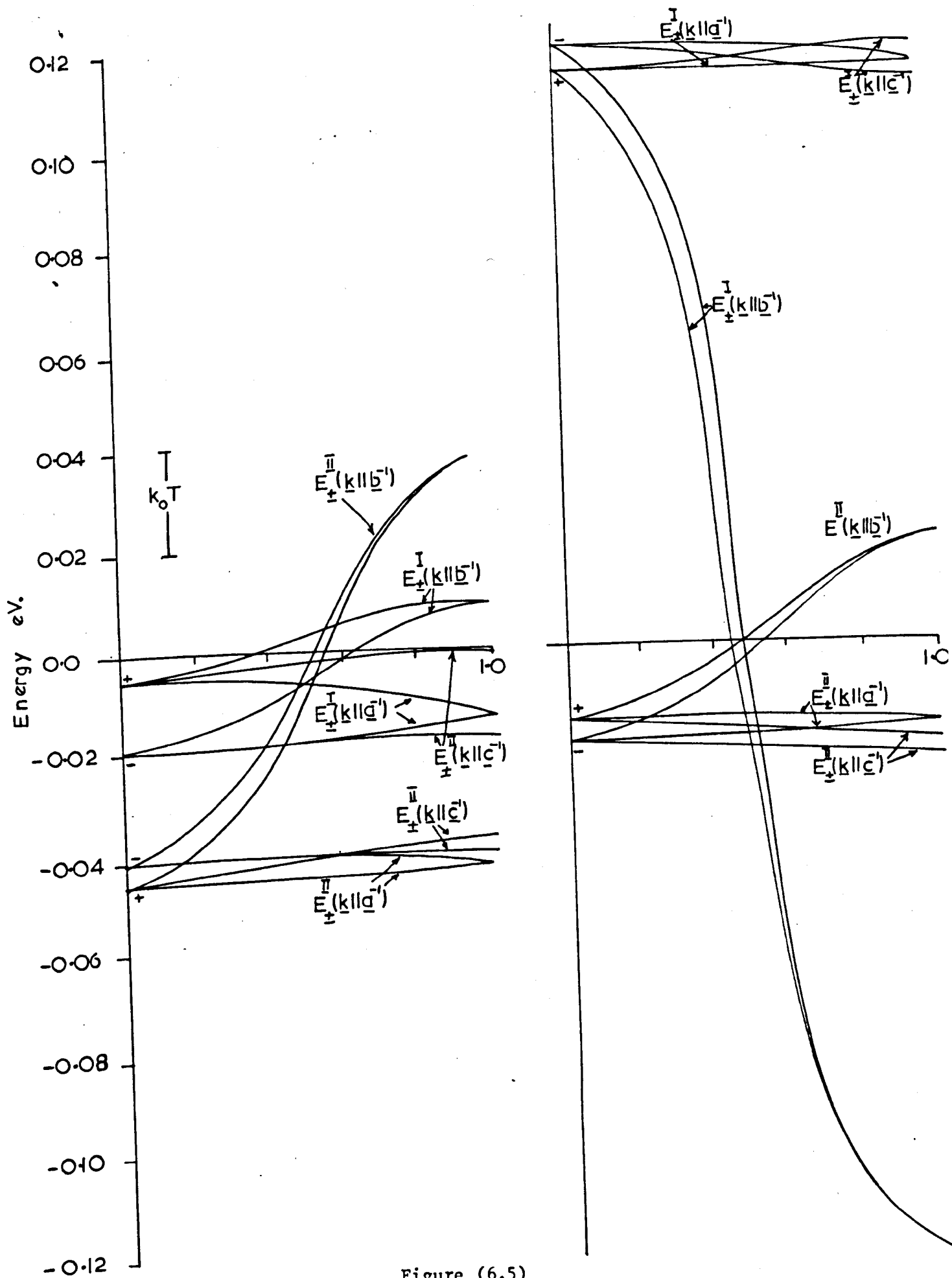
Figure (6.5)

Energy band structures of excess hole (left) and electron in coronene in the absence of band mixing.
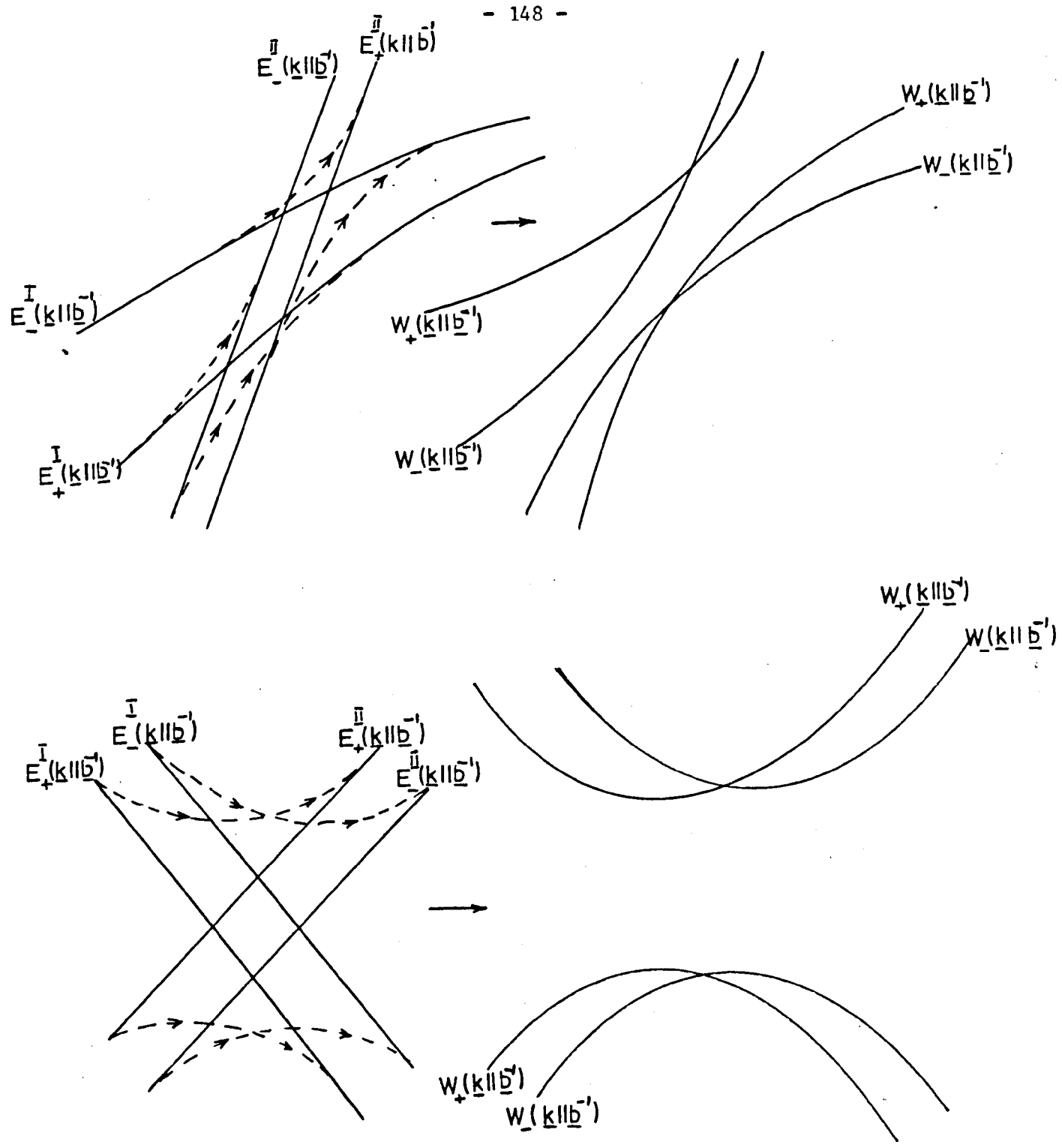
Figure (6.6)

Enlarged sections of the crossing regions of the excess

electron (c) and hole (a) bands and the energy band shapes

resulting from band-band repulsion. The superscripts on

$W_+(\underline{k})$ have been omitted for clarity.

axis they intersect, hence, one would expect band mixing effects to be of greater importance in this direction. This is substantiated by the close similarities between the "pure" energy bands in figure (6.5) and the corresponding energy bands in figure (6.3) along the $\underline{a}^{-1}$ and $\underline{c}^{-1}$ axes. Figure (6.6) shows an enlarged section of the crossing regions of figure (6.5) and the band shapes resuling from band-band repulsion. For low values of $\underline{k}$ ($\underline{k} < 0.4 \pi \underline{b}^{-1}$) $E_{\pm}^{I}(\underline{k}||\underline{b}^{-1})$ and $E_{\pm}^{II}(\underline{k}||\underline{b}^{-1})$ are reasonably well separated and the energy bands in figure (6.3) show a strong correlation with the pure energy bands of figure (6.5). In the region

$$0.4 \pi \underline{b}^{-1} < \underline{k} < 0.6 \pi \underline{b}^{-1}$$

the two sets of energy bands experience an increasing repulsion due to the presence of the other and this results in the energy bands changing direction and ultimately exchanging roles. The situation is illustrated in figure (6.6) (c), the dotted lines showing the bending of the energy bands due to mutual repulsion and the resulting band shapes are shown in figure (6.6) (d). For $\underline{k} > 0.6 \pi \underline{b}^{-1}$ the repulsion effects decrease and the energy bands again show a strong correlation with the pure energy bands.

Similar arguments can be used to explain the strange behaviour of the energy bands of excess holes along the $\underline{b}^{-1}$ axes. These are illustrated in figure (6.6) (a) and figure (6.6) (b).

The above effects are effectively an extension of the familiar non-crossing rule (203) into the energy bands in $\underline{k}$ - space. It should be noted that $E_{+}(\underline{k})$ and $E_{-}(\underline{k})$ belong to different symmetry species hence crossing of these energy bands as in figure (6.3) and figure (6.4) does not constitute a violation of the non-crossing rule.

The energy band structure of circumanthracene and ovalene, calculated using the transfer integrals with screening parameter 30.7 nm^{-1}, are shown in figure (6.8) and figure (6.7) respectively. The general shapes of the energy bands for ovalene calculated using the transfer integrals with the modified screening parameters are very similar to the ones shown and are not given here, however, if needed they can be easily calculated using the transfer integrals of table (6.3) and equation (3.12) of Chapter (3), section (3), page (47).

Unlike the linear polyacenes the energy bands of ovalene and circumanthracene show only small splitting between the two components of the energy band and, due to increased molecular size and the relatively short length of the $\underline{c}$ axis, have a relatively large band width in the $\underline{c}^{-1}$ direction. In addition $E_{\pm}(\underline{k}||\underline{b}^{-1})$ shows the same type of variation for both electrons and holes hence the lower energy states will be around the minimum at $\underline{k} = \pi b^{-1}$ for electrons and around the maximum $\underline{k} = 0$ for holes in ovalene, while the reverse is true for circumanthracene. It should be noted that the energy levels for excess holes are measured downwards from the top of the band. Thus $\dfrac{d^2(E_{\pm}(\underline{k}||b)}{dk_b^2}$ will be positive for excess electrons and negative for excess holes in ovalene and the same is true for circumanthracene. The effective mass, m^*, of a carrier of energy E and wave vector k can be written (204)

$$m^* = \frac{\hbar^2}{\dfrac{d^2E}{dk^2}} \qquad (6.1)$$

Hence the effective masses in the lower energy states will be positive for electrons and negative for holes and, since the energy band widths are several times k_0T at room temperature, it will be these states
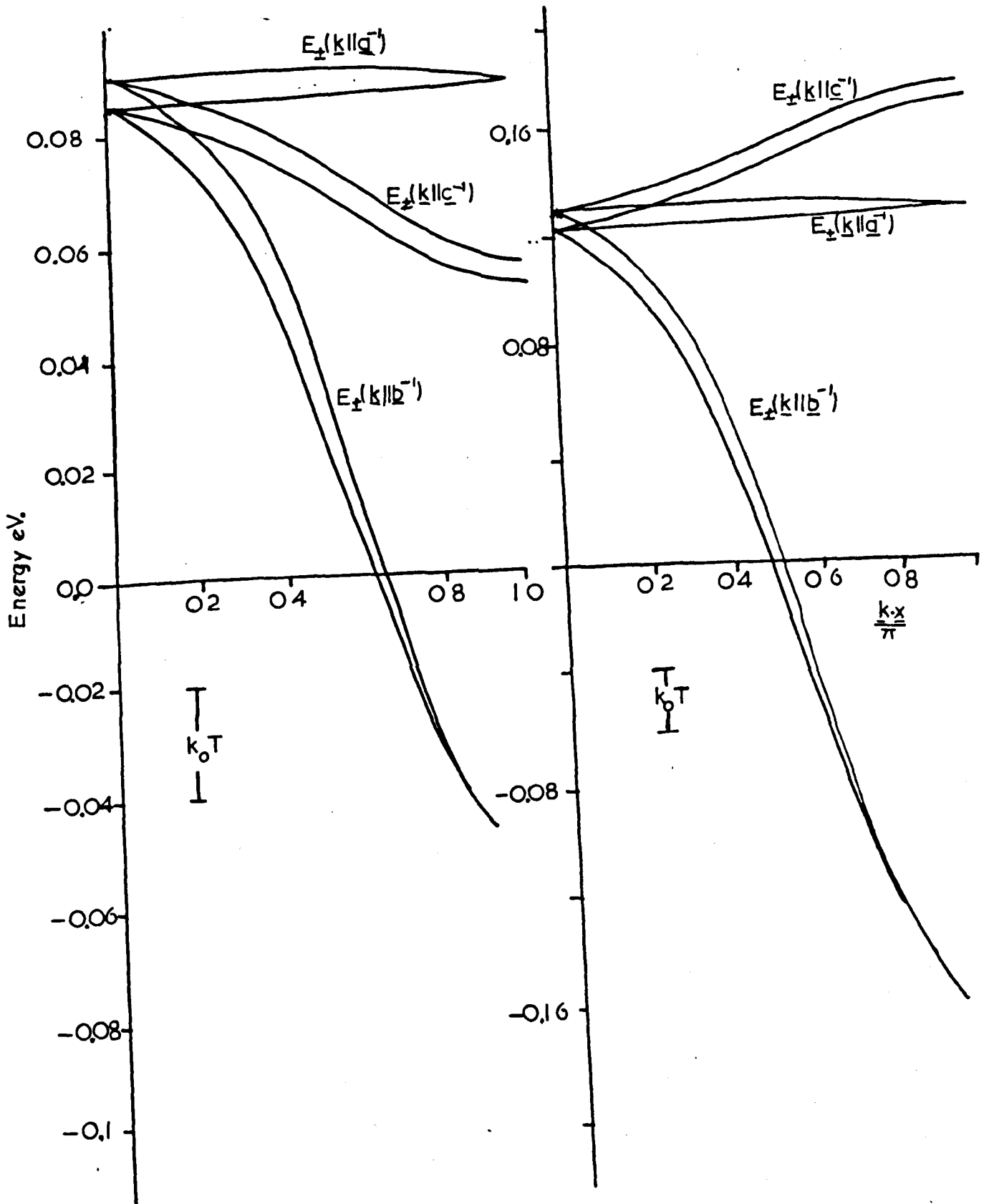
Figure (6.7)

Energy band structure of excess electrons (left) and

excess holes (right) in crystalline ovalene $|\langle \gamma^0|\chi^1\rangle|^2 = 1.0$.

(a)

(b)
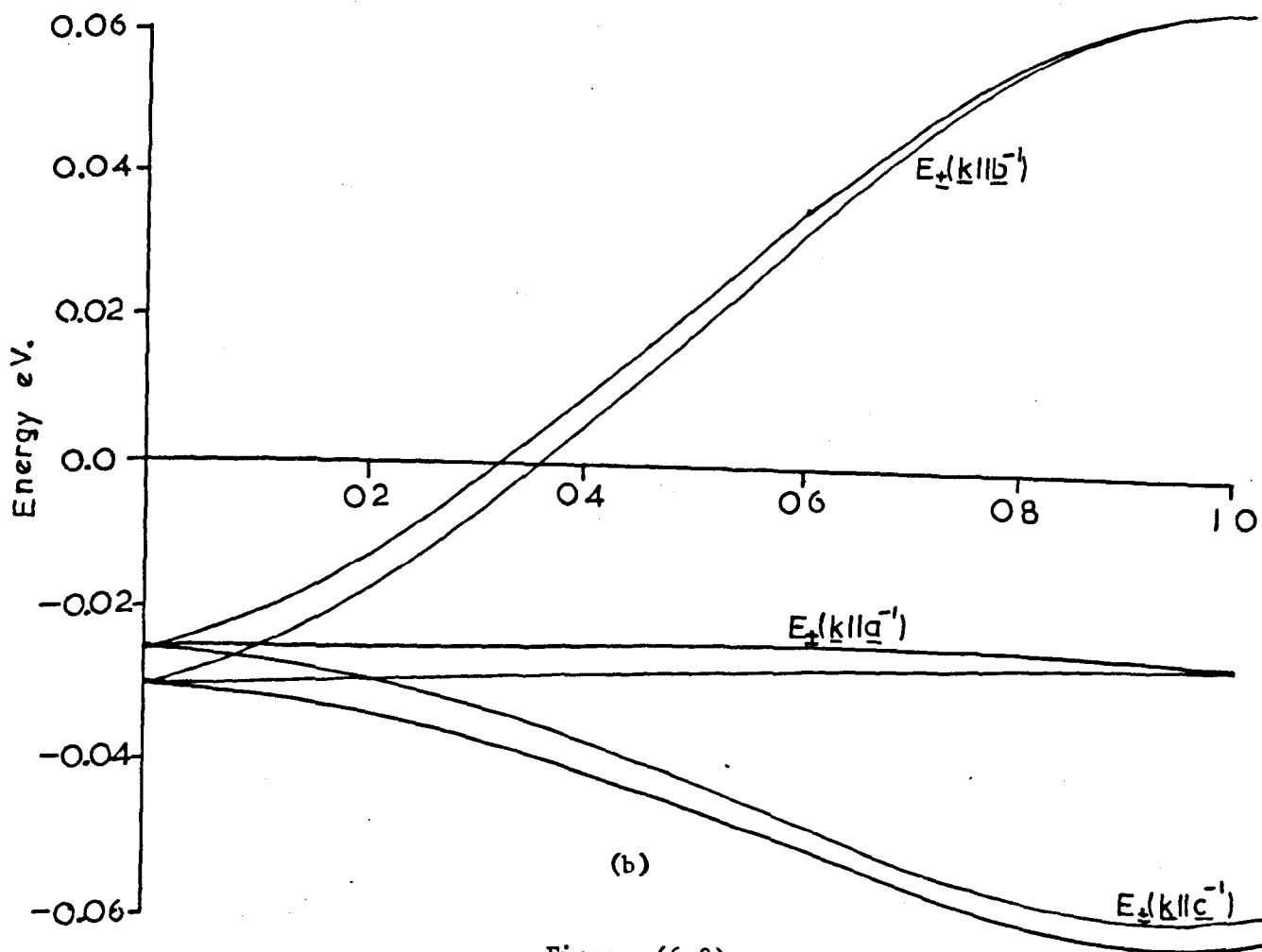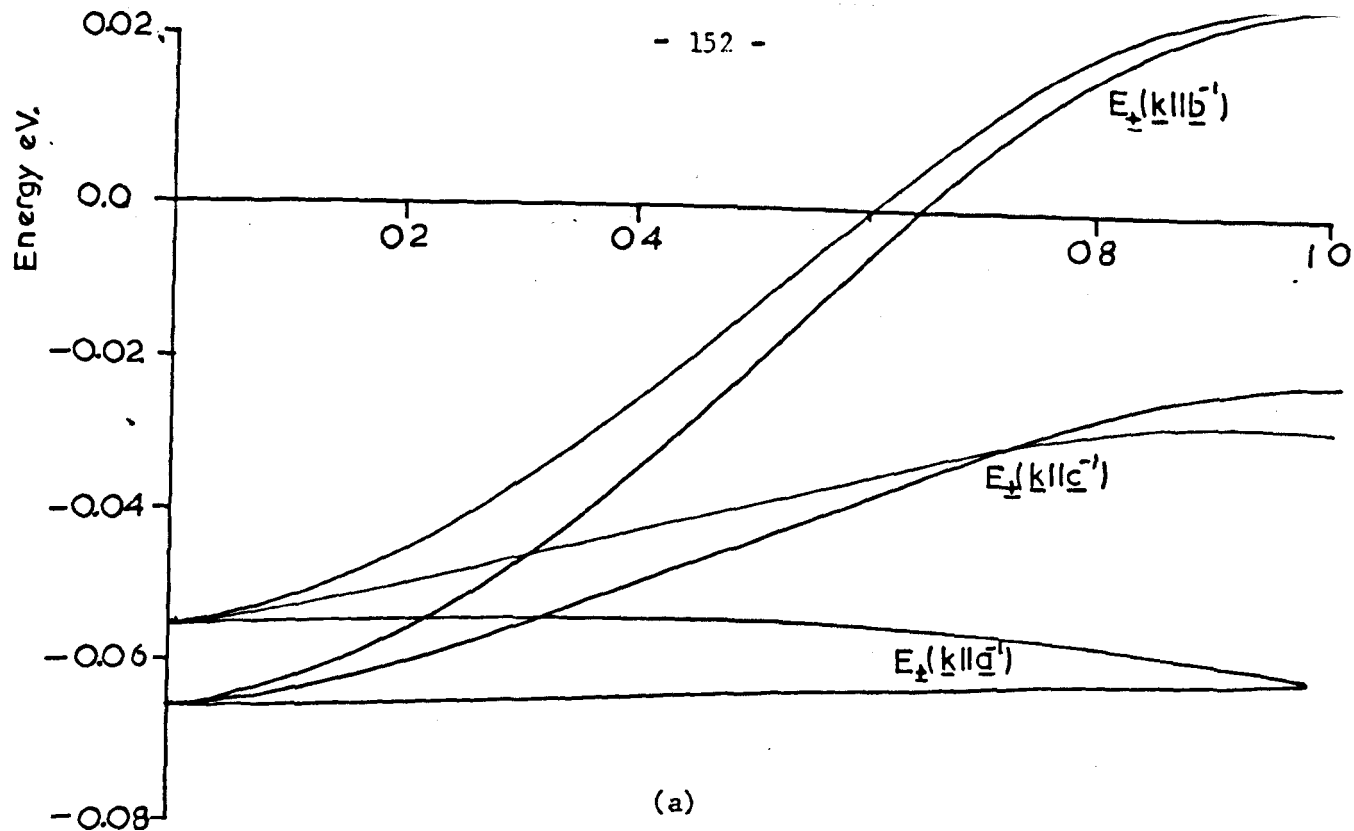
Figure (6.8)

Energy band structure of excess holes (a) and excess

electrons (b) in crystalline circumanthracene.

		Coronene			Ovalene	
	Electron	Electron	Hole	Hole	Electron	Hole
$E(\underline{k} \parallel \underline{a}')^{+}$	0.012	0.006	0.034	0.006	0.014	0.004
$E(\underline{k} \parallel \underline{a}')^{-}$	0.013	0.006	0.033	0.005	0.014	0.004
$E(\underline{k} \parallel \underline{b}')^{+}$	0.329	0.431	0.064	0.146	0.688	1.243
$E(\underline{k} \parallel \underline{b}')^{-}$	0.408	0.418	0.130	0.135	0.659	1.236
$E(\underline{k} \parallel \underline{c}')^{+}$	0.012	0.014	0.007	0.038	0.153	0.204
$E(\underline{k} \parallel \underline{c}')^{-}$	0.025	0.009	0.020	0.022	0.145	0.193
$\underline{c}$ splitting	0.067	0.008	0.079	0.005	0.022	0.018

Table(6.5)

Energy bandwidths* of the electron and hole bands in coronene and ovalene computed using single Slater functions with screening parameter ς = 24.6 nm^{-1}. Vibrational overlap factor unity.

*units: eV.

		Coronene				Ovalene		Circumanthracene	
		Electron	Electron	Hole	Hole	Electron	Hole	Electron	Hole
$E(\underline{k} \parallel \underline{a}')$	+	0.0017	0.0009	0.0062	0.0004	0.0019	0.0010	0.0022	0.0023
	−	0.0020	0.0012	0.0060	0.0002	0.0019	0.0010	0.0022	0.0023
$E(\underline{k} \parallel \underline{b}')$	+	0.0964	0.1041	0.0411	0.0584	0.1462	0.2948	0.0837	0.0919
	−	0.1002	0.1020	0.0532	0.0578	0.1423	0.2927	0.0881	0.0873
$E(\underline{k} \parallel \underline{c}')$	+	0.0010	0.0039	0.0012	0.0094	0.0341	0.0416	0.0333	0.0337
	−	0.0019	0.0033	0.0028	0.0082	0.0333	0.0407	0.0346	0.0358
$\underline{c}$ splitting		0.0047	0.0015	0.0150	0.0006	0.0031	0.0029	0.0031	0.0025

Table(6.6)

Energy bandwidths* in coronene ovalene and circumanthracene computed using single Slater functions with screening parameter ζ = 30.7 nm^{-1}.

Vibrational overlap factor unity.

*units: eV.

which are most densely populated. Therefore, in ovalene at least, one should not observe any anomalous effects in the electrical properties along the $\underline{b}$ axis. This provides an easy method of determining whether or not band theory is applicable to ovalene as the model predicts that the ratio μ^D/μ^H should be positive for both electrons and holes unlike in the case of linear polyacenes where the reverse is true. In the case of circumanthracene the ratio μ^D/μ^H should again be positive for both electrons and holes, although the effects of molecular vibrations may reduce the band width to the extent that the band width $< k_0 T$ and then the sign of μ^D/μ^H would be reversed.

6.3 Mobility Tensor

The ratios of the elements of the mobility tensor, calculated in the mean free time and mean free path approximations using the methods of Chapters (3) and (4) and the transfer integrals computed with single Slater functions characterized by both the normal and modified ($\zeta = 24.6$ nm^{-1}) screening parameters, are given in table (6.7) and table (6.8). The mobility ratios for coronene crystals containing excess electrons is relatively independent of the vibrational overlap factor and show the electron mobility in the $\underline{b}^{-1}$ direction to be several orders of magnitude greater than either the $\underline{a}^{-1}$ or $\underline{c}'^{-1}$ directions. In general

$$\mu_{aa} \sim \mu_{c'c'} \sim \frac{1}{1000}\left(\frac{1}{100}\right)\mu_{bb} \quad \text{for both energy bands}$$

where the figure in parentheses refers to the value calculated using the screening parameter $\zeta = 24.6$ nm^{-1}.

The variation of the hole mobility ratios with vibrational overlap factor is rather more complicated, the two energy bands showing opposite

variations as the factor is increased. If the hole mobility ratio μ_{aa}/μ_{bb} , calculated using $\zeta = 30.7$ nm^{-1} , is considered; for the band of lowest energy the mobility ratios decrease with increasing vibrational overlap factor while the reverse is true for the higher band. As with the rather peculiar behaviour of the energy bands in the Brillouin zone, the mobility ratios can be understood in terms of the mobilities in the "pure" energy bands, and the large band widths. For vibrational overlap factor unity the energy band width along $\underline{b}^{-1}$ is much larger than k_0T the excess hole will therefore be predominantly in the lower energy states which show a strong resemblence to the "pure" energy bands which leads to the higher band having the higher degree of anisotropy. For vibrational overlap factor 0.1 the band width along $\underline{b}^{-1}$ is less than k_0T resulting in the upper regions of energy band being more heavily populated and, since the relationship between actual energy bands and pure energy bands has been reversed, the anisotropy of the mobility ratios is reversed. Thus one would expect similarities between the mobility ratios in the first band with vibrational overlap factor 0.1 and the second band with vibrational overlap factor 1.0 and vice versa. Such correlations are amply illustrated in table (6.7). Similar trends are observed using screening parameter $\zeta = 24.6$ nm^{-1} , however, even with vibrational overlap 0.1 the energy band width is still $\sim k_0T$ and so the effect is not so pronounced.

The mobility ratios of ovalene and circumanthracene, with $\zeta = 30.7$ nm^{-1} , show some similarities in that the ratios for electrons and holes are approximately the same, μ_{aa}/μ_{bb} being less than $\mu_{c'c'}/\mu_{bb}$, and they are relatively insensitive to the degree of vibrational overlap. For $\zeta = 30.7$ nm

$$\mu_{aa} \sim \frac{1}{10}\,\mu_{aa} \sim \frac{1}{50}\,\mu_{bb} \quad \text{for ovalene}$$

and

$$\mu_{aa} \sim \frac{1}{20}\,\mu_{aa} \sim \frac{1}{20}\,\mu_{bb} \quad \text{for circumanthracene.}$$

	Coronene I			Coronene II			Ovalene			Circumanthrancene		
Vibrational Overlap	0.1	0.5	1.0	0.1	0.5	1.0	0.1	0.5	1.0	0.1	0.5	1.0
$\langle vbvb\rangle$*	4.38	114.56	442.96	3.13	65.06	197.04	54.95	850.92	2322.40	5.28	128.49	442.12
$\langle vbvb/\underline{v}(\underline{k})\rangle$**	1.19	6.43	12.99	0.99	4.09	6.27	5.27	18.73	27.74	1.23	6.03	10.74
$\frac{\mu_{aa}}{\mu_{bb}}$	0.11 (0.30)	0.08 (0.22)	0.05 (0.14)	0.05 (0.16)	0.07 (0.23)	0.11 (0.35)	0.01 (0.01)	0.01 (0.02)	0.02 (0.03)	0.03 (0.03)	0.02 (0.03)	0.03 (0.03)
$\frac{\mu_{cc}}{\mu_{bb}}$	0.03 (0.05)	0.03 (0.07)	0.04 (0.10)	0.03 (0.06)	0.03 (0.05)	0.03 (0.05)	0.09 (0.13)	0.14 (0.24)	0.21 (0.39)	0.68 (0.72)	0.68 (0.75)	0.75 (0.88)
$\frac{\mu_{ac}}{\mu_{bb}}$	-0.01 (-0.02)	-0.01 (-0.03)	-0.01 (-0.04)	-0.01 (-0.02)	-0.01 (-0.02)	-0.01 (-0.02)	-0.03 (-0.04)	-0.04 (-0.06)	-0.06 (-0.10)	-0.12 (-0.13)	-0.12 (-0.13)	-0.13 (-0.15)

(a)

Table(6.7)

Mobility ratios of excess holes(a) and electrons(b) in crystalline coronene, ovalene and circumanthracene computed in the mean free time and free path(in parentheses) approximations using single Slater functions with screening parameter τ = 30.7 nm^{-1}.

* units: $1_{10}6$ m^2/sec^2.

**units: $1_{10}3$ m/sec.

	I	Coronene		II			Ovalene			Circumanthrancene	
Vibrational Overlap	0.1	0.5	1.0	0.1	0.5	1.0	0.1	0.5	1.0	0.1	0.5	1.0
$\langle vbvb \rangle$*	15.96	287.06	728.68	22.97	535.80	1494.60	14.39	322.18	924.09	4.70	105.95	343.84
$\langle vbvb/\underline{v}(\underline{k}) \rangle$**	2.65	10.07	15.06	3.32	16.45	25.70	2.41	10.93	166.81	1.10	4.98	8.27
$\underline{\mu}_{aa}$	0.003	0.003	0.003	0.0 1	0.001	0.001	0.02	0.02	0.03	0.04	0.06	0.08
μ_{bb}	(0.010)	(0.007)	(0.007)	(0.005)	(0.003)	(0.002)	(0.02)	(0.03)	(0.04)	(0.05)	(0.08)	(0.12)
$\underline{\mu}_{cc}$	0.001	0.002	0.004	0.0~1	0.001	0.001	0.234	0.263	0.363	0.736	0.802	0.949
μ_{bb}	(0.010)	(0.015)	(0.021)	(0.006)	(0.005)	(0.006)	(0.288)	(0.357)	(0.551)	(0.776)	(0.869)	(1.070)
$\underline{\mu}_{ac}$	-0.001	-0.001	-0.002	-0.001	-0.001	-0.001	-0.063	-0.070	-0.097	-0.112	-0.115	-0.128
μ_{bb}	(-0.004)	(-0.005)	(-0.009)	(-0.002)	(-0.002)	(-0.002)	(-0.077)	(-0.095)	(-0.014)	(-0.122)	(-0.130)	(-0.149)

(b)

Table(6.7) cont.

Mobility ratios of excess holes(a) and electrons(b) in crystalline coronene, ovalene and circumanthracene computed in the mean free time and free path(in parentheses) approximations using single Slater functions with screening parameter $\underline{5}$ = 30.7 nm^{-1}.

* units: $1_{10}6 \ m^2/sec^2$.

**units: $1_{10}3 \ m/sec$.

	I	Coronene		II			Ovalene		
Vibrational Overlap	0.1	0.5	1.0	0.1	0.5	1.0	0.1	0.5	1.0
$\langle vbvb\rangle$*	37.66	786.27	1919.90	28.39	532.98	1581.30	611.58	2200.60	1868.50
$\langle vbvb/\underline{v}(\underline{k})\rangle$**	3.51	16.14	22.21	2.95	11.66	19.65	14.06	13.98	6.51
$\underline{\mu}_{aa}$	0.37	0.20	0.08	0.18	0.35	0.56	0.01	0.08	0.27
μ_{bb}	(0.46)	(0.24)	(0.11)	(0.29)	(0.50)	(0.67)	(0.03)	(0.22)	(0.92)
$\underline{\mu}_{cc}$	0.05	0.07	0.13	0.06	0.05	0.04	0.19	1.06	3.26
μ_{bb}	(0.08)	(0.16)	(0.35)	(0.08)	(0.06)	(0.05)	(0.37)	(2.37)	(8.11)
$\underline{\mu}_{ac}$	-0.02	-0.02	-0.05	-0.02	-0.01	-0.02	-0.05	-0.28	-0.86
μ_{bb}	(-0.03)	(-0.06)	(-0.02)	(-0.02)	(-0.02)	(-0.02)	(-0.10)	(-0.62)	(-2.07)

(a)

Table(6.8)

Mobility ratios of excess holes(a) and electrons(b) in crystalline coronene and ovalene computed in the mean free time and free path(in parentheses) approximations using single Slater functions with screening parameter ς = 24.6 nm^{-1}.

*units: $1_{10}6$ m^2/sec^2.

**units: $1_{10}3$ m/sec.

	Coronene I			Coronene II			Ovalene		
Vibrational Overlap	0.1	0.5	1.0	0.1	0.5	1.0	0.1	0.5	1.0
$\langle vbvb \rangle$*	197.19	1226.20	2167.50	359.38	2678.20	2288.10	277.12	2362.70	3904.60
$\langle vbvb/\underline{v}(\underline{k}) \rangle$**	8.02	19.84	34.72	12.94	25.63	13.88	10.45	23.13	23.58
μ_{aa}	0.01	0.01	0.01	0.003	0.003	0.007	0.02	0.04	0.07
μ_{bb}	(0.01)	(0.01)	(0.02)	(0.01)	(0.01)	(0.05)	(0.02)	(0.07)	(0.12)
μ_{cc}	0.003	0.008	0.02	0.002	0.008	0.04	0.22	0.56	1.02
μ_{bb}	(0.01)	(0.02)	(0.02)	(0.01)	(0.08)	(0.34)	(0.29)	(0.90)	(1.71)
μ_{ac}	-0.001	-0.002	-0.005	-0.001	-0.003	-0.015	-0.06	-0.15	-0.27
μ_{bb}	(-0.004)	(-0.008)	(-0.008)	(-0.004)	(-0.028)	(-0.129)	(-0.077)	(-0.242)	(-0.458)

(b)

Table(6.8)

Mobility ratios of excess holes(a) and electrons(b) in crystalline coronene and ovalene computed in the mean free time and free path(in parentheses) approximations using single Slater functions with screening parameter ς= 24.6 nm^{-1}.

* units: $1_{10}6$ m^2/sec^2 .

**units: $1_{10}3$ m/sec.
;

The mobility ratios of electrons and holes in crystalline ovalene calculated using screening parameter ζ = 24.6 nm^{-1} show a large variation with increase in vibrational overlap. For vibrational overlap factor 0.1 the mobility ratios for electrons and holes are very similar, however, due to the extreme widths of the energy band along $\underline{b}^{-1}$, this situation does not hold for any other value of the vibrational overlap factor. It is interesting to note that the mobility ratios for the electron band with vibrational overlap factor 1.0 and the mobility ratios for the hole band with vibrational overlap factor 0.5 show a strong correlation in keeping with the width of the hole band being twice that of the electron band.

6.4 Orientation of the principle axes of the mobility tensor

The direction cosines of the principle axes of the mobility tensor with respect to the orthogonal crystallographic axes $\underline{a}$, $\underline{b}$ and $\underline{c}'$ are obtained by diagonalization of the mobility tensor. The crystal symmetry is such that the crystallographic $\underline{b}$ - axis is always a principle axis and if the principle axes of the mobility tensor are represented by $\underline{A}$, $\underline{B}$ and $\underline{C}$ the array representing the relative orientation of the principle and crystallographic axes is of the form

	$\underline{a}$	$\underline{b}$	$\underline{c}'$
$\underline{A}$	$\underline{a}A$	-90	-aC
$\underline{B}$	90	0	90
$\underline{C}$	aC	90	aA

The values of the elements aA and aC for coronene, ovalene and circumanthracene are given in table (6.10). Unlike anthracene type crystals the principle axes of the electron and hole mobility tensors for both ovalene and circumanthracene are colinear and independent of the degree of vibrational overlap. In addition, the calculated

	L	M	N
a	84.8	44.2	133.7
b	85.6	46.7	43.7
c	6.9	96.8	89.6

Coronene

	L	M	N
a	44.7	78.5	132.4
b	51.5	74.4	42.7
c	70.8	160.5	86.2

Ovalene

	L	M	N
a	44.1	82.4	128.7
b	54.8	75.8	38.7
c	67.2	159.1	90.0

Circumanthracene

Table(6.9)

Orientation of the molecular axes L,M and N
to the crystal axes a, b and c.

Element	Vibrational	I Coronene Electron	II Electron	I Hole	II Hole	Ovalene Electron	Ovalene Hole	Circumanthracene Electron	Circumanthracene Hole
a.A	0.1	0.18	0.36	6.81	28.11	15.06	15.02	9.96	9.93
		(1.07)	(3.02)	(4.80)	(11.91)	(15.08)	(15.06)	(10.00)	(9.93)
a.C		-89.82	-89.63	-83.19	-61.89	74.94	74.97	80.04	80.07
		(-88.93)	(-86.98)	(-85.24)	(-70.09)	(74.92)	(74.94)	(80.00)	(80.04)
a.A	1.0	0.83	0.27	30.54	7.28	15.02	15.03	9.98	9.90
		(1.09)	(1.58)	(30.02)	(3.52)	(15.01)	(15.09)	(10.06)	(9.91)
a.C		-89.72	-89.72	-59.45	-82.72	74.98	74.97	80.02	80.10
		(-79.70)	(-88.42)	(-59.98)	(-86.48)	(74.99)	(74.91)	(79.95)	(80.09)

Table(6.10)

Orientation of the principle axes of the mobility tensor with respect to the crystallographic axes $\underline{a}, \underline{b}$ and $\underline{c}$ computed using single Slater functions with screening parameter $\zeta = 30.724$ nm^{-1} .

Element	Vibrational Overlap	I Electron	II Coronene*I Electron	Hole	II Hole	Ovalene* Electron	Hole	Ovalene** Electron	Hole
a.A		9.55	35.83	2.75	6.10	15.09	15.01	15.10	15.03
		(37.81)	(31.14)	(4.30)	(6.16)	(15.10)	(15.09)	(15.08)	(15.01)
a.C	0.1	-80.45	-54.17	-87.25	-83.89	74.91	74.92	74.90	74.97
		(-52.19)	(-58.86)	(-85.70)	(-83.84)	(74.90)	(74.91)	(74.92)	(74.97)
a.A		38.83	21.45	30.79	1.87	15.01	14.94	15.01	14.90
		(33.24)	(20.45)	(24.03)	(2.25)	(15.01)	(14.95)	(15.01)	(14.70)
a.C	1.0	-51.74	-68.55	-59.21	-88.13	74.99	75.06	74.99	75.10
		(-56.76)	(-69.15)	(-65.97)	(-87.53)	(74.99)	(75.05)	(74.99)	(75.38)

Table(6.10) cont.

Orientation of the principle axes of the mobility tensor with respect to the crystallographic axes a,b and c.

* computed using single Slater functions with screening parameter ς = 24.565 nm^{-1} .

**computed using single Slater functions with screening parameter ς = 22.676 nm^{-1} .

	(0,0,1)	(0,1,0)	(0,1,1)	(½,½,0)	(½,½,1)
Electron	548.92	2606.01	7.12	57.10	6.34
Hole	734.21	4741.29	13.21	26.14	13.17

Transfer integrals* for excess electrons and holes in ovalene computed using single Slater functions with screening parameter ς = 22.7 nm .

	Electron	Hole
$E(\underline{k} \parallel \underline{a}^{-1})$ +	0.0256	0.0052
−	0.0256	0.0052
$E(\underline{k} \parallel \underline{b}^{-1})$ +	1.0767	1.8799
−	1.0254	1.8695
$E(\underline{k} \parallel \underline{c}^{\prime})$ +	0.2337	0.3260
−	0.2227	0.3049

Energy bandwidths** of excess electrons and holes in ovalene.

	Electron			Hole		
Vibrational Overlap	0.1	0.5	1.0	0.1	0.5	1.0
$\langle vbvb \rangle$****	580.62	3334.20	4160.40	994.36	2290.4	848.60
$\langle vbvb/\underline{v}(\underline{k}) \rangle$***	14.63	24.24	18.78	15.81	10.18	1.93
μ_{aa}	0.02	0.06	0.11	0.02	0.16	1.05
μ_{bb}	(0.03)	(0.09)	(0.20)	(0.05)	(0.49)	(4.16)
μ_{cc}	0.23	0.77	1.56	0.29	1.99	11.51
μ_{bb}	(0.33)	(1.29)	(2.79)	(0.58)	(4.54)	(27.79)
μ_{ac}	−0.06	−0.21	−0.49	−0.08	−0.53	−2.99
μ_{bb}	(−0.06)	(−0.35)	(−0.75)	(−0.16)	(−1.68)	(−6.67)

Mobility ratios.

Table(6.11)

* units: 1_{10}−4 eV.

** units: eV.

*** units: 1_{10}3 m/sec.

****units: 1_{10}6 m²/sec².

values of aA and aC are the same whether the screening parameter $\zeta = 30.7$ nm^{-1} or $\zeta = 24.6$ nm^{-1} are used even though the mobility ratios μ_{aa}/μ_{bb} and $\mu_{c'c'}/\mu_b$ have changed by a factor of about 10. Thus it appears that, for ovalene at least, the relative orientations of the principle axes are independent of both vibrational overlap factor and screening parameter. To test this statement further the elements of the mobility tensor have been calculated using screening parameter $\zeta = 22.7$ nm^{-1}. The transfer integrals, energy band widths and ratios of the components of the mobility tensor are given in table (6.11). The values of elements aA and aC are consistent with those obtained using the previous two screening parameters indicating that the effect arises as a result of the crystal structure and relative orientation of the molecules within the unit cell. This is further substantiated by the correlation between the angles $\underline{a}.\underline{C}$, $\underline{A}.\underline{c}'$ of the mobility tensor with the angles $\underline{a}.\underline{M}$ and $\underline{L}.\underline{c}'$ (c.f. tables (5.9) and table (5.10)), where $\underline{M}$ and $\underline{L}$ are the molecular axes of the molecule. Thus the principle axes of the mobility tensor $\underline{A}$ and $\underline{C}$ approximately lie along the molecular axis $\underline{M}$ and $\underline{L}$, and the remaining axis $\underline{B}$ is coincident with the crystallographic axis $\underline{b}$.

Similar correlations are observed for circumanthracene, however, possibly due to band-band interactions the above effects are not observed in coronene.

6.5   Comparison of theory with experiment

Assuming the energy band model to be applicable to the conduction mechanism in coronene type crystals, then, by the methods described in Chapter (3), the relationship between the minimum value of the mobility and the energy band width is :

$$\mu_{ii} \overset{>}{\sim} \frac{e\,h}{k_0 T\,B} <<v_i\,v_i>> \qquad\qquad (6.2)$$

The mobilities calculated in this way are found to vary approximately
as the vibrational overlap factor and hence it would be an
advantage to have some idea of the magnitude of this factor.
Miller and Murrell (131) have shown that a common Franck-Condon factor,
which is essentially the square of the vibrational overlap integral
between the ground and first electronic excited states, can be used
to calculate the vibrational envelopes of a series of condensed
aromatic hydrocarbons. Assuming a similar situation to exist for
the vibrational overlap integral between the neutral molecule and
the ionised states then the value of the factor $|<\chi^0|\chi^1>|^2$ will
be of the order 0.5 (74). The validity of this assumption does not
effect the general conclusions in the following discussion.

Using the value $|<\chi^0|\chi^1>|^2 = 0.5$ together with the energy
band widths of table (6.5) and table (6.6) and the mean square
velocities given in table (6.8) and table (6.7) the minimum values
of the mobility, μ_{bb} , of electrons and holes in coronene are
1.5 (4.1) and 4.6 (6.3) cm^2/volt.sec., respectively, where the
figures in parentheses refer to values calculated using screening
parameter $\zeta = 24.6$ nm^{-1}. The electron and hole mobilities in each
of the pairs of energy bands are approximately equal.

Assuming the conductivity to be intrinsic and not affected
by traps then (205)

$$\sigma_0 = e(N_{0e}\,N_{0h})^{\frac{1}{2}} (\mu_h + \mu_e) \qquad\qquad (6.3)$$

where $\sigma 0$ is the pre-exponential factor, N_{0e} and N_{0h} are the
effective densities of states of the electron - hole conduction

bands, and μ_e and μ_h are the mobilities of free electrons and holes respectively. Theoretical considerations of Le Blanc on anthracene led to approximately equal densities of states for holes and electrons so that equation (6.3) reduces to :

$$\sigma 0 \ = \ e \ N_0 (\mu_h + \mu_e) \tag{6.4}$$

where N_0 is the geometric mean of N_{0_e} and N_{0_h} and e is the charge on the free electron. Quantitatively N_0 is about twice the molecular density and hence for coronene $N_0 = 2.6_{10}21 \ cm^{-3}$.

Equation (6.4) can be extended to conduction at any temperature, T , in which case

$$\sigma \ = \ e \ N(\mu_e + \mu_h) \tag{6.5}$$

where $N = N_0 \exp(E/2 \ k_0 T)$; E is the experimentally measured energy gap. Thus, for coronene at 15^oC, using the values $E(||ab)$ (193) and $E(\underline{1} \ ab)$ (193). N_0 has the values $6.6_{10}12 \ cm^{-3}$ and $2.4_{10}12 \ cm^{-3}$ giving values of $6_{10}12(1_{10}11) \ \Omega-cm$ and $2_{10}15(1_{10}14) \ \Omega-cm$ for the resistivity parallel and perpendicular to the ab plane respectively. As before the figures in parentheses refer to value calculated using $\zeta = 24.6 \ nm^{-1}$. The value of N is extremely sensitive to both E and T and in view of this the values of the resistivity can be considered in reasonable agreement with the observed values of $1_{10}12-1_{10}13 \ \Omega-cm$. and $1_{10}17-1_{10}18 \ \Omega-cm$. for the resistivity parallel and perpendicular to the ab plane respectively.

The effective density of states, N_0 , in circumanthracene is $1.8_{10}21 \ cm^{-3}$ and the calculated mobilities along the b axis are 1.2 and 1.9 $cm^2/volt.sec.$ for electrons and holes respectively. Using the value $E = 1.8 \ eV$ (196) the calculated resistivities $\rho(||\underline{b})$ is $6_{10}12 \ \Omega-cm$ which is in good agreement with the observed value (196).

Similarly using values of the mobility and energy gap in the __ab__ plane the predicted resistivity of 7×10^{13} Ω-cm. is in good agreement with the observed value of 2.5×10^{13} Ω-cm. (196). However, the predicted resistivity, calculated using E = 1.7 eV, of 3×10^{13} Ω-cm. is about four orders of magnitude too low. This vast discrepancy between theory and experiment cannot be explained in terms of an error in the calculated mobility since to give the observed resistivity would require a mobility of the order 1×10^{-5} cm /volt.sec. which is several orders of magnitude lower than those normally observed in materials of this type. Hence the discrepancy must lie either in an error in the observed value of E or to a breakdown of equation (6.5) due to trapping effects.

A similar situation is encountered in the case of crystalline ovalene where the calculated value of the resistivity, in the absence of trapping effects, using E = 1.13 eV. (194, 195) is of the order 1×10^{7} Ω-cm. which is about 8 orders of magnitude lower than observed experimentally. If, however, one uses a value E = 1.8 eV., intermediate between the values for coronene and circumanthracene, the resulting value for the resistivity of $\rho(||\underline{ab}) \sim 6 \times 10^{13}$ Ω-cm. is in much better agreement with experiment. This infers that the value of E determined by Inokuchi et al (195, 196) represents a trap depth rather than a band gap giving E_T = 0.59 eV. Using equation (6.5) in reverse, the number of free carriers, at room temperature, required to give the observed resistivity is of the order 1×10^{5} cm^3 thus the effective density of states, N_0, is of the order 3×10^{14} cm^{-3} which is of a similar order of magnitude to that observed in phenanthracene under space charge limited conditions (128).

Conclusion

The energy band structures of coronene, ovalene and circumanthracene have been calculated in the tight binding approximation

using single Slater functions to represent the carbon atomic orbitals.

The energy band structures of both excess electrons and holes in crystalline coronene consist of two sets of energy bands, corresponding to the two degenerate molecular energy levels in the free molecule, which exhibit a high degree of anisotropy with an average width ~ 0.05 eV. The energy dependence on the wave vector for $\underline{k}$ parallel to $\underline{b}^{-1}$ has several unusual features, however, the behaviour can be understood in terms of energy band-band interactions. Minimum values of the mobility, calculated such that the uncertainty principle is not violated, are 1.5 (4.1) cm^2/volt.sec. and 3.5 (6.3) cm^2/volt.sec., along the $\underline{b}^{-1}$ axis for electrons and holes respectively, and the mobilities along the remaining axes are related to this through

$$\mu_{aa} \sim \mu_{c'c'} \sim \frac{1}{1000} \left(\frac{1}{100}\right) \mu_{bb}$$

where the figures in parenthesis refer to values calculated using $\zeta = 24.6$ nm^{-1}.

The energy band structures of ovalene and circumanthracene are comparatively simple, again showing a high degree of anisotropy and large band width. It is noted that the energy bands along the $\underline{b}^{-1}$ axis should be of sufficient width (~ 0.1 eV) to effectively localize excess carriers around the band minimum thus removing the anomolous electrical and magnetic effects observed in anthracene type crystals. Minimum values of the mobility along the $\underline{b}^{-1}$ axis are 2.8 (3.1) and 3.8 (2.7) cm^2/volt.sec. for excess electrons and holes in ovalene, respectively, and 1.2 and 1.9 cm^2/volt.sec. for excess electrons and holes in circumanthracene. Approximate values for the mobilities along the two remaining axes can be obtained through the relations

$$\mu_{aa} \sim \frac{1}{10} \mu_{cc} \sim \frac{1}{50} \mu_{bb} \quad \text{for ovalene}$$

and

$$\mu_{aa} \sim \frac{1}{20} \mu_{cc} \sim \frac{1}{20} \mu_{bb} \quad \text{for circumanthracene.}$$

The mobility anisotropy of ovalene, calculated using $\zeta = 24.6 \text{ nm}^{-1}$, is very sensitive to the vibrational overlap factor and the above equation only holds for $|\langle\chi^0|\chi^1\rangle|^2 = 0.1$; for the mobility ratios for higher values of the vibrational overlap factor table (6.8) should be consulted.

In summary the energy band widths and carrier mobilities of condensed aromatic polyacenes are considerably larger than those previously obtained for lower aromatic hydrocarbons. It should be noted that the values of the mobility reported here represent the lower limit and simple hopping calculations of the type used on anthracene predict a value of the order 10 $\text{cm}^2/\text{volt.sec}$.

CHAPTER (7)

On the carrier mobilities in crystalline α-phenazine.

7.1   Introduction.

7.2   Molecular orbitals.

7.3   Numerical calculations.

7.4   Mobility tensor.

   (i)   Mobilities in the band approximation.

   (ii)   Mobilities in the localized representation.

7.5   Conclusion.

7.1 Introduction

In the previous calculations reported in this thesis the molecular orbital coefficients of the molecules in question have been calculated using the Hueckel approximation, an approximation which is known to give reasonable agreement when used to calculate physical properties of aromatic hydrocarbons. For heterocyclic molecules, however, the Hueckel approximation is much less reliable and when calculating the physical properties of such molecules SCF-LCAO-MO theory is generally used. In the present calculations the MO's representing the wave function of the positive or negative molecular ions have been obtained from solutions to the corresponding ground state problem. Fraga and Ransil (207) have noted that this approximation will lead to results that are not better than, and probably poorer than, the ground state, but which are still qualitatively useful.

As a basis for calculating the π-MO's of heterocyclic molecules use has been made of the Roothaan LCAO-SCF equations (147) suitably simplified by the "neglect of differential overlap" approximation (144, 145). This involves the neglect of products of pairs of different atomic orbitals in certain electron interaction integrals. This kind of treatment is intermediate in complexity between full LCAO-SCF calculations for π electrons and the very simple Hueckel approach which does not take into account electron interactions in any explicit manner.

Several methods have been derived for estimating the parameters needed in SCF calculations, thus introducing a certain degree of uncertainty into the molecular orbital coefficients. It is the object of this chapter to determine what effects the use of different parameters have when the resulting molecular orbitals are used in mobility calculations.

In the absence of any experimental data relating to the conduction mechanism in α-phenazine the carrier mobilities have been calculated using both the energy band and hopping models. The atomic wave functions of the carbon and nitrogen atoms are represented as single Slater functions using the normal screening parameters.

7.2 Molecular Orbitals

The molecular orbitals and energy levels were calculated using the LCAO-SCF-MO method with the simplifications introduced by Pariser and Parr (144) and Pople (145). The method assumes that the pi-electrons can be treated apart from the sigma-electrons, the pi-electrons moving in an effective field due to the core region composed of sigma electrons and nuclei . Parr (146) has given a set of sigma-pi separatability conditions which the wave functions of a set of molecular states must satisfy in order that they can be treated separately. In the pi-electron approximation correlation energies between the sigma and pi-electrons are necessarily neglected and the sigma parts of the wave functions are assumed to be invariant of the molecular state.

The Hamiltonian for a system containing 2n pi-electrons can be written :

$$H_\pi = \sum_{i=1}^{2n} H_{core}(i) + \sum_{i<j=1}^{2n} \frac{e^2}{r_{ij}} \qquad (7.1)$$

where $H_{core}(i) = T(i) + U_{core}(i)$ is the kinetic energy operator for electron i plus its potential energy in the field of the core.

The ground state wave function for a molecule with a closed shell is written as a single, normalised, Slater determinant :

$$\Psi_0 = det \, |\Phi_1 \, \overline{\Phi}_1 \, \Phi_2 \, \overline{\Phi}_2 \, \cdots \, \Phi_n \, \overline{\Phi}_n| \qquad (7.2)$$

where $\Phi_i = \psi_i \alpha$ and $\overline{\Phi}_i = \psi_i \beta$ are molecular spin orbitals. In the LCAO approximation the molecular ~~crystals~~ orbitals ψ_i are assumed to be linear combinations of a basis set of m-atomic orbitals, ϕ_μ :

$$\psi_i = \sum_{\mu=1}^{m} c_i^\mu \phi_\mu \qquad (7.3)$$

The atomic orbitals ϕ_μ are centred, one to each atom, on the various atoms contributing pi-electrons to the system under consideration. They are mutually orthogonal orbitals of such a nature that differential overlap is negligable. Although their exact analytical form is unknown they may be expected to resemble deformed $2p_\pi$ orbitals.

A procedure for the determination of the coefficients c_i^μ which minimise the total pi-electronic energy, $E_0 = \int \Psi_0^* H_\pi \Psi_0 \, d\tau$, has been given by Roothaan (147). However, the calculations are very tedious. The equations can be simplified considerably by the introduction of the zero differential overlap (Z.D.O.) approximation as suggested by Pariser and Parr (144) and Pople (145). The Z.D.O. approximation can be expressed as :

$$\phi_\mu^*(i) \, \phi_\nu(i) \, d\tau(i) = 0 \; ; \quad (\mu \neq \nu) \qquad (7.4)$$

It is rather difficult to determine theoretically whether or not the Z.D.O. assumption is a justifiable approximation, however, for hydrocarbons it appears to be a good first approximation but for heterocyclic molecules where the distribution of electrons is not so uniform one would expect overlap effects to play a greater role (146).

Within the Z.D.O. approximation, the coefficients c_i^μ and molecular orbital energies E_i are the eigenvectors and eigenvalues

of the Hartree - Fock matrix h^F whose elements are given by :

$$h^F_{\mu\mu} = \alpha_\mu + \frac{1}{2} P_{\mu\mu} \gamma_{\mu\mu} + \sum_{\nu \neq \mu} P_{\nu\nu} \gamma_{\mu\nu} \qquad (7.5)$$

$$h^F_{\mu\nu} = \beta_{\mu\nu} - \frac{1}{2} P_{\mu\nu} \gamma_{\mu\nu} \qquad (\mu \neq \nu) \qquad (7.6)$$

In these equations the quantity α_μ is the one-centre core matrix defined by :

$$\alpha_\mu = \int \phi_\mu^*(1) \underset{core}{H(1)} \phi_\mu(1) \, dv(1) \qquad (7.7)$$

the quantity $\beta_{\mu\nu}$ is the two-centre core matrix or resonance integral defined by :

$$\beta_{\mu\nu} = \int \phi_\mu^*(1) \underset{core}{H(1)} \phi_\nu(1) \, dv(1) \qquad (7.8)$$

the quantity $\gamma_{\mu\nu}$ is the coulomb repulsion integral defined by :

$$\gamma_{\mu\nu} = \int \phi_\mu^*(1) \phi_\nu^*(2) \frac{e^2}{r_{12}} \phi_\mu(1) \phi_\nu(2) \, dv(1) \, dv(2) \qquad (7.9)$$

and $P_{\mu\nu}$ is an element of the charge density - band order matrix P defined by :

$$P_{\mu\nu} = 2 \sum_{\substack{occupied \\ orbitals}} c_i^{\mu*} c_i^{\nu} \qquad (7.10)$$

The integral α_μ of equation (7) can be expanded according to Goepert - Meyer and Sklar(202)as :

$$\alpha_\mu = W_\mu - \sum_{\nu \neq \mu} (\mu\mu : \nu) + z_\nu \gamma_{\mu\nu} \qquad (7.11)$$

where z_ν is the number of electrons contributed to the pi-electron system by atom ν. The penetration integrals $(\mu\mu : \nu)$ are usually neglected. If, as suggested by McWeeny and Peacock (148), we choose the energy zero for the molecular orbital energies ε_i as

$$\varepsilon_0 = W_c + \frac{1}{2} \gamma_{cc}^{(0)}$$

then the Hartree - Fock Hamiltonian h^F assumes the form :

$$h_{\mu\mu}^F = \delta\omega_\mu + \frac{1}{2} P_{\mu\mu} \gamma_{\mu\mu} - \frac{1}{2} \gamma_{cc}^{(0)} + \sum_{\mu \neq \nu} (P_{\nu\nu} - z_\nu) \gamma_{\mu\nu} \qquad (7.12)$$

$$h_{\mu\nu}^F = \beta_{\mu\nu} - \frac{1}{2} P_{\mu\nu} \gamma_{\mu\nu} ; \qquad (\mu \neq \nu) \qquad (7.13)$$

where $\delta\omega_\mu = W_\mu - W_c$. Here W_μ measures the electron affinity of the single framework ion at μ and takes the value W_c for a carbon atom; while $\gamma_{cc}^{(0)}$ is the value of $\gamma_{\mu\mu}$ also for a carbon atom. The energy zero is then such that $h_{\mu\mu}^F = 0$ for a carbon atom in an alternant hydrocarbon. Because h^F depends on P, and hence on the c_i^{μ}'s, an iterative calculation must be used to determine the c_i^{μ}'s and ε_i's . A procedure for the direct iteration of the matrix R ($= \frac{1}{2} P$) utilising the method of steepest descents has been proposed by McWeeny (149). As it only involves the manipulation of matrices, it is particularly adaptable for electronic computation. The entire procedure was programmed in K.D.F.9 Algol, the input data consisting of the numerical values for z_μ, $\delta\omega_\mu$, $\beta_{\mu\nu}$ and $\gamma_{\mu\nu}$ defined by equation (7.11), (7.14), (7.8), and (7.9) and an initial estimate of the matrix P . At the end of each descent the idempotency of R was restored according to McWeeny's procedure (149). The procedure was regarded as self consistent when successive iterations did not change any of the elements of R by more than

1_{10}-4. The eigenvectors and eigenvalues of the self consistent Hamiltonian h^F were determined by diagonalising the matrix h^F utilising Householders method of rotations as developed by Wilkinson (150). The Algol text of the program is given in appendix (4) together with more detailed instructions for the construction of the data tape.

The energy levels of phenazine have been calculated using the coulomb integral parameters $\gamma_{\mu\mu}$ of McWeeny and Peacock (148) and Nishimoto and Forster (152) with the off diagonal elements calculated using the method of Mataga and Nishimoto (153). In addition $\gamma_{\mu\nu}$ have also been calculated using the Ohno approximation (154) and the integral of values of McWeeny and Peacock (148). In the construction of the resonance integral matrix it is assumed that $\beta_{\mu\nu}$ = 0 if μ and ν are not directly bonded and for adjacent atoms the values of Linderberg (156) have been used.

The molecular orbital coefficients of the excess electron and hole together with the electron densities of the neutral molecule, calculated using the above three sets of parameters are listed in table (7.1). Since it is the object of this chapter to show that different, but reasonable, values of the integral parameters do not drastically alter the general results in band structure calculations no attempt has been made to test the quality of the molecular orbital by computing the electronic, or physical, properties of the isolated molecule. However, all sets of parameters have been shown to give reasonable results when used in calculations on pyridine (148, 152). The points of interest for band structure calculations are that the three sets of wave functions are of the same symmetry and the corresponding molecular orbital coefficients are of the same sign varying only in magnitude.

	I			II			III		
	ψ_7	ψ_8	Electron Density	ψ_7	ψ_8	Electron Density	ψ_7	ψ_8	Electron Density
Symmetry	AxSy	SxSy		AxSy	SxSy		AxSy	SxSy	
1	0.07672	-0.15436	0.95538	0.07153	-0.14886	0.96457	0.01297	-0.19730	0.91295
2	-0.29399	-0.24875	1.00083	-0.29404	-0.24554	0.99786	-0.33317	-0.22065	0.99533
3	-0.20876	0.20144	0.99425	-0.20560	0.19770	0.99367	-0.21664	0.20000	0.98445
7	0.47867	0.49813	1.09938	0.48247	0.50730	1.08799	0.42930	0.49517	1.21506

I   Integral parameters from McWeeny(155). γ_{ij} calculated using Mataga-Nishimoto approximation.

II   Integral parameters from McWeeny(155). γ_{ij} calculated using Ohno approximation.

III Integral parameters from Nishimoto-Forster(152). γ_{ij} calculated using Mataga-Nishimoto approximation.

Table(7.1)

Molecular orbital coefficients of the highest occupied and lowest unhoccupied orbitals and electron densities of the neutral molecule in phenazine.

7.3 Numerical calculations

The crystal and molecular structure of α-phenazine has been
studied both at room temperature and 80°k (157 - 159). The crystal
structure is base centred monoclinic of space group P2$_1$/a (C$_{2h}^{(5)}$).
The main feature of the molecular packing may be visualized in terms
of molecular "stacks" which consist of molecules separated by unit
translations along 0 1 0 . Each molecule has three kinds of near
neighbours :   those within its own stack, those in stacks separated
by unit translation along 0 0 1 and those in stacks generated by
a glide plane. Within each stack the molecules are parallel,
separated by interplanar distance of 0.349 nm, and are staggered in
such a way as to minimise overlap. The shortest distance of approach
between carbon atoms separated by the length of the c-axis is
0.373 nm and in the molecule related by the glide plane 0.382 nm.
The molecules are inclined to the (0 1 0) plane at an angle of about
45° and thus molecules in stacks related by the glide plane are
approximately perpendicular. The molecular arrangement in
α-phenazine is closely similar to coronene and ovalene (161, 162), a
similarity which is reflected in the magnitudes of the principle
transfer integrals. Whereas in anthracene the conduction along the
$\underline{b}^{-1}$ axis occurs jointly through the interactions of the molecule at
(0, 0, 0) and those at (0, 1, 0) and ($\frac{1}{2}$, $\frac{1}{2}$, 0) in α-phenazine and
coronene, the latter interaction is much smaller than the former.
However, the interaction ($\frac{1}{2}$, $\frac{1}{2}$, 0) together with the interaction ($\frac{1}{2}$, $\frac{1}{2}$, 1),
which is also considerably smaller than (0, 1, 0) give rise to
conduction along the $\underline{a}$-axis. Hence the energy bands in phenazine
will exhibit a much higher degree of anisotropy in the $\underline{ab}$ plane
than in crystals having an anthracene type structure. In calculations
based on a hopping model the degree of anisotropy may be lowered by

the high quadratic moments of the smaller distribution functions.

Using the molecular orbital coefficients of section (2), the transfer integrals between the molecule at (0, 0, 0) and near neighbours have been calculated using the crystal data refined at $80^{\circ}K$. In addition the transfer integrals have been calculated using the molecular orbitals coefficients of set I and the room temperature crystal data. Due to the heterocyclic nature of phenazine the interactions between the molecule at the origin and the molecule at the general positions $(n\frac{a}{2}, m\frac{b}{2}, \ell)$ and $(n\frac{a}{2}, -m\frac{b}{2}, \ell)$ are no longer equivalent. The transfer and overlap integrals for the excess electron and hole are given in table (7.3) and table (7.2) respectively. The results of the calculations using the coefficients of sets I and II are extremely similar and show a strong correlation with the results of set III and, as was predicted on the basis of crystal structure, the anisotropy of the transfer integrals bears little resemblence to anthracene while showing a strong correlation to coronene type crystals (see chapter (6)).

The energy dependence on wave vector, $\underline{k}$, for α-phenazine can be written :

$$
\begin{aligned}
E'_{\pm}(\underline{k}) = \ & 2E_2 \ \cos(\underline{k} \circ \underline{c}) + 2E_3 \cos(\underline{k} \circ \underline{b}) \\
& + 2E_4 \ (\cos(\underline{k} \circ (\underline{b} + \underline{c})) + \cos(\underline{k} \circ (\underline{b} - \underline{c}))) \\
& + 2E_5 \ \cos(\underline{k} \circ \underline{a}) + 2E_6 \cos(\underline{k} \circ (\underline{c} + \underline{a})) \\
& + 2E_7 \ (\cos(\underline{k} \circ (\underline{a} + \underline{b})) + \cos(\underline{k} \circ (\underline{a} - \underline{b}))) \\
& + 2E_8 \ (\cos(\underline{k} \circ (\underline{a} + \underline{b} + \underline{c})) + \cos(\underline{k}(\underline{a} - \underline{b} + \underline{c}))) \\
& \pm 2E_9 \ \cos(\underline{k} \cdot \tfrac{1}{2}(\underline{a} + \underline{b})) \\
& \pm 2E_{10} \ \cos(\underline{k} \circ (\tfrac{1}{2}(\underline{a} + \underline{b}) + c) \\
& \pm 2E_{11} \ \cos(\underline{k} \circ \tfrac{1}{2}(\underline{a} - \underline{b})) \\
& \pm 2E_{12} \ \cos(\underline{k} \circ (\tfrac{1}{2}\underline{a} - \underline{b}) + c) \ .
\end{aligned}
$$

	I		II		III		I	
Position	Transfer	Overlap	Transfer	Overlap	Transfer	Overlap	Transfer	Overlap
0, 0, 1	16.01	-3.01	15.77	-2.98	12.89	-2.57	16.67	-3.13
0, 1, 0	-70.94	11.13	-70.80	11.23	-94.81	16.61	-58.16	9.38
0, 1, 1	-0.29	0.16	-0.31	0.17	-1.23	0.34	-0.19	0.18
$\frac{1}{2}$, $\frac{1}{2}$, 0	7.19	1.25	7.20	1.25	5.70	1.02	5.46	1.04
$-\frac{1}{2}$, $\frac{1}{2}$, 0	5.25	1.25	5.29	1.25	5.70	1.02	3.72	1.04
$\frac{1}{2}$, $\frac{1}{2}$, 1	-19.79	-3.57	-20.40	-3.69	-18.67	-3.43	-16.29	-3.45
$\frac{1}{2}$, $-\frac{1}{2}$, 1	-19.42	-3.57	-20.32	-3.69	-18.35	-3.43	-15.93	-3.45

Table(7.2)

Transfer* and overlap** integrals for excess holes in phenazine.The Roman numerals refer to the sets of molecular orbital coefficients of table(7.1).The first three sets of figures were calculated using crystal data obtained at 80° K,the fourth at room temperature.

* units: $1_{10}-4$ eV.

**units :$1_{10}-4$.

	I		II		III		I	
Position	Transfer	Overlap	Transfer	Overlap	Transfer	Overlap	Transfer	Overlap
0, 0, 1	-23.02	4.52	-22.47	4.50	-20.98	4.33	-23.96	4.71
0, 1, 0	268.52	-50.87	265.09	-50.51	291.02	-57.53	273.32	-45.51
0, 1, 1	26.70	5.00	-26.80	5.03	-32.81	6.11	-23.52	4.58
$\frac{1}{2}, \frac{1}{2}, 0$	23.88	-3.66	23.31	-3.61	21.58	-3.78	17.60	-2.65
$-\frac{1}{2}, \frac{1}{2}, 0$	13.08	-3.66	12.82	-3.61	13.77	-3.78	8.88	-2.65
$\frac{1}{2}, \frac{1}{2}, 1$	-4.66	1.45	-4.75	1.48	-5.68	1.76	-7.66	1.38
$\frac{1}{2}, -\frac{1}{2}, 1$	-4.66	1.45	-4.77	1.48	-5.68	1.76	-7.64	1.38

Table(7.3)

Transfer* and overlap** integrals for excess electrons in phenazine.The Roman numerals refer to the sets of molecular orbital coefficients of table(7.1).The first three sets of figures were calculated using crystal data obtained at $80°$ K,the fourth at room temperature.

* units: $1_{10}-4$ eV.

**units: $1_{10}-4$.

The numbering of the molecules in the crystal is shown in figure (7.2).
The energy band structures of excess electrons and holes along the
inverse $\underline{a}$, $\underline{b}$ and $\underline{c}$ axes are illustrated in figures (7.3) and
figure (7.4) and the energy band widths are given in table (7.4).

The energy band widths computed using the three sets
of transfer integrals are extremely similar, each showing the energy
band to be highly anisotropic. Comparisons with anthracene are
rather few, the energy band being similar to those of coronene and
ovalene, however, there is a limited correlation between the band
widths in phenazine along the $\underline{a}$ and $\underline{c}$ axes with those of anthracene
along the $\underline{c}$ and $\underline{a}$ axes corresponding to the approximately equal
lengths of these axes.

7.4   Mobility tensor

7.4(i)   Mobilities in the band approximation

In the energy band model the mobility tensor can be related to
the mean square velocity of the carriers in the mean free time
approximation through :

$$\mu_{ij} = \frac{e\,\tau}{k_0 T} \ll v_i\, v_j \gg$$

and in the mean free path approximation :

$$\mu_{ij} = \frac{e\,\lambda}{k_0 T} \ll v_i\, v_j / \underline{v}(\underline{k}) \gg$$

where the symbols have their usual meanings (160). The components
of the tensor $< v_{\underline{b}^{-1}}\, v_{\underline{b}^{-1}} >$ and $< v_{\underline{b}^{-1}}\, v_{\underline{b}^{-1}} / \underline{v}(\underline{k}) >$ and the ratios of
the non-zero elements of the tensor to these are given in table (7.5).
The mobility of excess electrons show a high degree of anisotropy in
both the $\underline{bc}'$ and $\underline{ab}$ planes whilst being practically isotropic in the
$\underline{ac}$ plane. The value of the mean square velocity of excess electrons
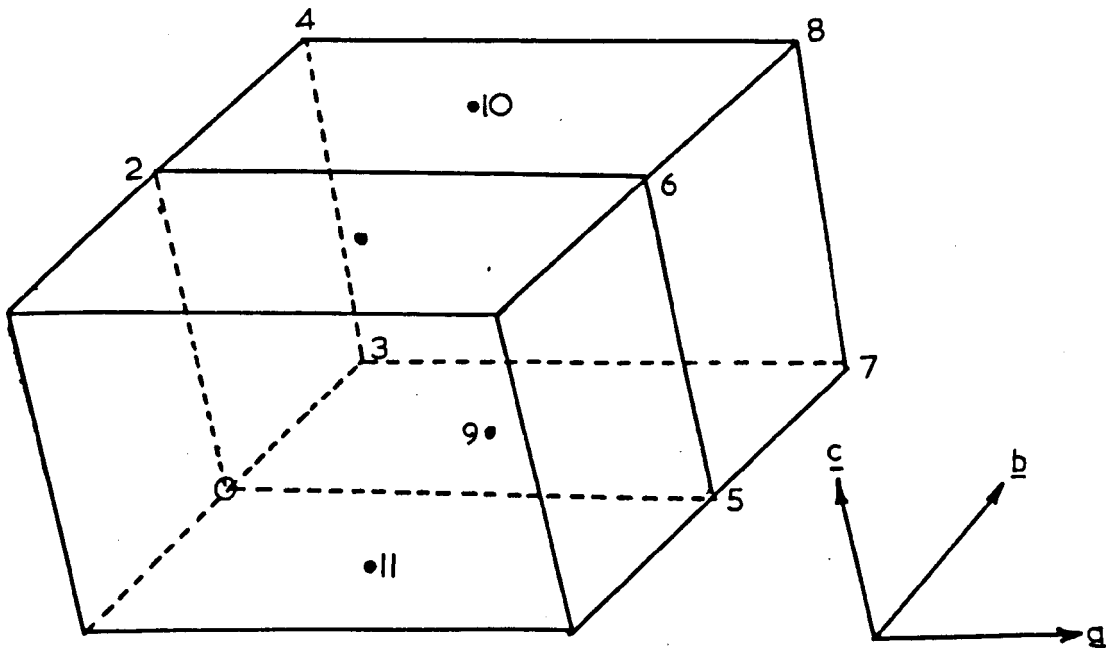
Figure (7.1)

Schematic representation of the unit cell of α-phenazine

showing the numbering of the molecules with the unit cell.
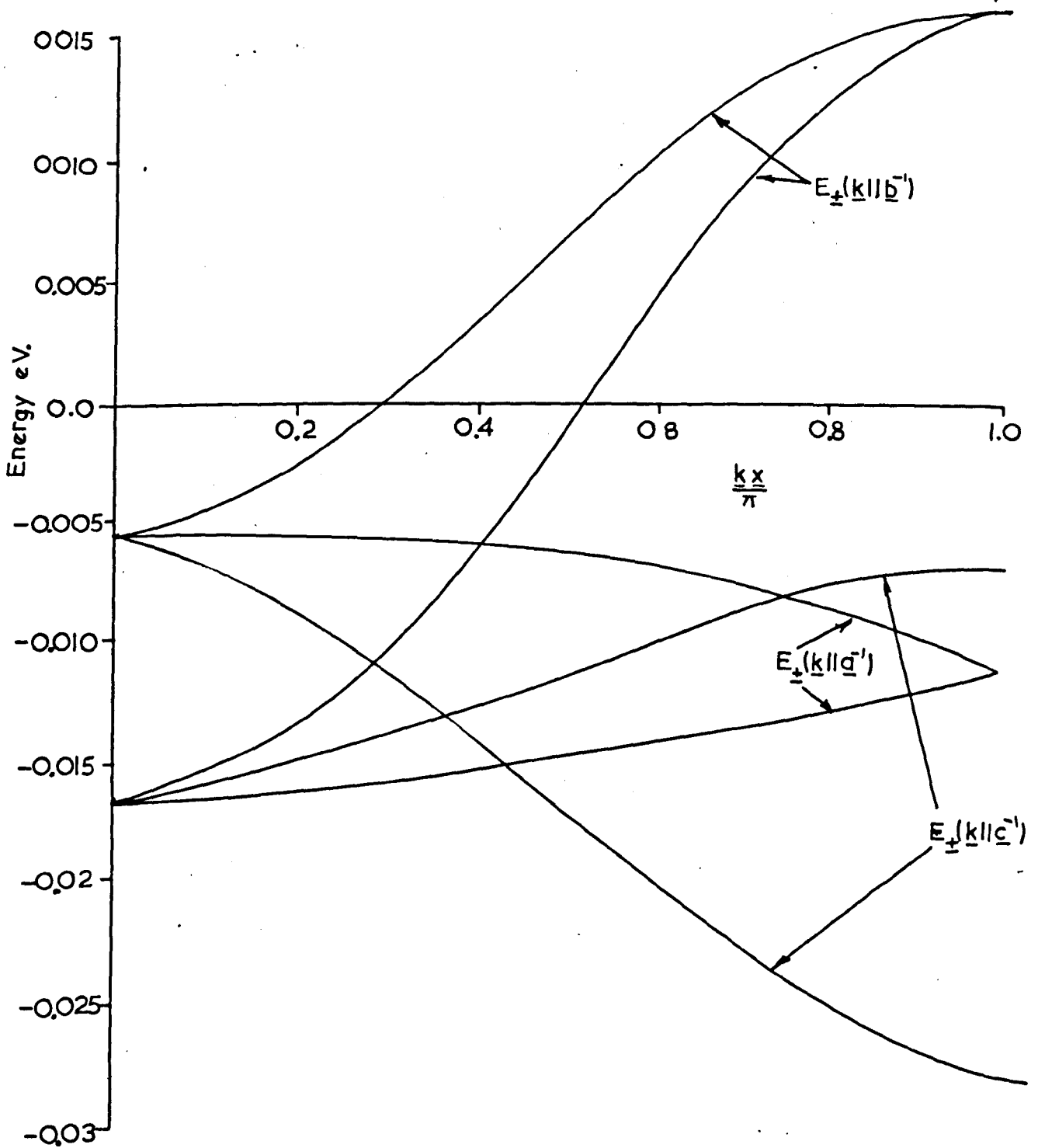
Figure (7.2)

Energy band structure of excess holes in α-phenazine.
The energy zero is arbitrarily chosen as the energy of
the lowest antibonding molecular orbital in the free
molecule.
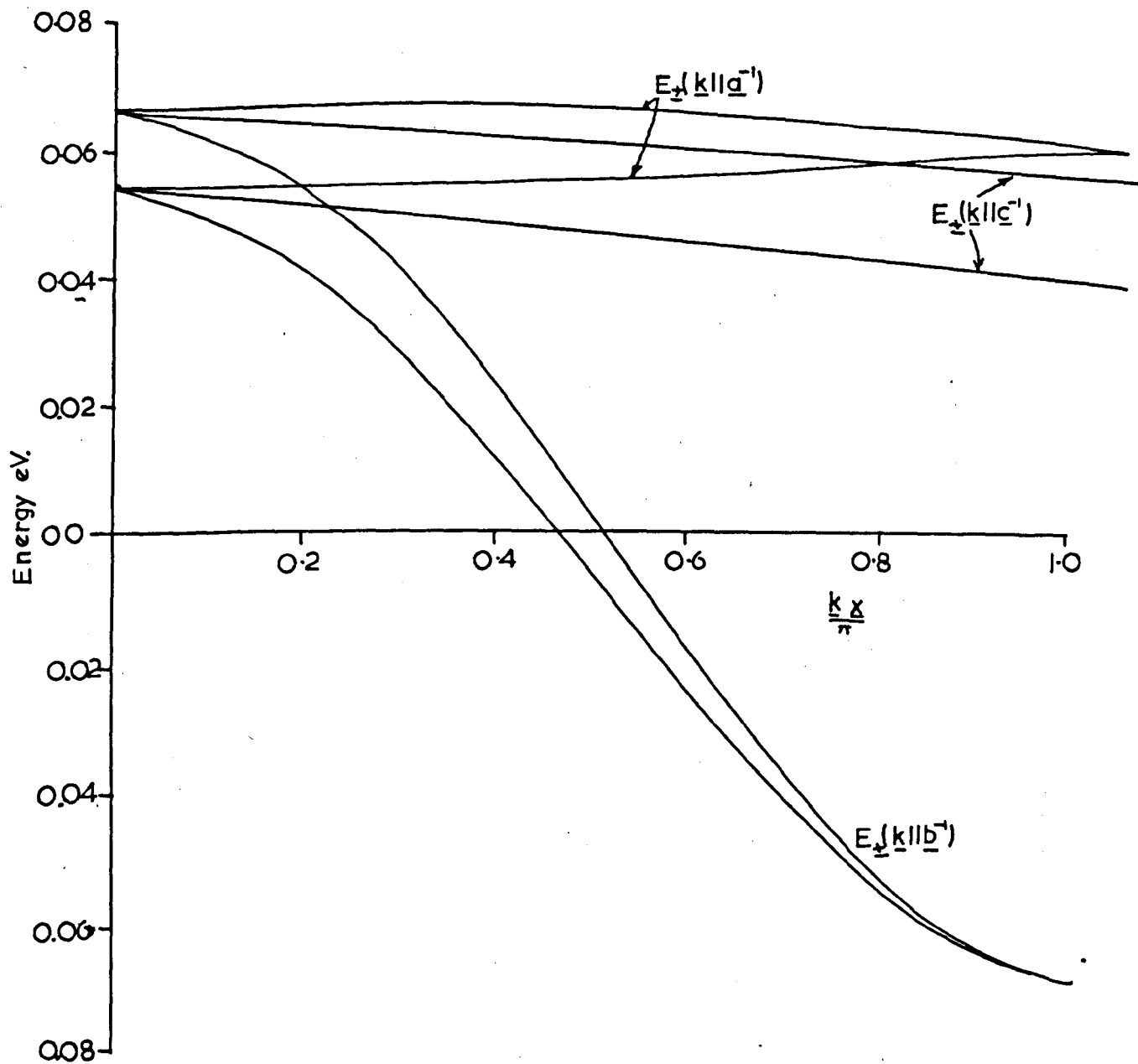
Figure (7.3)

Energy band structure of excess electrons in α-phenazine.

The energy zero is arbitrarily chosen as the energy of the

highest bonding molecular orbital in the free molecule.

		Low temp.		Room temp.	
		Electron	Hole	Electron	Hole
$E(\underline{k} \parallel \underline{a}')$	+	0.006	0.005	0.002	0.005
	−	0.006	0.005	0.002	0.005
$E(\underline{k} \parallel \underline{b}')$	+	0.123	0.034	0.074	0.028
	−	0.134	0.023	0.078	0.019
$E(\underline{k} \parallel \underline{c}')$	+	0.016	0.010	0.022	0.007
	−	0.008	0.022	0.035	0.020
c splitting		0.019	0.021	0.017	0.017

Table(7.4)

Energy bandwidths* in crystalline phenazine.

	Electron			Hole		
Vibrational Overlap	0.1	0.5	1.0	0.1	0.5	1.0
$\langle vbvb \rangle$**	9.383	138.330	272.490	0.658	15.150	50.027
$\langle vbvb/\underline{v}(\underline{k}) \rangle$***	2.032	6.468	7.396	0.405	1.999	3.593
$\dfrac{\mu_{aa}}{\mu_{bb}}$	0.08 (0.09)	0.14 (0.19)	0.29 (0.44)	0.23 (0.22)	0.22 (0.22)	0.24 (0.25)
$\dfrac{\mu_{cc}}{\mu_{bb}}$	0.05 (0.09)	0.16 (0.24)	0.29 (0.44)	0.32 (0.30)	0.26 (0.24)	0.23 (0.22)

(a)

	Electron			Hole		
Vibrational Overlap	0.1	0.5	1.0	0.1	0.5	1.0
$\langle vbvb \rangle$**	7.216	171.620	284.561	0.456	11.324	48.724
$\langle vbvb/\underline{v}(\underline{k}) \rangle$***	1.848	9.216	11.224	0.331	1.671	2.895
$\dfrac{\mu_{aa}}{\mu_{bb}}$	0.05 (0.07)	0.05 (0.07)	0.05 (0.07)	0.22 (0.22)	0.21 (0.21)	0.20 (0.22)
$\dfrac{\mu_{cc}}{\mu_{bb}}$	0.05 (0.07)	0.03 (0.04)	0.03 (0.04)	0.38 (0.35)	0.36 (0.33)	0.35 (0.33)

(b)

Table(7.5)

Mobility ratios of excess electrons and holes in phenazine at room(b) and low(a) temperatures.

* units: eV.

** units: $1 \times 10^6 \ m^2/sec^2$.

***units: $1 \times 10^3 \ m/sec$.

along the $\underline{b}^{-1}$ axis is about 5× the corresponding figure for anthracene and a similar behaviour is observed for the band widths giving rise to

$$\left(\mu_{\underline{b}^{-1}\underline{b}^{-1}} \right)^{\text{Phenazine}}_{\text{minimum}} - \left(\mu_{\underline{b}^{-1}\underline{b}^{-1}} \right)^{\text{Anthracene}}_{\text{minimum}}$$

A similar situation exists for excess holes. It is interesting to note for excess holes in α-phenazine $\mu_{aa} > \mu_{c'c'}$ the reverse being true for anthracene.

The ratios of the Hall to drift mobilities for excess electrons and holes, calculated using the method of Le Blanc (100) are, respectively, 7.885 and -32.126 at room temperature and 1.920 and -7.260 at 80°K, with vibrational overlap factor 0.1. These results are very similar to the values for anthracene and show the Hall mobility to be anomalous in both sign and magnitude.

7.4(ii)   Mobilities in the localized representation

The elements of the mobility tensor have been calculated using the method of Glaeser and Berry (44). The quadratic moments of the probability distributions $\tau(\underline{r}_i)$ for α-phenazine and anthracene at room temperature at 90°K are given in table (7.6) and the jump probabilities, jump frequencies, $\frac{1}{T_i}$, and diagonal elements of the mobility tensor are given in table (7.8) and table (7.7). Unlike the energy band model, the hopping model predicts the values for the hole mobility in phenazine to be very similar, both in magnitude and in the degree of anisotropy, to those of anthracene. Correlation between the two sets of electron mobilities are not quite so pronounced although, as predicted on the energy band model, there are some similarities between the mobility along the $\underline{c}'$ axis in phenazine and that along the $\underline{a}$ axis in anthracene.

Molecule	Phenazine xx	xy	xz	yy	yz	zz
0,0,1	5.59	-	-15.80	-	-	44.65
0,1,0	-	-	-	25.61	-	-
0,1,1	5.59	-11.97	-15.80	25.61	33.82	44.65
1,1,1	117.83	-	72.50	-	-	44.65
$\frac{1}{2},\frac{1}{2},0$	43.69	16.73	-	6.40	-	-
$\frac{1}{2},\frac{1}{2},1$	18.11	10.74	28.36	6.40	16.91	44.65

(a)

Molecule	Phenazine xx	xy	xz	yy	yz	zz
0,0,1	5.43	-	-15.53	-	-	44.35
0,1,0	-	-	-	24.81	-	-
0,1,1	5.43	-11.61	-15.53	24.81	33.17	44.35
1,1,1	113.12	-	70.83	-	-	44.35
$\frac{1}{2},\frac{1}{2},0$	42.04	16.15	-	6.20	-	-
$\frac{1}{2},\frac{1}{2},1$	17.24	10.34	27.65	6.20	16.59	44.35

(b)

Table(7.6)

Quadratic moments of phenazine and anthracene at room(a

*units: $1_{10}-2$ nm^2.

Anthracene

xx	xy	xz	yy	yz	zz
40.53	-	-58.54	-	-	84.55
-	-	-	36.557	-	-
40.53	-38.44	-58.54	36.55	55.52	84.55
4.82	-	20.19	-	-	-
18.33	12.92	-	9.14	-	-
4.35	-6.30	-19.18	9.14	27.76	84.55

Anthrancene

xx	xy	xz	yy	yz	zz
41.93	-	-58.57	-	-	81.82
-	-	-	36.02	-	-
41.93	-38.86	-58.57	36.02	54.29	81.82
3.87	-	17.80	-	-	81.82
17.82	12.67	-	9.01	-	-
5.08	-6.76	-20.39	9.01	27.14	81.82

) and low(b) temeratures.

Molecule	I $\tau(\underline{ri})$	I $1/ti$	Anthracene $\tau(\underline{ri})$	Anthracene $1/ti$
0,0,1	0.143	1.613	0.001	0.010
0,1,0	0.497	5.626	0.303	5.618
0,1,1	0.003	0.018	-	0.001
1,0,0	-	-	-	0.002
1,0,1	-	-	0.004	0.074
$\frac{1}{2}\frac{1}{2}$,0	0.079	0.444	0.493	4.570
$\frac{1}{2}\frac{1}{2}$,1	0.279	1.576	0.199	1.843

(a)

Molecule	I $\tau(\underline{ri})$	I $1/ti$	Anthracene $\tau(\underline{ri})$	Anthracene $1/ti$
0,0,1	0.068	2.313	0.002	0.050
0,1,0	0.678	22.957	0.164	4.383
0,1,1	0.134	2.275	-	-
1,0,0	-	-	-	0.001
1,0,1	-	-	0.001	0.015
$\frac{1}{2}\frac{1}{2}$,0	0.076	1.280	0.831	11.144
$\frac{1}{2}\frac{1}{2}$,1	0.044	0.741	0.003	0.034

(b)

	Hole I	Hole Anth.	Electron I	Electron Anth.
Average jump frequency	1.325	1.731	4.224	2.232
No. of jumps	3.501	4.324	16.157	9.983
μ aa	0.06	0.09	0.17	0.31
μ bb	0.11	0.15	0.70	0.27
μ cc	0.13	0.14	0.36	0.01

Table(7.7)

Jump probabilities, jump frequencies* and mobilities**

in phenazine and anthracene at room temperature.

* units: $1_{10}12$ sec^{-1}.

**units: $1_{10}-4$ m^2/volt-sec.

Molecule	I $\tau(\underline{r_i})$	I $1/t_i$	III $\tau(\underline{r_i})$	III $1/t_i$	Anthracene $\tau(\underline{r_i})$	Anthracene $1/t_i$
0,0,1	0.059	2.226	0.049	2.029	0.005	0.121
0,1,0	0.686	25.975	0.686	28.152	0.075	1.972
0,1,1	0.136	2.583	0.155	3.173	-	-
1,0,0	-	-	-	-	-	0.012
1,0,1	-	-	-	-	0.002	0.040
½,½,0	0.094	1.788	0.083	1.710	0.889	11.648
½,½,1	0.024	0.451	0.027	0.550	0.030	0.389

(a)

Molecule	$\tau(\underline{r_i})$	$1/t_i$	$\tau(\underline{r_i})$	$1/t_i$	$\tau(\underline{r_i})$	$1/t_i$
0,0,1	0.155	1.549	0.082	1.246	0.004	0.102
0,1,0	0.508	6.862	0.600	9.171	0.221	5.028
0,1,1	0.004	0.028	0.016	0.119	-	0.001
1,0,0	-	-	-	-	-	0.002
1,0,1	-	-	-	-	0.004	0.098
½,½,0	0.089	0.603	0.066	0.503	0.570	6.400
½,½,1	0.284	1.914	0.236	1.806	0.201	2.288

(b)

	Electron I	Electron III	Electron Anth.	Hole I	Hole III	Hole Anth
Average jump frequency	4.717	5.088	2.027	1.565	1.835	2.001
No. of jumps	18.492	20.056	10.519	4.262	6.070	5.264
μ_{aa}	0.73	0.74	1.0	0.29	0.32	0.37
μ_{bb}	2.84	3.13	0.71	0.46	0.76	0.49
μ_{cc}	1.30	1.49	0.18	0.55	0.65	0.55

Table (7.8)

Jump probabilities, jump frequencies* and mobilities**

in phenazine and anthracene at low temperature.

* units: 1×10^{12} sec^{-1}.

**units: 1×10^{-4} m^2/volt-sec.

Conclusion

The mobility tensor of crystalline α-phenazine has been calculated using both the energy band and hopping models of charge carrier transport. Three sets of integral parameters have been used to determine the orbital coefficients of the isolated molecule which were then used to estimate the transfer integrals. The differences in these integrals was found to be very small.

The minimum value of the mobility along the $\underline{b}$ axis in phenazine is predicted, on the basis of the energy band model, to be similar to that of anthracene with

$$\mu_{bb} \sim 5 \; \mu_{aa} \sim 3 \; \mu_{cc'} \quad \text{for excess holes, while for excess}$$

electrons $\mu_{bb} \sim 20 \; \mu_{aa} \sim 20 \; \mu_{cc'}$.

As in crystalline anthracene the ratio of the Hall to drift mobility is predicted to be anomalous in both sign and magnitude, the numerical values being similar to those of the parent hydrocarbon.

On the basis of the hopping model, the magnitude of the hole mobility along the $\underline{b}$ axis is similar to the corresponding value for anthracene, the mobilities along the remaining axes being related through

$$\mu_{bb} \sim \mu_{cc'} \sim 2 \; \mu_{aa}$$

while the electron mobility along the $\underline{b}$ axis is predicted to be about three times that of anthracene with

$$\mu_{bb} \sim 6 \; \mu_{aa} \sim 2 \; \mu_{cc'} \quad .$$

CHAPTER (8)

On the energy band structure and carrier mobilities

in crystalline β-phthalocyanine.

8.1   Introduction.

8.2   Molecular Orbitals.

8.3   Energy band structure.

8.4   Numerical calculations.

8.5   Mobility tensor.

    (i)   General.

    (ii)   Hall mobility.

   (iii)   Validity of the energy band model.

    (iv)   Mobilities in the localized representation.

8.6   Conclusion.

8.1 Introduction

The phthalocyanine molecular structure is built on the porphyrin ring system which is a basis of many naturally occurring compounds of biological interest. This, together with its high stability and relative ease of purification, has led to extensive study of its electrical properties. Together with its copper derivative, β-phthalocyanine is one of the relatively few organic crystals to have found application in the solid state field (163 - 165). In spite of this, at the instigation of these calculations very little theoretical work had been reported concerning the mechanism of charge carrier transport.

The applicability of the band model to the transport mechanism in metal free phthalocyanine has been suggested by Heilmeier, Warfield and Harrison (166), who, from Hall effect measurements and expressions applicable to wide band semiconductors, estimated the number of free carriers in phthalocyanine single crystals to be 2 to $12_{10}6$ cm^{-3}, in agreement with the value $1_{10}6$ to $1_{10}7$ derived from bulk measurements in single crystals. In addition, using the method of Fröhlich and Sewell (84) and the experimental value of the band width, they calculated a Hall mobility of 0.2 cm^2/volt.sec. which is in good agreement with their experimental value of 0.1 to 0.4 cm^2/volt.sec. More recently Barbe and Westgate (167) have successfully used equations based on the energy band model to interpret bulk trapping states in β-phthalocyanine single crystals.

The thermal activation energy for electrical conduction , first optical absorption and energy of initiation of photo-conductivity have all been found to be 1.68 eV. (168) indicating that carriers can be created by direct excitation of electrons from the valence band.

While this work was in preparation the energy band structure of
crystalline β-phthalocyanine has been published by Sukigara and
Nelson (169). The calculation is based on molecular wave functions
constructed from a molecular geometry in which the central hydrogen
atoms are situated on opposite nitrogen atoms. However, Chen (170)
has shown that much better agreement with the observed absorption
spectra can be obtained using a model in which the central hydrogen
atoms are shared between neighbouring nitrogen atoms in the form of
a hydrogen bond. In the calculations reported herein the "shared
hydrogen" model of molecular phthalocyanine is used.

More recently Chen (171) has published a calculation of the
energy band structure based on the shared hydrogen model. His
treatment of the energy band structure is very similar to the
one given here.

8.2   Molecular Orbitals

The molecular orbitals of phthalocyanine have recently been
investigated by Chen (170) in which he compared the merits of two
models. One in which the hydrogen atoms are localized on opposite
nitrogen atoms and the other in which the hydrogen atoms are shared
between neighbouring nitrogen atoms in the form of a hydrogen bond.
Calculations with a range of parameters showed the shared hydrogen
model to successfully predict the observed absorption frequencies
whilst with the localized hydrogen model agreement with experiment
was poor. Using the parameters of Chen we have recalculated the
energy levels of phthalocyanine using both Householder and Jacobi methods
to diagonalise   the secular determinant and while agreement is
obtained between the results of the two methods they are both slightly
different to those quoted by Chen. Following the procedure of Chen some

of the transitions in the ultra violet/visible region of the spectrum have been recalculated. The calculated transition frequencies are given in table (8.1).

The energy parameter β was calculated to give ν_1 the accepted value of 14306 cm^{-1}, and the parameters used in the secular equation were chosen to give the ratio of the doublet separation $\Delta\nu_1$ to the frequency ν_1 the experimental value 19.54 (calculated value 19.59).

<div align="center">Table (8.1)</div>

Transition		Calculated frequency	Experiment frequency (172)
$a_u \rightarrow b_{3g}^{*} (b_{2g}^{*})$	ν_1	14306 cm^{-1}	14306 cm^{-1}
$a_u \rightarrow b_{3g}^{**} (b_{2g}^{**})$	ν_2	33548 cm^{-1}	30380 cm^{-1}
$a_u \rightarrow b_{3g}^{***} (b_{2g}^{***})$	ν_3	46025 cm^{-1}	-
$b_{1u} \rightarrow b_{3g}^{**} (b_{2g}^{**})$	ν_2'	39099 cm^{-1}	34580 cm^{-1}
$b_{1u} \rightarrow b_{3g}^{***} (b_{2g}^{***})$	ν_3'	51579 cm^{-1}	-

<u>Calculated transition frequencies of β-phthalocyanine in the ultra violet region.</u>

The Hueckle coefficients of the highest bonding and two lowest antibonding molecular orbitals together with the electron densities of the neutral molecule and the parameters used are given in table (8.2).

The molecular orbitals of the positive ion were obtained by assigning the excess hole to the highest filled molecular orbital of the neutral molecule. Since this molecular orbital energy level is well separated from the next nearest level the energy band arising from these levels will be well separated so that, in treating conduction in the hole band, the effects of band mixing will be negligible. For the excess electron, however, the energy levels of the first and second antibonding orbitals are quite close together

Figure (8.1)

Molecular structure of phthalocyanine showing the

numbering of the atoms.

Atom	au	b3g	b2g	Electron Density
1	-0.12954	0.06781	0.14595	0.99886
2	0.12954	-0.14890	-0.07107	0.99805
3	0.16775	-0.03291	-0.13112	0.98149
4	-0.08006	0.15662	0.09842	1.02690
5	0.08006	-0.09898	-0.15442	1.02851
6	-0.16775	0.13301	0.04062	0.98047
7	0.00000	0.00000	0.34779	1.18716
8	0.27142	-0.26643	-0.10683	0.92726
9	0.00000	0.17935	-0.17077	1.45646
10	-0.27142	0.09518	0.26500	0.93376
11	0.00000	-0.34034	0.00000	1.14930
Energy of MO.	0.2950*	-0.2086	-0.2343	
	-1.0388**	0.7345	0.8250	

Table(8.2)

Molecular orbital coefficients of au,b3g and b2g

orbitals in phthalocyanine.

* Hueckel units.

** eV.

hence the energy bands arising from these levels will mix appreciably and subsequently the effects of band mixing must be taken into account when treating electronic conduction.

8.3 Energy band structure

The theory of band mixing in near degenerate energy bands has been discussed earlier in relation to conduction in the higher energy bands of anthracene. For aromatic hydrocarbons it was shown that the coulombic repulsion term $C_n^{\ell,m}$ can be ignored, however, in phthalocyanine due to the localization of charge densities at certain points in the molecule, this approximation no longer applies.

The conduction bands resulting from the interaction between the energy bands constructed from molecular orbitals of symmetry b_{2g} and b_{3g} can be written

$$W_{\pm}^{\pm}(\underline{k}) = \frac{1}{2}\{ H_{b_{2g},b_{2g}}^{\pm} + H_{b_{3g},b_{3g}}^{\pm} \pm (H_{b_{2g},b_{2g}}^{\pm} - H_{b_{3g},b_{3g}}^{\pm})^2 + 4 H_{b_{2g},b_{3g}}^{\pm} \}^{\frac{1}{2}} \quad (8.1)$$

where

$$H_{\ell,m}^{\pm} = E_\ell^{(o)} \delta_{\ell m} + \sum_{n \neq 0} C_n^{\ell,m} + \sum_{n \neq 0} (\pm 1)^n$$

$$|\langle \chi^0|\chi^1\rangle|^2 \; E_n^{\ell,m} \cos(\underline{k} \cdot \underline{r}_n) \quad (8.2)$$

and $\quad C_n^{\ell,m} = \langle\phi_\ell(\underline{r})|V(\underline{r} \cdot \underline{r}_n)|\phi_m(r)\rangle \quad (8.3)$

$$E_n^{\ell,m} = \langle\phi_\ell(\underline{r} - \underline{r}_n)|V(\underline{r} - \underline{r}_n)|\phi_m(\underline{r})\rangle \quad (8.4)$$

and $E_\ell^{(o)}$ is the energy of the molecular orbital ϕ_ℓ in the neutral molecule.

The evaluation of the transfer integral, $E_n^{\ell,m}$, has already been discussed in relation to the energy bands of aromatic hydrocarbons and so will not be discussed here. On substituting for the potential, $V(\underline{r} - \underline{r}_n)$, in equation (8.3) and expanding the molecular orbital, ϕ_ℓ, ϕ_m, in terms of their constituent atomic orbitals, u, it can be shown that :

$$C_n^{\ell,m} = \{ -e^2 \sum_{\alpha,\beta} c_\ell^\beta c_m^\beta \langle u_\beta(\underline{r}) | Z_\alpha/R_\alpha | u_\beta(\underline{r}) \rangle$$

$$- \langle u_\beta(\underline{r}) | \sum_{j\ occ} \phi_\alpha^{(j)} | r_{12}^{-1} | \phi_\alpha^{(j)} | u_\beta(r) \rangle$$

$$- \rho_\alpha \langle u_\beta(\underline{r}) \, u_\alpha(\underline{r} - \underline{r}_n) | r_{12}^{-1} | u_\alpha(\underline{r} - \underline{r}_n) \, u_\beta(\underline{r}) \rangle \qquad (8.5)$$

For large internuclear distances the electronic charge distributions in the second and third terms can be considered localized at centre α, therefore, if the number of core electrons on centre α is n_α, $C_n^{\ell,m}$ reduces to

$$C_n^{\ell,m} = -e^2 \sum_{\alpha,\beta} c_\ell^\beta c_m^\beta (z_\alpha - n_\alpha - \rho_\alpha) \langle u_\beta(\underline{r}) | 1/R_\alpha | u_\beta(\underline{r}) \rangle \qquad (8.6)$$

Unlike the transfer integrals, $E_n^{\ell,m}$, the two centre one electron coulomb integrals in equation (8.6) decrease very slowly with increased internuclear distance hence in calculating $\sum_{n\neq 0} C_n^{\ell,m}$ an extremely large number of molecules have to be taken into account and, although the integrals themselves are easily evaluated, to attempt such a large number of calculations is prohibitive in terms of computer time. The approximation (174)

$$e^2 \langle u_\beta(\underline{r}) | 1/R_\alpha | u_\beta(\underline{r}) \rangle = 14.41/R_{\alpha\beta} \qquad (8.7)$$

has therefore been used, where $R_{\alpha\beta}$ is the internuclear distance

o

(in Å) between centres α and β .

$$C_n^{\ell,m} = -\sum_{\alpha,\beta} c_\ell^\beta \ c_m^\beta \ (z_\alpha - n_\alpha - \rho_\alpha) \ 14.41/R_{\alpha\beta} \qquad (8.8)$$

The above result is similar to that used by Chen (171), however, since we have included both core states and pi-electrons in the potential the sum over α of $(z_\alpha - n_\alpha - \rho_\alpha)$ is zero hence, unlike Chen a 41st site at the centre of the molecule with $z_{41} = 2$ and $\rho_{41} = 0$, is not added.

8.4   Numerical calculations

The crystal structure of β-phthalocyanine has been determined by Roberson (173). The structure is monoclinic, of space group, $P2_1/a$, with two molecules per unit cell. The molecular structure of phthalocyanine is illustrated in figure (8.1). Depending upon whether a shared or localized hydrogen model is assumed one obtains either L and M or L' and M' as the symmetry axes in the molecular plane. However, as can be seen from the figure L', M' are not symmetry axes since the angles 14' - 7 - 8 $\neq$ 10 - 11 - 12 and this indicates that the hydrogen atoms are shared.

The electronic parts of the transfer integrals, calculated using Slater wave functions with the normal screening parameters for carbon and nitrogen and the methods given in Chapter (3), page (44), are given in table (8.3). In the estimation of the core state contribution to the transfer integral the central and peripheral nitrogen were assumed to be in the $1s^2$ $tr^{3/2}$ tr tr and $1s^2$ tr^2 tr tr core states respectively while the carbon atoms were assumed to be in the state $1s^2$ tr tr tr. The coulomb interactions terms, computed using the approximations outlined in section (8.3) are also given in table (8.3).

Position	au,au En	b2g,b2g En	b3g,b3g En	b2g,b3g En
0,1,0	323.47	243.84	74.17	-32.02
0,1,1	0.22	-	-0.39	-0.23
$\frac{1}{2},\frac{1}{2},0$	2.85	-1.88	33.10	1.79
$\frac{1}{2},\frac{1}{2},1$	3.56	-0.78	-2.94	4.24
$\frac{1}{2},\ ,1$	2.40	2.35	0.34	2.03
$Cn^{1,m}$	-0.27030	-0.32618	-0.32030	-0.07919

Table(8.3)

Transfer* and coulomb** integrals for phthalocyanine.

	Electron (b3g)	Electron (b2g)	Hole	1st. Cond.	2nd. Cond.
$E(\underline{k}\parallel\underline{a}')^{+}$	0.012	0.001	0.004	0.012	0.001
$E(\underline{k}\parallel\underline{a}')^{-}$	0.012	0.001	0.004	0.012	0.001
$E(\underline{k}\parallel\underline{b}')^{+}$	0.017	0.097	0.126	0.041	0.096
$E(\underline{k}\parallel\underline{b}')^{-}$	0.041	0.098	0.133	0.017	0.098
$E(\underline{k}\parallel\underline{c}')^{+}$	0.002	0.002	0.005	0.0004	0.003
$E(\underline{k}\parallel\underline{c}')^{-}$	0.003	0.003	0.005	0.0002	0.003
band splitting	0.001	0.007	0.048	0.012	0.001

Table(8.4)

Energy bandwidths** of the excess hole and electron bands in the abscense of band mixing and the conduction bands resulting from band mixing of the two. Vibrational overlap factor unity.

* units: $1_{\text{x}}-4$ eV.

** units: eV.

Due to the heterocyclic nature of phthalocyanine the transfer integrals between the molecule at the origin and those at $\frac{n}{2}$, $\frac{m}{2}$, ℓ and $\frac{n}{2}$, $-\frac{m}{2}$, ℓ are not necessarily equal as they are in anthracene, however, explicit calculation of such terms has shown them to be very nearly so and hence, for simplicity they are assumed equal.

The general features of the $\underline{k}$ dependent parts of the energy bands of excess electrons and holes in crystalline β-phthalocyanine are shown in figure (8.2) and figure (8.3). For all the states the energy bands are extremely anisotropic, the band widths along the $\underline{b}$ axis being an order of magnitude larger than in either of the remaining directions. The calculated band gap and separation of the two conduction bands at $\underline{k} = 0$ are 1.69 eV. and 0.19 eV., respectively, in good agreement with the experimental values of 1.68 eV. and 0.12 eV. However, the observed band splitting of 0.05 eV. is about five times the calculated value. The energy band widths and band splittings at $\underline{k} = 0$ are shown in table (8.4) and are of a similar order of magnitude to those obtained experimentally.

8.5 Mobility tensor

8.5(i) General

The component of the mobility tensor, along the $\underline{b}$ axis, without the constant premultiplicative factors $\frac{e\,\tau}{k_0 T}$ and $\frac{e\,\lambda}{k_0 T}$ and computed using the methods of Chapter (3) and Chapter (4), together with the ratio of the non-zero elements of the tensor to this are given in table (8.5) for various values of the vibrational overlap factor. The mobility ratios reflect the highly anisotropic nature of the energy bands and are relatively insensitive to the vibrational overlap factor.
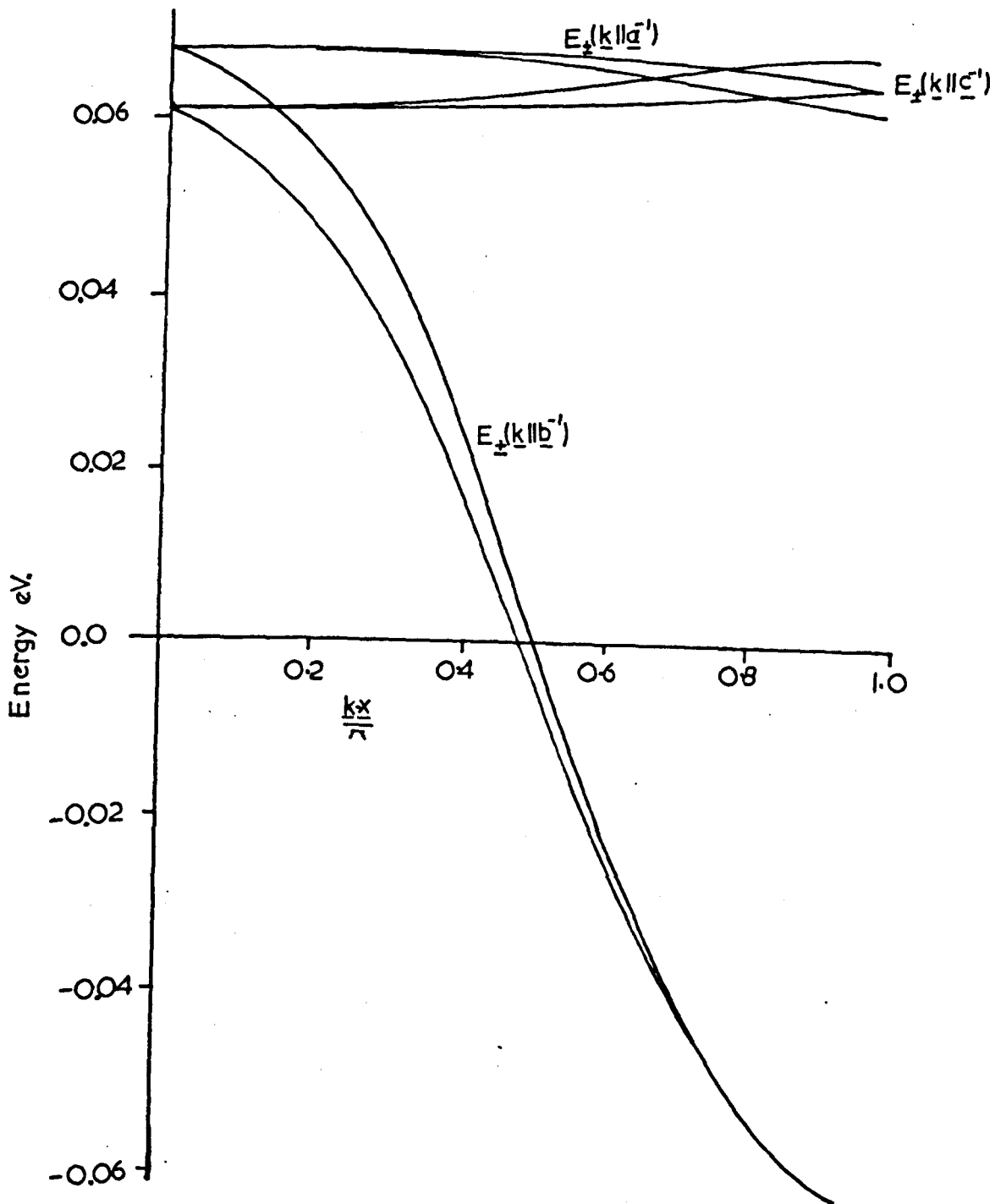
Figure (8.2)

Energy band structure of excess hole in crystalline

β-phthalocyanine. The energy zero is arbitrarily set at

$$\langle\phi_{au}|H|\phi_{au}\rangle + \sum_{n\neq 0} C_n^{au,au}$$
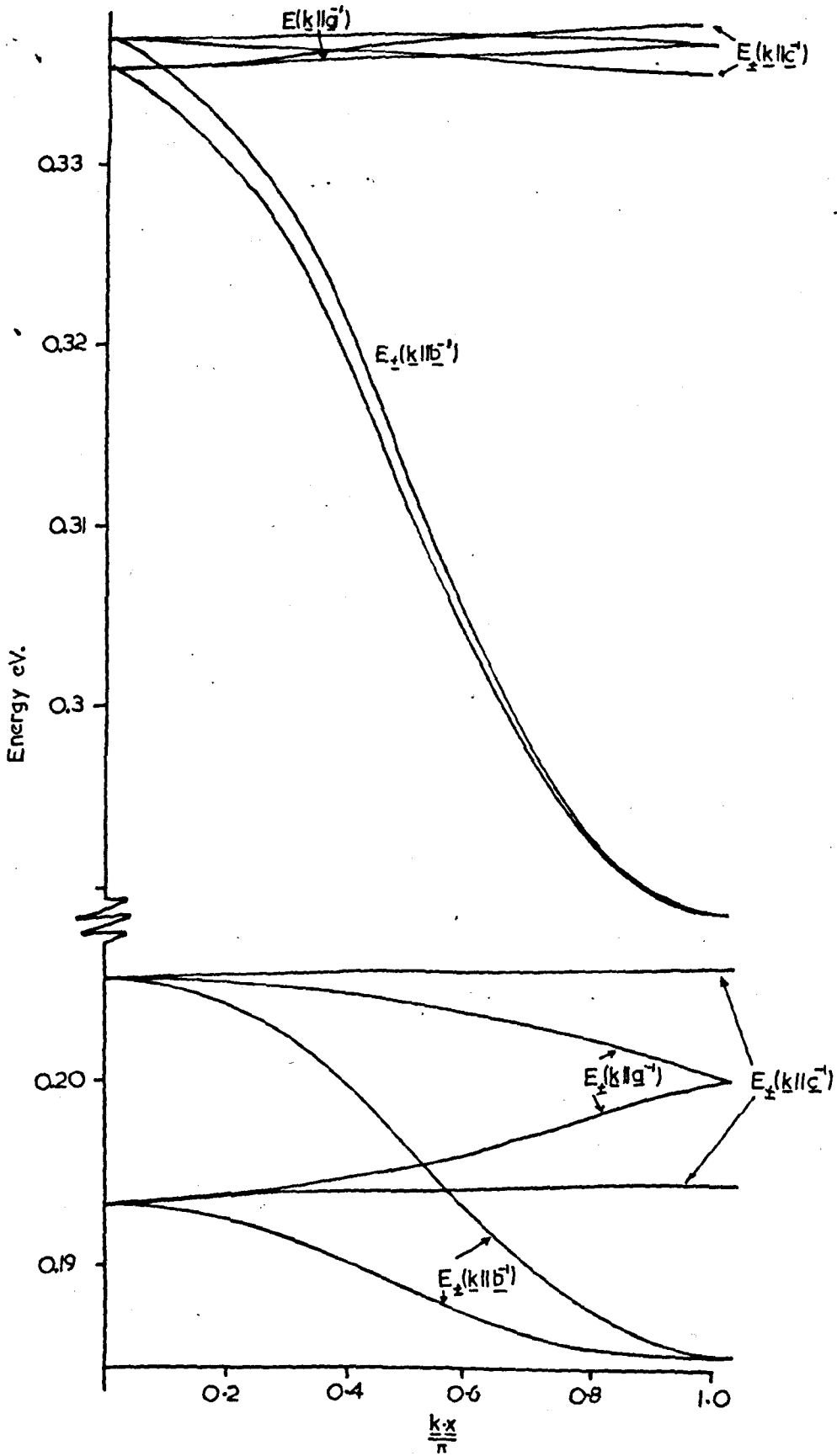
Figure (8.3)

Energy band structures of the first and second conduction

bands in crystalline ß-phthalocyanine.

Vibrational Overlap	b3g		b2g		au			
	0.1	1.0	0.1	1.0	0.1	0.2	0.5	1.0
$\langle vbvb \rangle$*	0.652	59.945	6.532	436.11	11.172	43.190	229.740	731.331
$\langle vbvb/\underline{v}(\underline{k}) \rangle$**	0.385	3.832	2.143	20.651	2.736	5.289	11.401	28.918
$\dfrac{\mu_{aa}}{\mu_{bb}}$	1.49	1.24	0.002	0.002	0.002	0.002	0.002	0.002
	(1.23)	(0.99)	(0.005)	(0.030)	(0.005)	(0.006)	(0.01)	(0.01)
$\dfrac{\mu_{cc'}}{\mu_{bb}}$	0.03	0.02	0.001	0.001	0.003	0.004	0.006	0.008
	(0.02)	(0.02)	(0.005)	(0.003)	(0.01)	(0.01)	(0.03)	(0.03)

Vibrational Overlap	1 st Cond.			2 nd Cond.		
	0.1	0.2	0.5	0.1	0.2	0.5
$\langle vbvb \rangle$*	0.785	3.118	19.021	6.626	26.553	159.380
$\langle vbvb/\underline{v}(\underline{k}) \rangle$**	0.364	0.728	1.818	1.983	3.981	9.711
$\dfrac{\mu_{aa}}{\mu_{bb}}$	4.04	3.98	3.78	0.001	0.001	0.001
	(2.94)	(2.89)	(2.73)	(0.002)	(0.001)	(0.001)
$\dfrac{\mu_{c'c'}}{\mu_{bb}}$	0.001	0.001	0.001	0.013	0.015	0.010
	(0.001)	(0.001)	(0.001)	(0.02)	(0.02)	(0.01)

Table(8.5)

Mobility ratios of excess electrons and holes(in parentheses) in
crystalline β - phthalocyanine.

* units: $1_{\text{в}}6$ m / sec .   ** units $1_{\text{в}}3$ m/sec.

No experimental data on the anisotropy of the mobility tensor
is available for comparison although the magnitude of the mobility
has been determined. Of the values reported several lie in the
range 1.8 cm^2/volt.sec. (175 - 178) although much lower values have
been reported. Westgate and Warfield (181) and Barbe and Westgate (167)
have reported drift mobilities of electrons and holes along the $\underline{c}'$
axis in the range 0.05 to 0.1 cm^2/volt.sec. while Kearns and Calvin (182)
estimated the mobility of carriers in amorphous films to be 0.001 -
0.002 cm^2/volt.sec.

8.5(ii)   Hall mobilities

The ratio of the Hall to drift mobilities for the hole and
isolated b_{2g} and b_{3g} bands, for various values of the vibration
overlap factor, have been calculated using the method of Le Blanc (100)
and are given in table (8.6).

Vibrational Overlap	Hole (au)	Electron (b_{2g})	Electron (b_{3g})
0.1	5.99	7.951	23.770
0.5	1.198	1.590	4.754
1.0	0.599	0.795	2.377

Table (8.6)

Ratios of the Hall to drift mobilities for various values of

the vibrational overlap factor.

The ratios μ_H/μ_D for metal free phthalocyanine are much smaller than
values for the copper derivative in which Hall mobilities two orders
of magnitude larger have been reported (184, 185).

An interesting result of the calculation is that the sign of the Hall effect is the same for both electrons and holes, the sign for holes being anomolous. A similar effect has been predicted theoretically for the aromatic hydrocarbon ovalene (186) which has a similar crystallographic structure to phthalocyanine, both crystals having an extremely short $\underline{b}$ axis. No experimental data is available as to the relative signs of the Hall to drift mobility ratio although a Hall mobility, along an unspecified direction, of 0.1 to 0.4 cm^2/volt.sec. has been reported (166).

8.5(iii)   Validity of the energy band model

For the energy band model to be applicable to the conduction mechanism in a particular organic solid certain criteria have to be obeyed. These criteria have been discussed in some detail in Chapter (2) and so will not be discussed further here.

The lower limits of the diagonal elements of the mobility tensor calculated such that the energy band model is physically meaningful are given in table (8.7). For a vibrational overlap factor 0.1 the uncertainty principle is obeyed in all bands and all directions. For higher values of the factor however, only the mobilities in the second conduction band are within the limits demanded. This raises the question of whether the band model is the best approach to account for charge carrier transport in crystalline β-phthalocyanine and in view of this the components of the mobility tensor have been recalculated with a change of basis from the Bloch to a localized representation.

8.5(iv)   Mobilities in the localized representation

The theory underlying the hopping model as developed by Glaeser and Berry (44) has been discussed in detail in Chapter (2).

Vibrational Overlap	Hole			1st Cond.			2nd Cond.		
	μ_{aa}	μ_{bb}	μ_{cc}	μ_{aa}	μ_{bb}	$\mu_{c'c'}$	μ_{aa}	μ_{bb}	$\mu_{c'c'}$
0.1	0.070	1.115	0.091	0.34	0.035	–	0.008	0.09	0.04
	(0.050)	(2.607)	(0.087)	(0.82)	(0.07)	–	(0.001)	(0.36)	(0.02)
0.2	0.140	2.156	0.212	1.33	0.07	0.007	0.014	0.17	0.09
	(0.121)	(5.040)	(0.227)	(1.61)	(0.13)	–	(0.003)	(0.73)	(0.03)
0.5	0.379	4.587	0.734	1.53	0.08	0.008	0.040	0.50	0.12
	(0.418)	(10.80)	(0.849)	(3.82)	(0.33)	–	(0.007)	(0.78)	(0.06)

Table(8.7)

Minimum values of the mobility* calculated such that the energy band model is internally consistant. The figures in parentheses refer to values computed from the mean free path.

* units: $1 \times -4 \ m^2$/volt-sec.

Molecule	x.x	x.y	x.z	y.y	y.z	z.z
0,0,1	62.38	-	-98.85	-	-	156.66
0,1,0	-	-	-	22.28	-	-
0,1,1	62.38	-38.28	-98.85	22.28	59.08	156.66
1,0,1	142.85	-	149.60	-	-	156.66
½,½,0	98.51	23.42	-	5.57	-	-
½,½,1	4.11	4.78	25.37	5.57	29.54	156.66

Quadratic moments*.

Molecule	$\tau(\underline{r}1)$	$1/t1$	$\tau(\underline{r}1)$	$1/t1$	$\tau(\underline{r}1)$	$1/t1$
0,0,1	-	-	-	-	-	-
0,1,0	0.961	31.291	0.505	7.175	0.979	23.588
0,1,1	0.001	0.022	0.005	0.037	-	-
1,0,1	-	-	-	-	-	-
½,½,0	0.017	0.276	0.450	3.202	0.015	0.181
½,½,1	0.021	0.034	0.040	0.284	0.006	0.075

Average jump frequency	4.562	1.528	3.406
No. of jumps	30.070	5.073	23.088

μaa	0.11	0.44	0.07
μbb	1.26	0.14	0.98
μcc	0.20	0.07	0.04

Table(8.8)

Jump probabilities, jump frequencies** and mobilities***

in phthalocyanine.

* units: $1_{10}-2 \ nm^2$.

** units: $1_{10}12 \ sec^{-1}$.

***units: $1_{10}-4 \ m^2/volt\text{-}sec$.

The crystal wave function is constructed as an antisymmetrized product of molecular wave functions in which one molecule is represented as either a positive or a negative ion and the remainder are perturbed by the ionic molecule. If these perturbations are small then the transfer integrals given in table (8.3) can be used to construct the non-stationary state wave function $\Phi(t)$ (see Chapter 2).

The jump frequencies and jump probabilities between the molecule of the origin and near neighbours, together with the respective quadratic moments, are given in table (8.8). The jump probabilities between molecules which give rise to conduction along the $\underline{a}$ and $\underline{c}'$ axes are rather small, however, this is partially off set by the large quadratic moments of these molecules giving rise to an appreciable value for the mobility along these axes. The predicted electron and hole mobilities along the $\underline{c}'$ axes are in good agreement with the values obtained by Westgate and Warfield (181). In general the degree of anisotropy predicted on the basis of the hopping model is much lower than predicted by the band model. Comparison of tables (8.5) with table (8.8) provides a very good example of this.

8.6   Conclusion

The energy band structure and anisotropy of the mobility tensor have been computed using both the energy band and hopping models and, while the energy band model yields band gaps and band widths in good agreement with those observed experimentally, the uncertainty principle as formulated by Fröhlich and Sewell is not strictly obeyed except for cases where the vibrational overlap factor < 0.2. The sign of the Hall effect is predicted to be anomolous for excess holes but not excess electrons, in agreement with the results of Nelson (169) but in contrast to the result of Chen (171) where both are predicted to be anomolous.

Mobilities calculated using the simple hopping model are of the same order of magnitude as those observed experimentally, the values along the $\underline{c}'$ axis being in good agreement with the values of Westgate and Warfield (181) and Barbe and Westgate (167).

CHAPTER (9)

Transfer and Overlap integrals for imidazole and purine.

9.1   Introduction.

9.2   Numerical calculations.

9.1 Introduction

The energy transfer integrals for imidazole and purine have been calculated using the methods previously described (Chapter 3). At the instigation of the project it was intended to calculate the energy band structure and carrier mobilities based on the energy band model, however, recent experimental data (113-115) has indicated that conduction occurs via protonic tunnelling. If this is the case then any calculations based on the models used in this thesis would be inapplicable and subsequently the calculations have been suspended. However, the transfer integrals may be useful for some alternative calculation and are therefore reported briefly.

9.2 Numerical calculations

The molecular orbital coefficients and electron densities were calculated by the SCF method using the parameters of Miller, Lykos and Schmeising (116) for purine, and Brown and Heffernan (117) for imidazole, from the Hamiltonians quoted in Orloff and Fitts (118). The coefficients of the molecular orbital containing the excess electron and hole and the electron densities of the neutral molecule are given in table (9.1). Figure (9.1) shows the molecular structure of purine and imidazole illustrating the numbering of the atoms in the molecules. Both compounds contain two types of nitrogen atom in the five membered ring, one is bonded to a hydrogen atom which in the crystalline state is extensively hydrogen bonded to the second nitrogen atom on a neighbouring molecule. For the purpose of calculating the contribution of the core states to the transfer integrals the two nitrogen atoms were assumed to be in the following valence states

$$N - H \qquad 1s^2 \; tr \; tr \; tr \; \pi^2$$

$$N \qquad 1s^2 \; tr^2 tr \; tr \; \pi$$
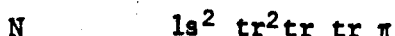
Both molecules crystallise with four molecules per unit cell, imidazole in a monoclinic lattice, space group $P2_1/a$ (119-121) while the purine crystal is orthorhombic with space group $P_n a2_1$ (122). The relationships between the four molecules per unit cell are as follows :

for imidazole

molecule (1) $\{ \; i \; | \; 0 \; \}$ molecule (2)

molecule (1) $\{\sigma_{ac} \; | \frac{b}{2} + \frac{c}{2} \}$ molecule (3)

molecule (1) $\{C_2 \; | \frac{b}{2} + \frac{c}{2} \}$ molecule (4)

and for purine

molecule (1) $\{C_2^{(c)} \; | \; \frac{1}{2} \underline{c} \}$ molecule (2)

molecule (1) $\{\sigma_{bc} \; | \; \frac{1}{2} \underline{a} + \frac{1}{2} \underline{b} + \frac{1}{2} \underline{c} \}$ molecule (3)

molecule (1) $\{\sigma_{ac} \; | \; \frac{1}{2} \underline{c} + \frac{1}{2} \underline{b} \}$ molecule (4)

The numerical evaluation of the transfer and overlap integrals was carried out using single Slater functions to represent the various atomic orbitals with the screening parameters :

carbon :

$$\zeta_{1s} \qquad = 107.7 \; nm^{-1}$$

$$\zeta_{tr} = \zeta_{\pi} = 30.7 \; nm^{-1}$$

nitrogen :

$$\zeta_{1s} \qquad = 126.7 \; nm^{-1}$$

$$\zeta_{tr} = \zeta_{\pi} = 36.8 \; nm^{-1}$$

The role of the labile proton in the molecular potential has
not been considered explicitly since the electron density on the
hydrogen atom is not known with any degree of certainty. Calculations
have been performed on the two extremes of the resonance structures
illustrated in figure (9.2). In both the diagrams the excess hole,
or electron, is considered to be on molecule (1) and the resonances
correspond to exchange of the labile proton between hydrogen bonded
molecules. Such a conduction mechanism has been proposed by
Brown and Aftergut (123), however, the more recent mechanisms are
rather more sophisticated (113). The intermolecular resonance and
overlap integrals for the two resonance structures of imidazole and
purine are given in table (9.2) and table (9.3) respectively.

	Imidazole			Purine		
	Hueckel Coeff.		Electron density	Hueckel Coeff.		Electron density
	Hole	Electron		Hole	Electron	
1	0.08256	0.41278	1.649	0.10053	-0.41185	1.272
2	-0.62532	-0.62741	1.101	0.35577	-0.13345	0.791
3	-0.48044	0.43152	1.099	0.22843	0.34120	1.239
4	0.23832	0.17889	1.034	-0.42954	-0.28478	0.941
5	0.56085	-0.46665	1.117	-0.47539	-0.05275	1.052
6				-0.29690	0.66602	0.782
7				-0.07922	-0.03200	1.779
8				0.44835	0.31786	0.911
9				0.32434	-0.25819	1.232

Table(9.1)

Hueckel coefficients of the highest bonding and lowest
antibonding molecular orbitals and π-electron densities
in imidazole and purine.
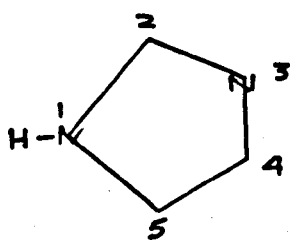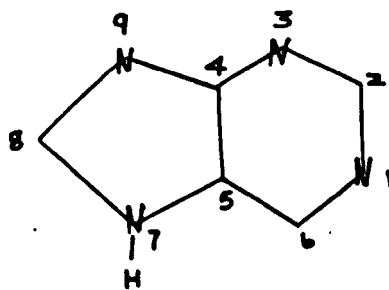
(a)   (b)

Numbering of the atoms in imidazole(a) and purine(b).

			I				II			
			Hole		Electron		Hole		Electron	
l	m	n	Trans.	Over.	Trans.	Over.	Trans.	Over.	Trans.	Over.
0, 1, 0			-69.37	15.54	5.67	2.44	-63.62	14.56	0.99	-2.47
0,-1, 0			-68.17	15.54	2.51	-2.44	-64.53	14.56	3.46	-2.47
1, 0, 1			-60.14	9.08	-30.57	3.47	4.53	-0.87	-26.38	3.56
0, ½, ½			4.61	-0.67	-10.58	0.91	-4.26	0.69	-5.56	0.95
0,-½,-½			-6.94	0.59	-0.47	0.91	-51.32	10.30	12.04	0.91
0,-½, ½			-1.11	0.59	-23.38	0.76	-62.25	10.30	-10.46	0.91
0, ½,-½			2.54	-0.67	-3.01	0.91	-1.38	0.69	-2.50	0.95
1, ½, $\frac{3}{2}$			12.01	-4.91	17.27	3.59	7.92	0.70	-17.15	3.71
1, ½, $\frac{3}{2}$			26.18	-4.91	-3.21	3.59	15.19	0.70	15.73	3.71

Table(9.2)

Transfer* and overlap** integrals for the resonance forms of imidazole.

* units 1×10^{-4} eV.

**units 1×10^{-4}.
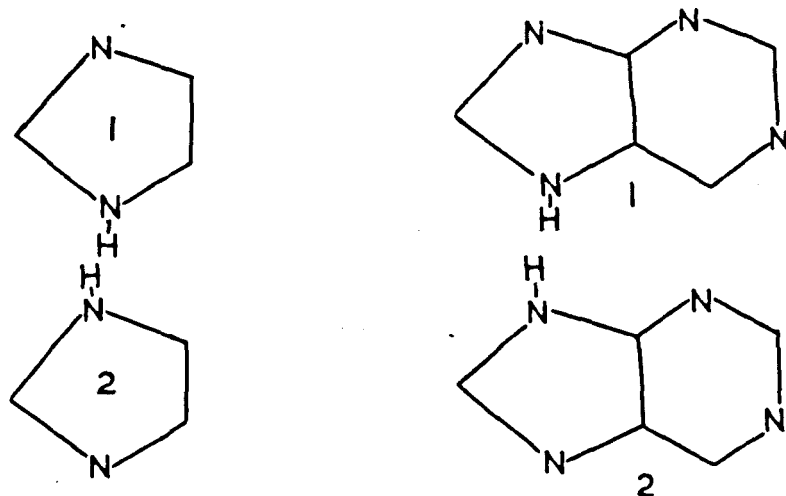
Figure (9.2)

			I				II			
l	m	n	Trans.	Over.	Trans.	Over.	Trans.	Over.	Trans.	Over.
Molecule related by translation l$\underline{a}$+m$\underline{b}$+n$\underline{c}$										
0,	0,	1	362.72	-102.70	145.24	-33.52	518.52	-119.29	134.97	-30.37
0,	0,	-1	465.54	-102.70	177.03	-33.52	512.13	-119.29	164.35	-30.37
0,	0,	2	0.05	-0.03	0.02	-0.01	0.08	-0.03	0.01	-0.01
0,	0,	-2	0.08	-0.03	0.01	-0.01	0.08	-0.03	0.01	-0.01
Molecule related by C2c followed by translation l$\underline{a}$+m$\underline{b}$+n$\underline{c}$										
0,	0,	½	0.55	-0.01	0.02	0.12	0.75	-0.04	0.06	0.12
0,	0,	-½	-2.00	-0.01	1.37	-0.12	-1.97	-0.04	1.38	-0.12
0,	0,	3/2	0.13	-0.05	0.01	-	0.11	-0.05	-0.01	-
0,	0,	-3/2	0.10	-0.05	-0.10	-	0.10	-0.05	-0.01	-
0,	1,	½	1.88	-0.72	10.28	-4.91	1.86	-0.72	10.27	-4.91
0,	1,	-½	2.99	-0.72	19.93	-4.91	2.97	-0.72	19.91	-4.91
Molecule related by σbc followed by translation l$\underline{a}$+m$\underline{b}$+n$\underline{c}$										
½,	½,	0	-18.68	3.43	12.78	-2.21	-19.42	3.63	12.70	-2.19
-½,	½,	0	-16.21	3.43	10.04	2.21	-18.44	3.63	9.93	-2.19
½,	½,	1	-0.29	0.08	0.09	-0.02	-0.30	0.09	-0.28	-0.02
-½,	½,	-1	-0.23	0.08	0.01	-0.21	-0.24	0.09	0.02	-0.02
½,	½,	-1	-4.09	0.90	2.00	-0.43	-4.22	0.95	1.96	-0.42
-½,	½,	1	-3.58	0.90	1.56	0.43	-2.79	0.95	1.51	-0.42
Molecule related by σac followed by translation l$\underline{a}$+m$\underline{b}$+n$\underline{c}$										
½,	½,	½	-22.47	4.68	-9.28	2.40	-9.90	4.99	-13.28	2.94
½,	-½,	-½	-5.73	4.68	-12.74	2.40	-20.90	4.99	-13.07	2.94
½,	-½,	½	14.34	-2.73	-1.24	-0.32	22.98	-3.87	-6.78	1.08
½,	½,	-½	14.09	-2.73	2.39	-0.32	21.94	-3.87	-6.27	1.08

Table(9.3)

Transfer* and overlap** integrals for the resonance forms of purine.

* units 1$_D$-4 eV.

**units 1$_D$-4.

References

1. N. Stoletov sited in A.T. Vartanian, Izv. Akad. Nauk. SSSR. Ser. Fiz., 16, 169(1952).

2. A. Pochettino, Atti. Accad. Naz. Lincei., 15(1),355(1906). 15(2),17(1906).

3. A. Byk and H. Borck, Ber. Deut. Phys. Ges., 8,867(1910).

4. M. Volmer, Ann. Physik, 40, 775(1913).

5. A. Szent-Gyorgyi, Nature(London),157,875(1946).

6. A. Szent-Gyorgyi, Nature(London),148,157(1941).

7. A. Szent-Gyorgyi, Science 93,609(1941).

8. See for example the review by F. Gutmann and L.E. Lyons, Organic semiconductors, J. Wiley and Sons,Inc.(1967) p492,638.

9. M. Pope,H. Kallmann and J. Giachino, J. Chem. Phys.,42, 2540(1965).

10. O. H. Le Blanc. Jr., Physics and Chemistry of the Organic Solid State, Interscience Publishers, New York, 3,133(1967).

11. R. G. Kepler, Phys. Rev.,119,1226(1960).

12. H. Kallmann and M. Pope, Nature,185,31(1960).

13. D. E. Weiss and R. A. Bolto, Physics and Chemistry of the Organic Solid State, D. Fox,M.M. Labes and A. Weisberger,Eds. Interscience,New York, 2,68(1965).

14. C. Bogus, Z.Physik,184,219(1965).

15. G. M. Delacote, J. Chem. Phys. 42,4315(1965).

16. R. Raman,L. Azarraga and S.P McGlynn, J. Chem. Phys.,41 2516(1964).

17. W. Belper, Z. Physik, 185,507(1965).

18. D.C. Hoesterey and G. M. Letson, J. Chem. Phys. 41,675 (1963).

19. F. J. Morrin, Phys. Rev., 93,1199(1954).

20. J. Yamashita and T. Kurowasa, Phys. Chem. Solids., 5, 34(1958).

21. J. Yamashita and T. Kurowasa, J. Phys. Soc. Japan, 15,802,1211(1960).

22. G. M. Delacote and M. Schotte, Solid State Comm., 4,177(1966).

23. Name sujjested in ref(10).

24. For a review of the method see B. Pullman, Prog. Nucleic Acids Res. Mol. Biol., 9,327(1969).

25. W. A. Little, Phys. Rev., 134A,1416(1964).

26. L. Brillouin, Cashiers Phys., 15,413(1961).

27. B. F. Rozsnayi, F. Martino and J. Ladik, J. Chem. Phys., 52,5708(1970).

28. C. A. Coulson and M. P. Barnett, Phil. Trans. Roy. Soc (London), 243,212(1951).

29. M. P. Barnett, PhD Thesis, University of London.

30. M. P. Barnett, Methods in Computational Physics, 2,95(1963).

31. F. J. Corbato and A. C. Switendick, ibid, 2,155(1963).

32. E.W. Hobson, Theory of Spherical and Ellipsoidal Harmonics, C. U. P.(1931).

33. J. C. Slater, Phys. Rev., 36,57(1930).

34. M. Kotani,A. Amemiya, E. Ishiguro and T. Kimura, Tables of Molecular Integrals., Maruzen Co. Ltd.(1963).

35 C. A. Coulson, Proc. Camb. Phil. Soc.,33,104(1937).

36. Ref(34)page

37. w, gautschi, Journal A.C.M.,8,38(1961).

38. O. H. Le Blanc Jr., J. Chem. Phys.,35,1275(1961).

39. G. P. Thaxton, R. C. Jarnagin and M. Silver, J. Phys. Chem., 66,2461(1962).

40. J. L. Katz, S. A. Rice, S. I. Choi and J. Jortner, J. Chem. Phys.,39,1683(1963).

41. R. Silbey, J. Jortner, S. A. Rice and M. T. Vala,

(a) J. Chem. Phys.,42,733(1965).

(b) J. Chem. Phys.,43,2925(1965).

42. Y. Harada, Y. Maruyama, H. Inokuchi and N. Matsubara, Bull. Chem. Soc. Japan. 38,129(1965).

43. L. Friedman, Phys. Rev., 133, A1668(1964).

44. R. M. Glaeser and R. S. Berry, J. Chem. Phys.,44,3797(1966).

45. I. Chen, J. Chem. Phys., 51,3241(1969).

46. R. Williams and J. Dresner, J. Chem. Phys,46,2133(1967).

47. A. Many, E. Harnik and D. Gerlich, J. Chem. Phys., 23, 1732(1955).

48. D. Yamamoto, Bull. Fac. Ag. Mei. Univ.,4,98(1955). quoted by H. Inokuchi and H. Akamatu, Solid state Phys., 12,93(1961).

49. D. D. Eley and G. D. Parfitt, Trans. Farad. Soc.,51,1529(1955).

50. Y. Toyozawa. Quoted in Ref(42).

51. P. Gosar and S. I. Choi, Phys. Rev.,150,529(1966).

52. D. D. Eley and D. I. Spivey, Trans. Farad. Soc.,56,1432(1960).

53. D. D. Eley and M. R. Willis, Symposium on the Electrical Conductivity in Organic solids. H. Kallmann and M. Silver eds., Interscience, New York.

54. D. D. Eley, H. Inokuchi and M. R. Willis, Disc. Farad. Soc., 28,54(1959).

55. H. A. Pohl and D. A. Opp. J. Phys. Chem. 66,2121(1962).

56. H. A. Pohl, Modern aspects of the Vitreous State. J. D. Mackenzie, Ed. Butterworth, London(1962),Chapter(2),p 105.

57. S. H. Glarum, J. Phys. Chem. Solids, 24,1577(1963).

58. W. Seibrand, J. Chem. Phys., 41,3574(1964).

59. R. C. Nelson. J. Chem. Phys.,30,406(1959).

60. R. A. Keller and H. E. Rast Jr., J. Chem. Phys.,36,2640(1962).

61. H. H. Cardew and D. D. Eley, Disc. Farad. Soc.,27,115(1959).

62. G. Kemeny and B. Rosenberg, J. Chem. Phys.,52,4151(1970).

63. R. A. Keller, J. Chem. Phys., 38,1076(1963).

64. R. H. Tredgegold, Proc. Phys. Soc.(London),80,807(1962).

65. D. R. Kearns, J. Chem. Phys., 35,2269(1961).

66. J. Halpern and L. E. Orgel, Disc. Farad. Soc.,29,32(1960).

67. C. Zener, Phys. Rev., 82,403(1951).

68. W. Shockley, Electrons and Holes in semiconductors, Van Nostrand Company,Inc.,New York.(1950),p300.

69. R. G. Kepler, Phys. Rev. 119, 1226(1960).

70. L. Friedman, Phys. Rev. 140, A1649(1965).

71. S. Glarum, J. Phys. Chem. Solids.,24,1577(1963).

72. R. Kubo and K. Tomita, J. Phys. Soc. Japan.,9,888(1954).

73. R. Kubo, J. Phys. Soc. Japan.,12,570(1957).

74. S. A. Rice and J. Jortner in Physics and Chemistry of the Organic solid state. Eds. D. Fox, M. M. Labes and A. Weissberger.,3,430(Table(IX.19))(1967). Interscience.

75. O. H. Le Blanc Jr., J. Chem. Phys.33,626(1960).

76. G. H. Wannier, Phys. Rev.,52,191(1937).

77. J. M. Ziman. Principles of the Theory of Solids,6.2 p 149 C.U.P.(1964).

78. S. Chandstrasekar, Rev. Mod. Phys., 15,1(1943).

79. C. Kittel, Elementary Statistical Physics. pp157→158, J. Wiley and Sons, New York,1958.

80. F. Bloch, Z. Physik.,52,555(1928).

81. J. C. Slater, Phys. Chem. Solids.,8,21(1959).

82. A. F. Ioffe, Can. J. Phys.,34,1342(1956).

83. A. F. Ioffe, Phys. Chem. Solids,8,6(1959).

84. H. Frolich and G. L. Sewell,Proc. Phys. Soc.(London), 74,643(1959).

85. J. C. Slater and J. G. Kirkwood, Phys. Rev.,37,682(1931).

86. B. J. McClelland, J. Chem. Phys.,46,4158(1967).

87. M. Sano, M. Pope and H. Kallmann,J. Chem. Phys.,43,2920(1965).

88. J. Jortner, S. A. Rice and J. L. Katz, J. Chem. Phys.,42, 309(1965).

89. E. Clementi and C. C. J. Roothaan, Phys. Rev.,127,1618(1962).

90. S. C. Abrahams, J. Montheath-Robertson and J. C. White, Acta. Cryst.,2,233(1949).

91. J. F. Batt, Solid State Phys.,4,199(1957).

92. D. W.J.Cruickshank, Rev. Mod. Phys.,30,163(1958).

93. For a reveiw see Ref(8),table(8.2),page706.

94. G. M. Delacote, J. Chem. Phys., 42,4315(1965).

95. I. Nakada and Y. Ishihara, J. Phys. Soc.Japan.,19,695(1964).

96. W. Helfrich and P. Mark, Z. Physik.,166,370(1962).

97. K. Pigon and H. Chojnaki,J. Chem. Phys.,31,272(1959).

98. R. Mason, Acta Cryst.,17,547(1964).

99. J. Dresner, Phys. Rev.,143,558(1966).

100. O. H. Le Blanc Jr., J. Chem. Phys.,39,2395(1963).

101. R. S. Berry, J. Jortner, J. C. Macki, E. S. Pysh and S. A. Rice, J. Chem. Phys.,42,1535(1965).

102. M. Silver, G. Delacote, M. Shotte, J. S. Kim, R. C. Jarnagin and Mentalecheta, paper presented at the Organic Crystal Symposium, University of Chicago, 1965(unpublished) quoted in Ref(99).

103. M. Sano, M. Pope and H. Kallmann, J. Chem. Phys.,43,2920(1965)

104. A. M. Hermann, Quoted in Ref(8), p 256.

105. S. C. Mathur and D. C. Singh, Chem. Phys. Letters,5(4), 249(1970).

106. S. I. Choi and S. A. Rice, J. Chem. Phys.,38,366(1963).

107. M. Silver, D. Olness, M. Swicord and R. C. Jarnagin,Phys. Rev.letters, 10,12(1963).

108. E. Heilbronner and D. A. Straub, HMO- Hueckel Molecular orbitals,Springer-Verlag, Berlin-Heidelberg-New York(1966).

109. I. Nakada and Y. I. Ishihara, J. Phys. Soc. Japan., 19, 695(1964).

110. J. Fourney and G. Delacote, J. Chem. Phys., 52, 1028(1969).

111. G. T. Pott and D. F. Williams, J. Chem. Phys., 51, 1901(1969).

112. D.W.J. Cruickshank, Acta. Cryst., 9, 915(1956).

113. N. Reihl, Energetics and mechanisms in Radiation Biology. Ed. G. O. Phillips, Academic Press(1968).

114. A. Kawada, A. R. Mc Ghie and M. M. Labes, J. Chem. Phys., 52, 3121(1970).

115. A. R. Mc Ghie, H. Blum and M. M. Labes, J. Chem. Phys., 52, 6141(1970).

116. R. L. Miller, P. G. Lykos and H. N. Schmiesing, J. Am. Chem. Soc., 84, 4623(1962).

117. R. D. Brown and M. L. Heffernan, Australian J. Chem. Soc. 12, 543(1960).

118. M. K. Orloff and D. D. Fitts, J. Am. Chem. Soc., 85, 3721(1963).

119. S. Martinez-Carrera, Acta. Cryst., 20, 783(1966).

120. G. Will, Z. Kristallog., 119, 1(1963).

121. G. Will, Nature(London), 198, 575 (1963).

122. D. G. Watson, R. M. Sweet and R. E. Marsh, Acta Cryst., 19, 573(1965).

123. G. D. Brown and S. Aftergut, J. Chem. Phys., 38, 1356(1963).

124. J. Jager. Phys. Stat. Solodi, 35, 731(1969).

125. J. Ladik, Acta Phys. Acad. Sci. Hungary, 18, 173(1965).

126. B. J. Ransil, Rev. Mod. Phys., 32, 239(1960).

127. S. Matsumoto and T. Tsukada, Bull. Chem. Soc. Japan., 37, 1545(1964).

128. S. Matsumoto, Bull. Chem. Soc. Japan, 37, 997(1964).

129. R. A. Arndt and A. C. Damask, J. Chem. Phys., 45, 4627(1966).

130. R. A. Arndt and A. C. Damask, J. Chem. Phys., 45, 755(1966).

131. K. Miller and J. N. Murrell, Theoret. chim. Acta(Berlin), 7, 69(1962).

132. See chapter(3), section(7).

133. See Chapter(4).

134. Ref(8), table(8.13), p 771.

135. I. S. Rez, A. S. Sonin, E. E. Tsepelevich and A. A. Filimonov, Soviet Phys.- Cryst.,$\underline{4}$,59(1960).

    I. S. Rez, Cesk. Casopis. Fys., $\underline{13}$,31(1963).

136. J. Gay, R. Kara and J. P. Mathieu, Bull. Soc. France Mineral Crist., $\underline{8}$)4,187(1961).

137. J. V. Euler quoted in Ref(8),p 618,table(10.3).

138. L. M. Beliaev, G. G. Belikova, V. M. Fridkin and I. S. Zheludev, Krystallografiya, $\underline{3}$,772(1958).

139. W. Von Baldus, Z. Angew. Physik, $\underline{6}$,481(1954).

140 H. Kallmann and B. Rosenberg, Phys. Rev., $\underline{97}$,1596(1955).

141. I. S. Zheludev and V. M. Fridkin, Soviet Phys.-Cryst., $\underline{3}$,319(1958).

142. J. R. Freeman, H. P. Kallmann and M. Silver, Rev. Mod. Phys. $\underline{33}$,553(1961).

143. K. W. Boer and U. Kuemmel, Ann. Physik, $\underline{V1-20}$,303(1957).

144. R. Pariser and R. G. Parr, J. Chem. Phys., $\underline{21}$,466,767(1953).

145. J. A. Pople, Trans. Farad. Soc.,$\underline{49}$,1375(1953).

146. R. G. Parr, Quantum theory of molecular electonic structure. W. A. Bengamin Inc. N.Y.(1963). Chapter(3).

147. C. C. J. Roothaan, Rev. Mod. Phys. $\underline{23}$,69(1951).

148. R. Mc Weeny and T. E. Peacock, Proc. Roy. Soc. London, Ser. A, $\underline{70}$,41(1957).

149. R. Mc Weeny, Proc. Roy. Soc. London, Ser. A,$\underline{235}$,496(1956).

150. Liverpool University Algol Library Procedures, LUA5→LUA 12.

151. G. Castro and J. F. Hornig, J. Chem. Phys.,$\underline{42}$,1459(1965).

152. K. Nishoto and L. S. Forster, Bull. Chem. Soc. Japan, $\underline{41}$,2254(1968).

153. N. Mataga and K. Nishimoto, Z. Physik. Chem.(Frankfurt), $\underline{12}$,335(1957).

154. K. Ohno. Theoret. Chim. Acta, $\underline{2}$,219(1964).

155. D. F. Eggars, N.W. Gregory, G.D. Halsey and B.S. Rabinovitch, "Physical Chemistry", J. Wiley and Sons Inc (1964)

156. J. Linderberg, Chem. Phys. Letters, $\underline{1}$,39(1967).

157. F. H. Herbstein and G. M. T. Schmidt, Acta Cryst., $\underline{8}$,399(1955).

158.   ibid $\underline{8}$,406(1955).

159. F. L. Hirschfeld and G. M. T. Scmidt, J. Chem. Phys., $\underline{26}$, 923(1957).

160. see chapter(2), section(5).

161. J. M. Robertson and J. G. White, J. Chem. Soc., 607(1945).

162. D. M. Donaldson and J. M. Robertson, Proc. Roy. Soc., $\underline{A220}$,157(1953).

163. D. Kleitman, U. S. Tech. Serv. Rept., DS111419(1953).

164. F. A. Haak and J. P. Notta, J. Chem. Phys., $\underline{38}$,2648(1963).

165. A. Sussman, Paper read at the Electrochemical Society Thin film symposium, Pittsburg, PA, April(1963) quoted in Ref(8).

166. G. H. Heilmeier, G. Warfield and S. E. Harrison, J. Applied Phys., $\underline{34}$, 2278(1963).

167. D. F. Barbe and C. R. Westgate, J. Chem. Phys., $\underline{52}$,4046 (1970).

168. P. Day and R. J. P. Williams, J. Chem. Phys.,$\underline{37}$,567(1962).

169. M. Sukigara and R. C. Nelson, Mol. Phys.,$\underline{17}$,387(1969).

170. I. Chen, J. Mol. Spect., $\underline{23}$,131(1967).

171. I. Chen, J. Chem. Phys., $\underline{51}$,3241(1969).

172. J. M. Assour and S. E. Harrison, J. Am. Chem. Soc., $\underline{87}$, 651(1965).

173. J. M. Robertson, J. Chem. Soc., 1195(1936).

174. J. A. Pople, Trans. Farad. Soc.,$\underline{49}$,1375(1953).

175. D. Kleitmann and G. Goldsmith, Phys. Rev., $\underline{98}$,1544(1955).

176. C. Y. Liang, E. G. Scalco and G. Oneal, J. Chem. Phys. $\underline{37}$,459(1962).

177. P. E. Fielding and F. Gutmann, J. Chem. Phys., $\underline{26}$,411(1957).

178. K. Winksne and A. E. Newkirk, J. Chem. Phys, 34,2184(1961).

179. S. E. Harrison and J. M. Assour, Organic Crystal Symp.,NRC, Ottawa,1962, p 175.

180. J. Curry and E. P. Cassidy, J. Chem. Phys., 37,2154(1962).

181. C. R. Westgate and G. Warfield, J. Chem. Phys.,46,94(1967).

182. D. R. Kearns and M. Calvin, J. Chem. Phys.,34,2022(1961).

183.

184. G. M. Delacote and M. Schotte, Phys. Stat. Solidi, 2, 1460(1962).

185. G. H. Heilmeier and S. E. Harrison, Phys. Rev. 132,2010 (1963).

186. See chapter(6).

187. G. H. Heilmeier, G. Warfield and S. E. Harrison, Phys. Rev,. letters, 8,309(1962).

188. Salford University Library procedure No. 41.

189. H. Inokuchi, Bull. Chem. Soc.Japan, 29,131(1956).

190. T. Uchida in H. Inokuchi and H. Akamatu, Solid State Physics, 3,117(1961).

191. D. D. Eley, G. D. Parfitt, M. D. Perry and D. H. Taysum, Trans. Farad. Soc., 49,79(1953).

192. D. C. Northrop, Proc. Phys. Soc(London), 74,756(1959).

193. H. Inokuchi, H. Kuroda and H. Akamatu, Bull. Chem. Soc. Japan, 34, 749(1961).

194. H. Akamatu, H. Inokuchi and T. Handa. Nature(London) 168,520(1951).

195.

196. H. Inokuchi, N. Matsubara, Y. Maruyama and E. Clar, Nature(London), 205,64(1965).

197. Y. Harada, Y. Maruyama, H. Inokuchi and M. Matsubara, Bull. Chem. Soc. Japan, 38,129(1965).

198. E. Clar, W.Kelly, J. Montheath-Robertson and M. G. Rossman J. Chem. Soc., 3878(1956).

199. J. Montheath-Robertson and J. G. White, J. Chem. Soc.,
      607(1945).

200. D. M. Donaldson and J. Montheath-Robertson, Proc. Roy.
      Soc, A220, 157(1953).

201. J. Montheath-Robertson, Private communication May 1969.

202. M. Goeppert-Mayer and A. L. Sklar, J. Chem. Phys.,
      6, 645(1938).

203. See for example J. N. Murrell, S. F. A. Kettle and J. M.
      Tedder, Valence Theory J. Wiley and Sons(1965),p 154.

204. See for example C. Kittel. Elementary Solid State Physics.
      J. Wiley and Sons.(1964), p158, eqn.(6.27).

205. See for example Ref(8) p 453.

206. K. Miller and J. N. Murrell, Theoret. chim. Acta(Berlin).
      7, 69(1967).

207. S. Fraga and B. J. Ransil, J. Chem. Phys., 35,669(1961).

Appendix(1).

Evaluation of the molecular integrals.

(A1.1) i.   Two centre - two electron integrals.

        ii.   Two centre - one electron integrals.

(A1.2) A computer program to evaluate two centre - one electron integrals.

        i.   General.

        ii.   Construction of the data tape.

        iii.   Text of the program.

(A1.3) Tables of Hybrid integrals between Carbon and Nitrogen atoms.

(A1.1) <u>Evaluation</u> <u>of</u> <u>the</u> <u>molecular</u> <u>integrals</u>.

(A1.1.1) <u>Two</u> <u>centre-two</u> <u>electron</u> <u>integrals</u>.

The method used to evaluate the two centre-two electron integrals was the Zeta function expansion method as developed by Coulson and Barnett(28,29), a brief synopsis of which is given here. A more detailed account of the method is given in the original(28,29) and related(30,31) papers.

The problem can be expressed as the evaluation of integrals of the form:

$$\int \psi\,(c1,A,1)\ \psi(c1,A,1)\ r_{12}^{-1}\ \psi\,(c2,B,2)\ \psi(c2,C,2)\ dV1\ dV2 \qquad (A1.1)$$

where r_{12} denotes the distance between electrons 1 and 2, the integration is over the spaces V1,V2 of these two electrons and the symbol $\Psi\,(c1,X,1)$ denotes a nodeless one electron atomic orbital of an electron,1,referred to an atomic nucleus ,X, as origin. The analytic form of ψ is specified by the label c1 which summarizes the the quantum numbers n1,l1,m1 and screening parameter k1. Formally if r_{x1}, θ_{x1} and ϕ_{x1} are the polar co-ordinates of electron 1 measured from the nucleus,X, as origin and some arbitrary polar axis and reference plane that passes through the origin then the orbital , ψ , is of the form:

$$N(n,l,m)r_{x1}^{n-1}\ exp(-kr_{x1})\ P_l^m(cos(\theta_{x1})exp(1m\,\phi) \qquad (A1.2)$$

The Legendre functions $P_l^m(cos(\theta))$ are those defined by Hobson (32) and N(1,m,n) denotes a normalization factor. A function , ψ , having the form of eqn(A1.2) is termed a Slater atomic orbital or Slater function. If the centres B and C in eqn(A1.1) are coincident the integral is termed a coulomb integral and if centre A is coincident with centre B but not with C they are termed hybrid(28) or ionic(34) integrals. The program given in this appendix is concerned with the evaluation of both types of integral for the cases where the wavefunctions of electron 2 are either 2py or 2pz atomic orbitals and the wave functions

of electron 1 can be any function with principal quantum number ,n, either 1 or 2.

The method is based on the expansion(35) of a molecular orbital on centre B about centre A:

$$r_b^{m-1} \exp(-\beta r_b) = \sum_{n=0}^{\infty} \frac{2n+1}{(R \times r_a)} P_n(\cos(\theta_a)) \zeta_{m,n}(\beta, r_a; R)$$

which can alternately be expressed as:

$$= \zeta^{1-m} \sum_{n=0}^{\infty} \frac{(2n+1)}{(t \times \tau)} P_n(\cos(\theta_a)) \zeta_{m,n}(1, t; \tau) \qquad (A1.3)$$

where r_a and r_b denote the distance of a point P from the two centres A and B that are separated by a distance R. The angle subtended at A by the line PB is denoted θ_a and

$$t = \beta r_a,$$
$$\tau = \beta R.$$

P_n is a Legendre polynomial of degree n and $\zeta_{n,m}(1, t;\ )$ is the so-called zeta function. When $m = 0, 1, 2$ the zeta functions are commonly denoted $\gamma_n(1, t; \tau)$, $p_n(1, t; \tau)$ and $q_n(1, t; \tau)$ respectively.

Barnett and Coulson have shown that any coulomb integral can be reduced to the form:

$$C(c1, c2, c3, c4) = N_c(c1, c2, c3, c4) \int t^{\frac{1}{2}} g_c(c1, c2, c3, c4) dt$$

and hybrid integrals to the form:

$$I(c1, c2, c3, c4) = N_1(c1, c2, c3, c4) \int t^{\frac{1}{2}} \exp(-k3 \times t/k4) \times$$
$$g_1(c1, c2, c3, c4) dt \qquad (A1.4)$$

The functions g_c and g_1 are products of zeta functions and a simple polynomial $J_n(r)$ and N_1, N_c are numerical constants. The analytical equations for the above functions are tablulated in ref.(28).

The zeta function $\zeta_{0,n}(1, t; \tau)$ can be expressed as products of Bessel functions of imaginary argument and half-odd integer order:

$$\zeta_{0,n}(1,t;\tau) = I_{n+\frac{1}{2}}(t)K_{n+\frac{1}{2}}(\tau) \quad t \leq \tau$$

$$= K_{n+\frac{1}{2}}(t)I_{n+\frac{1}{2}}(\tau) \quad \tau < t \qquad (A1.5)$$

and functions of higher order can be calculated by means of simple recurrence formulae:

$$\zeta_{m,n}(1,t;\tau) = \frac{t \times \tau}{(2n+1)} [_m\zeta_{1,n-1}(1,t;\tau) - {}_M\zeta_{1,n+1}(1,t;\tau)]$$

$$-(m-1)[\zeta_{m-2,n-2}(1,t;\tau) - \zeta_{m-2,n+1}(1,t;\tau)]$$

and

$$\zeta_{m,n}(1,t,\tau) = (t^2 + \tau^2)\,\zeta_{m-2,n}(1,t;\tau) - \frac{2t \times \tau}{(2n+1)}(nx$$

$$\zeta_{m-2,n-1}(1,t;\tau) + (n+1)\,\zeta_{m-2,n+1}(1,t;\tau))$$

$$(A1.6)$$

Repeated application of the above recurrence formulae can lead to lossof accuracy.However, m can be raised from 0 to 4 without loss of more than 1 or 2 figures which is sufficient for the pupoese of calculations based on atomic orbitals with quantum number $n \leq 2$. The Bessel functions $I_{n+\frac{1}{2}}(x)$, $K_{n+\frac{1}{2}}(x)$ show approximately exponential type behavior with x and for large values of x $I_{n+\frac{1}{2}}(x)$ can have values out side the range of normal computers.Hence,it is convenient to work with scaled Bessel functions defined by:

$$i_{n+\frac{1}{2}}(x) = I_{n+\frac{1}{2}}(x)/f_n(x) \qquad (A1.7)$$

$$k_{n+\frac{1}{2}}(x) = K_{n+\frac{1}{2}}(x) \times f_n(x) \qquad (A1.8)$$

where

$$f(x) = n!(2x)^n/(2n+1)! \quad , \quad n \geq 0$$

and

$$f_{-1}(x) = 1/(2x).$$

The recurrence relations between the scaled Bessel functions are

$$i_{n+\frac{1}{2}}(x) = i_{n+\frac{3}{2}}(x) + [x^2/((2n+3)(2n+5))]\,i_{n+\frac{5}{2}}(x) \quad (A1.9)$$

and

$$k_{n+\frac{1}{2}}(x) = [(2n-1)/(2n+1)] \, k_{n-\frac{1}{2}}(x) + [x^2/(4n^2-1)] \, k_{n-\frac{3}{2}}(x)$$

$$\text{(A1.10)}$$

$$k_{-\frac{1}{2}}(x) = \frac{1}{2x} k_{\frac{1}{2}}(x)$$

$$k_{\frac{1}{2}}(x) = \sqrt{\frac{\pi}{2x}} \exp(-x).$$

For small values of x use of the recurrence relations(34) leads to large errors in the calculated values of $i_{n+\frac{1}{2}}(x)$ and for such cases the series expansion

$$i_{n+\frac{1}{2}}(x) = \sqrt{\frac{2x}{\pi}} \sum_{j=0}^{\infty} s_j \, , \qquad n \geq 0 \qquad\qquad \text{(A1.11)}$$

$$s_0 = 0 \; ;$$

$$s_j = s_{j-1} x^2/(2j(2n+2j+1)), \quad j \geq 1$$

should be used.

In the calculation of the transfer integrals between two molecules of (say) 20 atoms of the order 2400 hybrid integrals have to be calculated.Thus to reduce the amount of computor time needed to perform the calculation,hybrid integrals have been calculated over a fixed grid of internuclear distances. The resulting tables are given in tables(A1.1)-(A1.4). Values of the hybrid integral for a particular internuclear distance. ,R, can be obtained from the tables by interpolation. Tests have shown that using an Aitken interpolation procedure,of low order(4 to 6),high accuracies can be obtained in the interpolated integrals with very low computation times.

(A1.1.11) Two centre-one electron integrals.

The one electron integrals are of the following types:

$$\int \psi(c1,A,1) \; \underline{Op} \; \psi(c2,B,1) \; dV1$$

$$\text{(A1.12)}$$

where the operator $\underline{Op}$ can be either $1/r_a$, resonance integral, or unity, overlap integral. Such integrals can be calculated using the zeta function expansion, however, there are alternative methods which are more efficient.

By transforming the above integrals into a system of prolate spheroidal co-ordinates(9) and performing a simple integration over the angular co-ordinate the above integrals can be reduced to a finite summation over products of functions of the type:

$$\sum_i c_i A_{n_i}(\alpha) B_{m_i}(\beta)$$

where

$$A_n(\alpha) = \int_1^\infty \lambda^n \exp(-\alpha\lambda) d \qquad (A1.13)$$

$$= (k_A + k_B) \times R/2$$

$$B_m(\beta) = \int_{-1}^1 \nu^m \exp(-\beta\nu) d\nu \qquad (A1.14)$$

$$= (k_A - k_B) \times R/2$$

The function $A_n(\alpha)$ can be readily computed using the recurrence formula:

$$A_0(\alpha) = \exp(-\alpha)/\alpha$$

and

$$A_n(\alpha) = (\exp(-\alpha) + nA_{n-1}(\alpha))/\alpha \qquad (A1.15)$$

which is applicable to all α. However, as a check, values of $A_n(\alpha)$ for large n can be calculated explicitly using the equation:

$$A_n(\alpha) = \exp(-\alpha) \times (1 + \frac{n}{\alpha} + \frac{n(n+1)}{\alpha^2} \cdots \frac{n}{\alpha^n})/$$

If, for the two atomic orbitals in equ(A1.1) and eqn(A1.14), $k_A = k_B$ then the function $B_m(\beta)$ reduces either to zero, if m is odd, or is a simple fraction, viz:

$$B_m(0) = \frac{2}{(m+1)} \qquad \text{m even}$$

$$= 0 \qquad \text{m odd}$$

For the case where $\beta \neq 0$ the function can be calculated using the recurrence formula:

$$B_m(\beta) = [(-1)^m \exp(\beta) + m \, B_{m-1}(\beta) - \exp(-\beta)] \qquad (A1.16)$$

Again for large values of m, $B_m(\beta)$ can be calculated using the equation:

$$B_m(\beta) = (-1)^m \frac{\exp(\beta)}{\beta}[1 - \frac{m}{\beta} + \frac{m(m-1)}{\beta^2} \ldots\ldots(-1)^m \frac{m}{\beta^m}]$$
$$- \frac{\exp(-\beta)}{\beta}[1 + \frac{m}{\beta} + \frac{m(m-1)}{\beta^2} \ldots\ldots \frac{m}{\beta^m}] \qquad (A1.17)$$

Problems arising in the numerical computation of the above integrals have been discussed by Gautschi(37), who concluded that upward recursion was applicable if $\beta \geq \beta_n$ whilst for $\beta < \beta_n$ $Bm_{max}(\beta)$ should be calculated using eqn(A1.17) followed by downward recursion using eqn(A1.16). Gautschi(37) calculated the value of β_n to be

$$\beta_n = [n + 0.5 \ln(n) + \ln(\sqrt{2\pi}(1+e))]/e \qquad (A1.18)$$

Procedures have been written in KDF 9 algol to compute the A and B functions, incorporating the Gautschi criterion, the texts of which are given in appendix(2) labeled avector and bvector respectively.

(A1.2) <u>Computer program to evaluate 2 centre-2 electron integrals.</u>
(A1.2.i) <u>General.</u>

The program calculates coulomb and hybrid integrals for the cases where the orbitals of electron 2 (see eqn(A1.1)) are either 2py or 2pz Slater type orbitals, characterized by the screening parameters k3 and k4. The orbitals of electron 1 are set as 1s,1s(with screening parameters k5 and k6),2s,2s, 2px,2px,2py,2py and 2pz,2pz(with screening parameters k1 and k2). In general k1 = k2 and k5 = k6.

The output of the program is in the following form:
INTERMOLECULAR DISTANCE   -   value of R(see section A1.2.ii).
IONIC(or coulombic)INTEGRAL
ELEMENT OF INTEGRATION

T	PY1S1SPY	PY2S2SPY	PYPXPXPY	PYPYPYPY	PYPZPZPY
*	*******	*******	*******	*******	*******

IPY1S1SPY ********

IPY2S2SPY ********

IPYPXPXPY ********

IPYPZPZPY ********

The values listed under ELEMENT OF INTEGRATION refer to the value of the integrand at the upper limit of the numerical integration and serve as an accuracy check. For a limit of accuracy of five figures in the calculated integrals the values in the ELEMENT OF INTEGRATION column should be of the order $1_{\times}-7$ less than the value of the integral.

(A1.2.ii) <u>Construction of the data tape.</u>

REPEAT:

k1 :   Screening parameter of the first orbital of
                electron 1 for quantum number n =2.

if k1 > 998 then goto TERMINATE.

k2   Screening parameter of the second orbital of

electron 1 for quantum number n =2.

k3: Screening parameter of the first orbital of electron 2.

k4: Screening parameter of the second orbital of electron 2.

k5: Screening parameter of the first 1s orbital.

k6: Screening parameter of the second 1s orbital.

lol: Lower limit of integration.

upl: Upper limit of integration.

eps: Maximum tolerable error when calculating Bessel functions by series expansion.

REPEAT FOR NEW INTERMOLECULAR DISTANCE.

R: Intermolecular distance.

if R > 998 then goto REPEAT.

n: Number of points in the numerical integration.

type: An integer which determins the types of integral calculated.

type = 2   Orbitals of electron assumed to be 2pz ,hybrid integrals calculated.

type = any other even number; Orbitals of electron 2 assumed to be 2py,hybrid integrals calculated.

type = 1   Orbitals of electron 2 assumed to be 2 pz,coulomb integrals calculated.

type = any other odd number;Orbitals of electron 2 assumed to be 2 py, coulomb integrals calculated.

goto REPEAT FOR NEW INTERMOLECULAR DISTANCE.

TERMINATE: program terminated.

(A1.2.111) Text of the program.

```
begin
real z0,z1,z2,z3,z4,k1,k2,k3,k4,k5,k6,ka,kb,kc,upl,
lol,X,Y,R,a,b,c,t,w,x,y,grid,eps,j1,j3,j7,j8   ;
integer n,i,type,f1,jj;
array CPY1S1SPY,CPY2S2SPY,CPYPXPXPY,CPYPZPZPY,
CPYPYPYPY,CPZ1S1SPZ,CPZ2S2SPZ,CPZPXPXPZ,CPZPZPZPZ,
IPY1S1SPY,IPY2S2SPY,IPYPXPXPY,IPYPZPZPY,IPYPYPYPY,
IPZ1S1SPZ,IPZ2S2SPZ,IPZPXPXPZ,IPZPZPZPZ[0:100],z[0:4];
real procedure INTEGRATE(n,x,A)   ;
value n,x  ;
real x  ;
integer n  ;
array A  ;
begin
real w1,w2  ;
integer i,j  ;
j := n/2-1  ;
w1 := A[1];
w2 := 0.0   ;
for i := 1 step 1 until j do
begin
w1  := w1+A[2×i+1]  ;
w2  := w2+A[2×i]
end  ;
INTEGRATE := x×(A[0]+4×w1+2×w2+A[n])/3.0  ;
end  ;
real procedure K(n,z)  ;
value n,z  ;
real z  ;
integer n  ;
begin
real error,x,y,yn  ;
```

```
      integer i,j,p,q,r,s,t  ;
      y := exp(-z)  ;
      yn := y  ;
      x := 1/z  ;
      if n < 0 then n := -n-1  ;
      if n = 0 then goto FGBC  ;
      t := 1  ;
      for j := 1 step 1 until n do
      begin
      p := n+j  ;
      q := (if n = j then 1 else n-j)  ;
      t := 2×t×j  ;
      y := y×x  ;
      r := 1  ;
      s := 1  ;
      for i := 1 step 1 until p do r := r×i  ;
      for i := 1 step 1 until q do s := s×i  ;
      error := y×r/(s×t)  ;
      yn := yn+error  ;
      end  ;
      FGBC  :
      K := sqrt(3.1415926536/(2×z))×yn  ;
      end  ;
      real procedure I(n,z)  ;
      value n,z  ;
      real z  ;
      integer n  ;
      begin
      real yn,x,xx,y,yy,error,Z  ;
      integer i,j,p,q,r,s,t  ;
      if n = -1 then
      begin
      Z := sqrt(1/(2×z×3.1415926536))×(exp(-z)+exp(z))  ;
```

```
      goto WDVRDX

      end ;

      if z ≤ 1.0 then

      begin

      r := 1 ;

      if n = 0 then goto UJMLKJ ;

      for i := 1 step 1 until n do r := r×i ;

      UJMLKJ :

      s := r ;

      p := 2×n+1 ;

      for i := n+1 step 1 until p do s := s×i ;

      yn := r/s ;

      x := 1.0 ;

      y := z×z ;

      t := 1 ;

      for j := 1 step 1 until 15 do

      begin

      t := t×j ;

      r := 1 ;

      s := 1 ;

      x := y×x ;

      p := n+j ;

      q := 2×n+2×j+1 ;

      for i := 1 step 1 until p do r := r×i ;

      for i := 1 step 1 until q do s := s×i ;

      error := x×r/(s×t) ;

      yn := yn+error ;

      if error ≤ eps/100 then gotoWDVTFC ;

      end ;

WDVTFC:

      z := sqrt((2×z)↑(n+1)/3.1415926536)×yn ;

      end else

      begin
```

```
    xx := exp(z) ;

    yy := (-1)↑(n+1)/xx  ;

    yn := xx+yy  ;

    if n = 0 then goto UJMOKN ;

    y := 1/z  ;

    x := -y  ;

    t := 1  ;

    for j := 1 step 1 until n do

    begin

    t := 2xtxj  ;

    p := n+j  ;

    q := (if n = j then 1 else n-j)  ;

    xx := xXxx  ;

    yy := yXyy  ;

    r := 1  ;

    s := 1  ;

    for i := 1 step 1 until p do r := rxi  ;

    for i := 1 step 1 until q do s := sxi  ;

    error := (yy+xx)xr/(sxt)  ;

    yn := yn+error  ;

    end  ;

    UJMOKN  :

    Z := sqrt(1/(3.1415926536xzx2))xyn  ;

    end  ;

    WDVRDX  :

    I := Z  ;

    end  ;

    real procedure J(n,a)  ;

    value n,a  ;

    real a  ;

    integer n  ;

    begin

    switch SWITCH := L1,L2,L3,L4,L5,L6,L7,L8  ;
```

```
    real x,y ;
    y := exp(-a) ;
    goto SWITCH[n] ;
 L1:    x := 2-(2+a)xy  ;
        goto exit ;
 L2:    x := 6-(6+4xa+axa)xy  ;
        goto exit ;
 L3:    x := 24-(24+18xa+6xa↑2+a↑3)xy  ;
        goto exit ;
 L4:    x := 8-(8+8xa+4xa↑2+a↑3)xy  ;
        goto exit ;
 L5:    x := 40-(40+40xa+20xa↑2+6xa↑3+a↑4)xy  ;
        goto exit ;
 L6:    x := 96+8xa↑2-(96+96xa+56xa↑2+22xa↑3+6xa↑4+a↑5)xy  ;
        goto exit ;
 L7:    x := 144-(144+144xa+72xa↑2+24xa↑3+6xa↑4+a↑5)xy  ;
        goto exit ;
 L8:    x := -24+4xa↑2+(24+24xa+8xa↑2+a↑3)xy  ;
exit :
 j := x ;
 end ;
real procedure zeta(m,n,a,b) ;
value m,n,a,b ;
real a,b ;
integer m,n ;
begin
real x,y ;
integer 1 ;
array Y[n-1:n+1] ;
if a ≥ b then
begin
x := a ;
y := b ;
```

```
      end else
      begin
      x := b ;
      y := a
      end ;
      if (m+2)×2 = m then
      begin
      for i := n,n-1,n+1 do
      begin
      X[i] := I(i,y)×K(i,x) ;
      if m = 0 then goto exit ;
      end
      end else
      begin
      for i := n,n-1,n+1 do
      begin
      X[i] := (I(i-1,y)×K(i-1,x)-I(i+1,y)×K(i+1,x))×a×b/
      (2×i+1) ;
      if m = 1 then goto exit ;
      end
      end ;
      X[n] := (a×a+b×b)×X[n]-2×a×b×(n×X[n-1]+(n+1)×X[n+1])
      /(2×n+1) ;
      exit :
      zeta := X[n] ;
      end ;
open(20) ;
open(30) ;
f1 := format([6s-d.ddddddₚ-nd]) ;
Repeat :
k1 := read(20) ;
if k1 > 998 then goto OUT ;
```

```
    k2 := read(20)  ;

    k3 := read(20)  ;

    k4 := read(20)  ;

    k5 := read(20)  ;

    k6 := read(20)  ;

    lol:= read(20)  ;

    upl:= read(20)  ;

    eps:= read(20)  ;

    RepeatR :

    R := read(20)  ;

    if R > 998 then goto EXIT  ;

    n := read(20)  ;

    type := read(20)  ;

    grid := (upl-lol)/n  ;

    i := -1  ;

    upl := upl+grid/10  ;

    write text(30,[[6s]INTERNUCLEAR*DISTANCE])  ;

    write(30,f1+2,R)  ;

    if (type+2)×2 =type then goto THMBJO  ;

    write text(30,[[6s]COULOMBIC*INTEGRALS[2c]])  ;

    ka := (k1+k2)/2  ;

    kb := (k3+k4)/2  ;

    kc := (k5+k6)/2  ;

    a := 2×kb×R  ;

    Y := sqrt((k1×k2×k3×k4)↑5/(2×kb×R))  ;

    write text(30,[[6s]ELEMENTS*OF*INTEGRATION[2c12s]
    t[14s]PY1S1SPY[10s]PY2S2SPY[11s]PYPXPXPY[10s]
    PYPYPYPY[11s]PYPZPZPY[2c]])  ;

    if type = 1 then goto TCBRYV  ;

    for t := lol step grid until upl do
begin
b := ka×t/kb  ;
```

```
 i := i+1  ;
 c := kcxt/kb  ;
 w := sqrt(t)  ;
 j1:= j(1,c)  ;
 j3 := j(3,b)  ;
 j7 := j(7,b)  ;
 j8 := j(8,b)  ;
 for jj := 0 step 2 until 4 do z[jj] := zeta(1,jj,t,a)  ;
 x := z[0]-z[2]  ;
 y := z[2]-z[4]  ;
 CPY1S1SPY[i] := txtxwxj1xx  ;
 CPY2S2SPY[i] := txtxwxj3xx  ;
 CPYPXPXPY[i] := wx(xxj8+j7x(x-3xy/7)/10)  ;
 CPYPYPYPY[i] := wx(xxj8/3+0.1xj7x(x-3xy/7))  ;
 CPYPZPZPY[i] := wx(j8xx/3+0.1xj7x(x/3+4xy/7))  ;
 L2:

 end  ;

 write(30,f1,t)  ;
 write(30,f1,CPY1S1SPY[i])  ;
 write(30,f1,CPY2S2SPY[i])  ;
 write(30,f1,CPYPXPXPY[i])  ;
 write(30,f1,CPYPYPYPY[i])  ;
 write(30,f1+2,CPYPZPZPY[i])  ;
 X := sqrt(k5↑3xk6↑3xk3↑5xk4↑5/(2xkbxR))/(24xkc↑3xkb↑4)x
 INTEGRATE(n,grid,CPY1S1SPY)  ;
 write text(30,[[6s]CPY1S1SPY])  ;
 write(30,f1+2,X)  ;
 X := Y/(288xka↑5xkb↑4)xINTEGRATE(n,grid,CPY2S2SPY)  ;
 write text(30,[[6s]CPY2S2SPY])  ;
 write(30,f1+2,X)  ;
 X := Y/(48xka↑7xkb↑2)xINTEGRATE(n,grid,CPYPXPXPY)  ;
 write text(30,[[6s]CPYPXPXPY])  ;
```

```
write(30,f1+2,X)  ;

 X := Y/(16×ka↑7×kb↑2)×INTEGRATE(n,grid,CPYPYPYPY)  ;

 write text(30,[[6s]CPYPYPYPY])  ;

 write(30,f1+2,X)  ;

 X := Y/(16×ka↑7×kb↑2)×INTEGRATE(n,grid,CPYPZPZPY)  ;

 write text(30,[[6s]CPYPZPZPY])  ;

 write(30,f1+2,X)  ;

 goto EEXXIITT  ;

 TCBRYV  :

 for t := lol step grid until upl do

 begin

 b := ka×t/kb  ;

 c := kc×t/kb  ;

 i := i+1  ;

 w := sqrt(t)  ;

 j8 := j(8,c)  ;

 j7 := j(7,c)  ;

 z0 := zeta(1,0,t,a)  ;

 z1 := zeta(1,1,t,a)  ;

 z2 := zeta(1,2,t,a)  ;

 z3 := zeta(3,0,t,a)  ;

 z4 := zeta(1,4,t,a)  ;

 x := z0-z2  ;

 y := z2-z4  ;

 CPZ1S1SPZ[i] := w×(j8×z0+0.5×j7×(z0-2×x/3))/(t×t)  ;

 j7 := j(7,b)  ;

 j8 := j(8,b)  ;

 CPZ2S2SPZ[i] := w×(j8×z3+0.5×j7×(z3-2×(z3-zeta(3,2,t,a))
/3))/(t×t)  ;

 CPZPXPXPZ[i] := w×(j8×x/3+0.1×j7×(x/3+4×y/7))  ;

 CPZPZPZPZ[i] := w×(a×a×(j8×z0+0.5×j7×(z0-2×x/3))/(t×t
)-2×a×(j8×z1+0.5×j7×(z1-0.4×(z1-zeta(1,3,t,a)))))
```

```
      /t+j8×(z0-2×x/3)+0.5×j7×(z0-0.8×x-8×y/35))  ;
      L3:
      end  ;
      write(30,f1,t)  ;
      write(30,f1,CPZ1S1SPZ[1])  ;
      write(30,f1,CPZ2S2SPZ[1])  ;
      write(30,f1,CPZPXPXPZ[1])  ;
      write(30,f1,CPZPZPZPZ[1])  ;
      write(30,f1+2,CPZPXPXPZ[1])  ;
      X := sqrt((k5×k6)↑5×(k3×k4)↑3/a)/(4×kc↑7)×
      INTEGRATE(n,grid,CPZ1S1SPZ)  ;
      write text(30,[[6s]CPZ1S1SPZ])  ;
      write(30,f1+2,X)  ;
      X := Y/(48×ka↑7×kb↑2)×INTEGRATE(n,grid,CPZ2S2SPZ)  ;
      write text(30,[[6s]CPZ2S2SPZ])  ;
      write(30,f1+2,X)  ;
      X := Y/(16×ka↑7×kb↑2)×INTEGRATE(n,grid,CPZPXPXPZ)  ;
      write text(30,[[6s]CPZPXPXPZ])  ;
      write(30,f1+2,X)  ;
      X := Y/(16×ka↑7×kb↑2)×INTEGRATE(n,grid,CPZPZPZPZ)  ;
      write text(30,[[6s]CPZPZPZPZ])  ;
      write(30,f1+2,X)  ;
      write text(30,[[p]])  ;
      goto EEXXIITT  ;
      THMBJO  :
      write text(30,[[2c6s]IONIC*INTEGRALS[2c]])  ;
      a := k4×R  ;
      ka := (k1+k2)/2  ;
      Y := sqrt((k1×k2×k3)↑5/R)  ;
      kc := (k5+k6)/2  ;
      write text(30,[[6s]ELEMENTS*OF*INTEGRATION[2c12s]t[10s]
PY1S1SPY[10s]PY2S2SPY[11s]PYPXPXPY[10s]PYPYPYPY[11s]
```

```
    PYPZPZPY[2c]]) ;

    if type = 2 then goto TFHKOL ;

    for t := lol step grid until upl do

    begin b := 2×ka×t/k4 ;

    c := kc×t×2/k4 ;

    l := l+1 ;

    j1 := J(1,c) ;

    j3 := J(3,b) ;

    j7 := J(7,b) ;

    j8 := J(8,b) ;

    x := zeta(1,0,t,a)-zeta(1,2,t,a) ;

    w := sqrt(t)×exp(-k3×t/k4) ;

    IPY1S1SPY[l] := t×t×w×j1×x ;

    for jj := 0 step 2 until 4 do z[jj] := zeta(1,jj,t,a) ;

    x := z[0]-z[2] ;

    y := z[2]-z[4] ;

    IPY2S2SPY[l] := t×t×w×j3×x ;

    IPYPXPXPY[l] := w×(x×j8+j7×(x-3×x×y/7)/10) ;

    IPYPZPZPY[l] := w×(x×j8/3+0.1×j7×(x/3+4×x×y/7)) ;

    IPYPYPYPY[l] := w×(x×j8/3+0.1×j7×(x-3×x×y/7)) ;

    L :

    end ;

    write(30,f1,t) ;

    write(30,f1,IPY1S1SPY[l]) ;

    write(30,f1,IPY2S2SPY[l]) ;

    write(30,f1,IPYPXPXPY[l]) ;

    write(30,f1,IPYPYPYPY[l]) ;

    write(30,f1+2,IPYPZPZPY[l]) ;

    X := 2×sqrt(k5↑3×k6↑3×k3↑5/R)/(3×kc↑3×k4↑2)×

    INTEGRATE(n,grid,IPY1S1SPY) ;

    write text(30,[[6s]IPY1S1SPY]) ;

    write(30,f1+2,X) ;
```

```
X := Y/(18×ka↑5×k4↑2)×INTEGRATE(n,grid,IPY2S2SPY)  ;

write text(30,[[6s]IPY2S2SPY])  ;

write(30,f1+2,X)  ;

X := Y/(12×ka↑7)×INTEGRATE(n,grid,IPYPXPXPY)  ;

write text(30,[[6s]IPYPXPXPY])  ;

write(30,f1+2,X)  ;

X := Y/(4×ka↑7)×INTEGRATE(n,grid,IPYPYPYPY)  ;

write text(30,[[6s]IPYPYPYPY])  ;

write(30,f1+2,X)  ;

X := Y/(4×ka↑7)×INTEGRATE(n,grid,IPYPZPZPY)  ;

write text(30,[[6s]IPYPZPZPY])  ;

write(30,f1+2,X)  ;

goto EEXXIITT  ;

TFHKOL  :

for t := lol step grid until upl do

begin

b := 2×ka×t/k4  ;

c := 2×kc×t/k4  ;

i := i+1  ;

j1 := J(1,c)  ;

j3 := J(3,b)  ;

j7 := J(7,b)  ;

j8 := J(8,b)  ;

z0 := zeta(1,0,t,a)  ;

z1 := zeta(1,1,t,a)  ;

z2 := zeta(1,2,t,a)  ;

z3 := zeta(1,3,t,a)  ;

z4 := zeta(1,4,t,a)  ;

w := sqrt(t)×exp(-k3×t/k4)  ;

x := z0-z2  ;

y := z2-z4  ;

IPZ1S1SPZ[i] := w×t×j1×(a×z1-t×(z0-2×x/3))  ;
```

```
    IPZ2S2SPZ[1] := wxtxj3x(axz1-tx(z0-2xx/3))   ;

    IPZPXPXPZ[1] := wx(ax(j8xz1+0.1xj7x(z1-z3))/t

    -j8x(z0-2xx/3)-0.2xj7x(x/6+2xy/7))   ;

    IPZPZPZPZ[1] := wx(ax(j8xz1+0.5xj7x(z1-.4x(z1-z3)

    ))/t-j8x(z0-2xx/3)-0.5xj7x(z0-0.8xx-8xy/35))   ;

    L4  :

    end  ;

    write(30,f1,t)   ;

    write(30,f1,IPZ1S1SPZ[1])   ;

    write(30,f1,IPZ2S2SPZ[1])   ;

    write(30,f1,IPZPXPXPZ[1])   ;

    write(30,f1,IPZPZPZPZ[1])   ;

    write(30,f1+2,IPZPXPXPZ[1])   ;

    X := 2xsqrt((k5xk6)↑3xk3↑5/R)/(kc↑3xk4↑5)x

    INTEGRATE(n,grid,IPZ1S1SPZ)   ;

    write text(30,[[6s]IPZ1S1SPZ])   ;

    write(30,f1+2,X)   ;

    X := Y/(6xka↑5xk4↑2)xINTEGRATE(n,grid,IPZ2S2SPZ)   ;

    write text(30,[[6s]IPZ2S2SPZ])   ;

    write(30,f1+2,X)   ;

    X := Y/(4xka↑7)xINTEGRATE(n,grid,IPZPXPXPZ)   ;

    write text(30,[[6s]IPZPXPXPZ])   ;

    write(30,f1+2,X)   ;

    X := Y/(4xka↑7)xINTEGRATE(n,grid,IPZPZPZPZ)   ;

    write text(30,[[6s]IPZPZPZPZ])   ;

    write(30,f1+2,X)   ;

    EEXXIITT  :

    goto RepeatR  ;

    EXIT  :

    goto Repeat  ;

    OUT  :
```

```
close(30)  ;
close(20)  ;
end PROGRAM
```

(A1.3) <u>Tables</u> <u>of</u> <u>hybrid</u> <u>integerals</u> between <u>carbon</u> and.

   <u>nitrogen</u> <u>atoms</u>.

   The screening parameters used in computing the tables

were as follows:

Carbon: 1s = 5.7 au.   (107.7 nm^{-1}.)

                       2x = 1.625 au.(30.7 nm^{-1}.)

Nitrogen: 1s = 6.7 au.   (126.7 nm^{-1}.)

                       2s = 1.950 au.(36.8 nm^{-1}.)

where x = 2s,2px,2py,2pz.

   The values of the integrals within the tables are given

in atomic units. To convert the integrals to eV multiply by the

factor 27.21. To convert the internuclear distances to nm.

multiply by the factor 0.05292.

R.	$\langle py1\,sI1\,spy\rangle$	$\langle py2sI2spy\rangle$	$\langle pypxIpxpy\rangle$
4.500	1.41650×10^{-2}	1.33097×10^{-2}	1.27477×10^{-2}
4.625	1.20952×10^{-2}	1.13918×10^{-2}	1.09167×10^{-2}
4.750	1.03177×10^{-2}	9.73936×10^{-3}	9.33826×10^{-3}
4.875	8.79301×10^{-3}	8.31776×10^{-3}	7.97953×10^{-3}
5.000	7.48687×10^{-3}	7.09644×10^{-3}	6.81155×10^{-3}
5.125	6.36910×10^{-3}	6.04851×10^{-3}	5.80881×10^{-3}
5.250	5.41379×10^{-3}	5.15056×10^{-3}	4.94909×10^{-3}
5.375	4.59807×10^{-3}	4.38201×10^{-3}	4.21282×10^{-3}
5.500	3.90222×10^{-3}	3.72493×10^{-3}	3.58299×10^{-3}
5.625	3.30922×10^{-3}	3.16378×10^{-3}	3.04480×10^{-3}
5.750	2.80433×10^{-3}	2.68504×10^{-3}	2.58539×10^{-3}
5.875	2.37485×10^{-3}	2.27703×10^{-3}	2.19362×10^{-3}
6.000	2.00980×10^{-3}	1.92960×10^{-3}	1.85985×10^{-3}
6.125	1.69978×10^{-3}	1.63404×10^{-3}	1.57574×10^{-3}
6.250	1.43668×10^{-3}	1.38280×10^{-3}	1.33412×10^{-3}
6.375	1.21358×10^{-3}	1.16944×10^{-3}	1.12880×10^{-3}
6.500	1.02454×10^{-3}	9.88371×10^{-4}	9.54478×10^{-4}
6.625	8.64466×10^{-4}	8.34833×10^{-4}	8.06578×10^{-4}
6.750	7.29005×10^{-4}	7.04733×10^{-4}	6.81192×10^{-4}
6.875	6.14450×10^{-4}	5.94571×10^{-4}	5.74967×10^{-4}
7.000	5.17646×10^{-4}	5.01360×10^{-4}	4.85042×10^{-4}
7.125	4.35866×10^{-4}	4.22531×10^{-4}	4.08957×10^{-4}
7.250	3.66832×10^{-4}	3.55915×10^{-4}	3.44627×10^{-4}
7.375	3.08589×10^{-4}	2.99653×10^{-4}	2.90271×10^{-4}
7.50	2.59477×10^{-4}	2.52162×10^{-4}	2.44368×10^{-4}
7.625	2.18086×10^{-4}	2.12100×10^{-4}	2.05626×10^{-4}
7.750	1.83221×10^{-4}	1.78322×10^{-4}	1.72948×10^{-4}
7.875	1.53866×10^{-4}	1.49857×10^{-4}	1.45398×10^{-4}
8.000	1.29163×10^{-4}	1.25882×10^{-4}	1.22183×10^{-4}
8.125	1.08416×10^{-4}	1.05715×10^{-4}	1.02647×10^{-4}
8.250	9.09125×10^{-5}	8.87168×10^{-5}	8.61741×10^{-5}
8.375	7.62518×10^{-5}	7.44440×10^{-5}	7.23367×10^{-5}
8.500	6.38955×10^{-5}	6.24263×10^{-5}	6.06808×10^{-5}

Table(A1.1)
Hybrid integrals between t⩾

$\langle pypy|pypy\rangle$	$\langle pypz|pzpy\rangle$
$1.35208_{\text{D}}-02$	$1.36606_{\text{D}}-02$
$1.15641_{\text{D}}-02$	$1.16946_{\text{D}}-02$
$9.87984_{\text{D}}-03$	$9.99998_{\text{D}}-03$
$8.43221_{\text{D}}-03$	$8.54154_{\text{D}}-03$
$7.18961_{\text{D}}-03$	$7.28815_{\text{D}}-03$
$6.12429_{\text{D}}-03$	$6.21243_{\text{D}}-03$
$5.21215_{\text{D}}-03$	$5.29045_{\text{D}}-03$
$4.43202_{\text{D}}-03$	$4.50118_{\text{D}}-03$
$3.76552_{\text{D}}-03$	$3.82629_{\text{D}}-03$
$3.19669_{\text{D}}-03$	$3.24986_{\text{D}}-03$
$2.71171_{\text{D}}-03$	$2.75804_{\text{D}}-03$
$2.29862_{\text{D}}-03$	$2.33884_{\text{D}}-03$
$1.94707_{\text{D}}-03$	$1.98188_{\text{D}}-03$
$1.64816_{\text{D}}-03$	$1.67821_{\text{D}}-03$
$1.39421_{\text{D}}-03$	$1.42008_{\text{D}}-03$
$1.17865_{\text{D}}-03$	$1.20086_{\text{D}}-03$
$9.95805_{\text{D}}-04$	$1.01483_{\text{D}}-03$
$8.40827_{\text{D}}-04$	$8.57095_{\text{D}}-04$
$7.09562_{\text{D}}-04$	$7.23446_{\text{D}}-04$
$5.98459_{\text{D}}-04$	$6.10287_{\text{D}}-04$
$5.04488_{\text{D}}-04$	$5.14584_{\text{D}}-04$
$4.25046_{\text{D}}-04$	$4.33591_{\text{D}}-04$
$3.57935_{\text{D}}-04$	$3.65182_{\text{D}}-04$
$3.01274_{\text{D}}-04$	$3.07413_{\text{D}}-04$
$2.53463_{\text{D}}-04$	$2.58656_{\text{D}}-04$
$2.13142_{\text{D}}-04$	$2.17530_{\text{D}}-04$
$1.79157_{\text{D}}-04$	$1.82860_{\text{D}}-04$
$1.50525_{\text{D}}-04$	$1.53648_{\text{D}}-04$
$1.26416_{\text{D}}-04$	$1.29047_{\text{D}}-04$
$1.06142_{\text{D}}-04$	$1.08355_{\text{D}}-04$
$8.90572_{\text{D}}-05$	$9.09190_{\text{D}}-05$
$7.47161_{\text{D}}-05$	$7.62792_{\text{D}}-05$
$6.26425_{\text{D}}-05$	$6.39557_{\text{D}}-05$

wo carbon atoms.

R.	$\langle py1sI1spy \rangle$	$\langle py2sI2spy \rangle$	$\langle pypxIpxpy \rangle$
8.625	5.35384ᴅ-05	5.23367ᴅ-05	5.08911ᴅ-05
8.750	4.48450ᴅ-05	4.38620ᴅ-05	4.26652ᴅ-05
8.875	3.75506ᴅ-05	3.67467ᴅ-05	3.57561ᴅ-05
9.000	3.14326ᴅ-05	3.07751ᴅ-05	2.99554ᴅ-05
9.125	2.63031ᴅ-05	2.57655ᴅ-05	2.50874ᴅ-05
9.250	2.20040ᴅ-05	2.15643ᴅ-05	2.10035ᴅ-05
9.375	1.84018ᴅ-05	1.80425ᴅ-05	1.75787ᴅ-05
9.500	1.53850ᴅ-05	1.50912ᴅ-05	1.47079ᴅ-05
9.625	1.28591ᴅ-05	1.26188ᴅ-05	1.23021ᴅ-05
9.750	1.07449ᴅ-05	1.05485ᴅ-05	1.02867ᴅ-05
9.875	8.97584ᴅ-06	8.81526ᴅ-06	8.59903ᴅ-06
10.000	7.49610ᴅ-06	7.36481ᴅ-06	7.18623ᴅ-06
10.125	6.25860ᴅ-06	6.15129ᴅ-06	6.00382ᴅ-06
10.250	5.22408ᴅ-06	5.13637ᴅ-06	5.01463ᴅ-06
10.375	4.35911ᴅ-06	4.28781ᴅ-06	4.18732ᴅ-06
10.500	3.63712ᴅ-06	3.57852ᴅ-06	3.49559ᴅ-06
10.625	3.03426ᴅ-06	2.98607ᴅ-06	2.91764ᴅ-06
10.750	2.52982ᴅ-06	2.49068ᴅ-06	2.43423ᴅ-06
10.875	2.10952ᴅ-06	2.07733ᴅ-06	2.03076ᴅ-06
11.00	1.75812ᴅ-06	1.73197ᴅ-06	1.69357ᴅ-06
11.125	1.46530ᴅ-06	1.44380ᴅ-06	1.41214ᴅ-06
11.250	1.22063ᴅ-06	1.20317ᴅ-06	1.17707ᴅ-06
11.375	1.01695ᴅ-06	1.00259ᴅ-06	9.81068ᴅ-07
11.500	8.46794ᴅ-07	8.35133ᴅ-07	8.17399ᴅ-07
11.625	6.55350ᴅ-07	6.46506ᴅ-07	6.32980ᴅ-07
11.750	5.86976ᴅ-07	5.79190ᴅ-07	5.67149ᴅ-07
11.875	4.88630ᴅ-07	4.82230ᴅ-07	4.72309ᴅ-07
12.000	4.05707ᴅ-07	4.0509ᴅ-07	3.92338ᴅ-07
12.125	3.38316ᴅ-07	3.34042ᴅ-07	3.27312ᴅ-07
12.250	2.81379ᴅ-07	2.77917ᴅ-07	2.72375ᴅ-07
12.375	2.34071ᴅ-07	2.31280ᴅ-07	2.26654ᴅ-07
12.500	1.94617ᴅ-07	1.92301ᴅ-07	1.88544ᴅ-07
12.625	1.61803ᴅ-07	1.59915ᴅ-07	1.56823ᴅ-07

Table(A1.1)
Hybrid integrals between t

⟨pypy|pypy⟩	⟨pypz|pzpy⟩
5.25087ⱪ-05	5.36103ⱪ-05
4.39987ⱪ-05	4.49222ⱪ-05
3.68552ⱪ-05	3.76288ⱪ-05
3.08112ⱪ-05	3.15089ⱪ-05
2.58336ⱪ-05	2.63755ⱪ-05
2.16182ⱪ-05	2.20713ⱪ-05
1.80850ⱪ-05	1.84636ⱪ-05
1.51247ⱪ-05	1.54410ⱪ-05
1.26452ⱪ-05	1.29093ⱪ-05
1.05692ⱪ-05	1.07895ⱪ-05
8.83151ⱪ-06	9.01524ⱪ-06
7.37754ⱪ-06	7.53069ⱪ-06
6.16122ⱪ-06	6.28883ⱪ-06
5.14411ⱪ-06	5.25039ⱪ-06
4.29381ⱪ-06	4.38230ⱪ-06
3.58317ⱪ-06	3.65680ⱪ-06
2.98968ⱪ-06	3.05091ⱪ-06
2.49343ⱪ-06	2.54437ⱪ-06
2.07945ⱪ-06	2.12178ⱪ-06
1.73358ⱪ-06	1.76876ⱪ-06
1.44502ⱪ-06	1.47424ⱪ-06
1.20408ⱪ-06	1.22836ⱪ-06
1.00328ⱪ-06	1.02342ⱪ-06
8.35637ⱪ-07	8.52363ⱪ-07
6.46833ⱪ-07	6.59705ⱪ-07
5.79455ⱪ-07	5.90966ⱪ-07
4.82419ⱪ-07	4.91961ⱪ-07
4.01638ⱪ-07	4.08552ⱪ-07
3.34130ⱪ-07	3.40685ⱪ-07
2.77971ⱪ-07	2.83405ⱪ-07
2.31250ⱪ-07	2.35750ⱪ-07
1.92315ⱪ-07	1.96043ⱪ-07
1.59918ⱪ-07	1.63005ⱪ-07

cont.
wo carbon atoms.

R.	$\langle py1sI1spy\rangle$	$\langle py2sI2spy\rangle$	$\langle pypxIpxpy\rangle$
12.750	$1.34509_{10}{-}07$	$1.32963_{10}{-}07$	$1.30418_{10}{-}07$
12.875	$1.11793_{10}{-}07$	$1.10533_{10}{-}07$	$1.08438_{10}{-}07$
13.00	$9.30319_{10}{-}08$	$9.20001_{10}{-}08$	$9.02755_{10}{-}08$
13.125	$7.71891_{10}{-}08$	$7.63482_{10}{-}08$	$7.49295_{10}{-}08$
13.250	$6.41266_{10}{-}08$	$6.34381_{10}{-}08$	$6.22701_{10}{-}08$
13.375	$5.32628_{10}{-}08$	$5.27017_{10}{-}08$	$5.17415_{10}{-}08$
13.500	$4.42343_{10}{-}08$	$4.37759_{10}{-}08$	$4.29860_{10}{-}08$
13.625	$3.67306_{10}{-}08$	$3.63562_{10}{-}08$	$3.57065_{10}{-}08$
13.750	$3.04964_{10}{-}08$	$3.01898_{10}{-}08$	$2.96556_{10}{-}08$
13.875	$2.53149_{10}{-}08$	$2.50651_{10}{-}08$	$2.46257_{10}{-}08$
14.00	$2.10740_{10}{-}08$	$2.08694_{10}{-}08$	$2.05079_{10}{-}08$
14.125	$1.74377_{10}{-}08$	$1.72708_{10}{-}08$	$1.69737_{10}{-}08$
14.250	$1.44694_{10}{-}08$	$1.43330_{10}{-}08$	$1.40888_{10}{-}08$
14.375	$1.20047_{10}{-}08$	$1.18933_{10}{-}08$	$1.16926_{10}{-}08$
14.500	$9.95854_{10}{-}09$	$9.86757_{10}{-}09$	$9.70257_{10}{-}09$
14.625	$8.26006_{10}{-}09$	$8.18575_{10}{-}09$	$8.05014_{10}{-}09$
14.750	$6.85038_{10}{-}09$	$6.78969_{10}{-}09$	$6.67823_{10}{-}09$
14.875	$5.68056_{10}{-}09$	$5.63098_{10}{-}09$	$5.53939_{10}{-}09$
15.00	$4.70991_{10}{-}09$	$4.66942_{10}{-}09$	$4.59416_{10}{-}09$
15.125	$3.90465_{10}{-}09$	$3.87158_{10}{-}09$	$3.80974_{10}{-}09$
15.250	$3.23667_{10}{-}09$	$3.20966_{10}{-}09$	$3.15885_{10}{-}09$
15.375	$2.68264_{10}{-}09$	$2.66058_{10}{-}09$	$2.61884_{10}{-}09$
15.50)	$2.22319_{10}{-}09$	$2.20517_{10}{-}09$	$2.17088_{10}{-}09$
15.625	$1.70872_{10}{-}09$	$1.69515_{10}{-}09$	$1.66912_{10}{-}09$
15.750	$1.52635_{10}{-}09$	$1.51433_{10}{-}09$	$1.49120_{10}{-}09$
15.875	$1.26450_{10}{-}09$	$1.25468_{10}{-}09$	$1.23569_{10}{-}09$
16.000	$1.04746_{10}{-}09$	$1.03944_{10}{-}09$	$1.02383_{10}{-}09$

Table(A1.1)

Hybrid integrals between t

⟨pypyIpypy⟩	⟨pypzIpzpy⟩
$1.32959_{\mathrm{D}}-07$	$1.35513_{\mathrm{D}}-07$
$1.10523_{\mathrm{D}}-07$	$1.12638_{\mathrm{D}}-07$
$9.19868_{\mathrm{D}}-08$	$9.37378_{\mathrm{D}}-08$
$7.63337_{\mathrm{D}}-08$	$7.77813_{\mathrm{D}}-08$
$6.34233_{\mathrm{D}}-08$	$6.46204_{\mathrm{D}}-08$
$5.26867_{\mathrm{D}}-08$	$5.36768_{\mathrm{D}}-08$
$4.37615_{\mathrm{D}}-08$	$4.45801_{\mathrm{D}}-08$
$3.63426_{\mathrm{D}}-08$	$3.70193_{\mathrm{D}}-08$
$3.01773_{\mathrm{D}}-08$	$3.07366_{\mathrm{D}}-08$
$2.50537_{\mathrm{D}}-08$	$2.55158_{\mathrm{D}}-08$
$2.08589_{\mathrm{D}}-08$	$2.12413_{\mathrm{D}}-08$
$1.72616_{\mathrm{D}}-08$	$1.75770_{\mathrm{D}}-08$
$1.43249_{\mathrm{D}}-08$	$1.45854_{\mathrm{D}}-08$
$1.18861_{\mathrm{D}}-08$	$1.21013_{\mathrm{D}}-08$
$9.86127_{\mathrm{D}}-09$	$1.00389_{\mathrm{D}}-08$
$8.18025_{\mathrm{D}}-09$	$8.32687_{\mathrm{D}}-09$
$6.78490_{\mathrm{D}}-09$	$6.90593_{\mathrm{D}}-09$
$5.62684_{\mathrm{D}}-09$	$5.72672_{\mathrm{D}}-09$
$4.66584_{\mathrm{D}}-09$	$4.74826_{\mathrm{D}}-09$
$3.86849_{\mathrm{D}}-09$	$3.93650_{\mathrm{D}}-09$
$3.20701_{\mathrm{D}}-09$	$3.26311_{\mathrm{D}}-09$
$2.65831_{\mathrm{D}}-09$	$2.70458_{\mathrm{D}}-09$
$2.20323_{\mathrm{D}}-09$	$2.24139_{\mathrm{D}}-09$
$1.69359_{\mathrm{D}}-09$	$1.72273_{\mathrm{D}}-09$
$1.51292_{\mathrm{D}}-09$	$1.53887_{\mathrm{D}}-09$
$1.25349_{\mathrm{D}}-09$	$1.27488_{\mathrm{D}}-09$
$1.03842_{\mathrm{D}}-09$	$1.05606_{\mathrm{D}}-09$

cont.
wo carbon atoms.

R.	$\langle pz1sI1spz\rangle$	$\langle pz2sI2spz\rangle$	$\langle pzpxIpxpz\rangle$
4.500	$6.61159_{10}-02$	$6.09658_{10}-02$	$5.81422_{10}-02$
4.625	$5.88117_{10}-02$	$5.44283_{10}-02$	$5.19387_{10}-02$
4.750	$5.21826_{10}-02$	$4.84577_{10}-02$	$4.62692_{10}-02$
4.875	$4.61911_{10}-02$	$4.30304_{10}-02$	$4.11121_{10}-02$
5.000	$4.07963_{10}-02$	$3.81181_{10}-02$	$3.64410_{10}-02$
5.125	$3.59554_{10}-02$	$3.36891_{10}-02$	$3.22265_{10}-02$
5.250	$3.16261_{10}-02$	$2.97104_{10}-02$	$2.84378_{10}-02$
5.375	$2.77655_{10}-02$	$2.61481_{10}-02$	$2.50432_{10}-02$
5.500	$2.43324_{10}-02$	$2.29683_{10}-02$	$2.20110_{10}-02$
5.625	$2.12875_{10}-02$	$2.01382_{10}-02$	$1.93103_{10}-02$
5.750	$1.85935_{10}-02$	$1.76260_{10}-02$	$1.69113_{10}-02$
5.875	$1.62153_{10}-02$	$1.54017_{10}-02$	$1.47858_{10}-02$
6.000	$1.41205_{10}-02$	$1.34368_{10}-02$	$1.29069_{10}-02$
6.125	$1.22791_{10}-02$	$1.17050_{10}-02$	$1.12497_{10}-02$
6.250	$1.06633_{10}-02$	$1.01817_{10}-02$	$9.79112_{10}-03$
6.375	$9.24828_{10}-03$	$8.84448_{10}-03$	$8.50988_{10}-03$
6.500	$8.01112_{10}-03$	$7.67280_{10}-03$	$7.38653_{10}-03$
6.625	$6.93125_{10}-03$	$6.64798_{10}-03$	$6.40335_{10}-03$
6.750	$5.99012_{10}-03$	$5.75308_{10}-03$	$5.54428_{10}-03$
6.875	$5.17112_{10}-03$	$4.97289_{10}-03$	$4.79488_{10}-03$
7.000	$4.45944_{10}-03$	$4.29375_{10}-03$	$4.14214_{10}-03$
7.125	$3.84179_{10}-03$	$3.70338_{10}-03$	$3.57439_{10}-03$
7.250	$3.30646_{10}-03$	$3.19090_{10}-03$	$3.08126_{10}-03$
7.375	$2.84306_{10}-03$	$2.74662_{10}-03$	$2.65352_{10}-03$
7.500	$2.18493_{10}-03$	$2.36195_{10}-03$	$2.28296_{10}-03$
7.625	$2.09635_{10}-03$	$2.02928_{10}-03$	$1.96232_{10}-03$
7.750	$1.79782_{10}-03$	$1.74193_{10}-03$	$1.68521_{10}-03$
7.875	$1.54054_{10}-03$	$1.49398_{10}-03$	$1.44599_{10}-03$
8.000	$1.31904_{10}-03$	$1.28027_{10}-03$	$1.23968_{10}-03$
8.125	$1.12864_{10}-03$	$1.09631_{10}-03$	$1.06201_{10}-03$
8.250	$9.64813_{10}-04$	$9.37963_{10}-04$	$9.08997_{10}-04$
8.375	$8.24343_{10}-04$	$8.01967_{10}-04$	$7.77523_{10}-04$
8.500	$7.03697_{10}-04$	$6.85124_{10}-04$	$6.64510_{10}-04$

Table(A1.1)
Hybrid integrals between t₁

$\langle pzpy|pypz\rangle$	$\langle pzpz|pzpz\rangle$
5.81422×10^{-02}	6.66130×10^{-02}
5.19387×10^{-02}	5.94075×10^{-02}
4.62692×10^{-02}	5.28346×10^{-02}
4.11121×10^{-02}	4.68670×10^{-02}
3.64410×10^{-02}	4.14722×10^{-02}
3.22265×10^{-02}	3.66142×10^{-02}
2.84378×10^{-02}	3.22555×10^{-02}
2.50432×10^{-02}	2.83578×10^{-02}
2.20110×10^{-02}	2.48829×10^{-02}
1.93103×10^{-02}	2.17940×10^{-02}
1.69113×10^{-02}	1.90554×10^{-02}
1.47858×10^{-02}	1.66335×10^{-02}
1.29069×10^{-02}	1.44967×10^{-02}
1.12497×10^{-02}	1.26155×10^{-02}
9.79112×10^{-03}	1.09628×10^{-02}
8.50988×10^{-03}	9.51367×10^{-03}
7.38653×10^{-03}	8.24535×10^{-03}
6.40335×10^{-03}	7.13724×10^{-03}
5.54428×10^{-03}	6.17068×10^{-03}
4.79488×10^{-03}	5.32893×10^{-03}
4.14214×10^{-03}	4.59697×10^{-03}
3.57439×10^{-03}	3.96136×10^{-03}
3.08126×10^{-03}	3.41017×10^{-03}
2.65352×10^{-03}	2.93282×10^{-03}
2.28296×10^{-03}	2.51992×10^{-03}
1.96232×10^{-03}	2.16319×10^{-03}
1.68521×10^{-03}	1.85535×10^{-03}
1.44599×10^{-03}	1.58997×10^{-03}
1.23968×10^{-03}	1.36145×10^{-03}
1.06201×10^{-03}	1.16491×10^{-03}
9.08997×10^{-04}	9.95893×10^{-04}
7.77523×10^{-04}	8.50856×10^{-04}
6.64510×10^{-04}	7.26354×10^{-04}

cont.
vo carbon atoms.

R.	$\langle pz1sI1spz \rangle$	$\langle pz2sI2spz \rangle$	$\langle pzpxIpxpz \rangle$
8.625	$6.00360_{10}-04$	$5.84924_{10}-04$	$5.67550_{10}-04$
8.750	$5.11867_{10}-04$	$4.99039_{10}-04$	$4.84404_{10}-04$
8.875	$4.36139_{10}-04$	$4.25484_{10}-04$	$4.13164_{10}-04$
9.000	$3.71371_{10}-04$	$3.62535_{10}-04$	$3.52170_{10}-04$
9.125	$3.16059_{10}-04$	$3.08713_{10}-04$	$2.99997_{10}-04$
9.250	$2.68817_{10}-04$	$2.62721_{10}-04$	$2.55396_{10}-04$
9.375	$2.28507_{10}-04$	$2.23449_{10}-04$	$2.17296_{10}-04$
9.500	$1.94136_{10}-04$	$1.89940_{10}-04$	$1.84774_{10}-04$
9.625	$1.64846_{10}-04$	$1.61367_{10}-04$	$1.57031_{10}-04$
9.750	$1.39903_{10}-04$	$1.37018_{10}-04$	$1.33381_{10}-04$
9.875	$1.18674_{10}-04$	$1.16282_{10}-04$	$1.13233_{10}-04$
10.000	$1.00613_{10}-04$	$9.86336_{10}-05$	$9.60781_{10}-05$
10.125	$8.52651_{10}-05$	$8.36231_{10}-05$	$8.14822_{10}-05$
10.250	$7.22221_{10}-05$	$7.08621_{10}-05$	$6.90694_{10}-05$
10.375	$6.11470_{10}-05$	$6.00203_{10}-05$	$5.85197_{10}-05$
10.500	$5.17462_{10}-05$	$5.08138_{10}-05$	$4.95582_{10}-05$
10.625	$4.37748_{10}-05$	$4.30015_{10}-05$	$4.19513_{10}-05$
10.750	$3.70111_{10}-05$	$3.63722_{10}-05$	$3.54942_{10}-05$
10.875	$3.12832_{10}-05$	$3.07536_{10}-05$	$3.00197_{10}-05$
11.000	$2.64273_{10}-05$	$2.59905_{10}-05$	$2.53773_{10}-05$
11.125	$2.23201_{10}-05$	$2.19576_{10}-05$	$2.14454_{10}-05$
11.250	$1.88412_{10}-05$	$1.85420_{10}-05$	$1.81144_{10}-05$
11.375	$1.59004_{10}-05$	$1.56525_{10}-05$	$1.52955_{10}-05$
11.500	$1.34121_{10}-05$	$1.32076_{10}-05$	$1.29097_{10}-05$
11.625	$1.05637_{10}-05$	$1.04067_{10}-05$	$1.01756_{10}-05$
11.750	$9.53365_{10}-06$	$9.39385_{10}-06$	$9.18663_{10}-06$
11.875	$8.03403_{10}-06$	$7.91830_{10}-06$	$7.74553_{10}-06$
12.000	$6.76719_{10}-06$	$6.67187_{10}-06$	$6.52787_{10}-06$
12.125	$5.69903_{10}-06$	$5.62004_{10}-06$	$5.50005_{10}-06$
12.250	$4.79723_{10}-06$	$4.73219_{10}-06$	$4.63224_{10}-06$
12.375	$4.03743_{10}-06$	$3.98354_{10}-06$	$3.90030_{10}-06$
12.500	$3.39651_{10}-06$	$3.35210_{10}-06$	$3.28279_{10}-06$
12.625	$2.85653_{10}-06$	$2.81991_{10}-06$	$2.76221_{10}-06$

Table(A1.1)
Hybrid integrals between t

$\langle p_z p_y | p_y p_z \rangle$	$\langle p_z p_z | p_z p_z \rangle$
5.67550ɴ-04	6.19673ɴ-04
4.84404ɴ-04	5.28309ɴ-04
4.13164ɴ-04	4.50124ɴ-04
3.52170ɴ-04	3.83266ɴ-04
2.99997ɴ-04	3.26145ɴ-04
2.55396ɴ-04	2.77372ɴ-04
2.17296ɴ-04	2.35756ɴ-04
1.84774ɴ-04	2.00273ɴ-04
1.57031ɴ-04	1.70038ɴ-04
1.33381ɴ-04	1.44292ɴ-04
1.13233ɴ-04	1.22381ɴ-04
9.60781ɴ-05	1.03745ɴ-04
8.14822ɴ-05	8.79047ɴ-05
6.90694ɴ-05	7.44475ɴ-05
5.85197ɴ-05	6.30214ɴ-05
4.95582ɴ-05	5.33249ɴ-05
4.19513ɴ-05	4.51019ɴ-05
3.54942ɴ-05	3.81284ɴ-05
3.00197ɴ-05	3.22214ɴ-05
2.53773ɴ-05	2.72169ɴ-05
2.14454ɴ-05	2.29820ɴ-05
1.81144ɴ-05	1.93973ɴ-05
1.52955ɴ-05	1.63664ɴ-05
1.29097ɴ-05	1.38033ɴ-05
1.01756ɴ-05	1.08689ɴ-05
9.18663ɴ-06	9.80830ɴ-06
7.74553ɴ-06	8.26384ɴ-06
6.52787ɴ-06	6.95987ɴ-06
5.50005ɴ-06	5.86002ɴ-06
4.63224ɴ-06	4.93211ɴ-06
3.90030ɴ-06	4.15004ɴ-06
3.28279ɴ-06	3.49072ɴ-06
2.76221ɴ-06	2.93530ɴ-06

cont.
wo carbon atoms.

R.	$\langle pz1sI1spz\rangle$	$\langle pz2sI2spz\rangle$	$\langle pzpxIpxpz\rangle$
12.750	$2.40190_{10}-06$	$2.37143_{10}-06$	$2.32342_{10}-06$
12.875	$2.01876_{10}-06$	$1.99380_{10}-06$	$1.95385_{10}-06$
13.000	$1.69637_{10}-06$	$1.67577_{10}-06$	$1.64254_{10}-06$
13.125	$1.42505_{10}-06$	$1.40805_{10}-06$	$1.38042_{10}-06$
13.250	$1.19672_{10}-06$	$1.18266_{10}-06$	$1.15979_{10}-06$
13.375	$1.00484_{10}-06$	$9.93268_{10}-07$	$9.74168_{10}-07$
13.500	$8.43446_{10}-07$	$8.33897_{10}-07$	$8.18023_{10}-07$
13.625	$7.07786_{10}-07$	$6.99911_{10}-07$	$6.86721_{10}-07$
13.750	$5.93808_{10}-07$	$5.87303_{10}-07$	$5.76344_{10}-07$
13.875	$4.98041_{10}-07$	$4.92682_{10}-07$	$4.83580_{10}-07$
14.000	$4.17621_{10}-07$	$4.13204_{10}-07$	$4.05645_{10}-07$
14.125	$3.50103_{10}-07$	$3.46461_{10}-07$	$3.40186_{10}-07$
14.250	$2.93431_{10}-07$	$2.90429_{10}-07$	$2.85219_{10}-07$
14.375	$2.45875_{10}-07$	$2.43400_{10}-07$	$2.39076_{10}-07$
14.500	$2.05979_{10}-07$	$2.03989_{10}-07$	$2.00351_{10}-07$
14.625	$1.72518_{10}-07$	$1.70836_{10}-07$	$1.67859_{10}-07$
14.750	$1.44460_{10}-07$	$1.43075_{10}-07$	$1.40605_{10}-07$
14.875	$1.20939_{10}-07$	$1.19789_{10}-07$	$1.17749_{10}-07$
15.000	$1.01227_{10}-07$	$1.00286_{10}-07$	$9.85873_{10}-08$
15.125	$8.47092_{10}-08$	$8.39339_{10}-08$	$8.25256_{10}-08$
15.250	$7.08722_{10}-08$	$7.02335_{10}-08$	$6.90660_{10}-08$
15.375	$5.92833_{10}-08$	$5.87572_{10}-08$	$5.77895_{10}-08$
15.500	$4.95795_{10}-08$	$4.91462_{10}-08$	$4.83442_{10}-08$
15.625	$3.85901_{10}-08$	$3.82599_{10}-08$	$3.76436_{10}-08$
15.750	$3.46566_{10}-08$	$3.43627_{10}-08$	$3.38121_{10}-08$
15.875	$2.89670_{10}-08$	$2.87249_{10}-08$	$2.82689_{10}-08$
16.000	$2.42069_{10}-08$	$2.40076_{10}-08$	$2.36298_{10}-08$

Table(A1.1)
Hybrid integrals between tu

⟨pzpy|pypz⟩	⟨pzpz|pzpz⟩
$2.32342_{10}-06$	$2.46747_{10}-06$
$1.95385_{10}-06$	$2.07370_{10}-06$
$1.64254_{10}-06$	$1.74223_{10}-06$
$1.38042_{10}-06$	$1.46332_{10}-06$
$1.15979_{10}-06$	$1.22862_{10}-06$
$9.74168_{10}-07$	$1.03147_{10}-06$
$8.18023_{10}-07$	$8.65646_{10}-07$
$6.86721_{10}-07$	$7.26293_{10}-07$
$5.76344_{10}-07$	$6.09219_{10}-07$
$4.83580_{10}-07$	$5.10886_{10}-07$
$4.05645_{10}-07$	$4.28321_{10}-07$
$3.40186_{10}-07$	$3.59013_{10}-07$
$2.85219_{10}-07$	$3.00848_{10}-07$
$2.39076_{10}-07$	$2.52048_{10}-07$
$2.00351_{10}-07$	$2.11115_{10}-07$
$1.67859_{10}-07$	$1.76790_{10}-07$
$1.40605_{10}-07$	$1.48014_{10}-07$
$1.17749_{10}-07$	$1.23894_{10}-07$
$9.85873_{10}-08$	$1.03683_{10}-07$
$8.25256_{10}-08$	$8.67505_{10}-08$
$6.90660_{10}-08$	$7.25684_{10}-08$
$5.77895_{10}-08$	$6.06926_{10}-08$
$4.83442_{10}-08$	$5.07501_{10}-08$
$3.76436_{10}-08$	$3.94926_{10}-08$
$3.38121_{10}-08$	$3.54638_{10}-08$
$2.82689_{10}-08$	$2.96371_{10}-08$
$2.36298_{10}-08$	$2.47631_{10}-08$

cont.
wo carbon atoms.

R.	$\langle py1sI1spy\rangle$	$\langle py2sI2spy\rangle$
4.500	1.01091×10^{-02}	9.49067×10^{-03}
4.625	8.51863×10^{-03}	8.01135×10^{-03}
4.750	7.17150×10^{-03}	6.75550×10^{-03}
4.875	6.03190×10^{-03}	5.69083×10^{-03}
5.000	5.06896×10^{-03}	4.78939×10^{-03}
5.125	4.25619×10^{-03}	4.02708×10^{-03}
5.250	3.57088×10^{-03}	3.38317×10^{-03}
5.375	2.99363×10^{-03}	2.83986×10^{-03}
5.500	2.50785×10^{-03}	2.38190×10^{-03}
5.625	2.09942×10^{-03}	1.99627×10^{-03}
5.750	1.75633×10^{-03}	1.67187×10^{-03}
5.875	1.46839×10^{-03}	1.39923×10^{-03}
6.000	1.22692×10^{-03}	1.17027×10^{-03}
6.125	1.02451×10^{-03}	9.78131×10^{-04}
6.250	8.54967×10^{-04}	8.17019×10^{-04}
6.375	7.13094×10^{-04}	6.82043×10^{-04}
6.500	5.94456×10^{-04}	5.69046×10^{-04}
6.625	4.95296×10^{-04}	4.74506×10^{-04}
6.750	4.12472×10^{-04}	3.95464×10^{-04}
6.875	3.43332×10^{-04}	3.29420×10^{-04}
7.000	2.85651×10^{-04}	2.74271×10^{-04}
7.125	2.37554×10^{-04}	2.28246×10^{-04}
7.250	1.97470×10^{-04}	1.89858×10^{-04}
7.375	1.64079×10^{-04}	1.57854×10^{-04}
7.500	1.36278×10^{-04}	1.31189×10^{-04}
7.625	1.13145×10^{-04}	1.08984×10^{-04}
7.750	9.39047×10^{-05}	9.05029×10^{-05}
7.875	7.79072×10^{-05}	7.51260×10^{-05}
8.000	6.46120×10^{-05}	6.23383×10^{-05}
8.125	5.35672×10^{-05}	5.17084×10^{-05}
8.250	4.43959×10^{-05}	4.28764×10^{-05}
8.375	3.67828×10^{-05}	3.55407×10^{-05}
8.500	3.04658×10^{-05}	2.94505×10^{-05}

Hybrid integrals between carbon and

$\langle pypx|pxpy\rangle$	$\langle pypy|pypy\rangle$	$\langle pypz|pzpy\rangle$
9.12706×10^{-03}	9.71645×10^{-03}	9.62849×10^{-03}
7.70762×10^{-03}	8.19734×10^{-03}	8.12906×10^{-03}
6.50205×10^{-03}	6.90865×10^{-03}	6.85579×10^{-03}
5.47953×10^{-03}	5.81688×10^{-03}	5.77607×10^{-03}
4.61339×10^{-03}	4.89310×10^{-03}	4.86168×10^{-03}
3.88060×10^{-03}	4.11238×10^{-03}	4.08826×10^{-03}
3.26135×10^{-03}	3.45330×10^{-03}	3.43485×10^{-03}
2.73862×10^{-03}	2.89750×10^{-03}	2.88344×10^{-03}
2.29783×10^{-03}	2.42927×10^{-03}	2.41860×10^{-03}
1.92651×10^{-03}	2.03519×10^{-03}	2.02713×10^{-03}
1.61401×10^{-03}	1.70383×10^{-03}	1.69778×10^{-03}
1.35126×10^{-03}	1.42547×10^{-03}	1.42095×10^{-03}
1.13053×10^{-03}	1.19181×10^{-03}	1.18846×10^{-03}
9.45226×10^{-04}	9.95808×10^{-04}	9.93350×10^{-04}
7.89791×10^{-04}	8.31523×10^{-04}	8.29743×10^{-04}
6.59521×10^{-04}	6.93941×10^{-04}	6.92668×10^{-04}
5.50424×10^{-04}	5.78805×10^{-04}	5.77909×10^{-04}
4.59116×10^{-04}	4.82509×10^{-04}	4.81894×10^{-04}
3.82749×10^{-04}	4.02026×10^{-04}	4.01617×10^{-04}
3.18919×10^{-04}	3.34799×10^{-04}	3.34540×10^{-04}
2.65603×10^{-04}	2.78680×10^{-04}	2.78529×10^{-04}
2.21093×10^{-04}	2.31860×10^{-04}	2.31785×10^{-04}
1.83957×10^{-04}	1.92820×10^{-04}	1.92797×10^{-04}
1.52988×10^{-04}	1.60282×10^{-04}	1.60294×10^{-04}
1.27178×10^{-04}	1.33178×10^{-04}	1.33214×10^{-04}
1.05678×10^{-04}	1.10613×10^{-04}	1.10663×10^{-04}
8.77786×10^{-05}	9.18367×10^{-05}	9.18934×10^{-05}
7.28818×10^{-05}	7.62182×10^{-05}	7.62775×10^{-05}
6.04903×10^{-05}	6.32328×10^{-05}	6.32917×10^{-05}
5.01870×10^{-05}	5.24410×10^{-05}	5.24974×10^{-05}
4.16241×10^{-05}	4.34762×10^{-05}	4.35290×10^{-05}
3.45102×10^{-05}	3.60318×10^{-05}	3.60803×10^{-05}
2.86027×10^{-05}	2.98525×10^{-05}	2.98965×10^{-05}

Table(A1.2)
nitrogen atoms with the potential due to the former.

R.	$\langle py1sI1spy \rangle$	$\langle py2sI2spy \rangle$
8.625	$2.52259_{10}-05$	$2.43961_{10}-05$
8.750	$2.08811_{10}-05$	$2.02030_{10}-05$
8.875	$1.72795_{10}-05$	$1.67254_{10}-05$
9.000	$1.42951_{10}-05$	$1.38423_{10}-05$
9.125	$1.18231_{10}-05$	$1.14530_{10}-05$
9.250	$9.77610_{10}-06$	$9.47369_{10}-06$
9.375	$8.08141_{10}-06$	$7.83427_{10}-06$
9.500	$6.67883_{10}-06$	$6.47689_{10}-06$
9.625	$5.51833_{10}-06$	$5.35333_{10}-06$
9.750	$4.55844_{10}-06$	$4.42362_{10}-06$
9.875	$3.76464_{10}-06$	$3.65448_{10}-06$
10.000	$3.10840_{10}-06$	$3.01839_{10}-06$
10.125	$2.56598_{10}-06$	$2.49244_{10}-06$
10.250	$2.11778_{10}-06$	$2.05770_{10}-06$
10.375	$1.74749_{10}-06$	$1.69841_{10}-06$
10.500	$1.44166_{10}-06$	$1.40157_{10}-06$
10.625	$1.18912_{10}-06$	$1.15637_{10}-06$
10.750	$9.80650_{10}-07$	$9.53896_{10}-07$
10.875	$8.08570_{10}-07$	$7.86714_{10}-07$
11.000	$6.66569_{10}-07$	$6.48715_{10}-07$
11.125	$5.49407_{10}-07$	$5.34822_{10}-07$
11.250	$4.52764_{10}-07$	$4.40850_{10}-07$
11.375	$3.73056_{10}-07$	$3.63324_{10}-07$
11.500	$3.07333_{10}-07$	$2.99383_{10}-07$
11.625	$2.53148_{10}-07$	$2.46654_{10}-07$
11.750	$2.08482_{10}-07$	$2.03179_{10}-07$
11.875	$1.71659_{10}-07$	$1.67335_{10}-07$
12.000	$1.41314_{10}-07$	$1.37792_{10}-07$
12.125	$1.16324_{10}-07$	$1.13450_{10}-07$
12.250	$9.57488_{10}-08$	$9.33987_{10}-08$
12.375	$7.87992_{10}-08$	$7.68789_{10}-08$
12.500	$6.48396_{10}-08$	$6.32720_{10}-08$
12.625	$5.33463_{10}-08$	$5.20662_{10}-08$

Hybrid integrals between carbon and

$\langle pypx|I|pxpy\rangle$	$\langle pypy|I|pypy\rangle$	$\langle pypz|I|pzpy\rangle$
2.36987×10^{-05}	2.47251×10^{-05}	2.47645×10^{-05}
1.96294×10^{-05}	2.04723×10^{-05}	2.05072×10^{-05}
1.62537×10^{-05}	1.69458×10^{-05}	1.69765×10^{-05}
1.34546×10^{-05}	1.40227×10^{-05}	1.40496×10^{-05}
1.11344×10^{-05}	1.16006×10^{-05}	1.16241×10^{-05}
9.21183×10^{-06}	9.59448×10^{-06}	9.61476×10^{-06}
7.61912×10^{-06}	7.93311×10^{-06}	7.95059×10^{-06}
6.30014×10^{-06}	6.55776×10^{-06}	6.57278×10^{-06}
5.20815×10^{-06}	5.41949×10^{-06}	5.43235×10^{-06}
4.30439×10^{-06}	4.47774×10^{-06}	4.48872×10^{-06}
3.55658×10^{-06}	3.69875×10^{-06}	3.70810×10^{-06}
2.93801×10^{-06}	3.05461×10^{-06}	3.06255×10^{-06}
2.42646×10^{-06}	2.52207×10^{-06}	2.52880×10^{-06}
2.00354×10^{-06}	2.08194×10^{-06}	2.08763×10^{-06}
1.65396×10^{-06}	1.71823×10^{-06}	1.72304×10^{-06}
1.36509×10^{-06}	1.41778×10^{-06}	1.42184×10^{-06}
1.12644×10^{-06}	1.16963×10^{-06}	1.17305×10^{-06}
9.29343×10^{-07}	9.64737×10^{-07}	9.67607×10^{-07}
7.66574×10^{-07}	7.95581×10^{-07}	7.97988×10^{-07}
6.32195×10^{-07}	6.55966×10^{-07}	6.57985×10^{-07}
5.21274×10^{-07}	5.40751×10^{-07}	5.42443×10^{-07}
4.29740×10^{-07}	4.45698×10^{-07}	4.47113×10^{-07}
3.54214×10^{-07}	3.67288×10^{-07}	3.68471×10^{-07}
2.91914×10^{-07}	3.02624×10^{-07}	3.03612×10^{-07}
2.40530×10^{-07}	2.49303×10^{-07}	2.50127×10^{-07}
1.98159×10^{-07}	2.05345×10^{-07}	2.06032×10^{-07}
1.63220×10^{-07}	1.69106×10^{-07}	1.69678×10^{-07}
1.34419×10^{-07}	1.39239×10^{-07}	1.39716×10^{-07}
1.10686×10^{-07}	1.14633×10^{-07}	1.15030×10^{-07}
9.11341×10^{-08}	9.43661×10^{-08}	9.46960×10^{-08}
7.50235×10^{-08}	7.76698×10^{-08}	7.79439×10^{-08}
6.17516×10^{-08}	6.39184×10^{-08}	6.41460×10^{-08}
5.08205×10^{-08}	5.25945×10^{-08}	5.27834×10^{-08}

Table(A1.2) cont.
nitrogen atoms with the potential due to the former.

R.	$\langle py1sI1spy \rangle$	$\langle py2sI2spy \rangle$
12.750	$4.38853_{10}-08$	$4.28397_{10}-08$
12.875	$3.60973_{10}-08$	$3.52433_{10}-08$
13.000	$2.96879_{10}-08$	$2.89905_{10}-08$
13.125	$2.44134_{10}-08$	$2.38439_{10}-08$
13.250	$2.00738_{10}-08$	$1.96087_{10}-08$
13.375	$1.65035_{10}-08$	$1.61237_{10}-08$
13.500	$1.35668_{10}-08$	$1.32566_{10}-08$
13.625	$1.11514_{10}-08$	$1.08981_{10}-08$
13.750	$9.16507_{10}-09$	$8.95824_{10}-09$
13.875	$7.53173_{10}-09$	$7.36284_{10}-09$
14.000	$6.18889_{10}-09$	$6.05096_{10}-09$
14.125	$5.08489_{10}-09$	$4.97226_{10}-09$
14.250	$4.17748_{10}-09$	$4.08550_{10}-09$
14.375	$3.43178_{10}-09$	$3.35660_{10}-09$
14.500	$2.81902_{10}-09$	$2.75753_{10}-09$
14.625	$2.31533_{10}-09$	$2.26509_{10}-09$
14.750	$1.90138_{10}-09$	$1.86038_{10}-09$
14.875	$1.56131_{10}-09$	$1.52784_{10}-09$
15.000	$1.28199_{10}-09$	$1.25465_{10}-09$
15.125	$1.05254_{10}-09$	$1.03021_{10}-09$
15.250	$8.64080_{10}-10$	$8.45850_{10}-10$
15.375	$7.09309_{10}-10$	$6.94428_{10}-10$
15.500	$5.82200_{10}-10$	$5.70054_{10}-10$
15.625	$4.77817_{10}-10$	$4.67899_{10}-10$
15.750	$3.92164_{10}-10$	$3.84059_{10}-10$
15.875	$3.22117_{10}-10$	$3.15497_{10}-10$
16.000	$2.65417_{10}-10$	$2.60050_{10}-10$

Hybrid integrals between carbon and

⟨pypxIpxpy⟩	⟨pypyIpypy⟩	⟨pypzIpzpy⟩
4.18192×10^{-08}	4.32716×10^{-08}	4.34282×10^{-08}
3.44073×10^{-08}	3.55963×10^{-08}	3.57262×10^{-08}
2.83057×10^{-08}	2.92790×10^{-08}	2.93866×10^{-08}
2.32830×10^{-08}	2.40797×10^{-08}	2.41688×10^{-08}
1.91494×10^{-08}	1.98015×10^{-08}	1.98752×10^{-08}
1.57476×10^{-08}	1.62813×10^{-08}	1.63423×10^{-08}
1.29486×10^{-08}	1.33854×10^{-08}	1.34359×10^{-08}
1.06458×10^{-08}	1.10033×10^{-08}	1.10451×10^{-08}
8.75171×10^{-09}	9.04424×10^{-09}	9.07876×10^{-09}
7.19374×10^{-09}	7.43312×10^{-09}	7.46164×10^{-09}
5.91252×10^{-09}	6.10840×10^{-09}	6.13196×10^{-09}
4.85893×10^{-09}	5.01920×10^{-09}	5.03866×10^{-09}
3.99272×10^{-09}	4.12386×10^{-09}	4.13992×10^{-09}
3.28065×10^{-09}	3.38795×10^{-09}	3.40119×10^{-09}
2.69536×10^{-09}	2.78316×10^{-09}	2.79407×10^{-09}
2.21420×10^{-09}	2.28604×10^{-09}	2.29503×10^{-09}
1.81873×10^{-09}	1.87750×10^{-09}	1.88492×10^{-09}
1.49375×10^{-09}	1.54183×10^{-09}	1.54795×10^{-09}
1.22676×10^{-09}	1.26608×10^{-09}	1.27112×10^{-09}
1.00738×10^{-09}	1.03955×10^{-09}	1.04370×10^{-09}
8.27167×10^{-10}	8.53480×10^{-10}	8.56903×10^{-10}
6.79137×10^{-10}	7.00662×10^{-10}	7.03483×10^{-10}
5.57545×10^{-10}	5.75148×10^{-10}	5.77470×10^{-10}
4.57672×10^{-10}	4.72061×10^{-10}	4.73970×10^{-10}
3.75685×10^{-10}	3.87460×10^{-10}	3.89033×10^{-10}
3.08570×10^{-10}	3.18283×10^{-10}	3.19600×10^{-10}
2.54125×10^{-10}	2.62352×10^{-10}	2.63516×10^{-10}

Table(A1.2) cont.
nitrogen atoms with the potential due to the former.

R.	$\langle pz1sI1spz\rangle$	$\langle pz2sI2spz\rangle$
4.500	5.19896×10^{-2}	4.82109×10^{-2}
4.625	4.55729×10^{-2}	4.23680×10^{-2}
4.750	3.98520×10^{-2}	3.71376×10^{-2}
4.875	3.47703×10^{-2}	3.24744×10^{-2}
5.000	3.02720×10^{-2}	2.83323×10^{-2}
5.125	2.63026×10^{-2}	2.46657×10^{-2}
5.250	2.28103×10^{-2}	2.14303×10^{-2}
5.375	1.97460×10^{-2}	1.85837×10^{-2}
5.500	1.70641×10^{-2}	1.60861×10^{-2}
5.625	1.47226×10^{-2}	1.39005×10^{-2}
5.750	1.26828×10^{-2}	1.19924×10^{-2}
5.875	1.09097×10^{-2}	1.03302×10^{-2}
6.000	9.37130×10^{-3}	8.88528×10^{-3}
6.125	8.03908×10^{-3}	7.63173×10^{-3}
6.250	6.88740×10^{-3}	6.54626×10^{-3}
6.375	5.89353×10^{-3}	5.60801×10^{-3}
6.500	5.03721×10^{-3}	4.79838×10^{-3}
6.625	4.30052×10^{-3}	4.10084×10^{-3}
6.750	3.66760×10^{-3}	3.50078×10^{-3}
6.875	3.12447×10^{-3}	2.98532×10^{-3}
7.000	2.65911×10^{-3}	2.54314×10^{-3}
7.125	2.26111×10^{-3}	2.16431×10^{-3}
7.250	1.92105×10^{-3}	1.84017×10^{-3}
7.375	1.63060×10^{-3}	1.56314×10^{-3}
7.500	1.38281×10^{-3}	1.32665×10^{-3}
7.625	1.17175×10^{-3}	1.12499×10^{-3}
7.750	9.92145×10^{-4}	9.53212×10^{-4}
7.875	8.39427×10^{-4}	8.07027×10^{-4}
8.000	7.09693×10^{-4}	6.82743×10^{-4}
8.125	5.99587×10^{-4}	5.77177×10^{-4}
8.250	5.06218×10^{-4}	4.87589×10^{-4}
8.375	4.27106×10^{-4}	4.11626×10^{-4}
8.500	3.60129×10^{-4}	3.47268×10^{-4}

Hybrid integrals between carbon and

$\langle pzpxIpxpz\rangle$	$\langle pzpyIpypz\rangle$	$\langle pzpzIpzpz\rangle$
$4.62261_{10}-02$	$4.62261_{10}-02$	$5.21805_{10}-02$
$4.06440_{10}-02$	$4.06440_{10}-02$	$4.58222_{10}-02$
$3.56439_{10}-02$	$3.56439_{10}-02$	$4.01251_{10}-02$
$3.11832_{10}-02$	$3.11832_{10}-02$	$3.50517_{10}-02$
$2.72187_{10}-02$	$2.72187_{10}-02$	$3.05540_{10}-02$
$2.37073_{10}-02$	$2.37073_{10}-02$	$2.65798_{10}-02$
$2.06070_{10}-02$	$2.06070_{10}-02$	$2.30770_{10}-02$
$1.78778_{10}-02$	$1.78778_{10}-02$	$1.99967_{10}-02$
$1.54819_{10}-02$	$1.54819_{10}-02$	$1.72950_{10}-02$
$1.33840_{10}-02$	$1.33840_{10}-02$	$1.49334_{10}-02$
$1.15515_{10}-02$	$1.15515_{10}-02$	$1.28740_{10}-02$
$9.95448_{10}-03$	$9.95448_{10}-03$	$1.10815_{10}-02$
$8.56558_{10}-03$	$8.56558_{10}-03$	$9.52469_{10}-03$
$7.36002_{10}-03$	$7.36002_{10}-03$	$8.17523_{10}-03$
$6.31557_{10}-03$	$6.31557_{10}-03$	$7.00765_{10}-03$
$5.41238_{10}-03$	$5.41238_{10}-03$	$5.99927_{10}-03$
$4.63267_{10}-03$	$4.63267_{10}-03$	$5.12981_{10}-03$
$3.96062_{10}-03$	$3.96062_{10}-03$	$4.38130_{10}-03$
$3.38224_{10}-03$	$3.38224_{10}-03$	$3.73787_{10}-03$
$2.88520_{10}-03$	$2.88520_{10}-03$	$3.18557_{10}-03$
$2.45865_{10}-03$	$2.45865_{10}-03$	$2.71212_{10}-03$
$2.09308_{10}-03$	$2.09308_{10}-03$	$2.30679_{10}-03$
$1.78016_{10}-03$	$1.78016_{10}-03$	$1.96019_{10}-03$
$1.51263_{10}-03$	$1.51263_{10}-03$	$1.66417_{10}-03$
$1.28416_{10}-03$	$1.28416_{10}-03$	$1.41164_{10}-03$
$1.08927_{10}-03$	$1.08927_{10}-03$	$1.19643_{10}-03$
$9.23207_{10}-04$	$9.23207_{10}-04$	$1.01322_{10}-03$
$7.81839_{10}-04$	$7.81839_{10}-04$	$8.57401_{10}-04$
$6.61612_{10}-04$	$6.61612_{10}-04$	$7.25004_{10}-04$
$5.59460_{10}-04$	$5.59460_{10}-04$	$6.12610_{10}-04$
$4.72743_{10}-04$	$4.72743_{10}-04$	$5.17280_{10}-04$
$3.99192_{10}-04$	$3.99192_{10}-04$	$4.36491_{10}-04$
$3.36861_{10}-04$	$3.36861_{10}-04$	$3.68082_{10}-04$

Table(A1.2) cont.
nitrogen atoms with the potential due to the former.

R.	$\langle pz1s I1spz\rangle$	$\langle pz2s I2spz\rangle$
8.625	$3.03467_{\mathrm{D}}-04$	$2.92786_{\mathrm{D}}-04$
8.750	$2.55567_{\mathrm{D}}-04$	$2.46699_{\mathrm{D}}-04$
8.875	$2.15102_{\mathrm{D}}-04$	$2.07742_{\mathrm{D}}-04$
9.000	$1.80942_{\mathrm{D}}-04$	$1.74836_{\mathrm{D}}-04$
9.125	$1.52125_{\mathrm{D}}-04$	$1.47060_{\mathrm{D}}-04$
9.250	$1.27830_{\mathrm{D}}-04$	$1.23629_{\mathrm{D}}-04$
9.375	$1.07360_{\mathrm{D}}-04$	$1.03877_{\mathrm{D}}-04$
9.500	$9.01233_{\mathrm{D}}-05$	$8.72358_{\mathrm{D}}-05$
9.625	$7.56172_{\mathrm{D}}-05$	$7.32243_{\mathrm{D}}-05$
9.750	$6.34164_{\mathrm{D}}-05$	$6.14337_{\mathrm{D}}-05$
9.875	$5.31598_{\mathrm{D}}-05$	$5.15175_{\mathrm{D}}-05$
10.000	$4.45424_{\mathrm{D}}-05$	$4.31823_{\mathrm{D}}-05$
10.125	$3.73058_{\mathrm{D}}-05$	$3.61796_{\mathrm{D}}-05$
10.250	$3.12319_{\mathrm{D}}-05$	$3.02996_{\mathrm{D}}-05$
10.375	$2.61361_{\mathrm{D}}-05$	$2.53645_{\mathrm{D}}-05$
10.500	$2.18631_{\mathrm{D}}-05$	$2.12246_{\mathrm{D}}-05$
10.625	$1.82816_{\mathrm{D}}-05$	$1.77534_{\mathrm{D}}-05$
10.750	$1.52812_{\mathrm{D}}-05$	$1.48442_{\mathrm{D}}-05$
10.875	$1.27685_{\mathrm{D}}-05$	$1.24071_{\mathrm{D}}-05$
11.000	$1.06652_{\mathrm{D}}-05$	$1.03663_{\mathrm{D}}-05$
11.125	$8.90521_{\mathrm{D}}-06$	$8.65808_{\mathrm{D}}-06$
11.250	$7.43314_{\mathrm{D}}-06$	$7.22886_{\mathrm{D}}-06$
11.375	$6.20235_{\mathrm{D}}-06$	$6.03351_{\mathrm{D}}-06$
11.500	$5.17372_{\mathrm{D}}-06$	$5.03419_{\mathrm{D}}-06$
11.625	$4.31432_{\mathrm{D}}-06$	$4.19903_{\mathrm{D}}-06$
11.750	$3.59656_{\mathrm{D}}-06$	$3.50132_{\mathrm{D}}-06$
11.875	$2.99720_{\mathrm{D}}-06$	$2.91860_{\mathrm{D}}-06$
12.000	$2.49696_{\mathrm{D}}-06$	$2.43213_{\mathrm{D}}-06$
12.125	$2.07968_{\mathrm{D}}-06$	$2.02617_{\mathrm{D}}-06$
12.250	$1.73173_{\mathrm{D}}-06$	$1.68753_{\mathrm{D}}-06$
12.375	$1.44157_{\mathrm{D}}-06$	$1.40508_{\mathrm{D}}-06$
12.500	$1.19970_{\mathrm{D}}-06$	$1.16958_{\mathrm{D}}-06$
12.625	$9.98153_{\mathrm{D}}-07$	$9.73294_{\mathrm{D}}-07$

Hybrid integrals between carbon and

⟨pzpxIpxpz⟩	⟨pzpyIpypz⟩	⟨pzpzIpzpz⟩
2.84079D-04	2.84079D-04	3.10199D-04
2.39419D-04	2.39419D-04	2.61260D-04
2.01658D-04	2.01658D-04	2.19912D-04
1.69753D-04	1.69753D-04	1.85002D-04
1.42815D-04	1.42815D-04	1.55549D-04
1.20086D-04	1.20086D-04	1.30715D-04
1.00921D-04	1.00921D-04	1.09789D-04
8.47707D-05	8.47707D-05	9.21662D-05
7.11692D-05	7.11692D-05	7.73345D-05
5.97211D-05	5.97211D-05	6.48590D-05
5.00908D-05	5.00908D-05	5.43709D-05
4.19942D-05	4.19942D-05	4.55585D-05
3.51906D-05	3.51906D-05	3.81577D-05
2.94765D-05	2.94765D-05	3.19457D-05
2.46797D-05	2.46797D-05	2.67339D-05
2.06551D-05	2.06551D-05	2.23635D-05
1.72799D-05	1.72799D-05	1.87005D-05
1.44507D-05	1.44507D-05	1.56313D-05
1.20801D-05	1.20801D-05	1.30593D-05
1.00946D-05	1.00946D-05	1.09060D-05
8.43244D-06	8.43244D-06	9.10681D-06
7.04156D-06	7.04156D-06	7.60346D-06
5.87806D-06	5.87806D-06	6.34506D-06
4.90518D-06	4.90518D-06	5.29222D-06
4.09199D-06	4.09199D-06	4.41295D-06
3.41253D-06	3.41253D-06	3.67888D-06
2.84497D-06	2.84497D-06	3.06586D-06
2.37109D-06	2.37109D-06	2.55421D-06
1.97558D-06	1.97558D-06	2.12737D-06
1.64560D-06	1.64560D-06	1.77139D-06
1.37034D-06	1.37034D-06	1.47456D-06
1.14080D-06	1.14080D-06	1.22714D-06
9.49457D-07	9.49457D-07	1.02097D-06

Table(A1.2) cont.
nitrogen atoms with the potential due to the former.

R.	$\langle pz1sI1spz\rangle$	$\langle pz2sI2spz\rangle$	$\langle pzpxIpxpz\rangle$
12.750	8.30262×10^{-07}	8.09745×10^{-07}	7.90007×10^{-07}
12.875	6.90434×10^{-07}	6.73504×10^{-07}	6.57163×10^{-07}
13.000	5.74016×10^{-07}	5.60048×10^{-07}	5.46522×10^{-07}
13.125	4.77113×10^{-07}	4.65590×10^{-07}	4.54396×10^{-07}
13.250	3.96479×10^{-07}	3.86974×10^{-07}	3.77711×10^{-07}
13.375	3.29399×10^{-07}	3.21556×10^{-07}	3.13892×10^{-07}
13.500	2.73610×10^{-07}	2.67137×10^{-07}	2.60798×10^{-07}
13.625	2.27214×10^{-07}	2.21878×10^{-07}	2.16635×10^{-07}
13.750	1.88643×10^{-07}	1.84247×10^{-07}	1.79912×10^{-07}
13.875	1.56588×10^{-07}	1.52965×10^{-07}	1.49381×10^{-07}
14.000	1.29956×10^{-07}	1.26969×10^{-07}	1.24006×10^{-07}
14.125	1.07831×10^{-07}	1.05638×10^{-07}	1.02919×10^{-07}
14.250	8.94552×10^{-08}	8.74257×10^{-08}	8.54015×10^{-08}
14.375	7.41970×10^{-08}	7.25242×10^{-08}	7.08515×10^{-08}
14.500	6.15304×10^{-08}	6.01516×10^{-08}	5.87697×10^{-08}
14.625	5.10160×10^{-08}	4.98798×10^{-08}	4.87383×10^{-08}
14.750	4.22904×10^{-08}	4.13544×10^{-08}	4.04115×10^{-08}
14.875	3.50509×10^{-08}	3.42798×10^{-08}	3.35011×10^{-08}
15.000	2.90459×10^{-08}	2.84107×10^{-08}	2.77677×10^{-08}
15.125	2.40654×10^{-08}	2.35422×10^{-08}	2.30106×10^{-08}
15.250	1.99356×10^{-08}	1.95048×10^{-08}	1.90665×10^{-08}
15.375	1.65119×10^{-08}	1.61571×10^{-08}	1.57974×10^{-08}
15.500	1.36739×10^{-08}	1.33816×10^{-08}	1.30830×10^{-08}
15.625	1.13216×10^{-08}	1.10808×10^{-08}	1.08118×10^{-08}
15.750	9.37294×10^{-09}	9.17482×10^{-09}	8.87146×10^{-09}
15.875	7.76202×10^{-09}	7.60041×10^{-09}	7.13893×10^{-09}
16.000	6.43899×10^{-09}	6.31055×10^{-09}	5.47032×10^{-09}

Table(A1.2)

Hybrid integrals between carbon and nitrogen atoms

$\langle pzpy|pypz\rangle$	$\langle pzpz|pzpz\rangle$
$7.90007_{10}-07$	$8.49219_{10}-07$
$6.57163_{10}-07$	$7.06184_{10}-07$
$5.46522_{10}-07$	$5.87101_{10}-07$
$4.54396_{10}-07$	$4.87980_{10}-07$
$3.77711_{10}-07$	$4.05500_{10}-07$
$3.13892_{10}-07$	$3.36883_{10}-07$
$2.60798_{10}-07$	$2.79815_{10}-07$
$2.16635_{10}-07$	$2.32363_{10}-07$
$1.79912_{10}-07$	$1.92918_{10}-07$
$1.49381_{10}-07$	$1.60134_{10}-07$
$1.24006_{10}-07$	$1.32895_{10}-07$
$1.02919_{10}-07$	$1.10267_{10}-07$
$8.54015_{10}-08$	$9.14740_{10}-08$
$7.08515_{10}-08$	$7.58694_{10}-08$
$5.87697_{10}-08$	$6.29154_{10}-08$
$4.87383_{10}-08$	$5.21630_{10}-08$
$4.04115_{10}-08$	$4.32403_{10}-08$
$3.35011_{10}-08$	$3.58373_{10}-08$
$2.77677_{10}-08$	$2.96968_{10}-08$
$2.30106_{10}-08$	$2.46041_{10}-08$
$1.90665_{10}-08$	$2.03814_{10}-08$
$1.57974_{10}-08$	$1.68807_{10}-08$
$1.30830_{10}-08$	$1.39789_{10}-08$
$1.08118_{10}-08$	$1.15737_{10}-08$
$8.87146_{10}-09$	$9.58154_{10}-09$
$7.13893_{10}-09$	$7.93589_{10}-09$
$5.47032_{10}-09$	$6.58737_{10}-09$

cont.
with the potential due to the former.

R.	$\langle py1sI1spy \rangle$	$\langle py2sI2spy \rangle$
4.500	$8.03655_{10}-03$	$7.67670_{10}-03$
4.625	$6.72069_{10}-03$	$6.43589_{10}-03$
4.750	$5.61494_{10}+02$	$5.38960_{10}-03$
4.875	$4.68682_{10}-03$	$4.50862_{10}-03$
5.000	$3.90867_{10}-03$	$3.76784_{10}-03$
5.125	$3.25700_{10}-03$	$3.14575_{10}-03$
5.250	$2.71184_{10}-03$	$2.62396_{10}-03$
5.375	$2.25625_{10}-03$	$2.18682_{10}-03$
5.500	$1.87584_{10}-03$	$1.82099_{10}-03$
5.625	$1.55842_{10}-03$	$1.51516_{10}-03$
5.750	$1.29380_{10}-03$	$1.25973_{10}-03$
5.875	$1.07346_{10}-03$	$1.04660_{10}-03$
6.000	$8.90120_{10}-04$	$8.68932_{10}-04$
6.125	$7.37647_{10}-04$	$7.20943_{10}-04$
6.250	$6.10937_{10}-04$	$5.97779_{10}-04$
6.375	$5.05717_{10}-04$	$4.95352_{10}-04$
6.500	$4.18402_{10}-04$	$4.10237_{10}-04$
6.625	$3.45985_{10}-04$	$3.39556_{10}-04$
6.750	$2.85964_{10}-04$	$2.80902_{10}-04$
6.875	$2.36243_{10}-04$	$2.32259_{10}-04$
7.000	$1.95080_{10}-04$	$1.91944_{10}-04$
7.125	$1.61018_{10}-04$	$1.58551_{10}-04$
7.250	$1.32849_{10}-04$	$1.30907_{10}-04$
7.375	$1.09563_{10}-04$	$1.08035_{10}-04$
7.500	$9.03231_{10}-05$	$8.91214_{10}-05$
7.625	$7.44336_{10}-05$	$7.34885_{10}-05$
7.750	$6.13174_{10}-05$	$6.05741_{10}-05$
7.875	$5.04943_{10}-05$	$4.99098_{10}-05$
8.000	$4.15677_{10}-05$	$4.11081_{10}-05$
8.125	$3.42077_{10}-05$	$3.38464_{10}-05$
8.250	$2.81421_{10}-05$	$2.78581_{10}-05$
8.375	$2.31448_{10}-05$	$2.29215_{10}-05$
8.500	$1.90293_{10}-05$	$1.88538_{10}-05$

YQ

Hybrid integrals between carbon and

$\langle py px I px py\rangle$	$\langle py py I py py\rangle$	$\langle py pz I pz py\rangle$
$7.34628_{10}-03$	$7.69497_{10}-03$	$7.98886_{10}-03$
$6.08268_{10}-03$	$6.44677_{10}-03$	$6.69706_{10}-03$
$5.10601_{10}-03$	$5.39523_{10}-03$	$5.60759_{10}-03$
$4.30292_{10}-03$	$4.51062_{10}-03$	$4.69018_{10}-03$
$3.61735_{10}-03$	$3.76741_{10}-03$	$3.91876_{10}-03$
$3.02661_{10}-03$	$3.14376_{10}-03$	$3.27097_{10}-03$
$2.52316_{10}-03$	$2.62104_{10}-03$	$2.72769_{10}-03$
$2.10199_{10}-03$	$2.18340_{10}-03$	$2.27260_{10}-03$
$1.75376_{10}-03$	$1.81738_{10}-03$	$1.89182_{10}-03$
$1.46062_{10}-03$	$1.51157_{10}-03$	$1.57356_{10}-03$
$1.21506_{10}-03$	$1.25630_{10}-03$	$1.30782_{10}-03$
$1.01024_{10}-03$	$1.04341_{10}-03$	$1.08616_{10}-03$
$8.39358_{10}-04$	$8.66008_{10}-04$	$9.01431_{10}-04$
$6.96906_{10}-04$	$7.18310_{10}-04$	$7.47613_{10}-04$
$5.78256_{10}-04$	$5.95439_{10}-04$	$6.19641_{10}-04$
$4.79507_{10}-04$	$4.93293_{10}-04$	$5.13256_{10}-04$
$3.97386_{10}-04$	$4.08440_{10}-04$	$4.24886_{10}-04$
$3.29139_{10}-04$	$3.37998_{10}-04$	$3.51531_{10}-04$
$2.72463_{10}-04$	$2.79559_{10}-04$	$2.90683_{10}-04$
$2.25426_{10}-04$	$2.31107_{10}-04$	$2.40242_{10}-04$
$1.86415_{10}-04$	$1.90962_{10}-04$	$1.98455_{10}-04$
$1.54079_{10}-04$	$1.57716_{10}-04$	$1.63857_{10}-04$
$1.27292_{10}-04$	$1.30201_{10}-04$	$1.35228_{10}-04$
$1.05114_{10}-04$	$1.07439_{10}-04$	$1.11552_{10}-04$
$8.67621_{10}-05$	$8.86201_{10}-05$	$9.19819_{10}-05$
$7.15837_{10}-05$	$7.30678_{10}-05$	$7.58138_{10}-05$
$5.90369_{10}-05$	$6.02220_{10}-05$	$6.24633_{10}-05$
$4.86698_{10}-05$	$4.96158_{10}-05$	$5.14439_{10}-05$
$4.01082_{10}-05$	$4.08630_{10}-05$	$4.23532_{10}-05$
$3.30404_{10}-05$	$3.36425_{10}-05$	$3.48565_{10}-05$
$2.72085_{10}-05$	$2.76887_{10}-05$	$2.86771_{10}-05$
$2.23982_{10}-05$	$2.27811_{10}-05$	$2.35853_{10}-05$
$1.84324_{10}-05$	$1.87375_{10}-05$	$1.93915_{10}-05$

Table(A1.3)
nitrogen atoms with the potential due to the latter.

R.	$\langle py1sI1spy \rangle$	$\langle py2sI2spy \rangle$
8.625	1.56410×10^{-05}	1.55031×10^{-05}
8.750	1.28525×10^{-05}	1.27441×10^{-05}
8.875	1.05582×10^{-05}	1.04730×10^{-05}
9.000	8.67126×10^{-06}	8.60436×10^{-06}
9.125	7.11969×10^{-06}	7.06725×10^{-06}
9.250	5.84436×10^{-06}	5.80307×10^{-06}
9.375	4.79630×10^{-06}	4.76304×10^{-06}
9.500	3.93530×10^{-06}	3.90823×10^{-06}
9.625	3.22812×10^{-06}	3.20702×10^{-06}
9.750	2.64747×10^{-06}	2.63175×10^{-06}
9.875	2.17078×10^{-06}	2.15871×10^{-06}
10.000	1.77957×10^{-06}	1.76988×10^{-06}
10.125	1.45856×10^{-06}	1.45089×10^{-06}
10.250	1.19524×10^{-06}	1.18927×10^{-06}
10.375	9.79260×10^{-07}	9.74578×10^{-07}
10.500	8.02163×10^{-07}	7.98477×10^{-07}
10.625	6.56972×10^{-07}	6.54077×10^{-07}
10.750	5.37973×10^{-07}	5.35701×10^{-07}
10.875	4.40448×10^{-07}	4.38665×10^{-07}
11.000	3.60543×10^{-07}	3.59143×10^{-07}
11.125	2.95082×10^{-07}	2.93983×10^{-07}
11.250	2.41467×10^{-07}	2.40604×10^{-07}
11.375	1.97559×10^{-07}	1.96882×10^{-07}
11.500	1.61608×10^{-07}	1.61076×10^{-07}
11.625	1.32168×10^{-07}	1.31750×10^{-07}
11.750	1.08082×10^{-07}	1.07754×10^{-07}
11.875	8.84123×10^{-08}	8.81544×10^{-08}
12.000	7.23383×10^{-08}	7.21353×10^{-08}
12.125	5.91556×10^{-08}	5.89962×10^{-08}
12.250	4.83479×10^{-08}	4.82229×10^{-08}
12.375	3.95152×10^{-08}	3.94171×10^{-08}
12.500	3.22986×10^{-08}	3.22216×10^{-08}
12.625	2.63949×10^{-08}	2.63344×10^{-08}

Hybrid integrals between carbon and

$\langle pypxIpxpy\rangle$	$\langle pypyIpypy\rangle$	$\langle pypzIpzpy\rangle$
$1.51638_{10}-05$	$1.54069_{10}-05$	$1.59385_{10}-05$
$1.24710_{10}-05$	$1.26647_{10}-05$	$1.30966_{10}-05$
$1.02533_{10}-05$	$1.04076_{10}-05$	$1.07583_{10}-05$
$8.42758_{10}-06$	$8.55042_{10}-06$	$8.83508_{10}-06$
$6.92496_{10}-06$	$7.02275_{10}-06$	$7.25369_{10}-06$
$5.68875_{10}-06$	$5.76658_{10}-06$	$5.95387_{10}-06$
$4.67196_{10}-06$	$4.73390_{10}-06$	$4.88572_{10}-06$
$3.83596_{10}-06$	$3.88524_{10}-06$	$4.00827_{10}-06$
$3.14876_{10}-06$	$3.18795_{10}-06$	$3.28761_{10}-06$
$2.58407_{10}-06$	$2.61523_{10}-06$	$2.69594_{10}-06$
$2.12014_{10}-06$	$2.14491_{10}-06$	$2.21025_{10}-06$
$1.73912_{10}-06$	$1.75882_{10}-06$	$1.81169_{10}-06$
$1.42626_{10}-06$	$1.44191_{10}-06$	$1.48468_{10}-06$
$1.16944_{10}-06$	$1.18188_{10}-06$	$1.21647_{10}-06$
$9.58654_{10}-07$	$9.68539_{10}-07$	$9.96505_{10}-07$
$7.85705_{10}-07$	$7.93562_{10}-07$	$8.16165_{10}-07$
$6.43829_{10}-07$	$6.50071_{10}-07$	$6.68335_{10}-07$
$5.27478_{10}-07$	$5.32435_{10}-07$	$5.47190_{10}-07$
$4.32067_{10}-07$	$4.36004_{10}-07$	$4.47921_{10}-07$
$3.53851_{10}-07$	$3.56977_{10}-07$	$3.66600_{10}-07$
$2.89739_{10}-07$	$2.92220_{10}-07$	$2.99989_{10}-07$
$2.37201_{10}-07$	$2.39171_{10}-07$	$2.45441_{10}-07$
$1.94153_{10}-07$	$1.95717_{10}-07$	$2.00776_{10}-07$
$1.58888_{10}-07$	$1.60129_{10}-07$	$1.64210_{10}-07$
$1.29996_{10}-07$	$1.30981_{10}-07$	$1.34272_{10}-07$
$1.06349_{10}-07$	$1.07130_{10}-07$	$1.09784_{10}-07$
$8.70283_{10}-08$	$8.76479_{10}-08$	$8.97881_{10}-08$
$7.12322_{10}-08$	$7.17240_{10}-08$	$7.34499_{10}-08$
$5.82723_{10}-08$	$5.86625_{10}-08$	$6.00538_{10}-08$
$4.76429_{10}-08$	$4.79524_{10}-08$	$4.90735_{10}-08$
$3.89524_{10}-08$	$3.91979_{10}-08$	$4.01012_{10}-08$
$3.18492_{10}-08$	$3.20439_{10}-08$	$3.27717_{10}-08$
$2.60361_{10}-08$	$2.61905_{10}-08$	$2.67767_{10}-08$

Table(A1.3) cont.
nitrogen atoms with the potential due to the latter.

R.	$\langle py1sI1spy \rangle$	$\langle py2sI2spy \rangle$	$\langle pypxIpxpy \rangle$
12.750	$2.15673_{10}-08$	$2.15199_{10}-08$	$2.12809_{10}-08$
12.875	$1.76208_{10}-08$	$1.75837_{10}-08$	$1.73923_{10}-08$
13.000	$1.43951_{10}-08$	$1.43661_{10}-08$	$1.42128_{10}-08$
13.125	$1.17587_{10}-08$	$1.17360_{10}-08$	$1.16132_{10}-08$
13.250	$9.60440_{10}-09$	$9.58657_{10}-09$	$9.48821_{10}-09$
13.375	$7.84396_{10}-09$	$7.82997_{10}-09$	$7.75119_{10}-09$
13.500	$6.40566_{10}-09$	$6.39469_{10}-09$	$6.33160_{10}-09$
13.625	$5.23058_{10}-09$	$5.22197_{10}-09$	$5.17145_{10}-09$
13.750	$4.27073_{10}-09$	$4.26398_{10}-09$	$4.22352_{10}-09$
13.875	$3.48669_{10}-09$	$3.48139_{10}-09$	$3.44900_{10}-09$
14.000	$2.84639_{10}-09$	$2.84223_{10}-09$	$2.81629_{10}-09$
14.125	$2.32346_{10}-09$	$2.32020_{10}-09$	$2.29943_{10}-09$
14.250	$1.89648_{10}-09$	$1.89392_{10}-09$	$1.87729_{10}-09$
14.375	$1.54783_{10}-09$	$1.54582_{10}-09$	$1.53250_{10}-09$
14.500	$1.26319_{10}-09$	$1.26162_{10}-09$	$1.25095_{10}-09$
14.625	$1.03081_{10}-09$	$1.02958_{10}-09$	$1.02103_{10}-09$
14.750	$8.41136_{10}-10$	$8.40166_{10}-10$	$8.33322_{10}-10$
14.875	$6.86306_{10}-10$	$6.85545_{10}-10$	$6.80067_{10}-10$
15.000	$5.59944_{10}-10$	$5.59348_{10}-10$	$5.54967_{10}-10$
15.125	$4.56814_{10}-10$	$4.56347_{10}-10$	$4.52842_{10}-10$
15.250	$3.72659_{10}-10$	$3.72292_{10}-10$	$3.69488_{10}-10$
15.375	$3.03991_{10}-10$	$3.03703_{10}-10$	$3.01458_{10}-10$
15.500	$2.47955_{10}-10$	$2.47730_{10}-10$	$2.45930_{10}-10$
15.625	$2.02224_{10}-10$	$2.02050_{10}-10$	$2.00607_{10}-10$
15.750	$1.64943_{10}-10$	$1.64804_{10}-10$	$1.63651_{10}-10$
15.875	$1.34706_{10}-10$	$1.34576_{10}-10$	$1.33656_{10}-10$
16.000	$1.10577_{10}-10$	$1.10404_{10}-10$	$1.09665_{10}-10$

Table(A1.3)

Hybrid integrals between carbon and nitrogen atoms

$\langle pypy|pypy\rangle$	$\langle pypz|pzpy\rangle$
2.14033×10^{-08}	2.18755×10^{-08}
1.74893×10^{-08}	1.78696×10^{-08}
1.42896×10^{-08}	1.45959×10^{-08}
1.16741×10^{-08}	1.19207×10^{-08}
9.53652×10^{-09}	9.73499×10^{-09}
7.78949×10^{-09}	7.94923×10^{-09}
6.36194×10^{-09}	6.49052×10^{-09}
5.19549×10^{-09}	5.29897×10^{-09}
4.24257×10^{-09}	4.32584×10^{-09}
3.46409×10^{-09}	3.53109×10^{-09}
2.82825×10^{-09}	2.88215×10^{-09}
2.30890×10^{-09}	2.35226×10^{-09}
1.88479×10^{-09}	1.91967×10^{-09}
1.53845×10^{-09}	1.56650×10^{-09}
1.25567×10^{-09}	1.27823×10^{-09}
1.02478×10^{-09}	1.04292×10^{-09}
8.36288×10^{-10}	8.50878×10^{-10}
6.82414×10^{-10}	6.94141×10^{-10}
5.56822×10^{-10}	5.66244×10^{-10}
4.54309×10^{-10}	4.61884×10^{-10}
3.70648×10^{-10}	3.76744×10^{-10}
3.02377×10^{-10}	3.07282×10^{-10}
2.46660×10^{-10}	2.50599×10^{-10}
2.01186×10^{-10}	2.04343×10^{-10}
1.64108×10^{-10}	1.66653×10^{-10}
1.34015×10^{-10}	1.36154×10^{-10}
1.09954×10^{-10}	1.11990×10^{-10}

cont.
with the potential due to the latter.

R.	$\langle pz1sI1spz\rangle$	$\langle pz2sI2spz\rangle$
4.500	$4.35474_{10}-02$	$4.08846_{10}-02$
4.625	$3.78602_{10}-02$	$3.56806_{10}-02$
4.750	$3.28378_{10}-02$	$3.10564_{10}-02$
4.875	$2.84180_{10}-02$	$2.69643_{10}-02$
5.000	$2.45413_{10}-02$	$2.33568_{10}-02$
5.125	$2.11513_{10}-02$	$2.01875_{10}-02$
5.250	$1.81954_{10}-02$	$1.74122_{10}-02$
5.375	$1.56248_{10}-02$	$1.49890_{10}-02$
5.500	$1.33947_{10}-02$	$1.28792_{10}-02$
5.625	$1.14646_{10}-02$	$1.10470_{10}-02$
5.750	$9.79763_{10}-03$	$9.45980_{10}-03$
5.875	$8.36096_{10}-03$	$8.08786_{10}-03$
6.000	$7.12511_{10}-03$	$6.90452_{10}-03$
6.125	$6.06395_{10}-03$	$5.88593_{10}-03$
6.250	$5.15434_{10}-03$	$5.01079_{10}-03$
6.375	$4.37592_{10}-03$	$4.26026_{10}-03$
6.500	$3.71080_{10}-03$	$3.61767_{10}-03$
6.625	$3.14332_{10}-03$	$3.06837_{10}-03$
6.750	$2.65981_{10}-03$	$2.59953_{10}-03$
6.875	$2.24840_{10}-03$	$2.19997_{10}-03$
7.000	$1.89879_{10}-03$	$1.85991_{10}-03$
7.125	$1.60205_{10}-03$	$1.57085_{10}-03$
7.250	$1.35048_{10}-03$	$1.32544_{10}-03$
7.375	$1.13743_{10}-03$	$1.11735_{10}-03$
7.500	$9.57198_{10}-04$	$9.41106_{10}-04$
7.625	$8.04884_{10}-04$	$7.91993_{10}-04$
7.750	$6.76290_{10}-04$	$6.65968_{10}-04$
7.875	$5.67820_{10}-04$	$5.59558_{10}-04$
8.000	$4.76407_{10}-04$	$4.69798_{10}-04$
8.125	$3.99435_{10}-04$	$3.94151_{10}-04$
8.250	$3.34678_{10}-04$	$3.30454_{10}-04$
8.375	$2.80239_{10}-04$	$2.76864_{10}-04$
8.500	$2.34510_{10}-04$	$2.31814_{10}-04$

Hybrid integrals between carbon and

⟨pzpx|pxpz⟩	⟨pzpy|pypz⟩	⟨pzpz|pzpz⟩
$3.89101_\text{D}-02$	$3.89101_\text{D}-02$	$4.48337_\text{D}-02$
$3.39872_\text{D}-02$	$3.39872_\text{D}-02$	$3.90670_\text{D}-02$
$2.96089_\text{D}-02$	$2.96089_\text{D}-02$	$3.39513_\text{D}-02$
$2.57306_\text{D}-02$	$2.57306_\text{D}-02$	$2.94319_\text{D}-02$
$2.23080_\text{D}-02$	$2.23080_\text{D}-02$	$2.54544_\text{D}-02$
$1.92982_\text{D}-02$	$1.92982_\text{D}-02$	$2.19661_\text{D}-02$
$1.66599_\text{D}-02$	$1.66599_\text{D}-02$	$1.89167_\text{D}-02$
$1.43541_\text{D}-02$	$1.43541_\text{D}-02$	$1.62588_\text{D}-02$
$1.23445_\text{D}-02$	$1.23445_\text{D}-02$	$1.39487_\text{D}-02$
$1.05976_\text{D}-02$	$1.05976_\text{D}-02$	$1.19461_\text{D}-02$
$9.08261_\text{D}-03$	$9.08261_\text{D}-03$	$1.02142_\text{D}-02$
$7.77191_\text{D}-03$	$7.77191_\text{D}-03$	$8.71974_\text{D}-03$
$6.64033_\text{D}-03$	$6.64033_\text{D}-03$	$7.43288_\text{D}-03$
$5.66535_\text{D}-03$	$5.66535_\text{D}-03$	$6.32706_\text{D}-03$
$4.82690_\text{D}-03$	$4.82690_\text{D}-03$	$5.37856_\text{D}-03$
$4.10716_\text{D}-03$	$4.10716_\text{D}-03$	$4.56644_\text{D}-03$
$3.49038_\text{D}-03$	$3.49038_\text{D}-03$	$3.87223_\text{D}-03$
$2.96268_\text{D}-03$	$2.96268_\text{D}-03$	$3.27976_\text{D}-03$
$2.51189_\text{D}-03$	$2.51189_\text{D}-03$	$2.77487_\text{D}-03$
$2.12736_\text{D}-03$	$2.12736_\text{D}-03$	$2.34522_\text{D}-03$
$1.79981_\text{D}-03$	$1.79981_\text{D}-03$	$1.98009_\text{D}-03$
$1.52116_\text{D}-03$	$1.52116_\text{D}-03$	$1.67020_\text{D}-03$
$1.28441_\text{D}-03$	$1.28441_\text{D}-03$	$1.40750_\text{D}-03$
$1.08350_\text{D}-03$	$1.08350_\text{D}-03$	$1.18506_\text{D}-03$
$9.13200_\text{D}-04$	$9.13200_\text{D}-04$	$9.96920_\text{D}-04$
$7.69009_\text{D}-04$	$7.69009_\text{D}-04$	$8.37964_\text{D}-04$
$6.47052_\text{D}-04$	$6.47052_\text{D}-04$	$7.03801_\text{D}-04$
$5.44004_\text{D}-04$	$5.44004_\text{D}-04$	$5.90670_\text{D}-04$
$4.57017_\text{D}-04$	$4.57017_\text{D}-04$	$4.95362_\text{D}-04$
$3.83656_\text{D}-04$	$3.83656_\text{D}-04$	$4.15141_\text{D}-04$
$3.21842_\text{D}-04$	$3.21842_\text{D}-04$	$3.47677_\text{D}-04$
$2.69802_\text{D}-04$	$2.69802_\text{D}-04$	$2.90986_\text{D}-04$
$2.26027_\text{D}-04$	$2.26027_\text{D}-04$	$2.43387_\text{D}-04$

Table(A1.3) cont.
nitrogen atoms with the potential due to the latter.

R.	$\langle pz1sI1spz\rangle$	$\langle pz2sI2spz\rangle$	$\langle pzpxIpxpz\rangle$
8.625	$1.96125_{10}-04$	$1.93972_{10}-04$	$1.89233_{10}-04$
8.750	$1.63928_{10}-04$	$1.62210_{10}-04$	$1.58331_{10}-04$
8.875	$1.36940_{10}-04$	$1.35569_{10}-04$	$1.32396_{10}-04$
9.000	$1.14333_{10}-04$	$1.13239_{10}-04$	$1.10645_{10}-04$
9.125	$9.54079_{10}-05$	$9.45354_{10}-05$	$9.24157_{10}-05$
9.250	$7.95750_{10}-05$	$7.88795_{10}-05$	$7.71481_{10}-05$
9.375	$6.63367_{10}-05$	$6.57825_{10}-05$	$6.43689_{10}-05$
9.500	$5.52746_{10}-05$	$5.48329_{10}-05$	$5.36795_{10}-05$
9.625	$4.60356_{10}-05$	$4.56838_{10}-05$	$4.47431_{10}-05$
9.750	$3.83238_{10}-05$	$3.80436_{10}-05$	$3.72768_{10}-05$
9.875	$3.18899_{10}-05$	$3.16668_{10}-05$	$3.10419_{10}-05$
10.000	$2.65250_{10}-05$	$2.63474_{10}-05$	$2.58384_{10}-05$
10.125	$2.20535_{10}-05$	$2.19122_{10}-05$	$2.14977_{10}-05$
10.250	$1.83286_{10}-05$	$1.82161_{10}-05$	$1.78788_{10}-05$
10.375	$1.52269_{10}-05$	$1.51375_{10}-05$	$1.48630_{10}-05$
10.500	$1.26455_{10}-05$	$1.25744_{10}-05$	$1.23511_{10}-05$
10.625	$1.04978_{10}-05$	$1.04413_{10}-05$	$1.02597_{10}-05$
10.750	$8.71184_{10}-06$	$8.66689_{10}-06$	$8.51931_{10}-06$
10.875	$7.22722_{10}-06$	$7.19149_{10}-06$	$7.07157_{10}-06$
11.000	$5.99366_{10}-06$	$5.96526_{10}-06$	$5.86785_{10}-06$
11.125	$4.96903_{10}-06$	$4.94647_{10}-06$	$4.86737_{10}-06$
11.250	$4.11832_{10}-06$	$4.10040_{10}-06$	$4.03618_{10}-06$
11.375	$3.41222_{10}-06$	$3.39799_{10}-06$	$3.34586_{10}-06$
11.500	$2.82640_{10}-06$	$2.81510_{10}-06$	$2.77280_{10}-06$
11.625	$2.34058_{10}-06$	$2.33161_{10}-06$	$2.29729_{10}-06$
11.750	$1.93765_{10}-06$	$1.93053_{10}-06$	$1.90270_{10}-06$
11.875	$1.60319_{10}-06$	$1.59754_{10}-06$	$1.57497_{10}-06$
12.000	$1.32584_{10}-06$	$1.32135_{10}-06$	$1.30306_{10}-06$
12.125	$1.09644_{10}-06$	$1.09288_{10}-06$	$1.07806_{10}-06$
12.250	$9.06756_{10}-07$	$9.03927_{10}-07$	$8.91916_{10}-07$
12.375	$7.49629_{10}-07$	$7.47384_{10}-07$	$7.37654_{10}-07$
12.500	$6.19514_{10}-07$	$6.17734_{10}-07$	$6.09853_{10}-07$
12.625	$5.11881_{10}-07$	$5.10470_{10}-07$	$5.04088_{10}-07$

Table (A1.3)

Hybrid integrals between carbon and nitrogen atoms

$\langle p_z p_y | p_y p_z \rangle$	$\langle p_z p_z | p_z p_z \rangle$
$1.89233_{D}-04$	$2.03450_{D}-04$
$1.58331_{D}-04$	$1.69968_{D}-04$
$1.32396_{D}-04$	$1.41915_{D}-04$
$1.10645_{D}-04$	$1.18428_{D}-04$
$9.24157_{D}-05$	$9.87755_{D}-05$
$7.71481_{D}-05$	$8.23424_{D}-05$
$6.43689_{D}-05$	$6.86093_{D}-05$
$5.36795_{D}-05$	$5.71395_{D}-05$
$4.47431_{D}-05$	$4.75651_{D}-05$
$3.72768_{D}-05$	$3.95774_{D}-05$
$3.10419_{D}-05$	$3.29167_{D}-05$
$2.58384_{D}-05$	$2.73655_{D}-05$
$2.14977_{D}-05$	$2.27412_{D}-05$
$1.78788_{D}-05$	$1.88909_{D}-05$
$1.48630_{D}-05$	$1.56865_{D}-05$
$1.23511_{D}-05$	$1.30209_{D}-05$
$1.02597_{D}-05$	$1.08043_{D}-05$
$8.51931_{D}-06$	$8.96203_{D}-06$
$7.07157_{D}-06$	$7.43133_{D}-06$
$5.86785_{D}-06$	$6.16009_{D}-06$
$4.86737_{D}-06$	$5.10469_{D}-06$
$4.03618_{D}-06$	$4.22885_{D}-06$
$3.34586_{D}-06$	$3.50224_{D}-06$
$2.77280_{D}-06$	$2.89970_{D}-06$
$2.29729_{D}-06$	$2.40024_{D}-06$
$1.90270_{D}-06$	$1.98619_{D}-06$
$1.57497_{D}-06$	$1.64266_{D}-06$
$1.30306_{D}-06$	$1.35793_{D}-06$
$1.07806_{D}-06$	$1.12252_{D}-06$
$8.91916_{D}-07$	$9.27950_{D}-07$
$7.37654_{D}-07$	$7.66846_{D}-07$
$6.09853_{D}-07$	$6.33497_{D}-07$
$5.04088_{D}-07$	$5.23234_{D}-07$

cont.
with the potential due to the latter.

R.	$\langle pz1sI1spz\rangle$	$\langle pz2sI2spz\rangle$
12.750	$4.22861_{10}\text{-}07$	$4.21742_{10}\text{-}07$
12.875	$3.49237_{10}\text{-}07$	$3.48350_{10}\text{-}07$
13.000	$2.88369_{10}\text{-}07$	$2.87666_{10}\text{-}07$
13.125	$2.38056_{10}\text{-}07$	$2.37499_{10}\text{-}07$
13.250	$1.96481_{10}\text{-}07$	$1.96040_{10}\text{-}07$
13.375	$1.62132_{10}\text{-}07$	$1.61783_{10}\text{-}07$
13.500	$1.33762_{10}\text{-}07$	$1.33486_{10}\text{-}07$
13.625	$1.10334_{10}\text{-}07$	$1.10116_{10}\text{-}07$
13.750	$9.09933_{10}\text{-}08$	$9.08198_{10}\text{-}08$
13.875	$7.50280_{10}\text{-}08$	$7.48905_{10}\text{-}08$
14.000	$6.18527_{10}\text{-}08$	$6.17439_{10}\text{-}08$
14.125	$5.09816_{10}\text{-}08$	$5.08955_{10}\text{-}08$
14.250	$4.20142_{10}\text{-}08$	$4.19460_{10}\text{-}08$
14.375	$3.46179_{10}\text{-}08$	$3.45639_{10}\text{-}08$
14.500	$2.85192_{10}\text{-}08$	$2.84764_{10}\text{-}08$
14.625	$2.34909_{10}\text{-}08$	$2.34571_{10}\text{-}08$
14.750	$1.93462_{10}\text{-}08$	$1.93195_{10}\text{-}08$
14.875	$1.59302_{10}\text{-}08$	$1.59090_{10}\text{-}08$
15.000	$1.31154_{10}\text{-}08$	$1.30986_{10}\text{-}08$
15.125	$1.07963_{10}\text{-}08$	$1.07830_{10}\text{-}08$
15.250	$8.88609_{10}\text{-}09$	$8.87560_{10}\text{-}09$
15.375	$7.31284_{10}\text{-}09$	$7.30457_{10}\text{-}09$
15.500	$6.01714_{10}\text{-}09$	$6.01057_{10}\text{-}09$
15.625	$4.95013_{10}\text{-}09$	$4.94485_{10}\text{-}09$
15.750	$4.07224_{10}\text{-}09$	$4.06813_{10}\text{-}09$
15.875	$3.35274_{10}\text{-}09$	$3.35028_{10}\text{-}09$
16.000	$2.76989_{10}\text{-}09$	$2.77064_{10}\text{-}09$

Hybrid integrals between carbon and

`<pzpxIpxpz>`	`<pzpyIpypz>`	`<pzpzIpzpz>`
$4.16575_{10}-07$	$4.16575_{10}-07$	$4.32076_{10}-07$
$3.44167_{10}-07$	$3.44167_{10}-07$	$3.56715_{10}-07$
$2.84280_{10}-07$	$2.84280_{10}-07$	$2.94436_{10}-07$
$2.34760_{10}-07$	$2.34760_{10}-07$	$2.42978_{10}-07$
$1.93824_{10}-07$	$1.93824_{10}-07$	$2.00473_{10}-07$
$1.59991_{10}-07$	$1.59991_{10}-07$	$1.65369_{10}-07$
$1.32036_{10}-07$	$1.32036_{10}-07$	$1.36386_{10}-07$
$1.08943_{10}-07$	$1.08943_{10}-07$	$1.12461_{10}-07$
$8.98715_{10}-08$	$8.98715_{10}-08$	$9.27164_{10}-08$
$7.41237_{10}-08$	$7.41237_{10}-08$	$7.64239_{10}-08$
$6.11241_{10}-08$	$6.11241_{10}-08$	$6.29834_{10}-08$
$5.03946_{10}-08$	$5.03946_{10}-08$	$5.18974_{10}-08$
$4.15412_{10}-08$	$4.15412_{10}-08$	$4.27557_{10}-08$
$3.42368_{10}-08$	$3.42368_{10}-08$	$3.52183_{10}-08$
$2.82121_{10}-08$	$2.82121_{10}-08$	$2.90051_{10}-08$
$2.32435_{10}-08$	$2.32435_{10}-08$	$2.38841_{10}-08$
$1.91470_{10}-08$	$1.91470_{10}-08$	$1.96644_{10}-08$
$1.57697_{10}-08$	$1.57697_{10}-08$	$1.61876_{10}-08$
$1.29861_{10}-08$	$1.29861_{10}-08$	$1.33237_{10}-08$
$1.06922_{10}-08$	$1.06922_{10}-08$	$1.09648_{10}-08$
$8.80222_{10}-09$	$8.80222_{10}-09$	$9.02235_{10}-09$
$7.24531_{10}-09$	$7.24531_{10}-09$	$7.42302_{10}-09$
$5.96274_{10}-09$	$5.96274_{10}-09$	$6.10623_{10}-09$
$4.90627_{10}-09$	$4.90627_{10}-09$	$5.02216_{10}-09$
$4.03697_{10}-09$	$4.03697_{10}-09$	$4.13047_{10}-09$
$3.32480_{10}-09$	$3.32480_{10}-09$	$3.39973_{10}-09$
$2.74895_{10}-09$	$2.74895_{10}-09$	$2.80761_{10}-09$

Table(A1.3) cont.

nitrogen atoms with the potential due to the latter.

R.	⟨py1sI1spy⟩	⟨py2sI2spy⟩	⟨pypxIpxpy⟩
4.500	$5.33987_{10}{-}03$	$5.09065_{10}{-}03$	$4.89461_{10}{-}03$
4.625	$4.38426_{10}{-}03$	$4.18771_{10}{-}03$	$4.02897_{10}{-}03$
4.750	$3.59588_{10}{-}03$	$3.44092_{10}{-}03$	$3.31254_{10}{-}03$
4.875	$2.94632_{10}{-}03$	$2.82418_{10}{-}03$	$2.72046_{10}{-}03$
5.000	$2.41176_{10}{-}03$	$2.31552_{10}{-}03$	$2.23182_{10}{-}03$
5.125	$1.97237_{10}{-}03$	$1.89656_{10}{-}03$	$1.82907_{10}{-}03$
5.250	$1.61159_{10}{-}03$	$1.55189_{10}{-}03$	$1.49754_{10}{-}03$
5.375	$1.31570_{10}{-}03$	$1.26870_{10}{-}03$	$1.22495_{10}{-}03$
5.500	$1.07326_{10}{-}03$	$1.03625_{10}{-}03$	$1.00109_{10}{-}03$
5.625	$8.74806_{10}{-}04$	$8.45680_{10}{-}04$	$8.17431_{10}{-}04$
5.750	$7.12515_{10}{-}04$	$6.89593_{10}{-}04$	$6.66915_{10}{-}04$
5.875	$5.79922_{10}{-}04$	$5.61879_{10}{-}04$	$5.43686_{10}{-}04$
6.000	$4.71657_{10}{-}04$	$4.57466_{10}{-}04$	$4.42883_{10}{-}04$
6.125	$3.83350_{10}{-}04$	$3.72188_{10}{-}04$	$3.60505_{10}{-}04$
6.250	$3.11373_{10}{-}04$	$3.02595_{10}{-}04$	$2.93242_{10}{-}04$
6.375	$2.52751_{10}{-}04$	$2.45850_{10}{-}04$	$2.38365_{10}{-}04$
6.500	$2.05043_{10}{-}04$	$1.99617_{10}{-}04$	$1.93632_{10}{-}04$
6.625	$1.66240_{10}{-}04$	$1.61975_{10}{-}04$	$1.57192_{10}{-}04$
6.750	$1.34741_{10}{-}04$	$1.31371_{10}{-}04$	$1.27549_{10}{-}04$
6.875	$1.09095_{10}{-}04$	$1.06460_{10}{-}04$	$1.03409_{10}{-}04$
7.000	$8.83315_{10}{-}05$	$8.62473_{10}{-}05$	$8.38119_{10}{-}05$
7.125	$7.14364_{10}{-}05$	$6.98120_{10}{-}05$	$6.78695_{10}{-}05$
7.250	$5.77699_{10}{-}05$	$5.64910_{10}{-}05$	$5.49421_{10}{-}05$
7.375	$4.66905_{10}{-}05$	$4.56863_{10}{-}05$	$4.44517_{10}{-}05$
7.500	$3.77192_{10}{-}05$	$3.69302_{10}{-}05$	$3.59465_{10}{-}05$
7.625	$3.04578_{10}{-}05$	$2.98381_{10}{-}05$	$2.90547_{10}{-}05$
7.750	$2.45835_{10}{-}05$	$2.40967_{10}{-}05$	$2.34730_{10}{-}05$
7.875	$1.98335_{10}{-}05$	$1.94514_{10}{-}05$	$1.89549_{10}{-}05$
8.000	$1.59948_{10}{-}05$	$1.56946_{10}{-}05$	$1.52998_{10}{-}05$
8.125	$1.28939_{10}{-}05$	$1.26582_{10}{-}05$	$1.23441_{10}{-}05$
8.250	$1.03901_{10}{-}05$	$1.02050_{10}{-}05$	$9.95523_{10}{-}06$
8.375	$8.36928_{10}{-}06$	$8.22394_{10}{-}06$	$8.02543_{10}{-}06$
8.500	$6.73896_{10}{-}06$	$6.62484_{10}{-}06$	$6.46710_{10}{-}06$

Table(A1.4)
Hybrid integrals between t

<pypyIpypy>	<pypzIpzpy>
5.14821ᴅ-03	5.22911ᴅ-03
4.23250ᴅ-03	4.30167ᴅ-03
3.47573ᴅ-03	3.53451ᴅ-03
2.85121ᴅ-03	2.90087ᴅ-03
2.33648ᴅ-03	2.37826ᴅ-03
1.91280ᴅ-03	1.94780ᴅ-03
1.56446ᴅ-03	1.59367ᴅ-03
1.27841ᴅ-03	1.30271ᴅ-03
1.04376ᴅ-03	1.06391ᴅ-03
8.51475ᴅ-04	8.68136ᴅ-04
6.94060ᴅ-04	7.07811ᴅ-04
5.65319ᴅ-04	5.76664ᴅ-04
4.60112ᴅ-04	4.69396ᴅ-04
3.74221ᴅ-04	3.81838ᴅ-04
3.04156ᴅ-04	3.10387ᴅ-04
2.47046ᴅ-04	2.52137ᴅ-04
2.00534ᴅ-04	2.04685ᴅ-04
1.62676ᴅ-04	1.66058ᴅ-04
1.31907ᴅ-04	1.34656ᴅ-04
1.06869ᴅ-04	1.09103ᴅ-04
8.65593ᴅ-05	8.83706ᴅ-05
7.00486ᴅ-05	7.15179ᴅ-05
5.66705ᴅ-05	5.78602ᴅ-05
4.58260ᴅ-05	4.67845ᴅ-05
3.69735ᴅ-05	3.78107ᴅ-05
2.99232ᴅ-05	3.05435ᴅ-05
2.41532ᴅ-05	2.46616ᴅ-05
1.94959ᴅ-05	1.99035ᴅ-05
1.57279ᴅ-05	1.60565ᴅ-05
1.26831ᴅ-05	1.29474ᴅ-05
1.02235ᴅ-05	1.04361ᴅ-05
8.23777ᴅ-06	8.40863ᴅ-06
6.63510ᴅ-06	6.77232ᴅ-06

wo nitrogen atoms.

R.	$\langle py1s|I1s|py\rangle$	$\langle py2s|I2s|py\rangle$	$\langle pypx|Ipx|py\rangle$
8.625	$5.42388_{10}{-}06$	$5.33470_{10}{-}06$	$5.20940_{10}{-}06$
8.750	$4.36455_{10}{-}06$	$4.29423_{10}{-}06$	$4.19471_{10}{-}06$
8.875	$3.51124_{10}{-}06$	$3.45573_{10}{-}06$	$3.37671_{10}{-}06$
9.000	$2.82293_{10}{-}06$	$2.77956_{10}{-}06$	$2.71684_{10}{-}06$
9.125	$2.26941_{10}{-}06$	$2.23526_{10}{-}06$	$2.18548_{10}{-}06$
9.250	$1.82362_{10}{-}06$	$1.79681_{10}{-}06$	$1.75732_{10}{-}06$
9.375	$1.46476_{10}{-}06$	$1.44380_{10}{-}06$	$1.41248_{10}{-}06$
9.500	$1.17840_{10}{-}06$	$1.16183_{10}{-}06$	$1.13694_{10}{-}06$
9.625	$9.20726_{10}{-}07$	$9.08163_{10}{-}07$	$8.88985_{10}{-}07$
9.750	$7.24610_{10}{-}07$	$7.14939_{10}{-}07$	$7.00056_{10}{-}07$
9.875	$6.13916_{10}{-}07$	$6.05852_{10}{-}07$	$5.93354_{10}{-}07$
10.000	$4.86848_{10}{-}07$	$4.80611_{10}{-}07$	$4.70806_{10}{-}07$
10.125	$3.91428_{10}{-}07$	$3.86502_{10}{-}07$	$3.78736_{10}{-}07$
10.250	$3.13636_{10}{-}07$	$3.09830_{10}{-}07$	$3.03647_{10}{-}07$
10.375	$2.51460_{10}{-}07$	$2.48473_{10}{-}07$	$2.43558_{10}{-}07$
10.500	$2.01466_{10}{-}07$	$1.99102_{10}{-}07$	$1.95251_{10}{-}07$
10.625	$1.61411_{10}{-}07$	$1.59556_{10}{-}07$	$1.56502_{10}{-}07$
10.750	$1.29305_{10}{-}07$	$1.27853_{10}{-}07$	$1.25434_{10}{-}07$
10.875	$1.03644_{10}{-}07$	$1.02503_{10}{-}07$	$1.00589_{10}{-}07$
11.000	$8.28523_{10}{-}08$	$8.19578_{10}{-}08$	$8.04429_{10}{-}08$
11.125	$6.63376_{10}{-}08$	$6.56359_{10}{-}08$	$6.44375_{10}{-}08$
11.250	$5.30811_{10}{-}08$	$5.25310_{10}{-}08$	$5.15832_{10}{-}08$
11.375	$4.24678_{10}{-}08$	$4.20362_{10}{-}08$	$4.12865_{10}{-}08$
11.500	$3.39653_{10}{-}08$	$3.36261_{10}{-}08$	$3.30333_{10}{-}08$
11.625	$2.72121_{10}{-}08$	$2.69464_{10}{-}08$	$2.64773_{10}{-}08$
11.750	$2.17415_{10}{-}08$	$2.15328_{10}{-}08$	$2.11620_{10}{-}08$
11.875	$1.73633_{10}{-}08$	$1.71996_{10}{-}08$	$1.69065_{10}{-}08$
12.000	$1.38771_{10}{-}08$	$1.37487_{10}{-}08$	$1.35171_{10}{-}08$
12.125	$1.10891_{10}{-}08$	$1.09885_{10}{-}08$	$1.08054_{10}{-}08$
12.250	$8.85950_{10}{-}09$	$8.78053_{10}{-}09$	$8.63586_{10}{-}09$
12.375	$7.07686_{10}{-}09$	$7.01491_{10}{-}09$	$6.90060_{10}{-}09$
12.500	$5.65188_{10}{-}09$	$5.60329_{10}{-}09$	$5.51298_{10}{-}09$
12.625	$4.51305_{10}{-}09$	$4.47494_{10}{-}09$	$4.40359_{10}{-}09$

Table(A1.4)
Hybrid integrals between t

⟨pypy❘pypy⟩	⟨pypz❘pzpy⟩
$5.34228_{10}-06$	$5.45244_{10}-06$
$4.29981_{10}-06$	$4.38816_{10}-06$
$3.45984_{10}-06$	$3.53065_{10}-06$
$2.78253_{10}-06$	$2.83930_{10}-06$
$2.23742_{10}-06$	$2.28288_{10}-06$
$1.79835_{10}-06$	$1.83474_{10}-06$
$1.44490_{10}-06$	$1.47403_{10}-06$
$1.16261_{10}-06$	$1.18593_{10}-06$
$9.08676_{10}-07$	$9.26828_{10}-07$
$7.15284_{10}-07$	$7.29487_{10}-07$
$6.06032_{10}-07$	$6.18101_{10}-07$
$4.81966_{10}-07$	$4.90262_{10}-07$
$3.86459_{10}-07$	$3.94177_{10}-07$
$3.09900_{10}-07$	$3.15901_{10}-07$
$2.48451_{10}-07$	$2.53280_{10}-07$
$1.99114_{10}-07$	$2.02962_{10}-07$
$1.59551_{10}-07$	$1.62616_{10}-07$
$1.27839_{10}-07$	$1.30284_{10}\ 07$
$1.02486_{10}-07$	$1.04433_{10}-07$
$8.19402_{10}-08$	$8.34899_{10}-08$
$6.56179_{10}-08$	$6.68520_{10}-08$
$5.25138_{10}-08$	$5.34961_{10}-08$
$4.20201_{10}-08$	$4.28018_{10}-08$
$3.36116_{10}-08$	$3.42334_{10}-08$
$2.69333_{10}-08$	$2.74283_{10}-08$
$2.15214_{10}-08$	$2.19149_{10}-08$
$1.71899_{10}-08$	$1.75025_{10}-08$
$1.37403_{10}-08$	$1.39888_{10}-08$
$1.09813_{10}-08$	$1.11787_{10}-08$
$8.77445_{10}-09$	$8.93127_{10}-09$
$7.00980_{10}-09$	$7.13435_{10}-09$
$5.59900_{10}-09$	$5.69790_{10}-09$
$4.47134_{10}-09$	$4.54987_{10}-09$

cont.
two nitrogen atoms.

R.	$\langle py1sI1spy\rangle$	$\langle py2sI2spy\rangle$
12.750	$3.60208_{10}-09$	$3.57219_{10}-09$
12.875	$2.88757_{10}-09$	$2.86403_{10}-09$
13.000	$2.16037_{10}-09$	$2.14314_{10}-09$
13.125	$1.83162_{10}-09$	$1.81719_{10}-09$
13.250	$1.45719_{10}-09$	$1.44591_{10}-09$
13.375	$1.16645_{10}-09$	$1.15758_{10}-09$
13.500	$9.29723_{10}-10$	$9.22782_{10}-10$
13.625	$7.41410_{10}-10$	$7.35965_{10}-10$
13.750	$5.91163_{10}-10$	$5.86892_{10}-10$
13.875	$4.71292_{10}-10$	$4.67943_{10}-10$
14.000	$3.75668_{10}-10$	$3.73042_{10}-10$
14.125	$2.99402_{10}-10$	$2.97343_{10}-10$
14.250	$2.38589_{10}-10$	$2.36974_{10}-10$
14.375	$190100_{10}-10$	$1.88834_{10}-10$
14.500	$1.51447_{10}-10$	$1.50454_{10}-10$
14.625	$1.20635_{10}-10$	$1.19856_{10}-10$
14.750	$9.60803_{10}-11$	$9.54697_{10}-11$
14.875	$7.65131_{10}-11$	$7.60341_{10}-11$
15.000	$6.09239_{10}-11$	$6.05484_{10}-11$
15.125	$4.85039_{10}-11$	$4.82095_{10}-11$
15.250	$3.86117_{10}-11$	$3.83808_{10}-11$
15.375	$3.07329_{10}-11$	$3.05519_{10}-11$
15.500	$2.44593_{10}-11$	$2.43173_{10}-11$
15.625	$1.94644_{10}-11$	$1.93532_{10}-11$
15.750	$1.54869_{10}-11$	$1.53995_{10}-11$
15.875	$1.23188_{10}-11$	$1.22504_{10}-11$
16.000	$9.80196_{10}-12$	$9.74680_{10}-12$

Hybrid integ

$\langle pypxIpxpy \rangle$	$\langle pypyIpypy \rangle$	$\langle pypzIpzpy \rangle$
$3.51585_{10}-09$	$3.56921_{10}-09$	$3.63152_{10}-09$
$2.81933_{10}-09$	$2.86154_{10}-09$	$2.91120_{10}-09$
$2.11014_{10}-09$	$2.14119_{10}-09$	$2.17808_{10}-09$
$1.78944_{10}-09$	$1.81550_{10}-09$	$1.84664_{10}-09$
$1.42406_{10}-09$	$1.44453_{10}-09$	$1.46915_{10}-09$
$1.14025_{10}-09$	$1.15644_{10}-09$	$1.17604_{10}-09$
$9.09124_{10}-10$	$9.21868_{10}-10$	$9.37377_{10}-10$
$7.25183_{10}-10$	$7.35207_{10}-10$	$7.47514_{10}-10$
$5.78383_{10}-10$	$5.86268_{10}-10$	$5.96029_{10}-10$
$4.61227_{10}-10$	$4.67433_{10}-10$	$4.75169_{10}-10$
$3.67742_{10}-10$	$3.72627_{10}-10$	$3.78757_{10}-10$
$2.93160_{10}-10$	$2.97005_{10}-10$	$3.01862_{10}-10$
$2.33675_{10}-10$	$2.36701_{10}-10$	$2.40548_{10}-10$
$1.86230_{10}-10$	$1.88611_{10}-10$	$1.91659_{10}-10$
$1.48400_{10}-10$	$1.50275_{10}-10$	$1.52687_{10}-10$
$1.18236_{10}-10$	$1.19711_{10}-10$	$1.21622_{10}-10$
$9.41916_{10}-11$	$9.53521_{10}-11$	$9.68651_{10}-11$
$7.50263_{10}-11$	$7.59393_{10}-11$	$7.71371_{10}-11$
$5.97536_{10}-11$	$6.04720_{10}-11$	$6.14200_{10}-11$
$4.75826_{10}-11$	$4.81478_{10}-11$	$4.88981_{10}-11$
$3.78865_{10}-11$	$3.83311_{10}\ 11$	$3.89249_{10}-11$
$3.01621_{10}-11$	$3.05118_{10}-11$	$3.09817_{10}-11$
$2.40100_{10}-11$	$2.42851_{10}-11$	$2.46568_{10}-11$
$1.91108_{10}-11$	$1.93272_{10}-11$	$1.96214_{10}-11$
$1.52085_{10}-11$	$1.53787_{10}-11$	$1.56113_{10}-11$
$1.20998_{10}-11$	$1.22338_{10}-11$	$1.24177_{10}-11$
$9.62943_{10}-12$	$9.73310_{10}-12$	$9.87877_{10}-12$

Table(A1.4) cont.
grals between two nitrogen atoms.

R.	$\langle pz1s\,I1s\,pz\rangle$	$\langle pz2s\,I2s\,pz\rangle$	$\langle pzpx\,Ipx\,pz\rangle$
4.500	$3.24552_{D}-02$	$3.05791_{D}-02$	$2.92905_{D}-02$
4.625	$2.76840_{D}-02$	$2.61553_{D}-02$	$2.50712_{D}-02$
4.750	$2.35576_{D}-02$	$2.23136_{D}-02$	$2.14038_{D}-02$
4.875	$2.00007_{D}-02$	$1.89899_{D}-02$	$1.82284_{D}-02$
5.000	$1.69446_{D}-02$	$1.61242_{D}-02$	$1.54883_{D}-02$
5.125	$1.43265_{D}-02$	$1.36613_{D}-02$	$1.31314_{D}-02$
5.250	$1.20894_{D}-02$	$1.15508_{D}-02$	$1.11102_{D}-02$
5.375	$1.01832_{D}-02$	$9.74742_{D}-03$	$9.38172_{D}-03$
5.500	$8.56267_{D}-03$	$8.21044_{D}-03$	$7.90748_{D}-03$
5.625	$7.18815_{D}-03$	$6.90370_{D}-03$	$6.65314_{D}-03$
5.750	$6.02478_{D}-03$	$5.79527_{D}-03$	$5.58839_{D}-03$
5.875	$5.04215_{D}-03$	$4.85711_{D}-03$	$4.68654_{D}-03$
6.000	$4.21153_{D}-03$	$4.06463_{D}-03$	$3.92421_{D}-03$
6.125	$3.53389_{D}-03$	$3.39654_{D}-03$	$3.28110_{D}-03$
6.250	$2.62192_{D}-03$	$2.83434_{D}-03$	$2.73955_{D}-03$
6.375	$2.47621_{D}-03$	$2.36206_{D}-03$	$2.28433_{D}-03$
6.500	$2.01610_{D}-03$	$1.96599_{D}-03$	$1.90232_{D}-03$
6.625	$1.68583_{D}-03$	$1.63434_{D}-03$	$1.58225_{D}-03$
6.750	$1.39735_{D}-03$	$1.35711_{D}-03$	$1.31454_{D}-03$
6.875	$1.15778_{D}-03$	$1.12556_{D}-03$	$1.09080_{D}-03$
7.000	$9.58469_{D}-04$	$9.32589_{D}-04$	$9.04237_{D}-04$
7.125	$7.92507_{D}-04$	$7.71817_{D}-04$	$7.48714_{D}-04$
7.250	$6.54751_{D}-04$	$6.38173_{D}-04$	$6.19362_{D}-04$
7.375	$5.40425_{D}-04$	$5.27154_{D}-04$	$5.11851_{D}-04$
7.500	$4.45646_{D}-04$	$4.35042_{D}-04$	$4.22604_{D}-04$
7.625	$3.67206_{D}-04$	$3.58712_{D}-04$	$3.48610_{D}-04$
7.750	$3.02304_{D}-04$	$2.95515_{D}-04$	$2.87317_{D}-04$
7.875	$2.48676_{D}-04$	$2.43249_{D}-04$	$2.36601_{D}-04$
8.000	$2.04402_{D}-04$	$2.00067_{D}-04$	$1.94678_{D}-04$
8.125	$1.67884_{D}-04$	$1.64422_{D}-04$	$1.60057_{D}-04$
8.250	$1.37789_{D}-04$	$1.35025_{D}-04$	$1.31493_{D}-04$
8.375	$1.13007_{D}-04$	$1.10803_{D}-04$	$1.07946_{D}-04$
8.500	$9.26230_{D}-05$	$9.08628_{D}-05$	$8.85531_{D}-05$

Table(A1.4)
Hybrid integrals between t

⟨pzpy|pypz⟩	⟨pzpz|pzpz⟩
$2.92905_{\mathrm{D}}-02$	$3.31562_{\mathrm{D}}-02$
$2.50712_{\mathrm{D}}-02$	$2.83237_{\mathrm{D}}-02$
$2.14038_{\mathrm{D}}-02$	$2.41332_{\mathrm{D}}-02$
$1.82284_{\mathrm{D}}-02$	$2.05129_{\mathrm{D}}-02$
$1.54883_{\mathrm{D}}-02$	$1.73960_{\mathrm{D}}-02$
$1.31314_{\mathrm{D}}-02$	$1.47210_{\mathrm{D}}-02$
$1.11102_{\mathrm{D}}-02$	$1.24321_{\mathrm{D}}-02$
$9.38172_{\mathrm{D}}-03$	$1.04788_{\mathrm{D}}-02$
$7.90748_{\mathrm{D}}-03$	$8.81637_{\mathrm{D}}-03$
$6.65314_{\mathrm{D}}-03$	$7.40482_{\mathrm{D}}-03$
$5.58839_{\mathrm{D}}-03$	$6.20905_{\mathrm{D}}-03$
$4.68654_{\mathrm{D}}-03$	$5.19824_{\mathrm{D}}-03$
$3.92421_{\mathrm{D}}-03$	$4.34547_{\mathrm{D}}-03$
$3.28110_{\mathrm{D}}-03$	$3.62742_{\mathrm{D}}-03$
$2.73955_{\mathrm{D}}-03$	$3.02391_{\mathrm{D}}-03$
$2.28433_{\mathrm{D}}-03$	$2.51752_{\mathrm{D}}-03$
$1.90232_{\mathrm{D}}-03$	$2.09332_{\mathrm{D}}-03$
$1.58225_{\mathrm{D}}-03$	$1.73851_{\mathrm{D}}-03$
$1.31454_{\mathrm{D}}-03$	$1.44226_{\mathrm{D}}-03$
$1.09080_{\mathrm{D}}-03$	$1.19507_{\mathrm{D}}-03$
$9.04237_{\mathrm{D}}-04$	$9.89293_{\mathrm{D}}-04$
$7.48714_{\mathrm{D}}-04$	$8.18025_{\mathrm{D}}-04$
$6.19362_{\mathrm{D}}-04$	$6.75795_{\mathrm{D}}-04$
$5.11851_{\mathrm{D}}-04$	$5.57760_{\mathrm{D}}-04$
$4.22604_{\mathrm{D}}-04$	$4.59920_{\mathrm{D}}-04$
$3.48610_{\mathrm{D}}-04$	$3.78916_{\mathrm{D}}-04$
$2.87317_{\mathrm{D}}-04$	$3.11913_{\mathrm{D}}-04$
$2.36601_{\mathrm{D}}-04$	$2.56548_{\mathrm{D}}-04$
$1.94678_{\mathrm{D}}-04$	$2.10844_{\mathrm{D}}-04$
$1.60057_{\mathrm{D}}-04$	$1.73151_{\mathrm{D}}-04$
$1.31493_{\mathrm{D}}-04$	$1.42090_{\mathrm{D}}-04$
$1.07946_{\mathrm{D}}-04$	$1.16518_{\mathrm{D}}-04$
$8.85531_{\mathrm{D}}-05$	$9.54819_{\mathrm{D}}-05$

cont.
two nitrogen atoms.

R.	$\langle pz1sI1spz\rangle$	$\langle pz2sI2spz\rangle$	$\langle pzpxIpxpz\rangle$
8.625	7.58632D-05	7.44593D-05	7.25933D-05
8.750	6.20955D-05	6.09766D-05	5.94699D-05
8.875	5.07980D-05	4.99045D-05	4.86885D-05
9.000	4.15260D-05	4.08151D-05	3.98343D-05
9.125	3.39285D-05	3.33621D-05	3.25713D-05
9.250	2.77050D-05	2.72536D-05	2.66165D-05
9.375	2.26094D-05	2.22504D-05	2.17373D-05
9.500	1.84710D-05	1.81841D-05	1.77703D-05
9.625	1.46794D-05	1.44579D-05	1.41336D-05
9.750	1.17495D-05	1.15765D-05	1.13208D-05
9.875	1.00607D-05	9.91506D-06	9.69810D-06
10.000	8.12063D-06	8.00624D-06	7.83344D-06
10.125	6.60750D-06	6.51627D-06	6.37744D-06
10.250	5.37310D-06	5.30078D-06	5.18930D-06
10.375	4.36785D-06	4.31021D-06	4.22072D-06
10.500	3.54866D-06	3.50302D-06	3.43119D-06
10.625	2.88228D-06	2.84571D-06	2.78810D-06
10.750	2.33969D-06	2.31090D-06	2.26469D-06
10.875	1.89864D-06	1.87574D-06	1.83870D-06
11.000	1.54001D-06	1.52180D-06	1.49220D-06
11.125	1.24871D-06	1.23427D-06	1.21052D-06
11.250	1.01213D-06	1.00068D-06	9.81627D-07
11.375	8.20049D-07	8.10955D-07	7.95702D-07
11.500	6.64186D-07	6.56959D-07	6.44749D-07
11.625	5.37734D-07	5.32009D-07	5.22238D-07
11.750	4.35213D-07	4.30671D-07	4.22855D-07
11.875	3.52117D-07	3.48514D-07	3.42262D-07
12.000	2.84790D-07	2.81943D-07	2.76934D-07
12.125	2.30261D-07	2.28042D-07	2.23999D-07
12.250	1.86112D-07	1.84307D-07	1.81122D-07
12.375	1.50380D-07	1.48949D-07	1.46404D-07
12.500	1.21472D-07	1.20343D-07	1.18305D-07
12.625	9.80905D-08	9.71953D-08	9.55678D-08

Table (A1.4)
Hybrid integrals between t

⟨pzpyIpypz⟩	⟨pzpzIpzpz⟩
7.25933_n-05	7.81912_n-05
5.94699_n-05	6.39899_n-05
4.86885_n-05	5.23364_n-05
3.98343_n-05	4.27767_n-05
3.25713_n-05	3.49435_n-05
2.66165_n-05	2.85280_n-05
2.17373_n-05	2.32768_n-05
1.77703_n-05	1.90117_n-05
1.41336_n-05	1.51062_n-05
1.13208_n-05	1.20880_n-05
9.69810_n-06	1.03490_n-05
7.83344_n-06	8.35184_n-06
6.37744_n-06	6.79392_n-06
5.18930_n-06	5.52376_n-06
4.22072_n-06	4.48921_n-06
3.43119_n-06	3.64666_n-06
2.78810_n-06	2.96096_n-06
2.26469_n-06	2.40331_n-06
1.83870_n-06	1.94983_n-06
1.49220_n-06	1.58118_n-06
1.21052_n-06	1.28184_n-06
9.81627_n-07	1.03877_n-06
7.95702_n-07	8.41461_n-07
6.44749_n-07	6.81377_n-07
5.22238_n-07	5.51549_n-07
4.22855_n-07	4.46304_n-07
3.42262_n-07	3.61017_n-07
2.76934_n-07	2.91930_n-07
2.23999_n-07	2.35986_n-07
1.81122_n-07	1.90703_n-07
1.46404_n-07	1.54060_n-07
1.18305_n-07	1.24419_n-07
9.55678_n-08	1.00451_n-07

cont.
;wo nitrogen atoms.

R.	$\langle pz1sI1spz \rangle$	$\langle pz2sI2spz \rangle$	$\langle pzpxIpxpz \rangle$
12.750	7.91653×10^{-08}	7.84563×10^{-08}	7.71569×10^{-08}
12.875	6.41537×10^{-08}	6.35895×10^{-08}	6.25478×10^{-08}
13.000	4.86624×10^{-08}	4.82442×10^{-08}	4.74650×10^{-08}
13.125	4.15879×10^{-08}	4.12352×10^{-08}	4.05745×10^{-08}
13.250	3.34462×10^{-08}	3.31676×10^{-08}	3.26421×10^{-08}
13.375	2.70501×10^{-08}	2.68287×10^{-08}	2.64080×10^{-08}
13.500	2.17875×10^{-08}	2.16123×10^{-08}	2.12771×10^{-08}
13.625	1.75546×10^{-08}	1.74158×10^{-08}	1.71485×10^{-08}
13.750	1.41405×10^{-08}	1.40307×10^{-08}	1.38176×10^{-08}
13.875	1.13877×10^{-08}	1.13008×10^{-08}	1.11310×10^{-08}
14.000	9.16839×10^{-09}	9.09957×10^{-09}	8.96428×10^{-09}
14.125	7.37981×10^{-09}	7.32533×10^{-09}	7.21756×10^{-09}
14.250	5.93881×10^{-09}	5.89570×10^{-09}	5.80984×10^{-09}
14.375	4.77801×10^{-09}	4.74390×10^{-09}	4.67552×10^{-09}
14.500	3.84328×10^{-09}	3.81628×10^{-09}	3.76183×10^{-09}
14.625	3.09068×10^{-09}	3.06932×10^{-09}	3.02597×10^{-09}
14.750	2.48492×10^{-09}	2.46802×10^{-09}	2.43351×10^{-09}
14.875	1.99745×10^{-09}	1.98407×10^{-09}	1.95661×10^{-09}
15.000	1.60527×10^{-09}	1.59470×10^{-09}	1.57285×10^{-09}
15.125	1.28981×10^{-09}	1.28144×10^{-09}	1.26406×10^{-09}
15.250	1.03613×10^{-09}	1.02952×10^{-09}	1.01569×10^{-09}
15.375	8.32177×10^{-10}	8.26951×10^{-10}	8.15948×10^{-10}
15.500	6.68246×10^{-10}	6.64110×10^{-10}	6.55357×10^{-10}
15.625	5.36511×10^{-10}	5.33237×10^{-10}	5.26277×10^{-10}
15.750	4.30638×10^{-10}	4.28052×10^{-10}	4.22519×10^{-10}
15.875	3.45553×10^{-10}	3.43516×10^{-10}	3.39120×10^{-10}
16.000	2.77312×10^{-10}	2.75692×10^{-10}	2.72185×10^{-10}

Table(A1.4)
Hybrid integrals between t

$\langle pzpy|pypz\rangle$	$\langle pzpz|pzpz\rangle$
$7.71569_{10}-08$	$8.10548_{10}-08$
$6.25478_{10}-08$	$6.56727_{10}-08$
$4.74650_{10}-08$	$4.98028_{10}-08$
$4.05745_{10}-08$	$4.25565_{10}-08$
$3.26421_{10}-08$	$3.42187_{10}-08$
$2.64080_{10}-08$	$2.76700_{10}-08$
$2.12771_{10}-08$	$2.22828_{10}-08$
$1.71485_{10}-08$	$1.79503_{10}-08$
$1.38176_{10}-08$	$1.44568_{10}-08$
$1.11310_{10}-08$	$1.16403_{10}-08$
$8.96428_{10}-09$	$9.37018_{10}-09$
$7.21756_{10}-09$	$7.54091_{10}-09$
$5.80984_{10}-09$	$6.06741_{10}-09$
$4.67552_{10}-09$	$4.88066_{10}-09$
$3.76183_{10}-09$	$3.92519_{10}-09$
$3.02597_{10}-09$	$3.15602_{10}-09$
$2.43351_{10}-09$	$2.53704_{10}-09$
$1.95661_{10}-09$	$2.03901_{10}-09$
$1.57285_{10}-09$	$1.63841_{10}-09$
$1.26406_{10}-09$	$1.31622_{10}-09$
$1.01569_{10}-09$	$1.05719_{10}-09$
$8.15948_{10}-10$	$8.48959_{10}-10$
$6.55357_{10}-10$	$6.81614_{10}-10$
$5.26277_{10}-10$	$5.47158_{10}-10$
$4.22519_{10}-10$	$4.39119_{10}-10$
$3.39120_{10}-10$	$3.52311_{10}-10$
$2.72185_{10}-10$	$2.82669_{10}-10$

cont.
;wo nitrogen atoms.

Appendix(2)

The Algol text of a program to calculate transfer integrals.

(A2.1) Introduction.

(A2.2) Construction of the data tape.

(A2.3) Text of the program.

(A2.1) <u>Introduction.</u>

The program evaluates the transfer integral between one molecule at the origin and another whose coordinates are given on the data tape. The two centre-two electron integrals are input as data for a fixed internuclear distance grid; and the values for any intermediate internuclear distance are obtained by an Aitken interpolation procedure. The one-electron integrals are evaluated analytically within the program using the methods outlined in Appendix(1). The program contains the text of the procedures used to determine the functions An(a) and Bm(b) referred to in the previous Appendix.

Several variations of the program are available, each being designed for a specific problem. The most important of these are:

(i)   A program for those cases in which the second molecule cannot be generated from the first by a symmetry operation, eg:- the unit cell of tetracene contains two molecules that are symmetrically unrelated.

(ii)   A program which allows the molecule at the origin to be rotated slightly about its equilibrium position, and the interaction between this displaced molecule and a second molecule at l,m,n is calculated.

(iii) A program to calculate the pi contribution to the transfer integrals without calculating the one electron integrals.

The output of the program consists of a synopsis of the input data, ie. crystal constants, atomic co-ordinates, Hueckel coefficients etc., which is essentially for checking and identification purposes followed by:

INTERMOLECULAR RESONANCE AND OVERLAP INTEGRALS BETWEEN THE
MOLECULE AT 0,0,0 AND THE MOLECULE AT **,**,**

	ELECTRON(au.)	HOLE(au.)	ELECTRON(eV.)	HOLE(eV.)
GAMMA	********	********	*********	******
RESA	*********	********	*********	*******
RESB	********	********	********	*******
OVERLAP	********	********	*********	*******

In addition to the four columns listed above, the output
contains two others which give the differences between
RESA, RESB and GAMMA, where GAMMA is the electronic contr-
ibution to the transfer integral and RESA, RESB are the
nuclear contributions to the transfer integral assuming
the excess electron(or hole) to be on molecule A or B
respectively.

(A2.2)   Construction of the data tape.

m — If $m < 4$ then the molecule is assumed
to have inversion symmetry, and the co-
ordinates of only half the atoms in the
molecule need to be specified.

DV — A device on which the output is to be read
(usually 30).

pp — The number of points in the integral tables
-1.(Note that there must be the same
number of points in each set of integral
tables.)

N — The number of atoms in the molecule.

mm — An integer fixing the possible types of
interaction.(See text.)

q — The order of the polynomial in the Aitken
interpolation procedure.

H[i]	The molecular orbital coefficients of the excess electron.
HI[i]	The molecular orbital coefficients of the excess hole.
HJ[i]	The electron density for the excess electron.
HK[i]	The electron density for the excess hole. In general HJ[i] = HK[i].
S[i]	Denotes the type of atom i. ie. C = 1, N = 2 and O = 3.
T[i]	The screening parameter of atom i.
Nu[i]	The nuclear charge of atom i.

The above values (H[i] $\rightarrow$ Nu[i]) are fed in for each atom i.

ie.

H[1] HI[1] HJ[1] HK[1] S[1] T[1] Nu[1]

H[2] HI[2] HJ[2] HK[2] S[2] T[2] Nu[2]

.   .   .   .

.   .   .   .

H[N] HI[N] HJ[N] HK[N] S[N] T[N] Nu[N]

XXX[j,i]	A 3×N array containing the atomic co-ordinates of atom i. The values should be fed in as follows:

x1;   y1;   z1;

x2;   y2;   z2;

.   .   .

xN;   yN   zN;

For a molecule possessing a centre of symmetry (m < 4) only the atomic co-ordinates of half the centres need to be specified.

angle[i]	A 1×N array containing the angles between atoms i-1,i and i+1. If i = N then the angle N-1,N,1 should be given and if i = 1 the angle N,1,2. Again if m < 4 only half the angles need be specified.

PCC[i,j]   A 5×pp array containing the hybrid(or coulomb)
            integrals for interactions between atoms
            corrosponding to S = 1. The values are fed
            in in sets of 5 in the order:-

   ⟨py1s1spy⟩   ⟨py2s2spy⟩   ⟨pypxpxpy⟩   ⟨pypypypy⟩   ⟨pypzpzpy⟩

OCC[i,j]   As above except that the ⟨pz----pz⟩ integrals
            replace the ⟨py----py⟩ integrals.

if mm =1 then goto MISS. (ie. The molecule contains one type of
                                     atom only)

if mm > 1 and < 5 and odd, then goto NO NITROGEN.

PCN[i,j]   A 5×pp array containing the hybrid(or coulomb)
            integrals between atoms denoted by S = 1 and
            S = 2 with the potential due to the former.

OCN[i,j]   As above only the ⟨py----py⟩ interactions
            are replaced by ⟨pz----pz⟩.

PNC[i,j]   A 5×pp array containing the hybrid(or coulomb)
            integrals between atoms denoted by S = 1 and
            S = 2 with the potential due to the latter.

ONC[i,j]   As above only the ⟨py----py⟩ interactions
            are replaced by ⟨pz----pz⟩.

PNN[i,j]   A 5×pp array containing hybrid integrals
            between atoms denoted S = 2.

ONN[i,j]   As above only the ⟨py----py⟩ interactions
            are replaced by ⟨pz----pz⟩.

NO NITROGEN:

if mm = 2 then goto MISS. (ie. only two types of atom in the
molecule)

PCO[i,j]   A 5×pp array containing the hybrid(or coulomb)
            integrals between atoms denoted by S = 1 and
            S = 3 with the potential due to the former.

OCO[i,j]   As above only the ⟨py----py⟩ interactions

are replaced by ⟨pz----pz⟩.

POC[i, j]   A 5×pp array containing the hybrid(or coulomb) integrals between atoms denoted by S = 1 and S = 3 with the potential due to the latter.

OOC[i, j]   As above only the ⟨py----py⟩ interactions are replaced by ⟨pz----pz⟩.

POO[i, j]   A 5×pp array containing hybrid integrals between atoms denoted S = 3.

OOO[i, j]   As above only the ⟨py----py⟩ interactions are replaced by ⟨pz----pz⟩.

if mm odd and < 5 then goto MISS.

PNO[i, j]   A 5×pp array containing the hybrid(or coulomb) integrals between atoms denoted by S = 2 and S = 3 with the potential due to the former.

ONO[i, j]   As above only the ⟨py----py⟩ interactions are replaced by ⟨pz----pz⟩.

PON[i, j]   A 5×pp array containing the hybrid(or coulomb) integrals between atoms denoted by S = 2 and S = 3 with the potential due to the latter.

ONO[i, j]   As above only the ⟨py----py⟩ interactions are replaced by ⟨pz----pz⟩.

MISS:

x[i]   A 1×pp array containing the internuclear distances corresponding to the above tables.

REPEAT CALCULATION:

a

if a < 0.0 then goto TERMINATE.

b

c   Crystal constants.

theta

eta

qq	The number of molecules considered in the calculation.
RR	The maximum internuclear distance considered. For values of the internuclear distances $>$ RR the integrals are assumed to be zero.
c1[i]	A 5X1 array containing the contribution of the i-th integral to the potential for atoms with S = 1.
c2[i]	As above for atoms with S = 2.
c3[i]	As above for atoms with S = 3.

These are repeated for the 5 components of the integral tables.

eg. If the carbon atom is assumed to be in the sp2 hybrid state then c1[1] = 2.0 since the 1s electrons are considered to be localized; c1[2] = c1[3] =c1[5] = 1.0 corresponding to the sp2 hybrid and c1[4] = 0.0.

Values derived in a similar manner should be given for c2 and c3. The result would then correspond to the core contribution to the transfer integral. For aromatic hydrocarbons having an even distribution of pi(py) electrons, the total transfer integral can be calculated by setting c1[4] = 1.0(no exchange) or 0.5 (exchange included). However this cannot be applied to heterocyclic molecules. In this case the pi interactions must be calculated seperately.

The ci s are fed in the following order:
c1[1]   c2[1]   c3[1]

.   .   .

c1[5] c2[5] c3[5]

REPEAT FOR ANOTHER MOLECULE OF THE SAME CRYSTAL SYMMETRY SPECIES:

SY[i,j]   A 3×3 array of the symmetry operation which

maps the molecule at (0,0,0) onto the molecule

at (l,m,n).

O[i,j]   The orthogonalization matrix for the crystall-

ographic system.

LL[i]   A vector containing the translational part of

the symmetry operation.

The figures from REPEAT FOR ANOTHER.......SYMMETRY SPECIES are

repeated for each of the qq calculations.

goto REPEAT CALCULATION.

TERMINATE: Program terminated.

(A2.3) Text of the program.

```
begin

real D,E,HH,a,b,c,theta,ALPHA,BETA,eta,esa,esb,ver,

RESA,RESB,OVER,HOLA,HOLB,HOLO,RR,SUM,xx,EE,SUM1  ;

integer l,i,j,N,pp,qq,mm,f1,f2,f3,f4,k,DV,p,q,m  ;

array c1,c2,c3[1:5],AA,BB[0:4],SY,O[1:3,1:3],ll,TR

[1:3]  ;

integer procedure format(str)  ;

string str  ;

format := layout(str)  ;

procedure AITKEN(x,f,n,xx,FF)  ;

value n,f,x,xx  ;

array x,f  ;

integer n  ;

real xx,FF  ;

begin

integer i,j  ;

for j := 0 step 1 until n-1 do

for i := j+1 step 1 until n do

f[i] := ((xx-x[j])×f[i]-(xx-x[i])×f[j])/(x[i]-x[j])  ;

FF := f[n]  ;

end AITKEN  ;

procedure INTERMOL(XX,O,TR,L,SYM,N,M,angle,int,cosa,cosb)  ;

value XX,N,M,L  ;

integer N,M  ;

array XX,O,L,TR,int,cosa,cosb,angle,SYM  ;

begin

real w,w1,r1,r2  ;

integer i,j,p  ;

array X[1:3,1:if M < 4 then 2×N else N],a[1:5,1:3]  ;

if M < 4 then

begin

for i := 1 step 1 until N do

for j := 1 step 1 until 3 do
```

```
begin
angle[i+N] := angle[i]  ;
XX[j,i+N] := -XX[j,i]  ;
end  ;
N := 2xN  ;
end  ;
for i := 1 step 1 until N do
for j := 1 step 1 until 3 do
begin w := 0.0  ;
for p := 1 step 1 until 3 do
w := w+XX[p,i]xSYM[p,j]  ;
X[j,i] := w  ;
end  ;
for i := 1 step 1 until N do
for j := 1 step 1 until 3 do
X[j,i] := X[j,i]+TR[j]xL[j]  ;
for i := 1 step 1 until N do
for j := 1 step 1 until 3 do
begin w := 0.0  ;
w1 := 0.0  ;
for p := 1 step 1 until 3 do
begin w := w+XX[p,i]xO[p,j]  ;
w1 := w1+X[p,i]xO[p,j]  ;
end  ;
XX[j,i] := w  ;
X[j,i] := w1 ;
end  ;
for j := 1 step 1 until N do
begin for p := 1 step 1 until 3 do
begin a[i,p] := XX[p,if j = 1 then N else j-1]-XX[p,j]  ;
```

```
a[2,p] := XX[p,if J = N then 1 else J+1]-XX[p,j] ;

end ;

w := 0.0 ;

w1 := 0.0 ;

for p := 1 step 1 until 3 do

begin w := a[1,p]xa[1,p]+w ;

w1 := a[2,p]xa[2,p]+w1 ;

end ;

r1 := sin(angle[j])xsqrt(wxw1) ;

for i := 1 step 1 until N do

begin for p := 1 step 1 until 3 do

begin a[3,p] := X[p,i] -XX[p,j] ;

a[4,p] := X[p,if i = 1 then N else i-1]-X[p,i] ;

a[5,p] := X[p,if i = N then 1 else i+1]-X[p,i] ;

end ;

w := 0.0 ;

w1 := 0.0 ;

for p := 1 step 1 until 3 do

begin w := w+a[4,p]xa[4,p] ;

w1:=w1+a[5,p]xa[5,p] ;

end ;

r2 := sin(angle[i])xsqrt(wxw1) ;

w := 0.0 ;

for p := 1 step 1 until 3 do

w := w+a[3,p]xa[3,p] ;

int[i,j] := sqrt(w) ;

w := 0.0 ;

w1 := 0.0 ;

for p := 1 step 1 until 3 do

begin
```

```
w := w+a[3,p]x(a[1,if p = 3 then 1 else  p+1]x
    a[2,if p > 1 then p-1 else 3]-a[2,if p = 3 then 1 else p+1]x
    a[1,if p > 1 then p-1 else 3])  ;
    w1:=w1-a[3,p]x(a[4,if p = 3 then 1 else p+1]x
    a[5,if p > 1 then p-1 else 3]-
    a[5,if p = 3 then 1 else p+1]x
    a[4,if p > 1 then p-1 else 3])  ;
    end ;
    cosa[i,j] := w/(r1xint[i,j])  ;
    cosb[i,j] := w1/(r2xint[i,j])  ;
    end
    end
    end  INTERMOL  ;
procedure avector(b,nmax,avalues)  ;
value b,nmax  ;
real b  ;
integer nmax  ;
array avalues  ;
begin
integer m  ;
avalues[0] := exp(-b)/b  ;
if nmax = 0 then goto exit  ;
for m := 1 step 1 until nmax do
avalues[m] := avalues[0]+mxavalues[m-1]/b  ;
exit  :
end avectors  ;
procedure bvector(a,n,b)  ;
value n,a  ;
integer n  ;
real a  ;
```

```
   array b ;
   begin real w,y,sum1    ;
   integer m,i,p  ;
   if abs(a) < 1ₙ-10 then
   begin for i := 0 step 1 until n do
   b[i] := if (i+2)×2 = 1 then 2/(i+1) else 0  ;
   goto exit ;
   end ;
   w := exp(a)  ;
   if abs(a) ≥ (n+n/6+3)/2.3 then
   begin y := 1/w  ;
   b[0] := (w-y)/a  ;
   if n = 0 then goto exit  ;
   for i := 1 step 1 until n do
   begin w := -w  ;
   b[i] := (w-y+i×b[i-1])/a  ;
   end ;
   goto exit  ;
   end ;
   i := n  ;
   sum1 := (-1)↑i×w/a-1/(a×w) ;
   y := 1/a  ;
   m := i  ;
   p := (-1)↑i  ;
   loop :
   p := -p  ;
   y := y×m/a  ;
   sum1 := sum1+y×w×p-y/w  ;
   m := m-1  ;
   if m > 0 then goto loop  ;
   b[i] := sum1  ;
   y := 1/w  ;
```

```
    m := n-1  ;
    if (n+2)×2 ≠ n then w := -w  ;
    for i := m step -1 until 0 do
    begin w := -w  ;
    b[i] := (w+y+axb[i+1])/(i+1)  ;
    end  ;
    exit  :
    end  bvectors  ;
    open(20)  ;
    m := read(20)  ;
    if m = -6 then goto XSGB  ;
    DV := read(20)  ;
    open(DV)  ;
    pp := read(20)  ;
    N := read(20)  ;
    mm := read(20)  ;
    q := read(20)  ;
begin integer array S[1:N]  ;
array angle,T,H,HI[1:N],cosa,cosb,R[1:N,1:N],XXX[1:3,1:N],
x[0:pp],PICC,PICN,PINN,PICO,PINO,PIOO,PINC,PIOC,PION,POCC,
POCN,PONN,POCO,PONO,POOO,POOC,POON,PONC[0:pp],PCC,OCC,PCN,
OCN,PNC,ONC,PNN,ONN,PNO,ONO,PON,OON,POO,OOO,PCO,OCO,POC,
OOC[1:5,0:pp],Nu,HJ,HK[1:N]   ;
switch SWITCH := CCC,CNN,COO,NNN,OOO,NOO  ;
procedure INTERPOLATE(x,F1,F2,P,xx,k,HH,q,EXIT)  ;
value x,xx,F1,F2,P,k,q  ;
integer P,q,k  ;
real xx,HH  ;
array F1,F2,x  ;
label EXIT  ;
```

```
begin real A,F ;
array x1,F3,F4[0:q] ;
integer s,i ;
s := 0 ;
HH := 0.0 ;
for i := 0 step 1 until P-1 do
begin if (x[i] ≥ xx and x[i+1] ≤ xx)
or (x[i] ≤ xx and x[i+1] ≥ xx) then
begin
if i ≥ q/2 and i < P-q/2 then s := i-q/2 else
if i ≥ q/2 and i ≥ P-q/2 then s := P-q-1 else
if i ≤ q/2 then s := 0 ;
goto njirgn ;
end ;
T111 :
end ;
njirgn :
A := D ;
for i := 0 step 1 until q do
begin x1[i] := x[i+s] ;
F3[i] := F1[i+s] ;
F4[i] := F2[i+s] ;
end ;
AITKEN(x1,F3,q,xx,F) ;
HH := HH+A×F ;
AITKEN(x1,F4,q,xx,F) ;
HH := HH+E×F ;
OUT :
goto EXIT ;
end INTERPOLATION ;
```

```
comment N - No of atoms in the molecule.

        PP - No of integrals to fed in-1.

        Q - No of molecules to be considered.

        MM - Denotes type of interaction

           eg MM = 1 ****C - C only.

              MM = 2 ****C - C,C - N,N - N only.

              MM = 3 ****C - C,C - O,O - O only.

              MM = 4 ***any combination of C,N and O  ;

  for i := 1 step 1 until N do

  begin H[i] := read(20)  ;

  HI[i] := read(20)  ;

  HJ[i] := read(20)  ;

  HK[i] := read(20)  ;

  S[i] := read(20)  ;

  T[i] := read(20)  ;

  Nu[i]:= read(20)

  end  ;

  comment HI,H(i) - Huckle Coefficients for the hole and
  electron respectively.

  HK,HJ(i) - Electron densities for the hole and electron
  respectively.

  S(i) - denotes the type of atom i.

  C = 1  N = 2  O = 3

  T(i) - Screening parameter for atom i.

  Nu(i)- Nuclear charge of atom i  ;

  for i := 1 step 1 until (if m < 4 then N/2 else N) do
  for j := 1 step 1 until 3 do

  XXX[j,i] := read(20)  ;

  for i := 1 step 1 until (if m < 4 then N/2 else N) do
  angle[i] := read(20)  ;
```

```
for j := 0 step 1 until pp do

for i := 1 step 1 until 5 do PCC[i,j] := read(20)  ;

for j := 0 step 1 until pp do

for i := 1 step 1 until 5 do OCC[i,j] := read(20)  ;

if mm = 1 then goto MISS  ;

if (mm+2)×2 ≠ mm and mm < 5 then goto No N  ;

for j := 0 step 1 until pp do

for i := 1 step 1 until 5 do PCN[i,j] := read(20)  ;

for j := 0 step 1 until pp do

for i := 1 step 1 until 5 do OCN[i,j] := read(20)  ;

for j := 0 step 1 until pp do

for i := 1 step 1 until 5 do PNC[i,j] := read(20)  ;

for j := 0 step 1 until pp do

for i := 1 step 1 until 5 do ONC[i,j] := read(20)  ;

for j := 0 step 1 until pp do

for i := 1 step 1 until 5 do PNN[i,j] := read(20)  ;

for j := 0 step 1 until pp do

for i := 1 step 1 until 5 do ONN[i,j] := read(20)  ;

No N  :

if mm = 2 then goto MISS  ;

for j := 0 step 1 until pp do

for i := 1 step 1 until 5 do PCO[i,j] := read(20)  ;

for j := 0 step 1 until ppdo

for i := 1 step 1 until 5 do OCO[i,j] := read(20)  ;

for j := 0 step 1 until pp do

for i := 1 step 1 until 5 do POC[i,j] := read(20)  ;

for j := 0 step 1 until pp do

for i := 1 step 1 until 5 do OOC[i,j] := read(20)  ;

for j := 0 step 1 until pp do

for i := 1 step 1 until 5 do POO[i,j] := read(20)  ;
```

```
for J := 0 step 1 until pp do
    for i := 1 step 1 until 5 do OOO[i,j] := read(20)  ;
    if (mm÷2)×2 ≠ mm and mm < 5 then goto MISS  ;
for J := 0 step 1 until pp do
    for i := 1 step 1 until 5 do PNO[i,j] := read(20)  ;
for J := 0 step 1 until pp do
    for i := 1 step 1 until 5 do ONO[i,j] := read(20)  ;
for J := 0 step 1 until pp do
    for i := 1 step 1 until 5 do PON[i,j] := read(20)  ;
for J := 0 step 1 until pp do
    for i := 1 step 1 until 5 do OON[i,j] := read(20)  ;
MISS  :

for i := 0 step 1 until pp do x[i] := read(20)  ;
Repeat Calculation  :
a := read(20)  ;
if a < 0 then goto XSGB  ;
b := read(20)  ;
c := read(20)  ;
theta := read(20)  ;
eta := read(20)  ;
qq := read(20)  ;
RR := read(20)  ;
for i := 1 step 1 until 5 do
begin c1[i] := read(20)  ;
c2[i] := read(20)  ;
c3[i] := read(20)  ;
end  ;
for i := 0 step 1 until pp do
begin PICC[i] := POCC[i] := PICN[i] := POCN[i] := PINC[i]
:= PONC[i] := PINN[i] := PONN[i] := PIOO[i] := POOO[i]
:= PICO[i] := POCO[i] := PIOC[i] := POOC[i] := PINO[i]
:= PONO[i] := PION[i] := POON[i] := 0.0  ;
for J := 1 step 1 until 5 do
```

```
begin
    PICC[1] := PICC[1]+c1[j]×PCC[j,1] ;
    POCC[1] := POCC[1]+c1[j]×OCC[j,1] ;
    if mm = 1 then goto PASS ;
    if(mm+2)×2 ≠ mm and mm < 5 then goto NON 2 ;
    PICN[1] := PICN[1]+c1[j]×PCN[j,1] ;
    POCN[1] := POCN[1]+c1[j]×OCN[j,1] ;
    PINC[1] := PINC[1]+c2[j]×PNC[j,1] ;
    PONC[1] := PONC[1]+c2[j]×ONC[j,1] ;
    PINN[1] := PINN[1]+c2[j]×PNN[j,1] ;
    PONN[1] := PONN[1]+c2[j]×ONN[j,1] ;
NON2 :
    if mm = 2 then goto PASS ;
    PICO[1] := PICO[1]+c1[j]×PCO[j,1] ;
    POCO[1] := POCO[1]+c1[j]×OCO[j,1] ;
    PIOC[1] := PIOC[1]+c3[j]×POC[j,1] ;
    POOC[1] := POOC[1]+c3[j]×OOC[j,1] ;
    PIOO[1] := PIOO[1]+c3[j]×POO[j,1] ;
    POOO[1] := POOO[1]+c3[j]×OOO[j,1] ;
    if (mm+2)×2 ≠ mm and mm < 5 then goto PASS ;
    PINO[1] := PINO[1]+c2[j]×PNO[j,1] ;
    PONO[1] := PONO[1]+c2[j]×ONO[j,1] ;
    PION[1] := PION[1]+c3[j]×PON[j,1] ;
    POON[1] := POON[1]+c3[j]×OON[j,1] ;
PASS :
    end ;
    end ;
f1 := format([2s-nd.d]) ;
f2 := format([5s-nd.ddddd]) ;
f3 := format([6s-d.dddddₚ-nd]) ;
f4 := format([4snd]) ;
```

```
write text(DV,[[4c6s]LATTICE*CONSTANTS[2c11s]A[13s]
B[13s]C[10s]BETA[10s]THETA[2c]]) ;

write(DV,f2,a) ;

write(DV,f2,b) ;

write(DV,f2,c) ;

write(DV,f2,eta) ;

write(DV,f2,theta) ;

write text(DV,[[2c6s]ATOMIC*CO-ORDINATES[2c11s]X[13s]
Y[13s]Z[11s]ANGLE[9s]H(1)[10s]HI(1)[8s]ELEC*DEN[8s]
T(1)[2c]]) ;

for i := 1 step 1 until N do

begin for j := 1 step 1 until 3 do

if m < 4 and i > N+2 then write(DV,f2,-XXX[j,N-i+1])
else write(DV,f2,XXX[j,i]) ;

if m < 4 and i > N+2 then write(DV,f2,angle[N-i+1])
else write(DV,f2,angle[i]) ;

write(DV,f2,H[i]) ;

write(DV,f2,HI[i]) ;

write(DV,f2,HK[i]) ;

write(DV,f2+2,T[i]) ;

end ;

write text(DV,[[2c]]) ;

p := 0 ;

EE := cos(theta) ;

Repeat :

p := p+1 ;

for i := 1 step 1 until 3 do

for j := 1 step 1 until 3 do

SY[j,i] := read(20) ;

for i := 1 step 1 until 3 do
```

```
for j := 1 step 1 until 3 do
O[j,1] := read(20) ;
ll[1] := a ;
LL[2] := b ;
ll[3] := c ;
for i := 1 step 1 until 3 do
TR[i] := read(20) ;
INTERMOL(XXX,O,TR,ll,SY,(if m < 4 then N/2 else N),
m,angle,R,cosa,cosb) ;
SUM1:= HOLA := HOLB := HOLO := SUM := RESA := RESB
:= OVER := 0.0 ;
i := 0 ;
Repeat i :
i := i+1 ;
j := 0 ;
if i = 1 then begin
write text(DV,[[2c3s]INTERMOLECULAR*RESONANCE*AND*OVERLAP
*INTEGRALS*BETWEEN*THE*MOLECULE*AT*0,0,0*AND[2c3s]THE*
MOLECULE*AT*]) ;
write(DV,f1,TR[1]) ;
write(DV,f1,TR[2]) ;
write(DV,f1+2,TR[3]) ;
end ;
Repeat j :
j := j+1 ;
E := cosa[j,i]xcosb[j,i] ;
if abs(E) > 1 then
begin
write text(30,[OVERFLOW[4s]]);
write(30,format([2snd]),i);
write(30,format([2sndc]),j);
if E > 1 then E := 1 else E := -1;
```

```
    end;
    D := EE-E  ;
    xx := R[j,i]  ;
    if xx > RR then goto BYE PASS  ;
    if abs(D) < 1ɒ-10 then k := 3 else k := 2  ;
    l := S[i]×S[j]  ;
    if l = 9 then l := 5  ;
    goto SWITCH[l]  ;
    CCC  :
    INTERPOLATE(x,PICC,POCC,pp,xx,k,HH,q,EXIT)  ;
    CNN  :
    if S[j] < S[i] then
    INTERPOLATE(x,PICN,POCN,pp,xx,k,HH,q,EXIT)
    else INTERPOLATE(x,PINC,PONC,pp,xx,k,HH,q,EXIT)  ;
    COO  :
    if S[j] < S[i] then
    INTERPOLATE(x,PICO,POCO,pp,xx,k,HH,q,EXIT)
    else INTERPOLATE(x,PIOC,POOC,pp,xx,k,HH,q,EXIT)  ;
    NNN  :
    INTERPOLATE(x,PINN,PONN,pp,xx,k,HH,q,EXIT)  ;
    OOO  :
    INTERPOLATE(x,PIOO,POOO,pp,xx,k,HH,q,EXIT)  ;
    NOO  :
    if S[j] < S[i] then
    INTERPOLATE(x,PINO,PONO,pp,xx,k,HH,q,EXIT)
    else INTERPOLATE(x,PION,POON,pp,xx,k,HH,q,EXIT)  ;
    EXIT  :
    SUM := HH×H[i]×H[j]×HJ[j]+SUM  ;
    SUM1 := SUM1+HI[i]×HI[j]×HK[j]×HH  ;
    ALPHA := (T[i]+T[j])×xx/2  ;
    BETA := (T[j]-T[i])×xx/2  ;
```

```
avector(ALPHA,4,AA) ;

bvector(BETA,4,BB) ;

esa := (xxXxxXT[i]XT[J])↑2.5×(((AA[3]-AA[1])×(BB[0]-BB[2])
    -(AA[2]-AA[0])×(BB[1]-BB[3]))×D+2×E×(AA[1]×BB[0]-AA[3]×BB[2]
    -AA[0]×BB[1]+AA[2]×BB[3]))/(16xxx) ;

esb := (xxXxxXT[i]XT[J])↑2.5×(((AA[3]-AA[1])×(BB[0]-BB[2])
    +(AA[2]-AA[0])×(BB[1]-BB[3]))×D+2×E×(AA[1]×BB[0]-AA[3]×BB[2]
    +AA[0]×BB[1]-AA[2]×BB[3]))/(16xxx) ;

ver := (xxXxxXT[i]XT[J])↑2.5×(((AA[4]-AA[2])×BB[0]-(AA[4]
    -AA[0])×BB[2]+(AA[2]-AA[0])×BB[4])×D+E×2×(AA[2]×BB[0]-AA[
    4]×BB[2]-AA[0]×BB[2]+AA[2]×BB[4]))/32 ;

RESA := RESA+H[i]×H[J]×Nu[J]×esa ;

RESB := RESB+H[i]×H[J]×Nu[i]×esb ;

OVER := OVER+H[i]×H[J]×ver ;

HOLA := HOLA+HI[i]×HI[J]×Nu[J]×esa ;

HOLB := HOLB+HI[i]×HI[J]×Nu[i]×esb ;

HOLO := HOLO+HI[i]×HI[J]×ver ;

BYEPASS :

if J < N then goto Repeat j ;

if i < N then goto Repeat i ;

write text(DV,[[17s]ELECTRON[12s]HOLE[2c]]) ;

write text(DV,[[3s]GAMMA[3s]]) ; write(DV,f3,SUM) ;

write(DV,f3,SUM1) ;

SUM := 27.21×SUM;

SUM1 := 27.21×SUM1;

write(30,f3,SUM);

write(30,f3+2,SUM1);

write text(DV,[[3s]RESA[4s]]) ;

write(DV,f3,RESA) ;

write(DV,f3,HOLA) ;

RESA := 27.21×RESA;

HOLA := 27.21×HOLA;
```

```
        write(DV,f3,RESA);
    write(DV,f3,HOLA);
    write(DV,f3,SUM-RESA);
    write(DV,f3+2,SUM1-HOLA);
    write text(DV,[[3s]RESB[4s]]) ;
    write(DV,f3,RESB)  ;
    write(DV,f3,HOLB)  ;
    RESB := 27.21×RESB;
    HOLB := 27.21×HOLB;
    write(DV,f3,RESB);
    write(DV,f3+2,HOLB);
    write(DV,f3,SUM-RESB);
    write(DV,f3+2,SUM1-HOLB);
    write text(DV,[[3s]OVERLAP]) ;
    write(DV,f3,OVER)  ;
    write(DV,f3+2,HOLO)  ;
    1 := 0  ;
    if p < qq then goto Repeat  ;
    goto Repeat Calculation  ;
    end ;
XSGB  :
close(20)  ;
close(DV)  ;
end PROGRAM
```

Appendix(3)

Calculation of the Energy band structure and the

elements of the mobility tensor in both the Bloch

and localized representations.

(A3.1) General.

(A3.2) Construction of the data tape.

    (i) The data tape for the first program.

    (ii)The data tape for the second program.

(A3.3) The text of the programs.

(A3.1) <u>General.</u>

In this appendix two computer programs are given which have been used to calculate the components of the mobility tensor in organic molecular crystals having monoclinic structures, space group $P2_1/a$, with two molecules per unit cell. The first, in KDF9 Algol, calculates the energy band structure and carrier mobilities, in both the mean free time and free path approximations, from parameters input as data. Several alternative programs have been developed for molecules having different space groups, eg. phenanthrene, and for the case where the molecular energy levels giving rise to the energy bands are degenerate.

The output from the program consists of the energy band structure along the three crystallographic axes and the components of the mobility tensor with respect to this system and also an orthogonal system defined by the vectors <u>a</u>,<u>b</u> and <u>a</u>×<u>b</u>. This program can also be used to calculate the components of the mobility tensor within the Glaeser and Berry scheme, however the results quoted in this thesis were obtained using the second program. This program, written in 903 Algol, calculates the components of the mobility tensor in the localized reprent- ation using both the Glaeser and Berry and Gosar and Choi models. As with the first program several alternative programs have been written for different space groups. An example of the output from this program is given in section(2.111).

(A3.2) <u>Constuction of the data tape.</u>

(A3.2.1) Data tape for the first program.

A	The vibrational overlap factor.
q	The number of points for the integration over ki.
r	The number of points for the integration over kj.
s	The number of points for the integration over kj.

hole	An integer = 1 for hole and any other number for a electron.
E2 → E14	The transfer integrals(see fig(3.1)).
n	The number of points used in the band structure plot.
Temp	The temperature.
aa	
bb	
cc	The crystal parameters.
alpha	Usually 90 .
beta	
gamma	Usually 90 .
ni	An integer = 1 for calculations on the band model only, = 2 for calculations on the hopping model only and any other number for both.

To terminate the program set E2 > 1ₓ8.

(A3.2.11$) Data tape for the second program.

T[i]	The transfer integrals E2,E3,E4,E5,E6,E9 and E10.
A	
B	The crystal parameters.
C	
BETA	
TEMP	The temperature.
	The polarization factor.
	The phonon interaction factor.

```
begin
real E2,E3,E4,E5,E6,E7,E8,E9,E10,E11,E12,E13,E14,temp,A,B,C,D,E,
F,G,H,alpha,gamma,aa,bb,cc,beta,sum1,sum2  ;
integer even1,evenj,evenk,r,s,p,q,m,n,ni,nj,nk,u,v,f1,f2,f3,
f4,hole  ;
array o,mu,vec[1:3,1:3],val[1:3],band[1:3]  ;
integer procedure format(str)  ;
string str  ;
format := layout(str)  ;


insert eigenvectors:


open(20)  ;
open(30)  ;
repeat  :
A  := read(20)  ;
q  := read(20)  ;
r  := read(20)  ;
s  := read(20)  ;
hole := read(20)  ;
E2  := read(20)×1₁₀-4×A  ;
if E2 > 998 then goto LLL  ;
E3  := read(20)×1₁₀-4×A  ;
E4  := read(20)×1₁₀-4×A  ;
E5  := read(20)×1₁₀-4×A  ;
E6  := read(20)×1₁₀-4×A  ;
E7  := read(20)×1₁₀-4×A  ;
E8  := read(20)×1₁₀-4×A  ;
E9  := read(20)×1₁₀-4×A  ;
E10:= read(20)×1₁₀-4×A  ;
E11:= read(20)×1₁₀-4×A  ;
E12:= read(20)×1₁₀-4×A  ;
```

```
E13:= read(20)×1ₙ-4×A  ;

E14:= read(20)×1ₙ-4×A  ;

n   := read(20)  ;

temp := read(20)  ;

aa  := read(20)  ;

bb  := read(20)  ;

cc  := read(20)  ;

alpha:= read(20)  ;

beta := read(20)  ;

gamma:= read(20)  ;

ni  := read(20)  ;


for p := 1 step 1 until 3 do
for v := 1 step 1 until 3 do
o[p,v] := 0.0  ;
sum1 := (cos(alpha)×cos(gamma)-cos(beta))/(sin(alpha)×sin(gamma));
o[1,1] := sin(gamma)  ;
o[1,3] := -sin(alpha)×sum1  ;
o[2,1] := cos(gamma)  ;
o[2,2] := 1  ;
o[2,3] := cos(alpha)  ;
o[3,3] := sin(alpha)×sqrt(1-sum1×sum1)  ;
if ni = 1 then goto Band only  ;
begin
array tr[1:3],x[1:7,1:3],tor,t[1:7],mu[1:3,1:3]  ;
integer array w[1:7]  ;
switch sw := L2,L3,L4,L5,L6,L7,L8  ;
integer i,j,k;
t[1] := E2  ;
t[2] := E3  ;
t[3] := E4  ;
```

```
    t[4] := E5 ;
    t[5] := E6 ;
    t[6] := E9 ;
    t[7] := E10 ;
    sum1 := 10000/A ;
,  for u := 1 step 1 until 7 do
    t[u] := t[u]xsum1 ;
    for u := 1 step 1 until 7 do
    for v := 1 step 1 until 3 do
    x[u,v] := 0.0 ;
    X[3,1] := X[1,1] := cos(beta)xcc;
    X[3,2] := X[2,2] := bb;
    X[5,1] := aa+X[1,1];
    X[6,1] := 0.5xaa;
    X[6,2] := X[7,2] := 0.5xbb;
    X[7,1] := 0.5xaa+X[1,1];
    X[1,3] := X[3,3] := X[5,3] := X[7,3] := ccxsin(beta);
    w[1] := w[2] := w[4] := w[5] := 2 ;
    w[3] := w[6] := w[7] := 4 ;
    for p := 1 step 1 until 7 do
    t[p] := abs(t[p])/10.3376 ;
    sum1 := 0.0 ;
    for p := 1 step 1 until 7 do
    sum1 := sum1+t[p]xw[p] ;
    for p := 1 step 1 until 7 do
    tor[p] := t[p]xw[p]/sum1 ;
    sum2 := 0.0 ;
    for p := 1 step 1 until 7 do
    sum2 := sum2+tor[p]xt[p] ;
    for p := 1 step 1 until 3 do
    for u := p step 1 until 3 do
begin
```

```
    sum1 := 0.0  ;

    for v := 1 step 1 until 7 do
    sum1 := sum1+tor[v]xx[v,u]xx[v,p]   ;
    mu[p,u] := mu[u,p] := sum2xsum1/(1.723312xtemp)  ;
    end  ;
    f1 := format([3s-ndd.ddd])  ;
    f2 := format([3snd])  ;
    write text(30,[[pc4s]JUMP*PROBABILITIES*AND*JUMP*FREQUENCIES
    *BETWEEN*THE*MOLECULE*AT*(0,0,0)*AND*NEAR*NEIGHBOURS[2c3s]
    MOL[4s]TOR(I)[5s]1/T(I)[2c]])  ;
    for u := 1 step 1 until 7 do
    begin
    write(30,f2,u)  ;
    write(30,f1,tor[u])  ;
    write(30,f1+2,t[u])  ;
    end  ;
    sum1 := 0.0  ;
    for p := 1 step 1 until 7 do
    sum1 := sum1+t[p]  ;
    write text(30,[[4s]AVERAGE*JUMP*FREQUENCY])  ;
    write(30,f1,sum1/7)  ;
    write text(30,[[2c4s]NO*OF*JUMPS])  ;
    write(30,f1+2,sum2)  ;
    write text(30,[[4s]MOBILITY*TENSOR[2c]])  ;
    for u := 1 step 1 until 3 do
    for v := 1 step 1 until 3 do
    write(30,if v = 3 then f1+2 else f1,mu[u,v])  ;
    write text(30,[[4s]EIGENVALUES*OF*MOBILITY*TENSOR[2c]])  ;
    eigenvectors(mu,3,3,val,vec)  ;
    for p := 1 step 1 until 3 do
    write(30,f1,val[p])  ;
```

```
write text(30,[[2c4s]RATIOS]);
write(30,f1,mu[1,1]/mu[2,2]);
write(30,f1+2,mu[3,3]/mu[2,2]);
write text(30,[[2c4s]EIGENVECTORS*OF*THE*MOBILITY*TENSOR[2c
4s]DIRECTION*COSINES[2c]]) ;
for u := 1 step 1 until 3 do
for v := 1 step 1 until 3 do
write(30,if v = 3 then f1+2 else f1,vec[u,v]) ;
write text(30,[[4s]ANGLES[2c]]) ;
for u := 1 step 1 until 3 do
for v := 1 step 1 until 3 do
write(30,if v = 3 then f1+2 else f1,
arctan(sqrt(abs(1-vec[u,v]↑2))/vec[u,v])×57.29577951) ;
write text(30,[[p]]) ;
end  Calculation of mobility tensor and principle axes
of th mobility tensor by the hopping model  ;


Band only  :
if ni = 2 then goto Hop only  ;
begin
real xi,xj,xk,x1,x2,x3,x4,y1,y2,y3,y4,z1,z2,z3,z4,gridi,gridj,
gridk,ui,uj,uk,li,lj,lk,Ep,Em,ki,kj,kk,STEP,EA,AE,SPLITA,EB,BE,
SPLITB,EC,CE,SPLITC,I,J,KA,KB,KC,KA2,KB2,K3B2,Emax,path  ;
array sum,sumi,sumj,sumk[1:6,1:6],dEp[1:3],dEm[1:3]  ;
Emax := 0.0  ;
f3 := format([2sd.ddd]) ;
f4 := format([4s-d.dddd])  ;
write text(30,[[p2c]EXCESS*]) ;
if hole = 1 then write text(30,[HOLE])
else write text(30,[ELECTRON]) ;
write text(30,[[s]BAND*AND*BAND*SPLITTINGS*IN*THE*
INVERSE*A,B*AND*C*DIRECTIONS[2c15s]POSITIVE**NEGATIVE
```

```
[14s]POSITIVE**NEGATIVE[14s]POSITIVE**NEGATIVE[2c8s]

X[11s]A[11s]A[6s]SPLITTING[5s]B[11s]B[6s]SPLITTING[

5s]C[11s]C[6s]SPLITTING[2c]]) ;

A := 2x(E2+E3+2xE4) ;

B := 2x(E5+E6+2xE7+2xE8+E12+2xE13) ;

C := 4x(E9+E10+E11+E14) ;

D := 2x(E2+E5+E6+E12) ;

E := 2x(E3+2xE4+2xE7+2xE8+2xE13) ;

F := 4x(E9+E10+E11) ;

G := 2x(E3+E5+2xE7+2xE9) ;

H := 2x(E2+2xE4+E6+2xE8+E12+2xE13+2x(E10+E11+E14)) ;

I := 2x(E3+E5+2xE7-2xE9) ;

J := 2x(E2+2xE4+E6+2xE8+E12+2xE13-2x(E10+E11+E14)) ;

gridi := 3.1415926536/n ;

f2 := format([4s-d.ddddn-nd]) ;

n := -1 ;

for STEP := 0.0 step gridi until 3.142 do

begin n := n+1 ;

KA := KB := KC := STEP ;

write(30,f4,STEP) ;

KA2 := KA/2 ;

KB2 := KB/2 ;

K3B2:= KBx3/2 ;

EA := A+Bxcos(KA)+Cxcos(KA2) ;

AE := A+Bxcos(KA)-Cxcos(KA2) ;

SPLITA := EA-AE ;

if n = 0 then

begin x1 := EA ;

x2 := AE ;

end ;
```

```
write(30,f4,EA) ;

write(30,f4,AE) ;

write(30,f4,SPLITA) ;

EB := D+Excos(KB)+Fxcos(KB2)+4xE14xcos(K3B2)  ;

BE := D+Excos(KB)-Fxcos(KB2)-4xE14xcos(K3B2)  ;

SPLITB := EB-BE ;

if n = 0 then

begin y1 := EB ;

y2 := BE ;

end ;

write(30,f4,EB) ;

write(30,f4,BE) ;

write(30,f4,SPLITB) ;

EC := G+Hxcos(KC) ;

CE := I+Jxcos(KC) ;

SPLITC := EC-CE ;

if n = 0 then

begin z1 := EC ;

z2 := CE ;

end ;

write(30,f4,EC) ;

write(30,f4,CE) ;

write(30,f4+2,SPLITC) ;

end ;

x1 := abs(EA-x1) ;

x2 := abs(AE-x2) ;

y1 := abs(EB-y1) ;

y2 := abs(BE-y2) ;

z1 := abs(EC-z1) ;

z2 := abs(CE-z2) ;

band[1] := if x1 > x2 then x1 else x2;

band[2] := if y1 > y2 then y1 else y2;
```

```
band[3] := if z1 > z2 then z1 else z2;
writetext(30,[[2c2s]BANDWIDTH]) ;
write(30,f4,x1) ;
write(30,f4,x2) ;
write text(30,[[11s]]) ;
write(30,f4,y1) ;
write(30,f4,y2) ;
write text(30,[[11s]]) ;
write(30,f4,z1) ;
write(30,f4+2,z2) ;
write text(30,[[p]]) ;
ui := 3.1415926536/aa ;
li := -ui ;
gridi := 2xui/q ;
ui := ui+gridi/10 ;
uj := 3.1415926536/bb ;
lj := -uj ;
gridj := 2xuj/r ;
uj := uj+gridj/10 ;
uk := 3.1415926536/cc ;
lk := -uk ;
gridk := 2xuk/s ;
uk := uk+gridk/10 ;
ni := -1 ;
temp := 8.61260ь-5xtemp ;
eveni := 1 ;
for p := 1 step 1 until 6 do
for v := p step 1 until 6 do
sumi[p,v] := sumi[v,p] := 0.0 ;
for ki := li step gridi until ui do
begin
ni := ni+1 ;
```

```
   x1  := k1xaa  ;

   x1  := cos(x1)  ;

   x2  := sin(x1)  ;

   x3  := cos(x1/2)  ;

   x4  := sin(x1/2)  ;

   nj  := -1  ;

   evenj := 1  ;

   for p := 1 step 1 until 6 do

   for u := p step 1 until 6 do

   sumj[p,u] := sumj[u,p] := 0.0  ;

   for kj := 1j step gridj until uj do

   begin nj := nj+1  ;

   xj  := kjxbb  ;

   y1  := cos(xj)  ;

   y2  := sin(xj)  ;

   y3  := cos(xj/2)  ;

   y4  := sin(xj/2)  ;

   nk  := -1  ;

   evenk := 1  ;

   for p := 1 step 1 until 6 do

   for u := p step 1 until 6 do

   sumk[p,u] := sumk[u,p] := 0.0  ;

   for kk := 1k step gridk until uk do

   begin nk := nk+1  ;

   xk := kkxcc  ;

   z1  := cos(xk)  ;

   z2  := sin(xk)  ;

   Ep := E2xz1+E3xy1+2xE4xy1xz1+E5xx1+E6x(z1xx1-z2xx2)

   +2xE7xx1xy1+2xE8x(x1xy1xz1-x2xy1xz2)

   +2xE9xx3xy3+2xE10x(z1xx3xy3-x4xy3xz2)+2xE14x(y1xy3-y2xy4)x

   (x3xz1-x4xz2)  ;
```

```
Em  := Ep-4xE9xx3xy3-4xE10x(z1xx3xy3-x4xy3xz2)-4xE14x
(y1xy3-y2xy4)x(x3xz1-x4xz2)  ;
Ep  := 2xEp  ;
Em  := 2xEm  ;
if hole = 1 then
begin
Ep  := Emax-Ep  ;
Em  := Emax-Em
end  ;
dEp[1] := 2xaax(-E5xx2-E6x(z1xx2+z2xx1)
-2xE7xx2xy1-2xE8x(x2xy1xz1+x1xy1xz2)-E9xx4xy3-E10x
(z1xx4xy3+x3xy3xz2)-E14x(y1xy3-y2xy4)x(x4xz1-x3xz2))x1ₒ-8;
dEm[1] := dEp[1]+4xaax(E9xx4xy3+E10x(z1xx4xy3+x3xy3xz2)
+E14x(y1xy3-y2xy4)x(x4xz1-x3xz2))x1ₒ-8  ;
dEp[2] := 2xbbx(-E3xy2-2xE4xy2xz1-2xE7xx1xy2-2xE8x(x1xy2xz1
-x2xy2xz2)-E9xx3xy4-E10x(z1xx3xy4-x4xy4xz2)-1.5xE14x(y2xy3+
y1xy4)x(x3xz1-x4xz2))x1ₒ-8;
dEm[2] := dEp[2]+4xbbx(E9xx3xy4+E10x(z1xx3xy4-x4xy4xz2)+1.5x
E14x(y2xy3+y1xy4)x(x3xz1-x4xz2))x1ₒ-8;
dEp[3] := 2xccx(-E2xz2-2xE4xy1xz2-E6x(z2xx1+z1xx2)-2xE8x(
x1xy1xz2+x2xy1xz1)-2xE10x(z2xx3xy3+x4xy3xz1)-2xE14x(y1xy3-
y2xy4)x(x3xz2+x4xz1))x1ₒ-8;
dEm[3] := dEp[3]+8x(E10x(z2xx3xy3+x4xy3xz1)+E14x(y1xy3-y2xy4)x
(x3xz2+x4xz1))xccx1ₒ-8  ;
z3 := exp(-Ep/temp)  ;
z4 := exp(-Em/temp)  ;
sum[4,1] := z3+z4  ;
for u := 1 step 1 until 3 do
for v := u step 1 until 3 do
 sum[u,v] := sum[v,u] := dEp[u]xdEp[v]xz3+dEm[u]xdEm[v]xz4  ;
path := 0.0  ;
for u := 1 step 1 until 3 do
```

```
    path := path+abs(dEp[u])  ;
    z3 := z3/path  ;
    path := 0.0  ;
    for u := 1 step 1 until 3 do
    path := path+abs(dEm[u])  ;
    z4 := z4/path  ;
    for u := 4 step 1 until 6 do
    for v := u step 1 until 6 do
    sum[u,v] := sum[v,u] := dEp[u-3]×dEp[v-3]×z3+dEm[u-3]×dEm[v-3]×z4;
    if nk = q then evenk := 1  ;
    for u := 1 step 1 until 3 do
    for v := u step 1 until 4 do
    sumk[u,v] := sumk[v,u] := sumk[u,v]+evenk×sum[v,u]  ;
    for u := 4 step 1 until 6 do
    for v := u step 1 until 6 do
    sumk[u,v] := sumk[v,u] := sumk[u,v]+evenk×sum[v,u]  ;
    if evenk = 1 or evenk = 4 then evenk := 2 else evenk := 4;
    end Calculation of elements for integration over kj;
    if nj = r then evenj := 1  ;
    for u := 1 step 1 until 3 do
    for v := u step 1 until 4 do
    sumj[u,v] := sumj[v,u] := sumk[u,v]×evenj+sumj[u,v];
    for u := 4 step 1 until 6 do
    for v := u step 1 until 6 do
    sumj[u,v] := sumj[v,u] := sumk[u,v]×evenj+sumj[u,v];
    if evenj = 1 or evenj = 4 then evenj := 2 else evenj := 4;
    end Calculation of elements for integration over ki  ;
    if ni = s then eveni := 1  ;
    for u := 1 step 1 until 3 do
    for v := u step 1 until 4 do
    sumi[u,v] := sumi[v,u] := sumj[u,v]×eveni+sumi[u,v];
    for u := 4 step 1 until 6 do
```

```
for v := u step 1 until 6 do

sum1[u,v] := sum1[v,u] := sumj[u,v]×even1+sum1[u,v];

if even1 = 1 or even1 = 4 then even1 := 2 else even1 := 4;

end Integration over k1  ;

for u := 1 step 1 until 3 do

for v := 1 step 1 until 3 do

sum1[u,v] := sum1[u,v]/(sum1[4,1]×4.32648ᴅ-21)  ;

for u := 4 step 1 until 6 do

for v := 4 step 1 until 6 do

sum1[u,v] := sum1[u,v]/(sum1[4,1]×6.581122ᴅ-11)  ;

write text(30,[[4s]COMPONENTS*OF*THE*MOBILITY*TENSOR*W.R.T.

*THE*CRYSTALOGRAPHIC*AXES*IN*THE*MEAN*FREE*TIME*APPROXIMATI

ON[2c]])  ;

for u := 1 step 1 until 3 do

for v := 1 step 1 until 3 do

write(30,if v = 3 then f2+2 else f2,sum1[u,v])  ;

write text(30,[[4s]COMPONENTS*OF*THE*MOBILITY*TENSOR*W.R.T.

*ORTHOGONAL*AXES*IN*THE*MEAN*FREE*TIME*APPROXIMATION[2c]])  ;

for u := 1 step 1 until 3 do

for v := 1 step 1 until 3 do

begin

sum1 := 0.0  ;

for r := 1 step 1 until 3 do

for p := 1 step 1 until 3 do

sum1 := sum1+o[v,p]×o[u,r]×sum1[p,r];

mu[u,v] := sum1;

write(30,if v = 3 then f2+2 else f2,mu[u,v])  ;

end  ;

write text(30,[[2c4s]RATIOS]);

write(30,f2,mu[1,1]/mu[2,2]);

write(30,f2+2,mu[3,3]/mu[2,2]);
```

```
write text(30,[[4s]LOWER*LIMITS*OF*THE*COMPONENTS*OF*THE*
MOBILITY*TENSOR*ALONG*THE*ORTHOGONAL*AXES[2c]]);
for u := 1 step 1 until 3 do
write(30,if u = 3 then f2+2 else f2, 6.5811₁₀-6 xmu[u,u]/(band[u]xtemp));
band[1] := aa;
band[2] := bb;
band[3] := cc;
write text(30,[[4s]EIGENVALUES*OF*THE*MOBILITY*TENSOR[2c]]) ;
eigenvectors(mu,3,3,val,vec) ;
for u := 1 step 1 until 3 do
write(30,f2,val[u]) ;
write text(30,[[2c4s]EIGENVECTORS*OF*THE*MOBILITY*TENSOR[2c
4s]DIRECTION*COSINES[2c]]) ;
for u := 1 step 1 until 3 do
for v := 1 step 1 until 3 do
write(30,if v = 3 then f2+2 else f2,vec[u,v]) ;
write text(30,[[4s]ANGLES[2c]]) ;
for u := 1 step 1 until 3 do
for v := 1 step 1 until 3 do
write(30,if v = 3 then f2+2 else f2,
arctan(sqrt(abs(1-vec[u,v]↑2))/vec[u,v])x57.29577951) ;
write text(30,[[p4s]COMPONENTS*OF*THE*MOBILITY*TENSOR*W.R.T.
*CRYSTALOGRAPHIC*AXES*IN*THE*MEAN*FREE*PATH*APPROXIMATION[2c]]). ;
for u := 4 step 1 until 6 do
for v := 4 step 1 until 6 do
write(30,if v = 6 then f2+2 else f2,sum1[u,v]) ;
write text(30,[[4s]COMPONENTS*OF*THE*MOBILITY*TENSOR*
W.R.T.*ORTHOGONAL*AXES*IN*THE*MEAN*FREE*PATH*APPROXIMATION
[2c]]) ;
for u := 4 step 1 until 6 do
for v := 4 step 1 until 6 do
begin
```

```
sum1 := 0.0  ;

for r := 4 step 1 until 6 do

for p := 4 step 1 until 6 do

sum1 := sum1+o[u-3,p-3]xo[v-3,r-3]xsum1[p,r];

mu[u-3,v-3] := sum1  ;

write(30,if v = 6 then f2+2 else f2,mu[u-3,v-3])  ;

end  ;

write text(30,[[2c4s]RATIOS]);

write(30,f2,mu[1,1]/mu[2,2]);

write(30,f2+2,mu[3,3]/mu[2,2]);

write text(30,[[4s]LOWER*LIMITS*OF*THE*COMPONENTS*OF*THE*
MOBILITY*TENSOR*ALONG*THE*ORTHOGONAL*AXES[2c]]);

for u := 1 step 1 until 3 do

write(30,if u = 3 then f2+2 else f2,'e3 rxband[u]xmu[u,u]/Temp);
write text(30,[[4s]EIGENVALUES*OF*THE*MOBILITY*TENSOR[2c]])  ;

eigenvectors(mu,3,3,val,vec)  ;

for u := 1 step 1 until 3 do

write(30,f2,val[u])  ;

write text(30,[[2c4s]EIGENVECTORS*OF*THE*MOBILITY*TENSOR[2c
4s]DIRECTION*COSINES[2c]])  ;

for u := 1 step 1 until 3 do

for v := 1 step 1 until 3 do

write(30,if v = 3 then f2+2 else f2,vec[u,v])  ;

write text(30,[[4s]ANGLES[2c]])  ;

for u := 1 step 1 until 3 do

for v := 1 step 1 until 3 do

write(30,if v = 3 then f2+2 else f2,
arctan(sqrt(abs(1-vec[u,v]↑2))/vec[u,v])x57.29577951)  ;
end Calculation of mobility within the band approximation  ;
Hop only  :


goto repeat  ;
```

```
LLL   :

close(20)  ;

close(30)  ;

end Program
```

```
      KR0069;
      "BEGIN"
      "REAL"  A,B,C,BETA,SUM1,SUM2,TEMP;
      "INTEGER" I,J,K ;
      "ARRAY"  TOR,T,W[1:7],X[1:7,1:3],MU[1:3,1:3]  ;
      "SWITCH" F := REPEAT  ;
      REPEAT  :
      "FOR" I := 1 "STEP" 1 "UNTIL" 7 "DO"
      "READ" T[I]  ;
      "READ" A,B,C,BETA,TEMP  ;
      "FOR" I := 1 "STEP" 1 "UNTIL" 7 "DO"
      "FOR" J := 1 "STEP" 1 "UNTIL" 3 "DO"
      X[I,J] := 0.0;
      X[3,1] := X[1,1] := C*COS(BETA)  ;
      X[3,2] := X[2,2] := B  ;
      X[5,1] := A+X[1,1]  ;
      X[6,1] := 0.5*A  ;
      X[6,2] := X[7,2] := 0.5*B  ;
      X[7,1] := 0.5*A+X[1,1]  ;
      X[1,3] := X[3,3] := X[5,3] := X[7,3] := C*SIN(BETA)  ;
      W[1] := W[2] := W[4] := W[5] := 2  ;
      W[3] := W[6] := W[7] := 4  ;
      "PRINT" 'MOLECULAR INTEGRALS
       (0,0,1)  (0,1,0)  (0,1,1)  (1,0,0)  (1,0,1)  (½,½,0)  (½,½,1)
      '  ;
      "FOR" I := 1 "STEP" 1 "UNTIL" 7 "DO"
      "PRINT" SAMELINE,ALIGNED(4,4),T[I];
      "PRINT" 'L2' ;
      "FOR" I := 1 "STEP" 1 "UNTIL" 7 "DO"
      T[I] := ABS(T[I])/10.3376  ;
      SUM1 := 0.0  ;
      "FOR" I := 1 "STEP" 1 "UNTIL" 7 "DO"
      SUM1 := SUM1 +T[I]*W[I]  ;
      "FOR" I := 1 "STEP" 1 "UNTIL" 7 "DO"
      TOR[I] := T[I]*W[I]/SUM1  ;
      SUM2 := 0.0  ;
      "FOR" I := 1 "STEP" 1 "UNTIL" 7 "DO"
      SUM2 := SUM2+TOR[I]*T[I]  ;
      SUM1 := 0.0  ;
      "FOR" I := 1 "STEP" 1 "UNTIL" 3 "DO"
      "FOR" J := 1 "STEP" 1 "UNTIL" 3 "DO"
      "BEGIN" SUM1 := 0.0  ;
      "FOR" K := 1 "STEP" 1 "UNTIL" 7 "DO"
      SUM1 := SUM1+TOR[K]*X[K,J]*X[K,I]  ;
      MU[I,J] := SUM1  ;
      "END"  ;
      BETA := 0.0;
      "PRINT" ' QUADRATIC MOMENTS
        X.X        X.Y        X.Z        Y.Y        Y.Z        Z.Z
      ' ;
      "FOR" I := 1 "STEP" 1 "UNTIL" 7 "DO"
      "BEGIN"
      "PRINT" SAMELINE,PREFIX('S2'),ALIGNED(3,3),
      X[I,1]*X[I,1],ALIGNED(3,3),X[I,1]*X[I,2],ALIGNED(3,3),
      X[I,1]*X[I,3],ALIGNED(3,3),X[I,2]*X[I,2],ALIGNED(3,3),
      X[I,2]*X[I,3],ALIGNED(3,3),X[I,3]*X[I,3],'L' ;
      "END";
      "PRINT" ' JUMP PROBABILITIES AND JUMP FREQUENCIES
        BETWEEN THE MOLECULE AT 0,0,0 AND NEAR NEIGHBOURS
          MOL    TOR(I)           1/T(I)
      ' ;
```

```
"PRINT"SAMELINE,PREFIX(**S4**),DIGITS(1),I,ALIGNED(1,3),TOR[I],
ALIGNED(2,3),T[I],**L**;
"END";
"FOR" I := 1 "STEP" 1 "UNTIL" 7 "DO"
BETA := BETA+T[I]/7;
"PRINT"* AVERAGE JUMP FREQUENCY *,SAMELINE,ALIGNED(2,3),BETA,
**L* NO OF JUMPS *,SAMELINE,ALIGNED(2,3),SUM2,*
DIFFUSION TENSOR
*;
"FOR" J := 1 "STEP" 1 "UNTIL" 3 "DO"
"FOR" I := 1 "STEP" 1 "UNTIL" 3 "DO"
"BEGIN"
"PRINT"SAMELINE,ALIGNED(5,4),MU[I,J] ;
"IF" I = 3 "THEN""PRINT"**L** ;
"END" ;
"PRINT" * MOBILITY TENSOR
*;
"FOR" J := 1 "STEP" 1 "UNTIL" 3 "DO"
"FOR" I := 1 "STEP" 1 "UNTIL" 3 "DO"
"BEGIN"
MU[I,J] := SUM2*MU[I,J]/(1.723312*TEMP) ;
"END" ;
"FOR" J := 1 "STEP" 1 "UNTIL" 3 "DO"
"FOR" I := 1 "STEP" 1 "UNTIL" 3 "DO"
"BEGIN"
"PRINT"SAMELINE,ALIGNED(5,4),MU[I,J] ;
"IF" I =3 "THEN" "PRINT"**L** ;
"END" ;
"PRINT" **L4** ;
"PRINT" *LINEAR RESPONSE THEORY OF THE MOBILITY*L**;
"FOR" I := 1 "STEP" 1 "UNTIL" 7 "DO"
T[I] := T[I]*10.3376;
"READ"A,B;
"PRINT"*POLARIZATION FACTOR*,SAMELINE,ALIGNED(5,4),A,
**L*PHONON ELECTRON INTERACTION FACTOR*,SAMELINE,
ALIGNED(5,4),B,**L**;
"FOR" I := 1 "STEP" 1 "UNTIL" 7 "DO"
TOR[I] := T[I]*2*(1+B)*W[I];
SUM1 := 0.0 ;
"FOR" I := 1 "STEP" 1 "UNTIL" 3 "DO"
"FOR" J := 1 "STEP" 1 "UNTIL" 3 "DO"
"BEGIN" SUM1 := 0.0 ;
"FOR" K := 1 "STEP" 1 "UNTIL" 7 "DO"
SUM1 := SUM1+TOR[K]*X[K,J]*X[K,I] ;
MU[I,J] := 3.1415926*SUM1/(TEMP*A);
"END" ;
"PRINT" * MOBILITY TENSOR
*;
"FOR" J := 1 "STEP" 1 "UNTIL" 3 "DO"
"FOR" I := 1 "STEP" 1 "UNTIL" 3 "DO"
"BEGIN"
"PRINT"SAMELINE,ALIGNED(5,4),MU[I,J] ;
"IF" I =3 "THEN" "PRINT"**L** ;
"END" ;
"PRINT" **L20** ;
"GOTO" REPEAT ;
"END"
```

FORMAT OF THE OUTPUT FROM KR0069.

MOLECULAR INTEGRALS

(0,0,1)	(0,1,0)	(0,1,1)	(1,0,0)	(1,0,1)	(½,½,0)	(½,½,1)
-4.2300	224.5100	-0.1600	1.5900	-5.0900	-403.6900	9.4600

QUADRATIC MOMENTS

X.X	X.Y	X.Z	Y.Y	Y.Z	Z.Z
40.532	0.000	-58.540	0.000	0.000	84.550
0.000	0.000	0.000	36.457	0.000	0.000
40.532	-38.441	-58.540	36.457	55.520	84.550
0.000	0.000	0.000	0.000	0.000	0.000
4.820	0.000	20.188	0.000	0.000	84.550
18.327	12.924	0.000	9.114	0.000	0.000
4.349	-6.296	-19.176	9.114	27.760	84.550

JUMP PROBABILITIES AND JUMP FREQUENCIES
BETWEEN THE MOLECULE AT 0,0,0 AND NEAR NEIGHBOURS

MOL	TOR(I)	1/T(I)
1	0.004	0.409
2	0.211	21.718
3	0.000	0.015
4	0.001	0.154
5	0.005	0.492
6	0.760	39.051
7	0.018	0.915

AVERAGE JUMP FREQUENCY   8.965
NO OF JUMPS   34.299
DIFFUSION TENSOR

14.2067	9.7015	-0.4957
9.7015	14.8092	0.5113
-0.4957	0.5113	2.2737

MOBILITY TENSOR

0.9425	0.6436	-0.0329
0.6436	0.9825	0.0339
-0.0329	0.0339	0.1508

LINEAR RESPONSE THEORY OF THE MOBILITY
POLARIZATION FACTOR   0.2760
PHONON ELECTRON INTERACTION FACTOR   0.4760
MOBILITY TENSOR

11.8015	8.3180	-0.0078
8.3180	9.5003	0.0098
-0.0078	0.0098	0.0372

Appendix(4)

A computer program to determine the energy levels
and molecular orbital coefficients of a molecule
by the SCF-LCAO method.

(A4.1) Introduction.

(A4.2) Construction of the data tape.

(A4.3) Text of the program.

(A4.1) Introduction.

The function of the program outlined in this appendix is two fold:

(1) To determine, from parameters input as data, the molecular energy levels and orbital coefficients of a particular molecule using the LCAO-SCF-MO method as discussed in chapter(7).

(2) To calculate the energy levels, molecular orbital coefficients and bond order-charge density matrix of a matrix input as data.

The data output for (1) consists of the idempotent density matrix and molecular Hamiltonian for each iteration and, if the data reaches self consistency and wh $\neq$ 1, the energy levels, orbital coeficients and density matrix. These are printed on the line printer. In addition the charge density matrix is output on punched tape.

The data output for case(2) consists of the eigenvalues and eigenvectors of the matrix followed by the charge density -bond order matrix.

(A4.2) Construction of the data tape.

n: The number of atoms in the molecule.

$z[i]$:   An n×1 array containing the number of electrons contributed by atom i to the pi system.

eV: An integer set equel to 1 if the units of energy are eV or 0 if the units are in Hueckel units.

max: The maximum number of iterations to be performed.

If the program is to be used to diagonalize a secular matrix max should be set> 998.

The position and value of the non-zero elements

of the matrix should then be input terminated by
setting the first position integer > 998.

This should be followed by £ENDJOB and the
remaining instructions ignored.

EXAMPLE To diagonalize a matrix of the form:

$$\begin{matrix} 1 & 0 & 1 \\ 0 & 1 & 0 \\ 1 & 0 & 1 \end{matrix}$$

The data(after max) would be of the form:

1;1;1;

1;3;1;

2;2;1;

3;3;1;

999;

£ENDJOB

The zero elements and symmetrically equivalent
(invertion) elements are constructed within the
program.

wh: An integer set equel to 1 if the resulting SCF
           Hamiltonian is not to be diagonalized.

idem: The maximum number of iterations required to
           restore idempotency (usually 2 or 3 are sufficient)

gc: The coulomb integral parameter for carbon.

dw[i]:   A nx1 array containing the differences in
           ionization potentials of carbon and atom i.

hc[i,j]:   A nxn array containing the approximate charge
           density-bond order matrix.

b[i,j]:   A nxn array containing the elements of the
           Resonance integral matrix.

g[i,j]:   A nxn array containing the elements of the
           Coulomb integral matrix.

(A4.3) The text of the program.

```
begin

real AA,gc;

integer i,j,n,fo,ft,ff,count,sum,max,idem,ev,wh,fw,k;

integer procedure format(str)   ;

string str   ;

format := layout(str)   ;

open(20);

open(30);

opout;

n:=read(20);

begin

array r,rm,s,b,h,hc,rs,g[1:n,1:n],
x,y,z,dw[1:n];

integer array u[1:n,1:n];

comment LUA 15 JUNE 1964;

procedure matmult (a,b,c,m,n,p);

value a,b,m,n,p;

integer m,n,p;

array a,b,c;

begin

integer i,j,k,r,s;

if m<0 then r:=-m else r:=m;

if p<0 then s:=-p else s:=p;

for i:=1 step 1 until r do

for j:=1 step 1 until s do

begin c[i,j]:=0;

for k:=1 step 1 until n do

c[i,j]:=c[i,j]+(if m<0 then a[k,i] else a[i,k])×
(if p<0 then b[j,k] else b[k,j])

end

end matmult;
```

```
procedure matinvert(x,r,y,error);
value x,r;
integer r;
real array x,y;
label error;
begin
comment Direct method (Todd) for matrix inversion.
The coefficients of the matrix to be inverted are
stored in the two dimensional array x , r  is the
number of rows (or columns, since the matrix is
square). On exit the inverted matrix is in the two
dimensional array y. Array x must have one extra
column for use as working space.  i.e. x must be
declared with dimensions [1:r,1:r+1]. error is the
label jumped to if x is a singular matrix;
integer s,l,v,z;
real max;
integer array rr[1:r];
for s:=1 step 1 until r do
begin
max:=0;
for l:=1 step 1 until r do
begin for v:=1 step 1 until s-1 do
if l=rr[v] then goto l1;
if abs(x[l,1])>abs(max) then
begin rr[s]:=l;
max:=x[l,1]
end;
l1:
```

```
end;
for l:=1 step 1 until r do
x[l,r+1]:=if l=rr[s] then 1 else 0;
if abs(max)<10-10 then goto error;
for l:=1 step 1 until r do
x[rr[s],l]:=x[rr[s],l+1]/max;
for l:=1 step 1 until r do
begin max:=x[l,1];
if l≠rr[s] then
for z:=1 step 1 until r do
x[l,z]:=x[l,z+1]-maxxx[rr[s],z]
end
end;
for z:=1 step 1 until r do
for l:=1 step 1 until r do
y[z,l]:=x[rr[z],l];
for z:=1 step 1 until r do
for l:=1 step 1 until r do
x[z,l]:=y[z,l];
for z:=1 step 1 until r do
for l:=1 step 1 until r do
y[l,rr[z]]:=x[l,z];
end;
comment LUA 12 APRIL 1964
LUA 5 APRIL 1964;
procedure householder tridiagonalisation (a,n,c,b);
value n;
integer n;
array a,b,c;
comment numerische mathematik 4.4 p.357 wilkinson, householders
    method for eigenvalues and eigenvectors;
```

```
begin

integer j,i,k;

real ai,sigma,h,bj,bigk,bi;

array q[1:n-1];

for i:=n step -1 until 3do

begin

sigma:=0;

for k:=1 step 1 until i-1 do

sigma:=sigma+a[i,k]xa[i,k];

ai:=a[i,i-1];

if ai>0 then bi:=-sqrt(sigma) else bi:= sqrt(sigma);

comment LUA 12 PAGE 2

LUA 5 PAGE 2;

b[i-1]:=bi;

if bi≠0 then

begin

h:=sigma-aixbi;

a[i,i-1]:=ai-bi;

for j:= i-1 step -1 until 1 do

begin

bj:=0;

for k:=i-1 step -1 until jdo

bj:=bj+a[k,j]xa[i,k];

for k:=j-1 step -1 until 1 do

bj:= bj+ a[j,k]xa[i,k];

q[j]:=bj/h

end j;

bigk:=0;

for j:=i-1 step -1 until 1do

bigk:=bigk+a[i,j]xq[j];
```

```
bigk:=bigk/(2×h);
forj:=i-1 step -1 until 1 do
q[j]:=q[j]-bigk×a[i,j];
for j:=i-1 step -1 until 1 do
begin
for k:=j step -1 until 1 do
a[j,k]:=a[j,k]-a[i,j]×q[k]-a[i,k]×q[j];
end j;
end
end i;
for i:=nstep -1 until 1 do
c[i]:= a[i,i];
b[i]:= a[2,1];
b[n]:=0
end householder tridiagonalisation;
comment LUA 12 PAGE 3
LUA 6 APRIL 1964;
procedure backtransformation (a,b,z,n,m1);
value n,m1;
integer n,m1;
array a,b,z;
comment numerische mathematik 4.4 p.358;
begin
integer i,j,k;
real s;
for j:= 1 step 1 until m1 do
for k:= 3 step 1 until n do
if b[k-1]≠0 then
begin
s:=0;
```

```
for i:= 1 step 1 until k-1 do

s:=s+a[k,i]×z[i,j];

s:=s/(b[k-1]×a[k,k-1]);

for i:=1 step 1 until k-1do

z[i,j]:=z[i,j]+s×a[k,i]

end

end backtransformation;

comment  LUA 12  PAGE 4

LUA 9  APRIL 1964;

procedure tridibisection 3 (c,b,n,m,t,gamma,w,norm);

value n,m,t,gamma;

integer n,m,t;

real gamma,norm;

array c,b,w;

begin

integer a1,i,j;

real p1,q1,y,lambda,l,g,h;

array p[1:n];

procedure sturms sequence;

begin integer i;

p1:=0;

q1:=1;

a1:=0;

for i:= 1 step 1 until n do

begin

y:=(c[i]-lambda)×q1-p[i]×p1;

p1:=q1; q1:=y;

if p1≥0 eqv q1≥0 then a1:=a1+1

end;

if q1=0 and p1>0 then a1:=a1-1

end;
```

```
comment LUA 12 PAGE 5 LUA 9 PAGE 2;

norm:= abs(c[1])+abs(b[1]);

for i:=2 step 1 until n do

begin l:= abs(b[i-1])+abs(c[i])+abs(b[i]);

if l>norm then norm:=l

end;

for i:=1 step 1 until n-1 do

begin

if b[i]=0 then p[i+1]:= gamma×norm×norm

else p[i+1]:=b[i]×b[i]

end;

p[1]:=0;

if m>n then m:=n;

for i:=1 step 1 until m do

begin

g:=norm;

h:=-norm;

for j:=1 step 1 until t do

begin lambda:=(g+h)/2;

sturms sequence;

if al>i then h:=lambda else g:=lambda

end;

w[i]:=(g+h)/2

end

end tridibisection;

comment LUA 12 PAGE 6

LUA 10 APRIL 1964;
```

```
procedure tridiinverse iteration 1 (c,b,n,w,norm,m1,macheps)
result:(z);
value n,m1,norm,macheps;
integer n,m1;
real norm,macheps;
arrayc,b,w,z;
comment numerische mathematik, 4, 368-376;
begin
integer i,j;
real bi,bi1,lambda,u,v,h,eps,eta;
array m,p,q,r,int[1:n],x[1:n+2];
lambda:=norm;
eps:=machepsxnorm;
for j:=1 step 1 until m1 do
begin lambda:=lambda-eps;
if w[j]<lambda then lambda:=w[j];
u:=c[1]-lambda;
v:=b[1];
if v=0 then v:=eps;
for i:=1 step 1 until n-1 do
begin
bi:=b[i];
if bi=0 then bi:= eps;
bi1:=b[i+1];
if bi1=0thenbi1:=eps;
comment  LUA 12   PAGE 7
LUA 10   PAGE 2;
if abs(bi)≥ abs(u) then
begin
m[i+1]:=u/bi;
if m[i+1]=0 and bi≤eps then m[i+1]:=1;
```

```
p[i]:=bi;

q[i]:=c[i+1]-lambda;

r[i]:=bi1;

u:=v-m[i+1]×q[i];

v:=-m[i+1]×r[i];

int[i+1]:=+1

end

else begin

m[i+1]:=bi/u;

p[i]:=u;

q[i]:=v;

r[i]:=0;

u:=c[i+1]-lambda-m[i+1]×v;

v:=bi1;

int[i+1]:=-1

end

end i;

p[n]:=u;

q[n]:= r[n]:=0;

x[n+1]:=x[n+2]:=0;

h:=0;

eta:=1/n;

for i:=n step -1 until 1 do

begin

u:=eta-q[i]×x[i+1]-r[i]×x[i+2];

if p[i]=0 then x[i]:=u/eps else x[i]:=u/p[i];

h:=h+abs(x[i])

end i;

comment  LUA 12  PAGE 8

LUA 10  PAGE 3;
```

```
h:=1/h;
for i:=1 step 1 until ndo
x[i]:=x[i]×h;
for i:= 2 step 1 until n do
begin
if int[i]>0 then
begin
u:=x[i-1];
x[i-1]:=x[i];
x[i]:=u-m[i]×x[i-1]
end
else x[i]:=x[i]-m[i]×x[i-1]
end i;
h:=0;
for i:=n step -1 until 1 do
begin
u:=x[i]-q[i]×x[i+1]-r[i]×x[i+2];
if p[i]=0 then x[i]:=u/eps
else x[i]:=u/p[i];
h:=x[i]×x[i]+h
endi;
h:=1/sqrt(h);
for i:=1 step 1 until n do
z[i,j]:=x[i]×h
endj
end tridiinverse iteration 1;
```

```
comment  LUA 12  PAGE 9;
procedure  eigenvectors (a,n,m,w,z);
value  n,m;
array a,w,z;
integer n,m;
begin
array b,c[1:n];
real norm;
householder tridiagonalisation (a,n,c,b);
tridibisection 3 (c,b,n,m,39,2↑(-78),w,norm);
tridiinverse iteration 1(c,b,n,w,norm,m,2↑(-39),z);
backtransformation (a,b,z,n,m)
end eigenvectors;
```

```
comment Construction of idempotent matrix-R;
procedure potent(idem,n,r,u,count,rs,lo);
value r,idem,n,u;
integer idem,count,n;
array r,rs;
integer array u;
label lo;
begin real a,be;
integer c,i,j;
array rm,s[1:n,1:n];
count:=0;
for c:=1 step 1 until idem do
begin count:=count+1;
matmult(r,r,s,n,n,n);
for i:=1 step 1 until n do
for j:=1 step 1 until n do
rm[i,j]:=rm[j,i]:=3.0×u[i,j]-2.0×r[i,j];
matmult(s,rm,rs,n,n,n);
for i:=1 step 1 until n do
for j:=1 step 1 until n do
if abs(rs[i,j]-r[i,j])>10-4 then goto lw;
goto lo;
lw:end;
a:=0.0;
for i:=1 step 1 until n do
a:=a+rs[i,i];
be:=(n÷2-a)/n;
for i:=1 step 1 until n do
for j:=1 step 1 until n do
rs[i,j]:=rs[j,i]:=rs[i,j]+be×u[i,j];
end potent;
```

```
comment Construction of new matrix-R;

procedure newr(u,r,h,g,s,n);

value u,r,h,g,n;

integer n;

array r,h,g,s;

integer array u;

begin real a,be,c,d;

integer i,j;

array ii,jj,rm[1:n,1:n],
          rs[1:n,1:n+1];

for i:=1 step 1 until n do

for j:=1 step 1 until n do

rs[i,j]:=rs[j,i]:=u[i,j]-r[i,j];

matmult(rs,h,rm,n,n,n);

matmult(rm,r,s,n,n,n);

for i:=1 step 1 until n do

for j:=1 step 1 until n do

begin ii[i,j]:=s[i,j]+s[j,i];
          jj[i,j]:=s[i,j]-s[j,i]

end;

matmult(ii,h,rs,n,n,n);

a:=0.0;

for i:=1 step 1 until n do

a:=a+rs[i,i];

matmult(ii,jj,s,n,n,n);

matmult(s,h,rs,n,n,n);

be:=0.0;

for i:=1 step 1 until n do

be:=be+rs[i,i];

for i:=1 step 1 until n do

for j:=1 step 1 until n do
```

```
rm[i,j]:=2.0×ll[i,i]×ll[j,j]-ll[i,j]×ll[i,j];

matmult(g,rm,rs,n,n,n);

c:=0.0;

for i:=1 step 1 until n do

c:=c+rs[i,i];

d:=-a/(2.0×be-c);

matmult(ll,ll,rm,n,n,n);

for i:=1 step 1 until n do

for j:=1 step 1 until n do

rs[i,j]:=u[i,j]+d×d×rm[i,j];

matinvert(rs,n,rm,ls);

for i:=1 step 1 until n do

for j:=1 step 1 until n do

rs[i,j]:=d×ll[i,j]+d×d×s[i,j];

matmult(rm,rs,s,n,n,n)

end newr;

for i := 1 step 1 until n do

z[i] := read(20)  ;

fo := format([_ss-ndd.ddddd_])  ;

ft := format([_ndc_])  ;

ff := format([_-nd.ddddc_])  ;

fw := format([_s-d.ddddd;_])  ;

ev := read(20)  ;

max := read(20)  ;

if max > 998 then

begin

for i := 1 step 1 until n do

for j := 1 step 1 until n do

h[i,j] := h[j,i] := 0.0;

xxxx:

i := read(20);
```

```
if i > 998 then goto out;

j := read(20);

AA:= read(20);

h[i,j] := h[j,i] := AA;

goto xxxx;

out:


wh := 2  ;

close(20)  ;

goto lf  ;

end;

wh := read(20)  ;

idem := read(20)  ;

gc:=(read(20))/2.0;

comment Reading in data;

for i:=1 step 1 until n do dw[i]:=read(20);

for i:=1 step 1 until n do

for j:=1 step 1 until n do

hc[i,j]:=r[i,j]:=0.5×read(20);

for i:=1 step 1 until n do

for j:=1 step 1 until n do

begin if i=j then u[i,j]:=1 else u[i,j]:=0;

          b[i,j]:=read(20)

end;

for i:=1 step 1 until n do

begin x[i]:=0.0;

for j:=1 step 1 until n do

begin g[i,j]:=read(20);

if i≠j then x[i]:=x[i]-z[j]×g[i,j]

end;
```

```
y[i]:=dw[i]-gc+x[i]

end;

close(20);

write text(30,[[10s]RESULTS*FOR*ITERATIVELY*CONSTRUCTED
*HARTREE-FOCK*HAMILTONIAN[cc]]);

sum:=-1;

lt:sum:=sum+1;

potent(idem,n,r,u,count,s,lo);

lo:for i:=1 step 1 until n do

for j:=1 step 1 until n do

r[i,j]:=r[j,i]:=s[i,j];

if sum≠0 then

begin for i:=1 step 1 until n do

for j:=1 step 1 until n do

if abs(r[i,j]-hc[i,j])>10-4 then

begin for i:=1 step 1 until n do

for j:=1 step 1 until n do

hc[i,j]:=hc[j,i]:=r[i,j];

goto lz

end;

goto lf

end;

lz:write text(30,[[ss]IDEMPOTENT*DENSITY*MATRIX[c]]);

write text(30,[[ss]ITERATIONS*REQUIRED*]);

write(30,ft,count);

for i:=1 step 1 until n do

begin

k := 0 ;

for j:=1 step 1 until n do

begin

k := k+1;
```

```
write(30,if j=nthen(if i=j then fo+2 else fo+1)else
 fo,r[i,j]);
if k = 11 then
begin
k := 0;
write text(30,[[c]]);
end
end
end;
for i:=1 step 1 until n do
begin
k := 0;
for j:=1 step 1 until n do
begin
k := k+1;
AA := R[i,j];
fixout(AA,1,1,5);
scout;
if k = 11 then
begin
k := 0;
crout(1)
end;
if j = n then crout(1);
end
end;
gapout(10);
comment Construction of hamiltonian-h;
for i:=1 step 1 until n do
begin x[i]:=0.0;
```

```
for j:=1 step 1 until n do

begin if i≠j then x[i]:=x[i]+2.0×r[j,j]×g[i,j];

rm[i,j]:=rs[i,j]:=0.0

end;

rm[i,i]:=y[i]+x[i]+r[i,i]×g[i,i];

for j:=i+1 step 1 until n do

rs[i,j]:=b[i,j]-r[i,j]×g[i,j];

for j:=1 step 1 until n do

h[i,j]:=h[j,i]:=rm[i,j]+rs[i,j]

end;

write text(30,[[ ss]HAMILTONIAN[ c]]);

for i:=1 step 1 until n do

begin

k := 0;

for j:=1 step 1 until n do

begin

k := k+1;

write(30,if j=n then (if i=j then fo+2 else fo+1)
 else fo,h[i,j]);

if k = 11 then

begin

k := 0;

write text(30,[[ c]]);

end;

end;

end;

if sum=max then goto lf;

newr(u,r,h,g,s,n);

for  i:=1 step 1 until n do

for j:=1 step 1 until n do

r[i,j]:=r[i,j]-s[i,j];
```

```
goto lt;

comment Construction of bond-order charge-density matrix;

lf:if wh=1 then goto ln;

eigenvectors(h,n,n,x,rm);

for i:=1 step 1 until n do

begin write text(30,[[ss]ENERGY*OF*MO*]);

write(30,ff,x[i]);

write text(30,[[ss]COEFFICIENTS*OF*ATOMIC*ORBITALS[c]]);

k := 0;

for j:=1 step 1 until n do

begin

k := k+1;

write(30,if j=n then fo+2 else fo,rm[j,i]);

if k = 11 then

begin

k := 0;

write text(30,[[c]]);

end;

r[i,j]:=0.0

end

end;

idem := 0  ;

for i := 1 step 1 until n do

idem := idem+z[i]  ;

if ev=1 then

begin max:=idem÷2+1 ;

for j:=1 step 1 until n do

for sum:=j step 1 until n do

for i:=max step 1 until n do
```

```
r[j,sum]:=r[sum,j]:=r[sum,j]+rm[sum,i]×rm[j,i]

end else

begin max:=idem÷2;

for j:=1 step 1 until n do

for sum:=j step 1 until n do

for i:=1 step 1 until max do

r[j,sum]:=r[sum,j]:=r[sum,j]+rm[sum,i]×rm[j,i]

end;

for i:=1 step 1 until n do

for j:=1 step 1 until n do

r[i,j]:=r[j,i]:=2.0×r[i,j];

write text(30,[[ss]BOND-ORDER*CHARGE-DENSITY*MATRIX[c]]);

for i:=1 step 1 until n do

begin

k := 0;

for j:=1 step 1 until n do

begin k := k+1;

write(30,if j=n then fo+1 else fo,r[i,j]);

if k = 11 then

begin

k := 0;

write text(30,[[c]]);

end

end

end;

for i := 1 step 1 until n do

begin

k := 0;

for j := 1 step 1 until n do

begin

k := k+1;
```

```
AA := r[i,j];

fixout(AA,1,1,5);

scout;

if j = n then crout(1);

if k = 11 then

begin

k := 0;

crout(1);

end

end

end;

goto ln;

ls:

write text(30,[MATRIX*SINGULAR]);

ln:

close(30);

clout;

end;

end
```